THE UNIVERSITY OF TOKYO

博士論文　DOCTORAL THESIS

Thermodynamic relations on irreversibility in nonequilibrium systems(非平衡系の不可逆性に関する熱力学的関係)

Author:
ヴー　バン　タン
Tan VAN VU

Supervisor:
Prof. Yoshihiko HASEGAWA

A thesis submitted in fulfillment of the requirements
for the degree of Doctor of Philosophy

in the

Department of Information and Communication Engineering
Graduate School of Information Science and Technology

January 20, 2021

Declaration of Authorship

I, Tan Van Vu, declare that this thesis titled, "Thermodynamic relations on irreversibility in nonequilibrium systems" and the work presented in it are my own. I confirm that:

- This work was done wholly or mainly while in candidature for a research degree at this University.
- Where any part of this thesis has previously been submitted for a degree or any other qualification at this University or any other institution, this has been clearly stated.
- Where I have consulted the published work of others, this is always clearly attributed.
- Where I have quoted from the work of others, the source is always given. With the exception of such quotations, this thesis is entirely my own work.
- I have acknowledged all main sources of help.
- Where the thesis is based on work done by myself jointly with others, I have made clear exactly what was done by others and what I have contributed myself.

Signed:

_____

Date:

_____

Abstract

Tan Van Vu

Thermodynamic relations on irreversibility in nonequilibrium systems

Physical systems in the real world are basically operated and maintained in nonequilibrium states. To carry out a particular function, the system unavoidably consumes energy from some resources or exchanges energy with its surroundings somehow. It is well known that thermodynamic systems undergoing irreversible processes are always accompanied by thermodynamic costs, which place fundamental limits on systems' operational performance. For example, molecular motors convert the chemical energy stored in ATP into a directed movement; thus, the more energy is dissipated, the farther the motor can travel. Moreover, one might intuitively expect a trade-off relation between the dissipation cost and the fluctuation of the displacement. Unveiling such latent relations distinguishes the possible from the impossible and deepens our understanding of the underlying mechanisms of physical systems, thus providing insights into the design principles of optimal artificial machines.

Over the past few decades, there has been a flurry of research to understand the thermodynamics of small systems, resulting in two comprehensive frameworks: stochastic thermodynamics and quantum thermodynamics. Stochastic thermodynamics mainly focuses on the thermodynamic aspects of classical systems far from equilibrium, whereas quantum thermodynamics deals with quantum systems in which quantum effects emerge. These theoretical frameworks allow us to investigate the physical properties of microscopic systems that are subject to significant fluctuations. One of the central quantities in thermodynamics is entropy production, which characterizes the *irreversibility* of thermodynamic processes. In nonequilibrium steady-state systems, entropy production quantifies the amount of heat dissipated into the environment. In the context of biological processes, entropy production reflects the free energy lost in the spontaneous relaxation to perform a specific function. Furthermore, entropy production sets universal limits on the efficiency of thermal machines, such as heat engines and refrigerators. Therefore, revealing new relations on irreversibility and estimating the degree of irreversibility have become important research topics.

In recent years, a powerful inequality known as thermodynamic uncertainty relation (TUR) has been discovered for nonequilibrium systems described by Markov jump processes and overdamped Langevin equations. The TUR asserts a trade-off between the *uncertainty* of time-integrated currents (a statistical measure) and entropy production (a thermodynamic measure), i.e., high precision of currents is unattainable without increasing the associated entropy production. Remarkably, the TUR not only quantifies our intuition — higher accuracy

requires more cost — for the first time but also imposes a lower bound on entropy production in terms of moments of currents. Nevertheless, questions remain about how entropy production constrains the current fluctuation in other stochastic dynamics and whether a tighter lower bound on entropy production can be derived given additional information.

Such research questions are addressed in two separate parts of this thesis. In the first part of this thesis, we focus on investigating the TUR in various dynamics from both theoretical and practical perspectives. Motivated by the numerical fact that the TUR is no longer valid in some stochastic dynamics, we derive novel TURs for a wide range of observables, which are not limited to time-integrated currents. Employing an information-theoretical approach, we obtain TURs for steady-state underdamped Langevin dynamics and for Langevin systems driven by an external time-dependent control protocol. Our derived bounds indicate that the entropy production cannot solely constrain the fluctuation of observables in the finite times, and other complementary contributions such as the dynamical activity are required. Going beyond the Markovian systems and adopting another approach based on the fluctuation theorem, we derive TURs for non-Markovian systems, including time delay, measurement and feedback control, and semi-Markov processes. The obtained TURs imply that in addition to the entropy production, non-Markovian contributions such as the information flow and memory effects play an important role in suppressing observable fluctuations. Along with theoretical results, we also propose a TUR-based method, which exactly estimates entropy production for overdamped Langevin dynamics and returns a tightest lower bound of entropy production for Markov jump processes. The proposed method provides an effective and efficient tool to infer dissipation in biological and physical systems from experimental data.

In the second part of the thesis, we aim to tighten the lower bound of the total entropy production, thus sharpening the second law of thermodynamics. Specifically, we derive geometrical bounds on the irreversibility in both quantum and classical Markovian open systems that satisfy the detailed balance condition. Using information geometry, we prove that irreversible entropy production is bounded from below by a modified Wasserstein distance between the initial and final states, thus strengthening the Clausius inequality in the reversible-Markov case. The modified metric can be regarded as a discrete-state generalization of the Wasserstein metric, which has been used to bound dissipation in continuous-state Langevin systems. Notably, the derived bounds can be interpreted as the quantum and classical speed limits, implying that the associated entropy production constrains the minimum time of transforming a system state.

The thesis presents various thermodynamic relations on the irreversibility of thermodynamic processes, which connect physical quantities such as dissipation, thermodynamic length, observable fluctuations, dynamical activity, and evolution speed in both classical and quantum open systems.

Acknowledgements

First and foremost, I would like to express my sincere gratitude to my supervisor Prof. Dr. Yoshihiko Hasegawa, for his continuous supervision and support throughout my doctoral course. I feel honored to have had the opportunity to work with him since my undergraduate days. In the meantime, I have learned a lot from him, ranging from physical biology to statistical physics and thermodynamics, especially his immense knowledge regarding stochastic processes, stochastic thermodynamics, and quantum thermodynamics. I have been greatly influenced by his enthusiasm for cutting-edge research and the way he approaches scientific problems. I have also enjoyed daily discussions with him, which are fruitful and helpful in formulating, solving, and opening new research questions. In addition to these scientific aspects, he has shared many invaluable thoughts to me as I build my future academic career. My gratitude goes far beyond this one paragraph.

I would like to thank my advisors during the first two years in my Ph.D., Prof. Dr. Yoshimasa Tsuruoka and Prof. Dr. Hidetsugu Irie, for their guidance and fruitful discussions. I am also grateful to Prof. Dr. Hitoshi Iba, Prof. Dr. Kenjiro Taura, Prof. Dr. Yoshimasa Tsuruoka, and Prof. Dr. Tetsuya J. Kobayashi for being part of my thesis committee.

My sincere thanks also go to Prof. Dr. Keiji Saito and Dr. Sosuke Ito for offering me the opportunities to talk about my research. I also would like to thank Prof. Dr. Shin-ichi Sasa and Dr. Andreas Dechant for helpful discussions. I am incredibly grateful to Prof. Dr. Keiji Saito for fruitful discussions on many topics, the careful reading of the manuscript, and the valuable comments.

I gratefully acknowledge the continuous support I received from the Sato Yo International Scholarship Foundation during my five years in graduate school. I am grateful not only for the financial support but also for the mental support of the Foundation staff.

I would like to thank my fellow labmates in the Hasegawa laboratory. Special thanks to Quoc Hoan Tran and Van Tuan Vo for creative collaborations, stimulating conversations, and lifelong friendships.

Finally, I owe the greatest gratitude to my family, especially my parents, for their love, endless support, and encouragement throughout my growth and academic endeavors. I want to express appreciation to my partner, Mai Dan, for her support and encouragement, both in my personal life and in completing my degree.

This thesis would not have been completed without the support of many people. I would also like to express my gratitude to other people who are not mentioned here.

Contents

List of Figures

Chapter 1

Introduction

1.1 Background and motivation

Thermodynamics is a phenomenological theory that studies heat and work, and their relation to energy and physical properties of matter. The theory of thermodynamics is originally invented with the purpose of investigating the working principle of heat engines, and then has been rapidly developed into several related branches such as statistical mechanics, nonequilibrium thermodynamics, and chemical thermodynamics. Since all systems in real world inevitably exchange energy with their surroundings in some form, thermodynamics has become a crucial framework to study a wide variety of problems in both science and engineering.

The framework of thermodynamics is basically built upon five axioms, which are commonly known as the laws of thermodynamics. The two central laws of these are the first and second laws, which are the statements about energy conservation and the irreversibility of thermodynamic processes, respectively. The first law states that the change of internal energy dE is determined by the amount of work δW exerted on the system and the heat δQ dissipated from the system to the environment,

$$dE = \delta W - \delta Q. \tag{1.1}$$

The second law of thermodynamics can be stated in multiple ways. The Clausius theorem [1] claims that for a thermodynamic system exchanging heat with a reservoir and undergoing a thermodynamic cycle,

$$-\oint \frac{\delta Q}{T} \leq 0, \tag{1.2}$$

where T denotes the temperature of the reservoir at a particular instant in time. The equality of Eq. (1.2) is attained for quasistatic processes, naturally suggesting us define a state function S for reversible processes as $dS = -\delta Q/T$. The quantity S is indeed the thermodynamic entropy of the system. Considering a cycle that takes the system from state A to state B under a irreversible process and transforms back to A along a reversible path, the Clausius inequality implies

$$\Delta S_{\mathrm{tot}} \coloneqq \Delta S + \Delta S_{\mathrm{m}} \geq 0, \tag{1.3}$$

where $\Delta S \coloneqq S_B - S_A$ is the entropy change of the system and $\Delta S_{\mathrm{m}} \coloneqq \int_A^B \delta Q/T$ can be regarded as the entropy change of the reservoir. Equation (1.3) is exactly a formula of the second law

of thermodynamics, which affirms that the total entropy production of the system and the reservoir is always nonnegative. Notably, the second law has an important implication for the arrow of time — all thermodynamic processes have a preferred direction (that increases the total entropy). Nevertheless, the traditional thermodynamics deals only with macroscopic systems being in (local) equilibrium states and with thermodynamic processes that bring the system from an equilibrium state to another one, during which fluctuations are negligible.

Over the last two decades, substantial progresses have been made in studying thermodynamics of small systems that are subject to significant fluctuations and driven out of equilibrium. A comprehensive theoretical framework, named stochastic thermodynamics [2–4], has been developed, allowing us to investigate thermodynamic properties of microscopic dynamics beyond the linear response regime [5, 6]. The notions of heat, work, and entropy production have been extended, and the first and second laws of thermodynamics have been established to the level of individual trajectories [7]. Because of non-negligible fluctuations, these thermodynamic quantities are no longer deterministic, but stochastic. Beyond the classical limit, one has to invoke the framework of quantum thermodynamics [8–10] to include quantum effects such as coherence, correlation, and entanglement. Quantum thermodynamics transfers the notions in the classical thermodynamics to quantum systems and derives analogs of the conventional thermodynamic relations in the quantum regime from the established quantum principles.

A key quantity in thermodynamics is entropy production, which is commonly used to quantify the degree of irreversibility of physical processes. From a qualitative perspective, entropy production characterizes the possibility of observing the time-reversed process; that is, the larger entropy production, the less likely the time-reversed process will occur. Quantitatively, entropy production indicates the amount of heat dissipated to the environment in nonequilibrium steady-state systems and the free energy lost in thermal relaxation processes. Moreover, the positivity of entropy production imposes fundamental limits on the efficiency of heat engines and the information-erasure cost via Landauer's principle [11–13]. The important role of entropy production in thermodynamics suggests that a better understanding of entropy production could lead to new directions in physics and other related fields. To date, the formulation of entropy production and the investigation of its properties have been extensively developed in various contexts, from classical to quantum systems [14].

Due to fluctuations in small systems, entropy production can be negative for some trajectory but is always nonnegative on average. Intriguingly, a universal property regarding the symmetry of the probability distribution of stochastic entropy productions was discovered as the fluctuation theorem [15–20], from which the second law of thermodynamics can be derived. The fluctuation theorem is a prominent result and has been applied to solve various problems in physics and biology. In recent years, the thermodynamic uncertainty relation (TUR), quantifying a trade-off between the fluctuation of an arbitrary current and the entropy production, has been another important discovery in nonequilibrium statistical physics [21]. Qualitatively, the TUR indicates that it is impossible to attain a small fluctuation without increasing dissipation quantified by the entropy production in the system. Unlike the fluctuation theorem, which is an equality encoding the distribution of entropy production,

the TUR is an inequality formulated as

$$\frac{\mathrm{Var}[\phi]}{\langle\phi\rangle^2} \geq \frac{2}{\Delta S_{\mathrm{tot}}}, \tag{1.4}$$

where ϕ is an arbitrary time-integrated current and $\langle\phi\rangle$ and $\mathrm{Var}[\phi] \coloneqq \langle\phi^2\rangle - \langle\phi\rangle^2$ are its mean and variance, respectively. For instance, a current that is antisymmetric under time reversal can be the distance traveled by a molecular motor or the heat flux in thermal machines. The TUR was first derived for biomolecular processes and later proven for continuous-time Markov jump processes [22, 23] and overdamped Langevin systems [24]. Subsequently, the violation of the bound has been found for other dynamics, e.g., for discrete-time Markov chains [25] and transport systems [26]. The TUR has been intensively refined in other contexts including both classical and quantum systems [27–48]. A remarkable application of the TUR is the estimation of entropy production (or dissipation) [49–51]. Generally, the underlying dynamics of the system are required to evaluate the dissipation. Nevertheless, the TUR enables a way to estimate dissipation without such prior knowledge of the system. That is, by observing various fluctuating currents, one can infer a lower bound on entropy production. In addition to entropy production, the current fluctuation is also lower bounded by the dynamical activity (which is also known as frenesy [52]) [29, 36],

$$\frac{\mathrm{Var}[\phi]}{\langle\phi\rangle^2} \geq \frac{1}{\langle n\rangle}, \tag{1.5}$$

where $\langle n\rangle$ denotes the average number of jumps between states in a Markov jump process. Notably, the bound in Eq. (1.5) is valid for generic counting observables and will be called the kinetic uncertainty relation (KUR) hereafter.

The TUR and KUR have two important implications. First, the (time-antisymmetric) entropy production and the (time-symmetric) dynamical activity constrain current fluctuations in nonequilibrium processes. To achieve high precision of currents, both dissipation and frenesy need to be increased. Given these two quantities, the order of fluctuations can be approximately estimated without knowing the microscopic details of the underlying dynamics. Second, the TUR sets a lower bound on entropy production; thus, dissipation during a finite-time process can be robustly inferred if the first and second moments of currents are provided. Nowadays, with the advent of the experimental techniques, such statistical information of fluctuating currents in small systems can be accessible without difficulty. Therefore, the TUR provides a powerful tool for thermodynamic inference, which especially benefits research in biology.

In this thesis, we investigate thermodynamic relations on irreversibility in nonequilibrium systems, focusing on the role of irreversibility in suppressing fluctuations and the refinement of the positivity of entropy production. These points are separately addressed in the two parts of the thesis.

In the first part, we put the TUR in a broader range of stochastic dynamics including non-Markovian systems, and study the connection between irreversibility and current fluctuations. The TUR is originally derived for steady-state continuous-time Markov jump processes, thus holding for overdamped Langevin systems. However, its violation can be numerically found

in other dynamics such as underdamped systems [53], Langevin systems driven by a control protocol [54], and non-Markovian systems [55–57]. This implies that entropy production cannot solely constrain current fluctuations in such dynamics. Thereby, we derive novel TURs and find that in addition to entropy production, other physical quantities such as dynamical activity, information flow, and memory terms are necessary to suppress fluctuations. These additional terms originate from the time-reversal symmetry breaking and the non-Markovian nature. Along with the theoretical investigation, we also consider the application of the TUR in the estimation of entropy production. The TUR establishes a saturable lower bound on entropy production in terms of moments of time-integrated currents. Nonetheless, from the practical point of view, it remains challenges to accurately infer entropy production from the observed data without access to details of the underlying dynamics. Accordingly, we propose a TUR-based method to exactly estimate entropy production of steady-state systems described by overdamped Langevin equations [58]. In the case of Markov jump processes, the method returns the tightest lower bound on entropy production. The study results confirm that fluctuations contain a wealth of information about physical processes and can be effectively exploited for thermodynamic inference.

In the second part, we refine the second law of thermodynamics for Markovian systems via a geometrical approach [59]. Most macroscopic natural phenomena are irreversible, although their microscopic physical processes are generally time-symmetric. According to the second law of thermodynamics, a system undergoing an irreversible process generates (on average) a positive entropy amount. This bound can be saturated only when operations are performed in the infinite-time quasistatic limit. However, as real processes must be completed in finite time, they are accompanied by a certain dissipation. Tightening the lower bound on entropy production not only deepens our understanding of how much heat must be dissipated, but also provides insights into quantum technologies such as quantum computation [60] and quantum heat engines [61]. Considering each possible state of the system as a point on a manifold, we prove that the entropy production is bounded from below by a modified Wasserstein distance between the initial and final states. This implies that the entropy production can be geometrically characterized beyond the linear response regime, thus shedding light on the problem of minimizing dissipation in discrete-state systems. Our study result also reveals that irreversibility constrains the state-transformation speed in quantum systems.

The thesis elucidates various relations between irreversibility and observable fluctuations, and characterizes irreversibility of thermodynamic processes from both information-theoretical and geometrical perspectives.

1.2 The structure of the thesis

The remainder of the thesis is organized as follows.

In chapter 2, we briefly introduce the framework of stochastic thermodynamics in both continuous-state Langevin systems and discrete-state Markov jump processes. The description of stochastic thermodynamics in this chapter is sufficient to understand all the results presented in the thesis. The notions of heat, work, and entropy production are generalized to the level of individual trajectories, and these thermodynamic quantities become stochastic.

The first and second laws of thermodynamics are then established and have analogous forms as in the classical thermodynamics. In addition, various versions of the fluctuation theorems and their derivations are also described.

Chapter 3 presents the framework of quantum thermodynamics and relevant concepts. The thermodynamics of closed and open quantum systems are discussed in a general setup. For systems that are weakly coupled to thermal reservoirs, several approximations can be applied, and the Lindblad master equation describing the dynamics of the reduced state is obtained. The notions of heat, work, and entropy production for open quantum systems governed by the Lindblad master equation are introduced.

In chapter 4, we consider Langevin systems for which the original TUR is inapplicable and derive novel TURs using the Cramér-Rao inequality. First, we focus on steady-state underdamped Langevin systems, in which the inertial effects cannot be neglected. The violation of the TUR is numerically found, which motivates us to investigate the relation between irreversibility and current fluctuations. We find that both irreversibility and dynamical activity complementarily constrain fluctuations of time-integrated currents. We illustrate our results with two systems, a single-well potential system and a periodically driven Brownian particle model, and numerically verify the inequalities. Next, we study Langevin systems driven by an arbitrary time-dependent protocol. For such systems, fluctuations of observables cannot be bounded solely by entropy production, even with an exponential bound. Therefore, we derive TURs for arbitrary observables satisfying a scaling condition in both overdamped and underdamped regimes. We prove that the observable fluctuation is constrained by both entropy production and a kinetic term. The derived bounds are applicable to both current and non-current observables and hold for arbitrary time-dependent protocols, thus providing a wide range of applicability. We illustrate our universal bounds with the help of three systems: a dragged Brownian particle, a Brownian gyrator, and a stochastic underdamped heat engine.

In chapter 5, we pay attention to non-Markovian systems and derive TURs for systems involving time delay, measurement and feedback control, and semi-Markov processes. First, we consider time-delayed Langevin systems and prove that the fluctuation of arbitrary dynamical observables is constrained by the Kullback-Leibler divergence between the distributions of the forward path and its reversed counterpart. Specifically, for observables that are antisymmetric under time reversal, the fluctuation is bounded from below by a function of a quantity that can be identified as a generalization of the total entropy production in Markovian systems. We also provide a lower bound for arbitrary observables that are odd under position reversal. The term in this bound reflects the extent to which the position symmetry has been broken in the system and can be positive even in equilibrium. Our results hold for finite observation times and a large class of time-delayed systems because detailed underlying dynamics are not required for the derivation. We numerically verify the derived uncertainty relations using two single time-delay systems and one distributed time-delay system. Next, we investigate the uncertainty of dynamical observables in classical systems manipulated by repeated measurements and feedback control; the precision should be enhanced in the presence of an external controller but limited by the amount of information obtained from the measurements. We prove that the entropy production and the information quantity constrain from below the fluctuation of arbitrary observables that are antisymmetric under time reversal.

The information term is the sum of the mutual entropy production and the Kullback-Leibler divergence, which characterizes the irreversibility of the measurement outcomes. The result holds for finite observation times and for both continuous- and discrete-time systems. We apply the derived relations to study the precision of a flashing Brownian ratchet. Last, we generalize the TUR and KUR for semi-Markov processes. Explicitly, we prove that, unlike in the Markovian case, the fluctuation of time-antisymmetric observables is bounded not only by entropy production but also by a memory term. For generic observables, we analogously show that the fluctuation is bounded by both dynamical activity and a memory term. Our results indicate that memory plays an important role in the bounds. Interestingly, with a proper form of the waiting-time distribution, the memory can decrease the observable fluctuation. When the waiting-time distribution is Poissonian (i.e., the process becomes Markov), the memory terms vanish, and the derived bounds reduce to the conventional bounds.

Chapter 6 closes the first part of the thesis, where we study a practical application of the TUR in thermodynamic inference. According to the TUR, we propose a deterministic method to estimate the entropy production from a single trajectory of system states. We explicitly and approximately compute an optimal current that yields the tightest lower bound using predetermined basis currents. Notably, the obtained tightest lower bound is intimately related to the multidimensional TUR. By proving the saturation of the TUR in the short-time limit, the exact estimate of the entropy production can be obtained for overdamped Langevin systems, irrespective of the underlying dynamics. For Markov jump processes, because the attainability of the TUR is not theoretically ensured, the proposed method provides the tightest lower bound for the entropy production. When entropy production is the optimal current, a more accurate estimate can be further obtained using the integral fluctuation theorem. We illustrate the proposed method using three systems: a four-state Markov chain, a periodically driven particle, and a multiple bead-spring model. The estimated results in all examples empirically verify the effectiveness and efficiency of the proposed method.

In chapter 7 which corresponds to the second part, we geometrically characterize irreversibility in Markovian systems and refine the positivity of entropy production. Particularly, we derive geometrical bounds on the irreversibility in both quantum and classical Markovian open systems that satisfy the detailed balance condition. Using information geometry, we prove that irreversible entropy production is bounded from below by a modified Wasserstein distance between the initial and final states, thus strengthening the Clausius inequality in the reversible-Markov case. The modified metric can be regarded as a discrete-state generalization of the Wasserstein metric, which has been used to bound dissipation in continuous-state Langevin systems. Notably, the derived bounds can be interpreted as the quantum and classical speed limits, implying that the associated entropy production constrains the minimum time of transforming a system state. We illustrate the results on several systems and show that a tighter bound than the Carnot bound for the efficiency of quantum heat engines can be obtained.

Chapter 8 ends the thesis with the conclusion and discussion on future research directions.

The last four chapters of the thesis are mainly based on the following works, which have been published in:

- T. Van Vu and Y. Hasegawa,
  "Uncertainty relations for underdamped Langevin dynamics",
  Phys. Rev. E **100**, 032130 (2019).
  © 2019 American Physical Society. Chapter 4 is based on this publication.

- T. Van Vu and Y. Hasegawa,
  "Thermodynamic uncertainty relations under arbitrary control protocols",
  Phys. Rev. Research **2**, 013060 (2020).
  © 2020 American Physical Society. Chapter 4 is based on this publication.

- T. Van Vu and Y. Hasegawa,
  "Uncertainty relations for time-delayed Langevin systems",
  Phys. Rev. E **100**, 012134 (2019).
  © 2019 American Physical Society. Chapter 5 is based on this publication.

- T. Van Vu and Y. Hasegawa,
  "Uncertainty relation under information measurement and feedback control",
  J. Phys. A: Math. Theor. **53**, 075001 (2020).
  © 2020 IOP Publishing Ltd. Chapter 5 is based on this publication.

- T. Van Vu and Y. Hasegawa,
  "Generalized uncertainty relations for semi-Markov processes",
  J. Phys.: Conf. Ser. **1593**, 012006 (2020).
  © 2020 IOP Publishing Ltd. Chapter 5 is based on this publication.

- T. Van Vu, V. T. Vo, and Y. Hasegawa,
  "Entropy production estimation with optimal current",
  Phys. Rev. E **101**, 042138 (2020) (selected as an Editors' Suggestion).
  © 2020 American Physical Society. Chapter 6 is based on this publication.

- T. Van Vu and Y. Hasegawa,
  "Geometrical bounds of the irreversibility in Markovian systems",
  Phys. Rev. Lett. **126**, 010601, (2021)
  © 2021 American Physical Society. Chapter 7 is based on this publication.

Below are further co-authored publications, which are not included in the thesis:

- Y. Hasegawa and T. Van Vu,
  "Uncertainty relations in stochastic processes: An information inequality approach",
  Phys. Rev. E **99**, 062126 (2019).

- Y. Hasegawa and T. Van Vu,
  "Fluctuation theorem uncertainty relation",
  Phys. Rev. Lett. **123**, 110602 (2019).

- V. T. Vo, T. Van Vu, and Y. Hasegawa,
  "Unified approach to classical speed limit and thermodynamic uncertainty relation",
  Phys. Rev. E **102**, 062132 (2020).

Chapter 2

Stochastic thermodynamics

In this chapter, we briefly introduce the framework of stochastic thermodynamics with the help of continuous-state systems described by Langevin equations, as well as discrete-state systems governed by Markov jump processes. We describe how the notions of heat, work, and entropy production are generalized to the level of stochastic trajectories. In addition, we also demonstrate the fluctuation theorems and their derivations in the above-mentioned dynamics. The content of this chapter is basically in line with the great explanation in Refs. [3, 62].

2.1 Microscopic dynamics

2.1.1 Langevin systems

To efficiently introduce the main concepts of stochastic thermodynamics, we consider a Brownian particle confined in a one spatial dimension. The particle is immersed in a thermal reservoir at the temperature T, and may be driven by an external agent through the control parameter λ. The state of the system (i.e., the particle) at time t is represented by its position $x(t)$ and velocity $v(t)$. The dynamics of the particle are governed by the underdamped Langevin equation:

$$\frac{dx}{dt} = v, \ m\frac{dv}{dt} = -\gamma v + F(x,\lambda) + \xi(t), \tag{2.1}$$

where m is the particle mass, $F(x,\lambda) = -\partial_x U(x,\lambda) + f(x,\lambda)$ is a systematic force exerted on the particle, and $\xi(t)$ is the Gaussian white noise with mean $\langle\xi(t)\rangle = 0$ and correlation $\langle\xi(t)\xi(t')\rangle = 2D\delta(t-t')$. We assume that changes in the system do not affect the equilibrium state of the reservoir (i.e., the reservoir instantly returns to equilibrium), and there is no correlation between them. In equilibrium, the diffusion constant D and the friction coefficient γ are related by the Einstein relation $D = k_{\mathrm{B}}T\gamma$, which is also known as the fluctuation-dissipation theorem. In order to make entropy dimensionless, we set Boltzmann's constant to unity, $k_{\mathrm{B}} \equiv 1$. The force $F(x,\lambda)$ consists of two contributions. The first term arises from a conservative potential $U(x,\lambda)$ and the second from an external force $f(x,\lambda)$ that is applied to the particle directly. The control parameter λ is varied from $\lambda(0) = \lambda_0$ to $\lambda(\tau) = \lambda_\tau$ according to some prescribed protocol. The interaction between the system and the reservoir is reflected by the thermal noise $\xi(t)$ and the friction force $-\gamma v$.

Two equivalent representations corresponding to Eq. (2.1) are the Fokker–Planck equation (FPE) [63, 64] and the path integral. Let $p(x,v,t)$ be the probability distribution function

to find the particle at state (x, v) at time t, then the time evolution of $p(x, v, t)$ obeys the following FPE:

$$\partial_t p(x,v,t) = \mathcal{L}[p(x,v,t)] = -\partial_x[vp(x,v,t)] - \partial_v\left\{\frac{1}{m}\left[-\gamma v + F(x,\lambda) - \frac{T\gamma}{m}\partial_v\right]p(x,v,t)\right\} \tag{2.2}$$

$$= -\partial_x j_x(x,v,t) - \partial_v j_v(x,v,t), \tag{2.3}$$

where $j_x(x, v, t)$ and $j_v(x, v, t)$ are the probability currents given by

$$j_x(x,v,t) = vp(x,v,t), \tag{2.4}$$

$$j_v(x,v,t) = \frac{1}{m}\left[-\gamma v + F(x,\lambda) - \frac{T\gamma}{m}\partial_v\right]p(x,v,t). \tag{2.5}$$

In the absence of the external control $\lambda(t)$ and the external force $f(x, \lambda)$, the system will relax to an equilibrium state (a Maxwell–Boltzmann distribution) after a sufficiently long time. Specifically,

$$\lim_{t\to\infty} p(x,v,t) = p^{\mathrm{eq}}(x,v) = C\exp\left[-\frac{1}{T}\left(\frac{mv^2}{2} + U(x)\right)\right], \tag{2.6}$$

where C is the normalizing constant. However, it is not the case when the system is simultaneously coupled to multiple reservoirs at different temperatures. In this scenario, the system will reach a nonequilibrium steady state.

While the FPE describes the dynamics of the probability distribution, the path integral quantifies the likelihood of observing a trajectory $\Gamma = \{x(t), v(t)\}_{0\le t\le\tau}$ as a stochastic realization of the process. Specifically, the conditional likelihood of the trajectory Γ given the initial state $(x(0), v(0))$ can be expressed as

$$\mathcal{P}(\Gamma|x(0),v(0)) = \mathcal{N}\exp(-\mathcal{A}[\Gamma]), \tag{2.7}$$

where $\mathcal{N}$ is a normalization term and $\mathcal{A}[\Gamma]$ is an Onsager–Machlup action functional, defined as

$$\mathcal{A}[\Gamma] = \int_0^\tau \frac{1}{4T\gamma}[m\dot{v} + \gamma v - F(x,\lambda)]^2 dt. \tag{2.8}$$

Note that the Ito product has been employed in the action functional above. Particularly, the crossing term $\int_0^\tau \gamma F(x,\lambda)v dt$ should be interpreted as $\int_0^\tau \gamma F(x,\lambda)\cdot v dt$, where $\cdot$ denotes the Ito product[1]. On the other hand, if the Stratonovich convention is employed, it should be interpreted as $\int_0^\tau \gamma F(x,\lambda)\circ v dt$, where $\circ$ denotes the Stratonovich product[2]. Rewriting $\mathcal{A}$ in the Stratonovich-type integral leads to a slightly different expression of $\mathcal{P}$ as

$$\mathcal{P}(\Gamma|x(0),v(0)) = \mathcal{N}\exp\left(\frac{\tau\gamma}{2m}\right)\exp\left(-\int_0^\tau \frac{1}{4T\gamma}[m\dot{v} + \gamma v - F(x,\lambda)]^2 dt\right). \tag{2.9}$$

[1] The Ito integral is the limit of the pre-point discretization, i.e., $\int \Lambda(x)\cdot dx = \lim_{K\to\infty}\sum_{k=0}^{K-1}\Lambda(x_k)(x_{k+1} - x_k)$.

[2] In the Stratonovich convention, the integral is the limit of the mid-point discretization, i.e., $\int \Lambda(x)\cdot dx = \lim_{K\to\infty}\sum_{k=0}^{K-1}\Lambda\left(\frac{x_k+x_{k+1}}{2}\right)(x_{k+1} - x_k)$.

Consequently, the path probability $\mathcal{P}(\Gamma)$ is given by

$$\mathcal{P}(\Gamma) \propto p(x(0), v(0), 0) \exp\left(-\int_0^\tau \frac{1}{4T\gamma}[m\dot{v} + \gamma v - F(x,\lambda)]^2 dt\right), \tag{2.10}$$

which is known as the path integral representation. For further details, see the Appendix A.2. Hereafter, the Stratonovich product is implicitly used unless stated otherwise. As will be shown later, these representations are useful in establishing and justifying the notions of heat and entropy production in stochastic thermodynamics of microscopic dynamics.

The first law.—Energy is exchanged between the system, the reservoir, and the external agent for each stochastic realization of the given process. Now, we wish to formulate the first law of thermodynamics (the law of energy balance) on the trajectory level. To this end, we need to identify the internal energy, heat, and work along a single trajectory. Since, the reservoir exerts a force $-\gamma v + \xi$ on the particle, $(\gamma v - \xi) \circ dx$ is the energy dissipated from the system to the reservoir. Note that the Stratonovich product allows us to use usual rules of calculus about the differentials. This energy transfer is then defined as the heat,

$$dq \coloneqq (\gamma v - \xi) \circ dx. \tag{2.11}$$

With this definition, dq denotes the amount of heat that the reservoir received from the system. Using the Langevin equation (2.1), the heat can be rewritten as

$$dq = \left(F(x,\lambda) - m\frac{dv}{dt}\right) \circ dx = \left(f(x,\lambda) - m\frac{dv}{dt} - \partial_x U(x,\lambda)\right) \circ dx. \tag{2.12}$$

Note that

$$m\frac{dv}{dt} \circ dx = m\frac{dv}{dt} \circ v dt = d\left(\frac{mv^2}{2}\right), \tag{2.13}$$

$$\partial_x U(x,\lambda) \circ dx = dU(x,\lambda) - \partial_\lambda U(x,\lambda) \circ d\lambda. \tag{2.14}$$

Substituting these relations into Eq. (2.12), we obtain

$$d\left(\frac{mv^2}{2} + U(x,\lambda)\right) = -dq + (\partial_\lambda U(x,\lambda) \circ d\lambda + f(x,\lambda) \circ dx)\,. \tag{2.15}$$

Identifying the internal energy e of the system as the sum of kinetic and potential energy,

$$e \coloneqq \frac{mv^2}{2} + U(x,\lambda), \tag{2.16}$$

then Eq. (2.15) uniquely defines the stochastic work as

$$dw \coloneqq \partial_\lambda U(x,\lambda) \circ d\lambda + f(x,\lambda) \circ dx = de + dq. \tag{2.17}$$

As seen, the work increment arises from changing the potential (at fixed particle position) and applying a non-conservative force to the particle. Equation (2.17) can be regarded as the microscopic expression of the first law of thermodynamics.

Now, integrating heat and work along the stochastic trajectory Γ, we obtain following expressions:

$$q[\Gamma] = \int_0^\tau [F(x,\lambda) - m\dot{v}] \circ \dot{x} dt, \tag{2.18}$$

$$w[\Gamma] = \int_0^\tau \left[\partial_\lambda U(x,\lambda) \circ \dot{\lambda} + f(x,\lambda) \circ \dot{x}\right] dt, \tag{2.19}$$

where the dot denotes the time derivative. Consequently, the first law of thermodynamics on the level of an individual trajectory can be written as

$$\Delta e = -q[\Gamma] + w[\Gamma] = \frac{m}{2}\left[v(\tau)^2 - v(0)^2\right] + U(x(\tau),\lambda_\tau) - U(x(0),\lambda_0). \tag{2.20}$$

Note that Eq. (2.20) holds for an arbitrary realization of the stochastic process. Both heat and work are path-dependent quantities, whereas the internal energy is path-independent and depends only on the starting and ending points.

The second law.—To derive the second law on the level of single trajectories, we need to define the corresponding entropy productions of the system and the reservoir. The entropy production Δs_m of the reservoir can be associated with the heat dissipated from the system to the reservoir as

$$\Delta s_\mathrm{m}[\Gamma] \coloneqq q[\Gamma]/T. \tag{2.21}$$

The stochastic entropy of the system can be defined as the Shannon entropy [7]

$$s(t) \coloneqq -\ln p(x,v,t), \tag{2.22}$$

where $p(x,v,t)$ is the solution of the FPE in Eq. (2.3). Thus, the change in the system entropy is obtained as $\Delta s[\Gamma] = -\ln p(x(\tau),v(\tau),\tau) + \ln p(x(0),v(0),0)$. Consequently, the total entropy change along a trajectory is defined as $\Delta s_\mathrm{tot}[\Gamma] \coloneqq \Delta s[\Gamma] + \Delta s_\mathrm{m}[\Gamma]$. In the following, we will show that the ensemble average of Δs_tot is always positive,

$$\langle \Delta s_\mathrm{tot}[\Gamma]\rangle = \int \mathcal{P}(\Gamma)\Delta s_\mathrm{tot}[\Gamma]\mathcal{D}\Gamma \geq 0, \tag{2.23}$$

which is exactly the second law of thermodynamics. To this end, we consider a time-reversed (backward) process of the given (forward) process as follows. A phase space point (x,v) is sampled from the final distribution $p(x(\tau),v(\tau),\tau)$ and the corresponding point $(x,-v)$ is set to the initial state. Subsequently, the particle is driven under a time-reversed control parameter $\lambda^\dagger(t) = \lambda(\tau - t)$ from $t = 0$ to $t = \tau$. For each trajectory $\Gamma = \{x(t),v(t)\}_{0\leq t\leq\tau}$, we define a time-reversed trajectory $\Gamma^\dagger = \{x(\tau-t),-v(\tau-t)\}_{0\leq t\leq\tau}$. Then, the probability of observing the trajectory $\Gamma^\dagger$ in the backward process is

$$\mathcal{P}_\mathrm{B}[\Gamma^\dagger] \propto p(x(\tau),v(\tau),\tau)\exp\left(-\int_0^\tau \frac{1}{4T\gamma}[m\dot{v} - \gamma v - F(x,\lambda)]^2 dt\right). \tag{2.24}$$

Here, the subscript B is referred to as the backward process. Combining Eqs. (2.10) and (2.24), the log of ratio of the path probabilities in the forward and backward processes can

be calculated as

$$\ln \frac{\mathcal{P}(\Gamma)}{\mathcal{P}_{\mathrm{B}}(\Gamma^\dagger)} = -\ln p(x(\tau), v(\tau), \tau) + \ln p(x(0), v(0), 0) - \frac{1}{T}\int_0^\tau [m\dot{v} - F(x,\lambda)] \circ \dot{x} dt \tag{2.25}$$

$$= \Delta s[\Gamma] + \Delta s_{\mathrm{m}}[\Gamma] = \Delta s_{\mathrm{tot}}. \tag{2.26}$$

Thus, the total entropy production $\langle \Delta s_{\mathrm{tot}} \rangle$ can be rewritten as

$$\langle \Delta s_{\mathrm{tot}}[\Gamma] \rangle = \int \mathcal{P}(\Gamma) \ln \frac{\mathcal{P}(\Gamma)}{\mathcal{P}_{\mathrm{B}}(\Gamma^\dagger)} \mathcal{D}\Gamma =: D(\mathcal{P}||\mathcal{P}_{\mathrm{B}}). \tag{2.27}$$

Since the Kullback–Leibler (KL) divergence $D(\mathcal{P}||\mathcal{P}_{\mathrm{B}})$ is always nonnegative, the inequality $\langle \Delta s_{\mathrm{tot}}[\Gamma] \rangle \geq 0$ is immediately proved. It is worth noting that the stochastic entropy production $\Delta s_{\mathrm{tot}}[\Gamma]$ can be negative for some trajectory Γ.

Now let us examine the ensemble average of the entropy production rate. First, the rate of the system entropy production $\dot{s}(t)$ reads

$$\dot{s}(t) = -\frac{\partial_t p(x,v,t)}{p(x,v,t)} - \frac{\partial_x p(x,v,t)}{p(x,v,t)} \circ \dot{x} - \frac{\partial_v p(x,v,t)}{p(x,v,t)} \circ \dot{v} \tag{2.28}$$

Combining this with the rate of the reservoir entropy production, $\dot{s}_{\mathrm{m}}(t) = -[m\dot{v} - F(x,\lambda)] \circ \dot{x}/T$, gives an expression of the total entropy production rate $\dot{s}_{\mathrm{tot}}$ as

$$\dot{s}_{\mathrm{tot}}(t) = -\frac{\partial_t p(x,v,t)}{p(x,v,t)} - \left[\frac{\partial_x p(x,v,t)}{p(x,v,t)} + \frac{m\dot{v} - F(x,\lambda)}{T}\right] \circ \dot{x} - \frac{\partial_v p(x,v,t)}{p(x,v,t)} \circ \dot{v} \tag{2.29}$$

$$= \frac{\partial_t p(x,v,t)}{p(x,v,t)} - \left[\frac{\partial_x p(x,v,t)}{p(x,v,t)} - \frac{F(x,\lambda)}{T}\right] \circ \dot{x} - \left[\frac{\partial_v p(x,v,t)}{p(x,v,t)} + \frac{mv}{T}\right] \circ \dot{v} \tag{2.30}$$

Taking the ensemble average in Eq. (2.30) and performing some calculus calculations, we obtain

$$\langle \dot{s}_{\mathrm{tot}}(t) \rangle = \iint \frac{m^2}{T\gamma} \frac{j^{\mathrm{ir}}(x,v,t)^2}{p(x,v,t)} dxdv, \tag{2.31}$$

where $j^{\mathrm{ir}}(x,v,t)$ is the irreversible current, given by

$$j^{\mathrm{ir}}(x,v,t) \coloneqq -\frac{1}{m}\left[\gamma v + \frac{T\gamma}{m}\partial_v\right] p(x,v,t). \tag{2.32}$$

To obtain Eq. (2.31), we have used the natural boundary conditions of $p(x,v,t)$ and the relations $\langle g(x,v,t) \circ \dot{x} \rangle = \iint g(x,v,t) j_x(x,v,t) dxdv$ and $\langle g(x,v,t) \circ \dot{v} \rangle = \iint g(x,v,t) j_v(x,v,t) dxdv$ for an arbitrary function $g(x,v,t)$. In equilibrium, this irreversible current vanishes; thus, the total entropy production is zero. However, if the system is in a nonequilibrium steady state, $\langle \dot{s}_{\mathrm{tot}}(t) \rangle$ is always positive.

Dynamics without inertia.—When the time resolution of our interest is much larger than m/γ (i.e., $\tau \gg m/\gamma$), Eq. (2.1) can be approximated by the following equation without the inertia term,

$$\gamma \dot{x} = F(x,\lambda) + \xi(t). \tag{2.33}$$

This equation is known as the overdamped Langevin equation. The FPE describing the time evolution of the probability distribution $p(x,t)$ is written as

$$\partial_t p(x,t) = -\partial_x \left\{ \gamma^{-1} \left[F(x,\lambda) - T\partial_x \right] p(x,t) \right\} = -\partial_x j_x(x,t), \tag{2.34}$$

where $j_x(x,t) \coloneqq \gamma^{-1} \left[F(x,\lambda) - T\partial_x \right] p(x,t)$ is the probability current. The path integral representations in the Ito and Stratonovich conventions, respectively, are as follows:

$$\mathcal{P}(\Gamma) \propto p(x(0),0) \exp\left(-\int_0^\tau \frac{1}{4T\gamma} [\gamma\dot{x} - F(x,\lambda)]^2 dt \right), \tag{2.35}$$

$$\mathcal{P}(\Gamma) \propto p(x(0),0) \exp\left(-\int_0^\tau \left\{ \frac{1}{4T\gamma} [\gamma\dot{x} - F(x,\lambda)]^2 + \frac{1}{2\gamma} \partial_x F(x,\lambda) \right\} dt \right). \tag{2.36}$$

Following the same idea as in the underdamped case, the heat and work can be defined as

$$q[\Gamma] \coloneqq \int_0^\tau F(x,\lambda) \circ \dot{x} dt, \tag{2.37}$$

$$w[\Gamma] \coloneqq \int_0^\tau \left[\partial_\lambda U(x,\lambda) \circ \dot{\lambda} + f(x,\lambda) \circ \dot{x} \right] dt. \tag{2.38}$$

Similarly, construct a backward process with the initial distribution $p(x,\tau)$ and the time-reversed control protocol $\lambda^\dagger(t) = \lambda(\tau - t)$, then the total entropy production can be expressed as

$$\langle \Delta s_{\mathrm{tot}}[\Gamma] \rangle = \int \mathcal{P}(\Gamma) \ln \frac{\mathcal{P}(\Gamma)}{\mathcal{P}_{\mathrm{B}}(\Gamma^\dagger)} \mathcal{D}\Gamma = D(\mathcal{P} || \mathcal{P}_{\mathrm{B}}) \geq 0, \tag{2.39}$$

where $\Gamma^\dagger = \{x(\tau - t)\}_{0 \leq t \leq \tau}$ is the time-reversed trajectory of Γ. The total entropy production $\langle \Delta s_{\mathrm{tot}} \rangle$ can also be calculated via the following integral formula:

$$\langle \Delta s_{\mathrm{tot}}[\Gamma] \rangle = \int_0^\tau \langle \dot{s}_{\mathrm{tot}}(t) \rangle dt, \tag{2.40}$$

where the entropy production rate $\langle \dot{s}_{\mathrm{tot}}(t) \rangle$ is given by

$$\langle \dot{s}_{\mathrm{tot}}(t) \rangle = \int \frac{\gamma}{T} \frac{j_x(x,t)^2}{p(x,t)} dx \geq 0. \tag{2.41}$$

When the control parameter λ is time independent, the system will reach a stationary state $p^{\mathrm{ss}}(x,\lambda)$ after a long time. In the absence of the external force (i.e., $f(x,\lambda) = 0$), this stationary state becomes the thermal equilibrium, given by

$$p^{\mathrm{eq}}(x,\lambda) = \exp\left\{ [\mathcal{F}(\lambda) - U(x,\lambda)]/T \right\}, \tag{2.42}$$

where $\mathcal{F}(\lambda)$ is the free energy defined as

$$\mathcal{F}(\lambda) \coloneqq -T \ln \left\{ \int \exp[-U(x,\lambda)/T] dx \right\}. \tag{2.43}$$

Herein we exclusively focus on the case that a genuine nonequilibrium steady state will finally be reached,

$$p^{\rm ss}(x,\lambda) = \exp[-\phi(x,\lambda)], \tag{2.44}$$

where $\phi(x,\lambda)$ is referred to as a nonequilibrium potential. This can be achieved in the presence of the nonconservative force $f(x,\lambda)$ or under coupling to multiple reservoirs at different temperatures. In this case, the systematic force $F(x,\lambda)$ can be expressed in terms of the steady-state probability current $j_x^{\rm ss}(x,\lambda)$ as

$$F(x,\lambda) = \gamma j_x^{\rm ss}(x,\lambda)/p^{\rm ss}(x,\lambda) - T\partial_x\phi(x,\lambda). \tag{2.45}$$

Using this relation, the heat can be decomposed into two contributions [65],

$$q[\Gamma] = q_{\rm hk}[\Gamma] + q_{\rm ex}[\Gamma], \tag{2.46}$$

where the housekeeping heat $q_{\rm hk}$ is the heat required to maintain the nonequilibrium steady state and the excess $q_{\rm ex}$ is the heat associated with changing the control parameter λ. Specifically, $q_{\rm hk}$ and $q_{\rm ex}$ explicitly read

$$q_{\rm hk}[\Gamma] = \int_0^\tau \gamma \frac{j_x^{\rm ss}(x,\lambda)}{p^{\rm ss}(x,\lambda)} \circ \dot{x}dt, \tag{2.47}$$

$$q_{\rm ex}[\Gamma] = -T\int_0^\tau \partial_x\phi(x,\lambda)\circ\dot{x}dt = T[-\Delta\phi + \int_0^\tau \partial_\lambda\phi(x,\lambda)\dot{\lambda}dt], \tag{2.48}$$

where $\Delta\phi \coloneqq \phi(x(\tau),\lambda_\tau) - \phi(x(0),\lambda_0)$. The total entropy production can be decomposed into two contributions as $\Delta s_{\rm tot} = \Delta s_{\rm a} + \Delta s_{\rm na}$, where $\Delta s_{\rm a} = q_{\rm hk}/T$ and $\Delta s_{\rm na} = \Delta s + q_{\rm ex}/T$ are the so-called adiabatic and nonadiabatic entropy productions, respectively, and their ensemble averages are nonnegative. By noticing that $j_x(x,t)/p(x,t) - j_x^{\rm ss}(x,\lambda)/p^{\rm ss}(x,\lambda) = -\gamma^{-1}T\partial_x(\ln[p(x,t)/p^{\rm ss}(x,\lambda)])$ and

$$\int p(x,t)\frac{j_x^{\rm ss}(x,\lambda)}{p^{\rm ss}(x,\lambda)}\left(\frac{j_x(x,t)}{p(x,t)} - \frac{j_x^{\rm ss}(x,\lambda)}{p^{\rm ss}(x,\lambda)}\right)dx = -\gamma^{-1}T\int j_x^{\rm ss}(x,\lambda)\partial_x\left(\frac{p(x,t)}{p^{\rm ss}(x,\lambda)}\right)dx = 0, \tag{2.49}$$

one can derive the explicit expressions of these entropy production rates as [66]

$$\langle \dot{s}_{\rm a}(t)\rangle = \int \frac{\gamma p(x,t)}{T}\left(\frac{j_x^{\rm ss}(x,\lambda)}{p^{\rm ss}(x,\lambda)}\right)^2 dx, \tag{2.50}$$

$$\langle \dot{s}_{\rm na}(t)\rangle = \int \frac{\gamma p(x,t)}{T}\left(\frac{j_x(x,t)}{p(x,t)} - \frac{j_x^{\rm ss}(x,\lambda)}{p^{\rm ss}(x,\lambda)}\right)^2 dx, \tag{2.51}$$

which immediately prove the positivity of both adiabatic and nonadiabatic entropy productions.

2.1.2 Markov jump processes

We consider a system with a finite set of states $\{n\}$. The system is in contact with a single reservoir at the inverse temperature $\beta = T^{-1}$. Due to interaction with the environment, the

stochastic transition from state m to state n occurs with a rate $R_{nm}(t)$. These transition rates may be controlled by an external protocol $\lambda(t)$. In the absence of the external control, the system always relaxes to a unique equilibrium state irrespective of the initial distribution, provided that the system is ergodic (i.e., any two states are connected via several transitions). Let $p_n(t)$ be the probability that the system is in state n at time t, then the dynamics of $p_n(t)$ obey the master equation,

$$\partial_t p_n(t) = \sum_{m(\neq n)} [R_{nm}(t)p_m(t) - R_{mn}(t)p_n(t)] = \sum_{m(\neq n)} j_{nm}(t), \tag{2.52}$$

where $j_{nm}(t) \coloneqq R_{nm}(t)p_m(t) - R_{mn}(t)p_n(t)$ is the probability current. For each state, the instantaneous total exit rate is defined as $-R_{nn}(t) = \sum_{m(\neq n)} R_{mn}(t)$. Let $\Gamma = \{n(t)\}_{0\leq t\leq \tau}$ be a stochastic trajectory that starts at state $n(0) = n_0$ and jumps at time t_j from n_j^- to n_j^+ for each $j = 1, \ldots, J$, and ends up at $n(\tau) = n_\tau$. Here, J denotes the number of jumps in the trajectory Γ. The conditional probability for a trajectory evolving without any jump is given by $p(n(s) = m, \forall s \in [0,t] | n(0) = m) = \exp\left(\int_0^t R_{mm}(s)ds\right)$. Thus, the probability of observing the trajectory Γ under the given dynamics can be calculated as

$$\mathcal{P}(\Gamma) = p_{n_0}(0) \exp\left(\int_{t_0}^{t_1} R_{n_0 n_0}(s)ds\right) \prod_{j=1}^{J} R_{n_j^+ n_j^-}(t_j) \exp\left(\int_{t_j}^{t_{j+1}} R_{n_j^+ n_j^+}(s)ds\right), \tag{2.53}$$

where $t_0 = 0$ and $t_{J+1} = \tau$.

Now, let us establish the notions of heat, work, and entropy production on the level of individual trajectories. Let $E_n(t)$ be the instantaneous energy of state n at time t. We assume that the transition rates satisfy the (global) detailed balance condition (DBC), $R_{mn}(t)e^{-\beta E_n(t)} = R_{nm}(t)e^{-\beta E_m(t)}$ for all $m \neq n$. This assumption implies that the probability distribution $p_n^{\mathrm{eq}}(t) \propto e^{-\beta E_n(t)}$ is the instantaneous equilibrium state of the system. Work along the trajectory Γ can be defined in analogy to Eq. (2.19) as

$$w[\Gamma] \coloneqq \int_0^\tau \partial_\lambda E_{n(t)}(t)\dot{\lambda}dt, \tag{2.54}$$

which is the change of energy due to the external control parameter. On the other hand, each jump from state n_j^- to state n_j^+ is associated with a change of energy, $E_{n_j^-}(t_j) - E_{n_j^+}(t_j)$, which can be regarded as the heat dissipated from the system to the reservoir. Therefore, heat along the trajectory can be defined as

$$q[\Gamma] \coloneqq \sum_{j=1}^{J} [E_{n_j^-}(t_j) - E_{n_j^+}(t_j)] = T \sum_{j=1}^{J} \ln \frac{R_{n_j^+ n_j^-}(t_j)}{R_{n_j^- n_j^+}(t_j)}. \tag{2.55}$$

The first law of thermodynamics on the single-trajectory level is then represented as

$$\Delta e = -q[\Gamma] + w[\Gamma] = E_{n_\tau}(\tau) - E_{n_0}(0). \tag{2.56}$$

Taking the ensemble average of each of these thermodynamic quantities gives explicit expressions,

$$\langle q[\Gamma]\rangle = \int_0^\tau \sum_{m\neq n} [E_m(t) - E_n(t)] R_{nm}(t) p_m(t) dt, \tag{2.57}$$

$$\langle w[\Gamma]\rangle = \int_0^\tau \sum_n \partial_t E_n(t) p_n(t) dt, \tag{2.58}$$

$$\langle \Delta e\rangle = \sum_n E_n(\tau) p_n(\tau) - \sum_n E_n(0) p_n(0). \tag{2.59}$$

Then, the relation $-\langle q[\Gamma]\rangle + \langle w[\Gamma]\rangle = \langle \Delta e\rangle$ can be verified as follows:

$$-\langle q[\Gamma]\rangle + \langle w[\Gamma]\rangle = \int_0^\tau \sum_{m\neq n} [E_n(t) - E_m(t)] R_{nm}(t) p_m(t) dt + \int_0^\tau \sum_n \partial_t E_n(t) p_n(t) dt \tag{2.60}$$

$$= \frac{1}{2}\int_0^\tau \sum_{m\neq n} [E_n(t) - E_m(t)] j_{nm}(t) dt + \int_0^\tau \sum_n \partial_t E_n(t) p_n(t) dt \tag{2.61}$$

$$= \int_0^\tau \sum_{m\neq n} E_n(t) j_{nm}(t) dt + \int_0^\tau \sum_n \partial_t E_n(t) p_n(t) dt \tag{2.62}$$

$$= \int_0^\tau \sum_n E_n(t) \sum_{m(\neq n)} j_{nm}(t) dt + \int_0^\tau \sum_n \partial_t E_n(t) p_n(t) dt \tag{2.63}$$

$$= \int_0^\tau \sum_n E_n(t) \partial_t p_n(t) dt + \int_0^\tau \sum_n \partial_t E_n(t) p_n(t) dt \tag{2.64}$$

$$= \int_0^\tau \partial_t \left(\sum_n E_n(t) p_n(t) \right) dt = \langle \Delta e\rangle. \tag{2.65}$$

Here, we have used the equality $j_{mn}(t) = -j_{nm}(t)$ in the third line and Eq. (2.52) in the fifth line.

The stochastic entropy on the single-trajectory level can be analogously defined. Using the Shannon entropy, the system entropy can be defined as $s(t) \coloneqq -\ln p_{n(t)}(t)$, and the corresponding entropy production is then obtained as $\Delta s = -\ln p_{n_\tau}(\tau) + \ln p_{n_0}(0)$. The entropy production of the reservoir can be calculated using the heat transferred from the system as

$$\Delta s_{\mathrm{m}} \coloneqq \beta q[\Gamma] = \sum_{j=1}^{J} \ln \frac{R_{n_j^+ n_j^-}(t_j)}{R_{n_j^- n_j^+}(t_j)}. \tag{2.66}$$

The total entropy production then reads

$$\Delta s_{\mathrm{tot}} = \Delta s + \Delta s_{\mathrm{m}}. \tag{2.67}$$

Note that this stochastic quantity can be negative; nevertheless, its ensemble average $\langle \Delta s_{\mathrm{tot}}\rangle$ is always nonnegative, which is regarded as the second law of thermodynamics. The inequality $\langle \Delta s_{\mathrm{tot}}\rangle \geq 0$ can be proved in several ways. Taking the continuous limit, the entropy production

rates of the system and the reservoir can be expressed as

$$\dot{s}(t) = -\frac{\partial_t p_{n(t)}(t)}{p_{n(t)}(t)} - \sum_j \delta(t-t_j) \ln \frac{p_{n_j^+}(t_j)}{p_{n_j^-}(t_j)}, \tag{2.68}$$

$$\dot{s}_{\rm m}(t) = \sum_j \delta(t-t_j) \ln \frac{R_{n_j^+ n_j^-}(t_j)}{R_{n_j^- n_j^+}(t_j)}. \tag{2.69}$$

Consequently, the total entropy production rate reads

$$\dot{s}_{\rm tot}(t) = -\frac{\partial_t p_{n(t)}(t)}{p_{n(t)}(t)} + \sum_j \delta(t-t_j) \ln \frac{R_{n_j^+ n_j^-}(t_j) p_{n_j^-}(t_j)}{R_{n_j^- n_j^+}(t_j) p_{n_j^+}(t_j)}, \tag{2.70}$$

and its ensemble average can be calculated as

$$\langle \dot{s}_{\rm tot}(t) \rangle = \frac{1}{2} \sum_{m \neq n} [R_{nm}(t) p_m(t) - R_{mn}(t) p_n(t)] \ln \frac{R_{nm}(t) p_m(t)}{R_{mn}(t) p_n(t)} \geq 0. \tag{2.71}$$

Note that $(x-y)\ln(x/y) \geq 0$ for all $x, y > 0$. The positivity of $\langle \Delta s_{\rm tot} \rangle$ is then affirmed from the relation $\langle \Delta s_{\rm tot} \rangle = \int_0^\tau \langle \dot{s}_{\rm tot}(t) \rangle dt$.

The total entropy production can also be expressed in terms of the path probabilities in the forward and backward processes, as in Eq. (2.27). Consider the backward process in which the initial distribution is $\{p_n(\tau)\}$ and the control parameter is time reversed, i.e., $R^\dagger_{mn}(t) := R_{mn}(\tau - t)$. For each trajectory Γ, define the time-reversed trajectory $\Gamma^\dagger = \{n^\dagger(t)\}_{0 \leq t \leq \tau}$ that starts at state $n^\dagger(0) = n_\tau$ and jumps at time $t_j^\dagger = \tau - t_{J-j+1}$ from n^+_{J-j+1} to n^-_{J-j+1} for each $j = 1, \ldots, J$, and ends up at $n^\dagger(\tau) = n_0$. The probability of observing the path $\Gamma^\dagger$ under the backward dynamics is

$$\mathcal{P}_{\rm B}(\Gamma^\dagger) = p_{n_\tau}(\tau) \exp\left(\int_{t_J}^{\tau} R_{n_\tau n_\tau}(s) ds \right) \prod_{j=1}^{J} R_{n^-_{J-j+1} n^+_{J-j+1}}(t_{J-j+1}) \exp\left(\int_{t_{J-j}}^{t_{J-j+1}} R_{n^-_{J-j+1} n^-_{J-j+1}}(s) ds \right). \tag{2.72}$$

Note that $n_1^- = n_0$, $n_J^+ = n_\tau$, and $n_j^+ = n_{j+1}^-$. From Eqs. (2.53) and (2.72), we have

$$\ln \frac{\mathcal{P}(\Gamma)}{\mathcal{P}_{\rm B}(\Gamma^\dagger)} = -\ln p_{n_\tau}(\tau) + \ln p_{n_0}(0) + \sum_{j=1}^{J} \ln \frac{R_{n_j^+ n_j^-}(t_j)}{R_{n_j^- n_j^+}(t_j)} = \Delta s + \Delta s_{\rm m} = \Delta s_{\rm tot}. \tag{2.73}$$

Consequently, the total entropy production can be written in terms of the KL divergence as

$$\langle \Delta s_{\rm tot} \rangle = \int \mathcal{P}(\Gamma) \ln \frac{\mathcal{P}(\Gamma)}{\mathcal{P}_{\rm B}(\Gamma^\dagger)} \mathcal{D}\Gamma = D(\mathcal{P} || \mathcal{P}_{\rm B}) \geq 0. \tag{2.74}$$

Equations (2.71) and (2.74) mathematically prove the second law of thermodynamics for the Markov jump processes.

Local detailed balance condition.— In the analysis above, we have assumed that the DBC is fulfilled. In the following, we discuss the case where the DBC is violated (e.g., when the system is simultaneously in contact with multiple reservoirs at different temperatures). For systems that do not fulfill the DBC, the probability currents $\{j_{mn}\}$ do not vanish even

when a steady state is reached. Since steady fluxes are maintained at steady state, basically one cannot assign internal energies to all states such that the DBC holds. In such scenario, the transition rates are assumed to satisfy the *local* DBC,

$$\ln \frac{R_{mn}(t)}{R_{nm}(t)} = \Delta S_{mn}, \ \forall m \neq n. \tag{2.75}$$

The local DBC implies that each jump from state n to state m is associated with a change ΔS_{mn} in the entropy of the reservoirs. With this assumption, the change in the entropy of the reservoirs along the trajectory Γ can be written as in Eq. (2.66), and accordingly the form of the total entropy production rate remains unchanged as in Eq. (2.70).

Let $p_n^{\rm ss}(\lambda_t)$ denote the stationary distribution of the system when the control parameter is fixed to λ_t. Similar to the case of overdamped Langevin dynamics, the entropy production of the reservoir can be split into the housekeeping and excess contributions as

$$\Delta s_{\rm m} = \Delta s_{\rm hk} + \Delta s_{\rm ex}, \tag{2.76}$$

where $\Delta s_{\rm hk}$ and $\Delta s_{\rm ex}$ characterize, respectively, the entropy changes associated with maintaining the corresponding steady state and with the time-dependent driving, and given by

$$\Delta s_{\rm hk} \coloneqq \sum_{j=1}^{J} \ln \frac{p_{n_j^-}^{\rm ss}(\lambda_{t_j}) R_{n_j^+ n_j^-}(t_j)}{p_{n_j^+}^{\rm ss}(\lambda_{t_j}) R_{n_j^- n_j^+}(t_j)}, \tag{2.77}$$

$$\Delta s_{\rm ex} \coloneqq -\sum_{j=1}^{J} \ln \frac{p_{n_j^-}^{\rm ss}(\lambda_{t_j})}{p_{n_j^+}^{\rm ss}(\lambda_{t_j})}. \tag{2.78}$$

The total entropy production $\Delta s_{\rm tot}$ can be decomposed into the adiabatic and nonadiabatic contributions as [67]

$$\Delta s_{\rm tot} = \Delta s_{\rm a} + \Delta s_{\rm na}, \tag{2.79}$$

where $\Delta s_{\rm a} = \Delta s_{\rm hk}$ and $\Delta s_{\rm na} = \Delta s + \Delta s_{\rm ex}$. It is worth noting that the averages of these contributions are both nonnegative, $\Delta s_{\rm a} \geq 0$ and $\Delta s_{\rm na} \geq 0$. When the system satisfies the DBC, $\Delta s_{\rm a} = 0$. On the other hand, if the time scale of the relaxation is smaller than that of the control parameter, it is easy to check that the nonadiabatic term vanishes on average, $\langle \Delta s_{\rm na} \rangle = 0$.

2.2 Fluctuation theorems

Historically, a fluctuation theorem was first numerically discovered in the simulation of sheared fluids [15, 68]. Shortly thereafter, related fluctuation theorems were proved for deterministic dynamics [16], stochastic dynamics [18, 69–72], and Hamiltonian systems [73, 74]. For detailed reviews of fluctuation theorems, see Refs. [19, 75–77]. In what follows, we present several fluctuation theorems and their derivations. The key ingredient underlying the derivations of fluctuation theorems is time reversal (i.e., they are basically dependent on the construction of the time-reversed process).

Integral fluctuation theorems.—As shown in the previous section, the stochastic entropy production can be expressed in terms of the path probabilities in the forward and backward processes, provided that the backward process is properly constructed with the time-reversed control protocol. Specifically, the stochastic entropy production reads

$$\Delta s_{\rm tot}[\Gamma] = \ln \frac{\mathcal{P}(\Gamma)}{\mathcal{P}_{\rm B}(\Gamma^\dagger)}, \tag{2.80}$$

which can be rewritten as $e^{-\Delta s_{\rm tot}[\Gamma]}\mathcal{P}(\Gamma) = \mathcal{P}_{\rm B}(\Gamma^\dagger)$. Taking the integral of both sides of this equality over all possible trajectories Γ, we obtain the rigorous relation

$$\langle e^{-\Delta s_{\rm tot}} \rangle = 1. \tag{2.81}$$

This equality is known as the integral fluctuation theorem (IFT) for the total entropy production. If the distribution $p(\Delta s_{\rm tot})$ is Gaussian, then the IFT implies

$$\langle\langle \Delta s_{\rm tot} \rangle\rangle = 2\langle \Delta s_{\rm tot} \rangle, \tag{2.82}$$

which relates the mean and variance of $\Delta s_{\rm tot}$. Applying Jensen's inequality to the convex function e^{-x}, the second law of thermodynamics can be immediately obtained

$$1 = \langle e^{-\Delta s_{\rm tot}} \rangle \geq e^{-\langle \Delta s_{\rm tot} \rangle} \Rightarrow \langle \Delta s_{\rm tot} \rangle \geq 0. \tag{2.83}$$

There are two important implications that can be derived from the IFT. First, the IFT indicates that the probability of negative entropy production is nonzero except the degenerate case [i.e., the probability distribution function of the total entropy production in the forward process is a delta function, $p(\Delta s_{\rm tot}) = \delta(\Delta s_{\rm tot})$]. The second law of *classical* thermodynamics (which deals with macroscopic systems whose fluctuations are negligible) states that the entropy production is always nonnegative; however, this is not the case for small systems, in which fluctuations are significant and a trajectory accompanying by a negative entropy production can be observed. On the other hand, it may take an infinite amount of time to observe such trajectories at the macroscopic limit. Second, an upper bound on the probability of negative entropy production can be derived as a result. Particularly, for an arbitrary number $\theta > 0$, we can prove that

$$p(\Delta s_{\rm tot} < -\theta) \leq \int_{-\infty}^{-\theta} p(\Delta s_{\rm tot}) e^{-\theta - \Delta s_{\rm tot}} d\Delta s_{\rm tot} \leq e^{-\theta}. \tag{2.84}$$

This inequality implies that the probability that entropy production is less than $-\theta$ vanishes at least exponentially with θ.

Conjugate dynamics and unification of IFTs.—In the derivation of the IFT for the total entropy production, we have employed the original dynamics under time reversal in the backward process. However, more general IFTs can be obtained as well by constructing a generic backward process using a conjugate dynamics. For simplicity, hereafter we consider only the case of overdamped Langevin systems. The same results can be analogously derived for Markov jump processes. For a trajectory $\Gamma^\dagger = \{x^\dagger(t)\}$, a conjugate dynamics are governed

by the overdamped Langevin equation,

$$\gamma^\dagger \dot{x}^\dagger = F^\dagger(x^\dagger, \lambda^\dagger) + \xi^\dagger, \tag{2.85}$$

where the noise satisfies $\langle \xi^\dagger \rangle = 0$ and $\langle \xi^\dagger(t)\xi^\dagger(t')\rangle = 2T^\dagger\gamma^\dagger\delta(t-t')$. In what follows, we consider only the case that the friction coefficient and the temperature are unchanged, $\gamma^\dagger = \gamma$ and $T^\dagger = T$. The conjugate dynamics can be defined from the original one via a one-to-one mapping as follows:

$$\{x(t), \lambda(t), F\} \mapsto \{x^\dagger(t), \lambda^\dagger(t), F^\dagger\}. \tag{2.86}$$

First, one can consider the backward process as a stochastic realization of the original dynamics under time reversal, i.e.,

$$x^\dagger(t) = x(\tau - t),\ \ \lambda^\dagger(t) = \lambda(\tau - t),\ \ F^\dagger(x, \lambda) = F(x, \lambda). \tag{2.87}$$

By assigning a general distribution function $p_{\rm f}(x)$ [instead of $p(x,\tau)$] to the initial distribution in the backward process, the following relation can be easily derived [7],

$$\left\langle e^{-\Delta s_{\rm m}} p_{\rm f}(x(\tau))/p(x(0),0) \right\rangle = 1. \tag{2.88}$$

In the absence of the external force, considering the case that the system starts from an equilibrium distribution $p(x,0) = p^{\rm eq}(x,\lambda_0) = \exp\{[\mathcal{F}(\lambda_0) - U(x,\lambda_0)]/T\}$ and setting $p_{\rm f}(x) = p^{\rm eq}(x,\lambda_\tau) = \exp\{[\mathcal{F}(\lambda_\tau) - U(x,\lambda_\tau)]/T\}$ in the backward process, we obtain

$$\langle e^{-\Delta s_{\rm m} + (\Delta\mathcal{F} - \Delta e)/T} \rangle = 1 \Rightarrow \langle e^{-w/T} \rangle = e^{-\Delta\mathcal{F}/T}, \tag{2.89}$$

where $\Delta\mathcal{F} = \mathcal{F}(\lambda_\tau) - \mathcal{F}(\lambda_0)$ denotes the free energy difference between two equilibrium states. The relation in Eq. (2.89) is known as the Jarzynski equality [73], which was originally derived for a Hamiltonian dynamics. The Jarzynski equality indicates that the free energy difference, which is a genuine equilibrium quantity, can be estimated from nonequilibrium measurements of work.

Second, one can employ a dual dynamics without time reversal for the backward process [78],

$$x^\dagger(t) = x(t),\ \ \lambda^\dagger(t) = \lambda(t),\ \ F^\dagger(x,\lambda) = F(x,\lambda) - 2\gamma \frac{j_x^{\rm ss}(x,\lambda)}{p^{\rm ss}(x,\lambda)}. \tag{2.90}$$

Note that this dual dynamics keep the stationary distribution unchanged and reverse the sign of the stationary current, i.e., $p^{\rm ss}(x,\lambda)^\dagger = p^{\rm ss}(x,\lambda)$ and $j_x^{\rm ss}(x,\lambda)^\dagger = -j_x^{\rm ss}(x,\lambda)$. Choosing $p_{\rm f}(x) = p(x,0)$, we can calculate the log-ratio of path probabilities as

$$\ln \frac{\mathcal{P}(\Gamma)}{\mathcal{P}_{\rm B}(\Gamma^\dagger)} = \int_0^\tau \left[\frac{j_x^{\rm ss}(x,\lambda)}{T p^{\rm ss}(x,\lambda)} \circ (\gamma\dot{x} - F(x,\lambda)) + \frac{\gamma}{T}\left(\frac{j_x^{\rm ss}(x,\lambda)}{p^{\rm ss}(x,\lambda)}\right)^2 - \partial_x \left(\frac{j_x^{\rm ss}(x,\lambda)}{p^{\rm ss}(x,\lambda)}\right)\right] dt \tag{2.91}$$

$$= q_{\rm hk}[\Gamma]/T. \tag{2.92}$$

To obtain the last line, we have used the relation $F(x,\lambda) = \left[\gamma j_x^{\rm ss}(x,\lambda) + T\partial_x p^{\rm ss}(x,\lambda)\right]/p^{\rm ss}(x,\lambda)$ and the stationary property $\partial_x j_x^{\rm ss}(x,\lambda) = 0$. Consequently, the IFT for the house keeping heat

can be obtained [79]

$$\langle e^{-q_{\rm hk}/T}\rangle = 1. \tag{2.93}$$

This can also be regarded as the IFT for the adiabatic entropy production, $\langle e^{-\Delta s_{\rm a}}\rangle = 1$.

Last, we consider the following dual-reversed dynamics:

$$x^\dagger(t) = x(\tau - t),\ \ \lambda^\dagger(t) = \lambda(\tau - t),\ \ F^\dagger(x,\lambda) = F(x,\lambda) - 2\gamma\frac{j_x^{\rm ss}(x,\lambda)}{p^{\rm ss}(x,\lambda)}. \tag{2.94}$$

Assume that the system is initially in a nonequilibrium steady state, $p(x,0) = p^{\rm ss}(x,\lambda_0)$, then choosing $p_{\rm f}(x) = p^{\rm ss}(x,\lambda_\tau)$ yields the following equality:

$$\ln\frac{\mathcal{P}(\Gamma)}{\mathcal{P}_{\rm B}(\Gamma^\dagger)} = \Delta\phi + q_{\rm ex}[\Gamma]/T. \tag{2.95}$$

Thus, the IFT for the excess heat can also be analogously obtained,

$$\langle e^{-(\Delta\phi + q_{\rm ex}/T)}\rangle = 1. \tag{2.96}$$

This equality is also known as the Hatano–Sasa relation [65]. When the system starts from an arbitrary distribution $p(x,0)$, then choosing $p_{\rm f}(x) = p(x,\tau)$ results in the following IFT:

$$\langle e^{-(\Delta s + q_{\rm ex}/T)}\rangle = 1. \tag{2.97}$$

Since $\Delta s_{\rm na} = \Delta s + q_{\rm ex}/T$, Eq. (2.97) indicates that the nonadiabatic entropy production follows the IFT, $\langle e^{-\Delta s_{\rm na}}\rangle = 1$.

Detailed fluctuation theorems.—A stronger class of fluctuation theorems, called detailed fluctuation theorems (DFTs), can be obtained under some special conditions. Let us turn to the definition of $p(\Delta s_{\rm tot})$ and perform the following calculations:

$$\begin{aligned}
p(\Delta s_{\rm tot}) &= \int \delta\left(\Delta s_{\rm tot} - \ln\frac{\mathcal{P}(\Gamma)}{\mathcal{P}_{\rm B}(\Gamma^\dagger)}\right)\mathcal{P}(\Gamma)\mathcal{D}\Gamma && \text{(2.98a)}\\
&= \int e^{\Delta s_{\rm tot}}\delta\left(\Delta s_{\rm tot} - \ln\frac{\mathcal{P}(\Gamma)}{\mathcal{P}_{\rm B}(\Gamma^\dagger)}\right)\mathcal{P}_{\rm B}(\Gamma^\dagger)\mathcal{D}\Gamma && \text{(2.98b)}\\
&= \int e^{\Delta s_{\rm tot}}\delta\left(\Delta s_{\rm tot} + \ln\frac{\mathcal{P}_{\rm B}(\Gamma^\dagger)}{\mathcal{P}(\Gamma)}\right)\mathcal{P}_{\rm B}(\Gamma^\dagger)\mathcal{D}\Gamma && \text{(2.98c)}\\
&= \int e^{\Delta s_{\rm tot}}\delta\left(-\Delta s_{\rm tot} - \ln\frac{\mathcal{P}_{\rm B}(\Gamma^\dagger)}{\mathcal{P}(\Gamma)}\right)\mathcal{P}_{\rm B}(\Gamma^\dagger)\mathcal{D}\Gamma^\dagger && \text{(2.98d)}\\
&= e^{\Delta s_{\rm tot}}p_{\rm B}(-\Delta s_{\rm tot}). && \text{(2.98e)}
\end{aligned}$$

Here, $p_{\rm B}(\cdot)$ denotes the probability distribution function of quantity $\Delta s_{\rm tot}^\dagger = \ln[\mathcal{P}_{\rm B}(\Gamma^\dagger)/\mathcal{P}(\Gamma)]$ in the backward process. When the forward and backward processes are identical, i.e., $\mathcal{P} \equiv \mathcal{P}_{\rm B}$, the DFT for the total entropy production can be obtained,

$$\frac{p(\Delta s_{\rm tot})}{p(-\Delta s_{\rm tot})} = e^{\Delta s_{\rm tot}}. \tag{2.99}$$

This can be achieved with time-reversal symmetry systems that satisfy two conditions: (i) the

initial and final distributions are the same, $p(x,0) = p(x,\tau)$, and (ii) the control parameter is time symmetric, $\lambda(t) = \lambda(\tau - t)$. These conditions are fulfilled, for example, with steady-state systems under a fixed control parameter or with periodic systems driven by a time-symmetric control protocol.

Now, we consider the setup in which the Jarzynski relation was obtained in Eq. (2.89). Let $p(w)$ and $p_{\rm B}(w)$ be the probability distributions of work exerted on the system in the forward and backward processes, respectively. Then, following the same steps as in Eq. (2.98), we arrive at the following relation:

$$\frac{p(w)}{p_{\rm B}(-w)} = e^{(w-\Delta\mathcal{F})/T}\,, \tag{2.100}$$

which is also known as the Crooks fluctuation theorem [17]. When the initial distributions in the forward and backward processes are the same equilibrium distributions and the control protocol is time symmetric, the free energy difference vanishes, $\Delta\mathcal{F} = 0$, and $\mathcal{P} \equiv \mathcal{P}_{\rm B}$. Consequently, the DFT for work can be immediately derived,

$$\frac{p(w)}{p(-w)} = e^{w/T}\,. \tag{2.101}$$

Chapter 3

Quantum thermodynamics

This chapter briefly introduces quantum thermodynamics, which establishes the concepts of heat, work, and entropy production in the quantum regime. The notions of entropy and thermal state and the description of quantum dynamics of closed and open systems are introduced. The first and second laws of thermodynamics are described for generic open quantum systems, especially for quantum dynamics governed by the Lindblad master equation. The content of this chapter is partially based on the explanation in Ref. [80].

3.1 Entropy and the thermal state

Given a density matrix ρ, von Neumann introduced the notion of entropy of ρ, called the von Neumann entropy, defined by

$$S(\rho) \coloneqq -\mathrm{tr}\{\rho \ln \rho\} = -\sum_n p_n \ln p_n, \tag{3.1}$$

where $\rho = \sum_n p_n |\psi_n\rangle\langle\psi_n|$ is the spectral decomposition of ρ, $\{p_n\}$ are nonnegative eigenvalues, and $\{|\psi_n\rangle\}$ are the corresponding eigenvectors satisfying $\sum_n |\psi_n\rangle\langle\psi_n| = I$. It can be observed that the von Neumann entropy is equal to the Shannon entropy of the distribution given by the eigenvalues of the density matrix. Let us discuss some important properties of the von Neumann entropy. First, this entropy is always nonnegative and well-defined. The zero entropy is attained when ρ is a pure state. From Eq. (3.1), one can easily prove that the von Neumann entropy is bounded from above as $S(\rho) \leq \ln \dim \mathcal{H}$, where $\mathcal{H}$ is the Hilbert space of the density matrices. Notably, if a density matrix $\rho_{AB} \in \mathcal{S}(\mathcal{H}_A \otimes \mathcal{H}_B)$ is a pure state, then $S(\rho_A) = S(\rho_B)$, where $\rho_A = \mathrm{tr}_B\{\rho_{AB}\}$ and $\rho_B = \mathrm{tr}_A\{\rho_{AB}\}$. Moreover, the von Neumann entropy is subadditive, $S(\rho_A \otimes \rho_B) = S(\rho_A) + S(\rho_B)$, and is invariant under unitary transforms, $S(\rho) = S(U\rho U^\dagger)$. In the context of thermodynamics, the von Neumann entropy is commonly used to characterize the entropy of quantum systems.

An important quantity which measures the difference between two density matrices is the quantum relative entropy, defined by

$$S(\rho_1 || \rho_2) \coloneqq \mathrm{tr}\{\rho_1 \ln \rho_1 - \rho_1 \ln \rho_2\}. \tag{3.2}$$

This relative entropy is always nonnegative but not a measure of "distance" because $S(\rho_1||\rho_2) \neq S(\rho_2||\rho_1)$. Analogous to the von Neumann entropy, the relative entropy is invariant under unitary transforms, $S(\rho_1||\rho_2) = S(U\rho_1U^\dagger||U\rho_2U^\dagger)$, and is subadditive, $S(\rho_A\otimes\rho_B||\sigma_A\otimes\sigma_B) = S(\rho_A||\sigma_A) + S(\rho_B||\sigma_B)$. Moreover, it is a jointly convex function, i.e., $\theta S(\rho_1||\sigma_1) + (1-\theta)S(\rho_2||\sigma_2) \geq S(\theta\rho_1 + (1-\theta)\rho_2||\theta\sigma_1 + (1-\theta)\sigma_2)$ for all $\theta \in [0,1]$. When ρ_1 and ρ_2 commute, $[\rho_1,\rho_2] = 0$, the quantum relative entropy reduces to the KL divergence between two distributions given by the eigenvalues of the density matrices,

$$S(\rho_1||\rho_2) = \sum_n p_n \ln\frac{p_n}{q_n}, \tag{3.3}$$

where $\rho_1 = \sum_n p_n|\psi_n\rangle\langle\psi_n|$ and $\rho_2 = \sum_n q_n|\psi_n\rangle\langle\psi_n|$. The most intriguing property of the relative entropy is that it is contractive under a physical map. That is

$$S(\rho_1||\rho_2) \geq S(\Lambda[\rho_1]||\Lambda[\rho_2]) \tag{3.4}$$

for arbitrary density matrices ρ_1,ρ_2 and completely positive trace-preserving map Λ.

In the canonical ensemble, the thermal state (Gibbs state) is given by

$$\rho^{\text{eq}} = e^{-\beta H}/Z,\ Z = \text{tr}\left\{e^{-\beta H}\right\}, \tag{3.5}$$

where H denotes the Hamiltonian of the system, $\beta = 1/T$ is the inverse temperature, and Z is the partition function. If the system is in contact with a thermal reservoir, then the thermal state is expected to well describe the system when it reaches equilibrium. The thermal state is also closely related to the von Neumann entropy via a principle of maximal entropy. That is the thermal state maximizes the von Neumann entropy under the condition of a fixed mean energy $\langle H\rangle$. For any state ρ that has the same mean energy as the thermal state (i.e., $\text{tr}\{\rho H\} = \text{tr}\{\rho^{\text{eq}}H\}$), we have

$$S(\rho) = -\text{tr}\{\rho\ln\rho\} = -\text{tr}\{\rho\ln\rho^{\text{eq}}\} - S(\rho||\rho^{\text{eq}}) \tag{3.6}$$

$$\leq -\text{tr}\{\rho\ln\rho^{\text{eq}}\} = -\text{tr}\{\rho^{\text{eq}}\ln\rho^{\text{eq}}\} = S(\rho^{\text{eq}}). \tag{3.7}$$

Here, we have used the fact $S(\rho||\rho^{\text{eq}}) \geq 0$. An equivalent statement with the principle of maximal entropy is that the thermal state minimizes the mean energy for a fixed von Neumann entropy.

3.2 Closed quantum systems

We consider a quantum system that does not exchange any heat or matter with the surroundings. If the system is initially in some pure state $|\psi(0)\rangle$, then the time evolution of the pure state $|\psi(t)\rangle$ is described by the Schrödinger equation,

$$\partial_t|\psi(t)\rangle = -\frac{i}{\hbar}H(t)|\psi(t)\rangle, \tag{3.8}$$

where $H(t)$ is the time-dependent Hamiltonian of the system, which can be driven by an external controller. Throughout this thesis, the Planck constant is set to unity, $\hbar = 1$, for simplicity. The solution of $|\psi(t)\rangle$ can be represented in terms of the unitary propagator $U(t)$ as

$$|\psi(t)\rangle = U(t)|\psi(0)\rangle, \tag{3.9}$$

where $U(t) = \mathbb{T}\exp\left\{-i\int_0^t H(s)ds\right\}$. The time ordering operator $\mathbb{T}$ means that in the power series expansion the Hamiltonians under the multiple integrals must be ordered from the left to the right in decreasing order of their time-arguments. When the Hamiltonian is time independent, the unitary propagator reads $U(t) = \exp(-iHt)$. Next, we consider the case that the system starts from a mixed state characterized by the density matrix

$$\rho(0) = \sum_n p_n|\psi_n(0)\rangle\langle\psi_n(0)|, \tag{3.10}$$

where $\{p_n\}_n$ are positive weights satisfying $\sum_n p_n = 1$ and $\{|\psi_n(0)\rangle\}_n$ are normalized pure states. From the linearity of the Schrödinger equation, the state of the system at time t can be explicitly calculated as

$$\rho(t) = \sum_n p_n U(t)|\psi_n(0)\rangle\langle\psi_n(0)|U^\dagger(t) = U(t)\rho(0)U^\dagger(t). \tag{3.11}$$

Differentiating both sides of Eq. (3.11) with respect to time t, a motion equation for the density matrix can be obtained,

$$\partial_t\rho(t) = -i[H(t), \rho(t)], \tag{3.12}$$

where $[X, Y] \coloneqq XY - YX$ denotes the commutator. Equation (3.12) is referred to as the von Neumann equation.

Now, let us establish the first law of thermodynamics in closed systems. The internal energy of the system at time t can be defined as

$$E(t) \coloneqq \mathrm{tr}\left\{H(t)\rho(t)\right\}. \tag{3.13}$$

Then the change of the internal energy of the system during time period τ is given by

$$\Delta E \coloneqq E(\tau) - E(0) = \int_0^\tau \left[\mathrm{tr}\left\{\partial_t H(t)\rho(t)\right\} + \mathrm{tr}\left\{H(t)\partial_t\rho(t)\right\}\right] dt. \tag{3.14}$$

The first term in the right-hand side corresponds to the energy change caused by the action of the external agent on the Hamiltonian and thus can be identified as the work exerted on the system,

$$\Delta W \coloneqq \int_0^\tau \mathrm{tr}\left\{\partial_t H(t)\rho(t)\right\} dt. \tag{3.15}$$

Consequently, the second term can be determined as the heat transferred from the surroundings into system,

$$-\Delta Q \coloneqq \int_0^\tau \mathrm{tr}\left\{H(t)\partial_t\rho(t)\right\} dt. \tag{3.16}$$

Since $\partial_t \rho(t) = -i[H(t), \rho(t)]$, one can easily derive that $\Delta Q = 0$. This is reasonable because the closed system does not exchange heat with the surroundings. Equation (3.14) can be rewritten as $\Delta E = \Delta W - \Delta Q = \Delta W$, which is regarded as the first law of thermodynamics. From this relation, one can see that the internal energy in closed systems is changed only due to the work done on the system.

Analogous to the Shannon entropy in the classical case, it is common to employ the von Neumman entropy to characterize the entropy of quantum systems. One can check that the von Neumann entropy $S(\rho)$ does not change under unitary dynamics,

$$S(\rho(t)) = -\mathrm{tr}\left\{U(t)\rho(0)U^\dagger(t)\ln[U(t)\rho(0)U^\dagger(t)]\right\} = -\mathrm{tr}\left\{\rho(0)\ln\rho(0)\right\} = S(\rho(0)). \tag{3.17}$$

This means that the entropy production in the unitary dynamics is always zero, leading to an important physical implication. That is, to reduce the system entropy we have to let the system interact with another system (e.g., a heat bath).

The analysis above is based on the formulation in the Schrödinger picture. In the next sections, we introduce other useful pictures and discuss their relevance.

3.2.1 Heisenberg picture

In the Schrödinger picture, the density matrix $\rho(t)$ evolves in time according to the von Neumann equation. In contrast, the Heisenberg picture is an equivalent description which transfers the time dependence from the density matrix to the operators on the same Hilbert space. That is the density matrix does not change with time, whereas the operators carry time dependence. Assume that at initial time $t = 0$, the quantum states in both pictures coincide, $\rho_H(0) = \rho(0)$, then the operators in these pictures are related through the following transformation:

$$A_H(t) = U^\dagger(t)A(t)U(t), \tag{3.18}$$

where the operator $A(t)$ in the Schrödinger picture can be time-dependent. Hereafter, the subscript H is referred to as the Heisenberg picture. It is easy to see that the expectation value of the physical observable $A(t)$ is identical in both pictures,

$$\langle A_H(t)\rangle = \mathrm{tr}\left\{A_H(t)\rho_H(0)\right\} = \mathrm{tr}\left\{A(t)U(t)\rho(0)U^\dagger(t)\right\} = \mathrm{tr}\left\{A(t)\rho(t)\right\} = \langle A(t)\rangle. \tag{3.19}$$

Differentiating both sides of Eq. (3.18) with respect to time t, we obtain the Heisenberg equation of motion of $A_H(t)$ as

$$\frac{d}{dt}A_H(t) = i[H_H(t), A_H(t)] + (\partial_t A(t))_H\,, \tag{3.20}$$

where $H_H(t) = U^\dagger(t)H(t)U(t)$ is the system Hamiltonian in the Heisenberg picture. When both the Schrödinger operator $A(t)$ and the Hamiltonian $H(t)$ are time-independent, $H_H(t) = H$ and Eq. (3.20) becomes

$$\frac{d}{dt}A_H(t) = i[H, A_H(t)]. \tag{3.21}$$

3.2.2 Interaction picture

Interaction picture is a more general representation which recovers both the Schrödinger picture and the Heisenberg picture in some limits. Unlike in the aforementioned pictures (in which either the density matrices or the operators carry time dependence), both of the density matrices and the operators in the interaction picture evolve in time. As will be shown in the next section, the interaction picture is useful to derive a master equation describing motion of the density matrix in open quantum systems.

We start with decomposing the Hamiltonian of the system as the sum of two parts,

$$H(t) = H_0 + H_1(t). \tag{3.22}$$

The explicit forms of these terms depend upon the particular problem under consideration. In general, H_0 can be the sum of the Hamiltonians of subsystems and $H_1(t)$ is thus the Hamiltonian induced by interaction between subsystems. Here we assume that H_0 is time-independent. Subsequently, the unitary time evolution operators $U_0(t)$ and $U_I(t)$ are introduced,

$$U_0(t) \coloneqq \exp(-iH_0t), \tag{3.23}$$

$$U_I(t) \coloneqq U_0^\dagger(t)U(t). \tag{3.24}$$

Using these operators, the density matrix and the operator in the interaction picture can be defined in the following:

$$\rho_I(t) \coloneqq U_I(t)\rho(0)U_I^\dagger(t), \tag{3.25}$$

$$A_I(t) \coloneqq U_0^\dagger(t)A(t)U_0(t). \tag{3.26}$$

One can observe that the expectation of the observable $A(t)$ remains unchanged,

$$\langle A(t)\rangle = \mathrm{tr}\left\{A(t)U_0(t)U_I(t)\rho(0)U_I^\dagger(t)U_0^\dagger(t)\right\} = \mathrm{tr}\left\{A_I(t)\rho_I(t)\right\}. \tag{3.27}$$

The time evolution of the density matrix can be described by the von Neumann equation,

$$\frac{d}{dt}\rho_I(t) = -i[H_I(t), \rho_I(t)], \tag{3.28}$$

where $H_I(t) = U_0^\dagger(t)H_1(t)U_0(t)$ denotes the interaction Hamiltonian in the interaction picture. Equation (3.28) is consistent with the von Neumann equation in the interaction picture. It can also be rewritten in the integral form as

$$\rho_I(t) = \rho_I(0) - i\int_0^t [H_I(s), \rho_I(s)]ds. \tag{3.29}$$

3.3 Open quantum systems

We consider an open system S that is coupled to another quantum system R, which is considered as a reservoir[1] throughout this thesis. Unlike in the case of closed systems, the open system S exchanges heat with the reservoir due to interaction between them. The composite system $S+R$ is assumed to be a closed system and follows the unitary dynamics. However, the state of the system S is affected not only by the internal dynamics but also by interaction with the reservoir, and thus no longer obeys the unitary dynamics. In what follows, the system S is referred to as the reduced system and its state is called the reduced state or the reduced density matrix.

Let $\mathcal{H}_S$ and $\mathcal{H}_R$, respectively, denote the Hilbert spaces of the system and the reservoir, then the Hilbert space of the composite system is the tensor product space $\mathcal{H} = \mathcal{H}_S \otimes \mathcal{H}_R$. The total Hamiltonian of the composite system is given by

$$H(t) = H_S(t) + V(t) + H_R, \tag{3.30}$$

where $H_S(t)$ is the time-dependent Hamiltonian of the system S, H_R is the free Hamiltonian of the reservoir, and $V(t)$ is the Hamiltonian characterizing the interaction between the system and the reservoir. The density matrix of the composite system evolves according to the unitary dynamics,

$$\partial_t \rho(t) = -i[H(t), \rho(t)], \tag{3.31}$$

and can be expressed in terms of the unitary propagator as

$$\rho(t) = U(t)\rho(0)U^\dagger(t). \tag{3.32}$$

The reduced density matrix $\rho_S(t)$ can be obtained by taking the partial trace over the reservoir,

$$\rho_S(t) = \mathrm{tr}_R\{\rho(t)\} = \mathrm{tr}_R\left\{U(t)\rho(0)U^\dagger(t)\right\}. \tag{3.33}$$

We assume that the initial state of the composite system is an uncorrelated product state $\rho(0) = \rho_S(0) \otimes \rho_R$, where ρ_R is some reference state of the reservoir, for example, the thermal equilibrium state. Given a fixed time t, then the time evolution of the system state can be regarded as a dynamical map $\Lambda_t : \mathcal{H}_S \to \mathcal{H}_S$, which transforms the initial state $\rho_S(0)$ to the final state $\rho_S(t)$. The relation between this dynamical map and the unitary evolution of the composite system is described in Fig. 3.1. The map Λ_t can be completely characterized by operators pertaining to the Hilbert space $\mathcal{H}_S$. Using the spectral decomposition, the reference state of the reservoir can be represented as

$$\rho_R = \sum_\nu \lambda_\nu |\varphi_\nu\rangle\langle\varphi_\nu|, \tag{3.34}$$

where $\{\lambda_\nu\}_\nu$ are nonnegative eigenvalues satisfying $\sum_\nu \lambda_\nu = 1$ and the eigenvectors $\{|\varphi_\nu\rangle\}_\nu$ form an orthonormal basis in the space $\mathcal{H}_R$. Substituting this representation of the reference

[1] The reservoir considered here is an environment that has an infinite number of degrees of freedom such that the frequencies of the reservoir modes form a continuum.

$$\begin{array}{ccc} \rho(0) = \rho_S(0) \otimes \rho_R & \xrightarrow{\text{unitary evolution}} & \rho(t) = U(t)\rho(0)U^\dagger(t) \\ \Big\downarrow \mathrm{tr}_R & & \Big\downarrow \mathrm{tr}_R \\ \rho_S(0) & \xrightarrow[\text{dynamical map}]{} & \rho_S(t) = \Lambda_t[\rho_S(0)] \end{array}$$

Figure 3.1: Commutative diagram showing the action of a dynamical map Λ.

state to Eq. (3.33), one can perform calculations of the partial trace and obtain

$$\rho_S(t) = \mathrm{tr}_R \left\{ U(t)\rho_S(0) \otimes \sum_\nu \lambda_\nu |\varphi_\nu\rangle\langle\varphi_\nu| U^\dagger(t) \right\} \tag{3.35}$$

$$= \sum_\mu \langle\varphi_\mu| U(t)\rho_S(0) \otimes \sum_\nu \lambda_\nu |\varphi_\nu\rangle\langle\varphi_\nu| U^\dagger(t) |\varphi_\mu\rangle \tag{3.36}$$

$$= \sum_{\mu,\nu} \sqrt{\lambda_\nu}\langle\varphi_\mu| U(t) |\varphi_\nu\rangle \rho_S(0) \sqrt{\lambda_\nu}\langle\varphi_\nu| U^\dagger(t) |\varphi_\mu\rangle \tag{3.37}$$

$$= \sum_{\mu,\nu} K_{\mu\nu}(t)\rho_S(0)K^\dagger_{\mu\nu}(t) = \Lambda_t[\rho_S(0)], \tag{3.38}$$

where operators $\{K_{\mu\nu}(t)\}$ are defined as $K_{\mu\nu}(t) \coloneqq \sqrt{\lambda_\nu}\langle\varphi_\mu| U(t) |\varphi_\nu\rangle$. These operators are called Kraus operators and Eq. (3.38) is called the Kraus operator sum representation of the dynamical map Λ_t. It should be noted that the operators $\{K_{\mu\nu}(t)\}$ satisfy the condition

$$\sum_{\mu\nu} K^\dagger_{\mu\nu}(t)K_{\mu\nu}(t) = \sum_{\mu,\nu} \sqrt{\lambda_\nu}\langle\varphi_\nu| U^\dagger(t) |\varphi_\mu\rangle \sqrt{\lambda_\nu}\langle\varphi_\mu| U(t) |\varphi_\nu\rangle \tag{3.39}$$

$$= \sum_\nu \lambda_\nu \langle\varphi_\nu| U^\dagger(t) \sum_\mu |\varphi_\mu\rangle\langle\varphi_\mu| U(t) |\varphi_\nu\rangle \tag{3.40}$$

$$= \sum_\nu \lambda_\nu \langle\varphi_\nu| U^\dagger(t)U(t) |\varphi_\nu\rangle \tag{3.41}$$

$$= I_S, \tag{3.42}$$

which ensures that the trace of the density matrix is preserved under the map Λ_t, $\mathrm{tr}\{\rho_S(t)\} = \mathrm{tr}\{\Lambda_t[\rho_S(0)]\} = \mathrm{tr}\{\rho_S(0)\} = 1$. The linearity and positivity of the map Λ_t can also be easily confirmed as below:

$$\Lambda_t[a_1\rho_1 + a_2\rho_2] = a_1\Lambda_t[\rho_1] + a_2\Lambda_t[\rho_2], \tag{3.43}$$

$$\langle\phi|\Lambda_t[\rho]|\phi\rangle = \sum_n p_n |\langle\phi|K_{\mu\nu}(t)|\psi_n\rangle|^2 \geq 0 \ \forall|\phi\rangle, \tag{3.44}$$

where the spectral decomposition $\rho = \sum_n p_n |\psi_n\rangle\langle\psi_n|$ has been used.

In the following sections, we focus on the thermodynamic aspect and discuss the first and second laws of thermodynamics in open quantum systems. We assume that the reservoir is a thermal bath at the inverse temperature $\beta = 1/T$, and the reference state of the reservoir is a thermal equilibrium state,

$$\rho_R = \rho_R^{\mathrm{eq}} \coloneqq \exp(-\beta H_R)/Z_R. \tag{3.45}$$

Here, $Z_R = \mathrm{tr}\{\exp(-\beta H_R)\}$ is the partition function.

3.3.1 The first law

Analogous to the case of closed quantum systems, the work done on the system can be defined as the energy change of the composite system,

$$\Delta W \coloneqq \mathrm{tr}\{H(\tau)\rho(\tau)\} - \mathrm{tr}\{H(0)\rho(0)\} = \int_0^\tau \mathrm{tr}\left\{\dot{H}(t)\rho(t)\right\} dt = \int_0^\tau \mathrm{tr}\left\{[\dot{H}_\mathrm{S}(t) + \dot{V}(t)]\rho(t)\right\} dt. \tag{3.46}$$

Here, we have used the fact that $\mathrm{tr}\{H(t)\dot{\rho}(t)\} = 0$. The heat transferred from the system to the reservoir is determined via the change in the internal energy of the reservoir,

$$\Delta Q \coloneqq \mathrm{tr}\{H_R\rho(\tau)\} - \mathrm{tr}\{H_R\rho(0)\} = \int_0^\tau \mathrm{tr}\{H_R\dot{\rho}(t)\}\, dt = -\int_0^\tau \mathrm{tr}\{[H_\mathrm{S}(t) + V(t)]\dot{\rho}(t)\}\, dt. \tag{3.47}$$

The energy change of the system S is contributed by the internal Hamiltonian and the interaction term,

$$\Delta E \coloneqq \mathrm{tr}\{[H_S(\tau) + V(\tau)]\rho(\tau)\} - \mathrm{tr}\{[H_S(0) + V(0)]\rho(0)\}. \tag{3.48}$$

Given the definitions of internal energy, heat, and work above, the first law of thermodynamics can be written as

$$\Delta E = \Delta W - \Delta Q. \tag{3.49}$$

Note that this relation is always valid irrespective of whether the initial state of the composite system is a product state or not.

3.3.2 The second law

Next we establish the second law of thermodynamics for open quantum systems [81]. We consider the case that the system is initially in the product state $\rho(0) = \rho_S(0) \otimes \rho_R^{\mathrm{eq}}$. The entropy of the system at time t is characterized by the von Neumann entropy

$$S(t) = -\mathrm{tr}\{\rho_S(t)\ln\rho_S(t)\}, \tag{3.50}$$

where $\rho_S(t) = \mathrm{tr}_R\{\rho(t)\}$ is the density matrix of the system S at time t. Since the von Neumann entropy is invariant under the unitary dynamics, we have

$$-\mathrm{tr}\{\rho(\tau)\ln\rho(\tau)\} = -\mathrm{tr}\{\rho(0)\ln\rho(0)\} = -\mathrm{tr}\{\rho_S(0)\ln\rho_S(0)\} - \mathrm{tr}\left\{\rho_R^{\mathrm{eq}}\ln\rho_R^{\mathrm{eq}}\right\}. \tag{3.51}$$

Using this equality, the entropy production of the system during time period τ can be calculated as

$$\begin{aligned}
\Delta S &\coloneqq -\mathrm{tr}\{\rho_S(\tau)\ln\rho_S(\tau)\} + \mathrm{tr}\{\rho_S(0)\ln\rho_S(0)\} && (3.52)\\
&= -\mathrm{tr}\{\rho(\tau)\ln\rho_S(\tau)\} + \mathrm{tr}\{\rho(\tau)\ln\rho(\tau)\} - \mathrm{tr}\left\{\rho_R^{\mathrm{eq}}\ln\rho_R^{\mathrm{eq}}\right\} && (3.53)\\
&= -\mathrm{tr}\left\{\rho(\tau)\ln\left[\rho_\mathrm{S}(\tau)\otimes\rho_R^{\mathrm{eq}}\right]\right\} + \mathrm{tr}\{\rho(\tau)\ln\rho(\tau)\} + \mathrm{tr}\left\{(\rho_R(\tau) - \rho_R^{\mathrm{eq}})\ln\rho_R^{\mathrm{eq}}\right\}. && (3.54)
\end{aligned}$$

The entropy production of the reservoir is associated with the heat transferred from the system as

$$\Delta S_{\mathrm{m}} \coloneqq \beta \Delta Q = \beta \left[\mathrm{tr} \left\{ H_R \rho(\tau) \right\} - \mathrm{tr} \left\{ H_R \rho(0) \right\} \right] = \mathrm{tr} \left\{ \left[\rho(\tau) - \rho(0) \right] \ln \rho_R^{\mathrm{eq}} \right\}. \tag{3.55}$$

Taking the sum of these entropy productions, we obtain the following formula for the total entropy production,

$$\Delta S_{\mathrm{tot}} \coloneqq \Delta S + \Delta S_{\mathrm{m}} = D(\rho(\tau) || \rho_S(\tau) \otimes \rho_R^{\mathrm{eq}}). \tag{3.56}$$

Since the relative entropy is always nonnegative, the second law of thermodynamics is immediately derived, $\Delta S_{\mathrm{tot}} \geq 0$. Equation (3.56) implies that the total entropy production can be quantified via correlation between the system and the reservoir. ΔS_{tot} is equal to zero if and only if $\rho(\tau) = \rho_S(\tau) \otimes \rho_R^{\mathrm{eq}}$, which means that the system and the reservoir remain uncorrelated.

3.4 Quantum master equations

In the previous section, we have showed that the time evolution of the state of the reduced system S can always be described by a family of dynamical maps $\{\Lambda_t\}_{t \geq 0}$. Since these dynamical maps depend on the unitary propagator and the degrees of freedom of the reservoir, it is generally difficult to obtain a closed motion equation of the reduced density matrix without further approximations. Under the condition of short correlation times (i.e., memory effects can be neglected in the reduced system dynamics), the concept of a quantum dynamical semigroup can be adopted, and a quantum Markovian master equation describing the motion of $\rho_S(t)$ can be mathematically derived. Basically, memory effects are always present due to the coupling between the system and the reservoir; however, they can be safely ignored in the weak coupling limit. In what follows, we first discuss the property of quantum dynamical semigroups and demonstrate a mathematical derivation of the Markovian quantum master equation. Then, we present a microscopic derivation that clarifies the physical conditions underlying the Markovian approximation. Finally, we discuss the first and second laws of thermodynamics for systems whose dynamics obey the quantum master equation.

The dynamical maps $\{\Lambda_t\}_t$ with $\Lambda_0 = I_S$ have the semigroup property if the following condition holds,

$$\Lambda_t = \Lambda_{t-s} \Lambda_s \ \forall 0 \leq s \leq t. \tag{3.57}$$

Under certain conditions, the map Λ_t can be expressed in terms of a semigroup generator $\mathcal{L}$ as

$$\Lambda_t = \exp(\mathcal{L} t), \tag{3.58}$$

from which the first-order differential equation describing the motion of the reduced density matrix can be readily obtained,

$$\frac{d}{dt} \rho_S(t) = \mathcal{L}(\rho_S(t)). \tag{3.59}$$

In the following, we will investigate a general form of the generator $\mathcal{L}$. To this end, we choose an orthonormal basis $\{F_n\}_{1 \leq n \leq N^2}$ of the Hilbert space $\mathcal{H}_S$, where $N = \dim \mathcal{H}_{\mathrm{S}}$. Specifically,

the operators F_n can be chosen to satisfy

$$\langle F_n, F_m \rangle := \mathrm{tr}\left\{F_n^\dagger F_m\right\} = \delta_{nm} \ \forall n, m = 1, \ldots, N^2, \tag{3.60}$$

$F_{N^2} = I_S/\sqrt{N}$, and $\mathrm{tr}\{F_n\} = 0$ for all $1 \leq n \leq N^2 - 1$. Such construction of the basis is always possible, for example, the set of Pauli matrices is a good choice for the $N = 2$ case and the generalized Gell-Mann matrices can be used for the general case. From the completeness of the basis, the Kraus operators $K_{\mu\nu}$ can be expressed in terms of $\{F_n\}$ as

$$K_{\mu\nu} = \sum_n \langle F_n, K_{\mu\nu} \rangle F_n. \tag{3.61}$$

Consequently, the dynamical map $\Lambda_t[\rho_S]$ can be written in the following form:

$$\Lambda_t[\rho_S] = \sum_{n,m=1}^{N^2} c_{nm}(t) F_n \rho_S F_m^\dagger, \tag{3.62}$$

where $c_{nm}(t)$ is given by

$$c_{nm}(t) = \sum_{\mu,\nu} \langle F_n, K_{\mu\nu} \rangle \langle F_m, K_{\mu\nu} \rangle^*. \tag{3.63}$$

One can easily verify that the matrix $\mathsf{C} = [c_{nm}]_{n,m=1}^{N^2}$ is Hermitian and positive semidefinite. From Eq. (3.62), one can take the short-time limit and obtain

$$\mathcal{L}(\rho_S) = \lim_{t \to 0} \frac{\Lambda_t[\rho_S] - \rho_S}{t} \tag{3.64}$$

$$= -i[H, \rho_S] + \{G, \rho_S\} + \sum_{n,m=1}^{N^2-1} a_{nm} F_n \rho_S F_m^\dagger. \tag{3.65}$$

Here, $\{X, Y\} = XY + YX$ denotes the anticommutator and

$$a_{N^2 N^2} = \lim_{t \to 0} \frac{c_{N^2 N^2}(t) - N}{t}, \tag{3.66}$$

$$a_{nm} = \lim_{t \to 0} \frac{c_{nm}(t)}{t} \ \forall (n, m) \neq (N^2, N^2), \tag{3.67}$$

$$F = \frac{1}{\sqrt{N}} \sum_{n=1}^{N^2-1} a_{nN^2} F_n, \tag{3.68}$$

$$G = \frac{1}{2N} a_{N^2 N^2} I_S + \frac{1}{2}(F + F^\dagger), \tag{3.69}$$

$$H = \frac{1}{2i}(F^\dagger - F). \tag{3.70}$$

Note that H is Hermitian and the matrix $\mathsf{A} = [a_{nm}]_{n,m=1}^{N^2-1}$ is Hermitian and positive semidefinite. Since Λ_t is a trace-preserving map, the following equality must hold for all ρ_S,

$$0 = \mathrm{tr}\{\mathcal{L}(\rho_S)\} = \mathrm{tr}\left\{\left(2G + \sum_{n,m=1}^{N^2-1} a_{nm} F_m^\dagger F_n\right) \rho_S\right\}, \tag{3.71}$$

which immediately derives

$$G = -\frac{1}{2}\sum_{n,m=1}^{N^2-1} a_{nm} F_m^\dagger F_n. \tag{3.72}$$

Hence, a standard form of the generator $\mathcal{L}$ is obtained as follows:

$$\mathcal{L}(\rho_S) = -i[H,\rho_S] + \sum_{n,m=1}^{N^2-1} a_{nm}\left(F_n\rho_S F_m^\dagger - \frac{1}{2}\left\{F_m^\dagger F_n, \rho_S\right\}\right). \tag{3.73}$$

Since A is self-adjoint and positive, one can diagonalize A using a unitary matrix $\mathsf{U} = [u_{nm}]$ as

$$\mathsf{U}\mathsf{A}\mathsf{U}^\dagger = \mathrm{diag}(\gamma_1, \ldots, \gamma_{N^2-1}), \tag{3.74}$$

where $\{\gamma_n\}$ are nonnegative eigenvalues of A. Defining the new matrices $\{L_n\}$ via the relation,

$$F_n = \sum_{m=1}^{N^2-1} u_{mn} L_m, \tag{3.75}$$

we get the following diagonal form of the generator $\mathcal{L}$,

$$\mathcal{L}(\rho_S) = -i[H,\rho_S] + \sum_{n=1}^{N^2-1} \gamma_n\left(L_n\rho_S L_n^\dagger - \frac{1}{2}\left\{L_n^\dagger L_n, \rho_S\right\}\right). \tag{3.76}$$

We make some remarks regarding Eq. (3.76). First, this form of the generator $\mathcal{L}$ is mathematically derived under some Markovian conditions without any physical justifications. It can be concluded that the master equation of a quantum Markovian process satisfying the semigroup property can always be written in this form. The Hermitian H can be interpreted as the Hamiltonian of the system (plus a correction called the Lamb shift). The operators L_n are usually referred to as the Lindblad operators (or jump operators), and Eq. (3.59) is known as the Lindblad master equation [82]. The nonnegative coefficients γ_n play the role of relaxation rates for the different decay modes of the open system. Moreover, one can prove that the dynamical map in the Lindblad form is always a positive trace-preserving map.

In the following section, we provide a microscopic derivation of the Lindblad master equation that justifies physical conditions under which Markovian assumptions are reasonable.

3.4.1 Microscopic derivation

We consider the case that the system is weakly coupled to the reservoir. For simplicity, the system Hamiltonian H_S is assumed to be time-independent. It is convenient to use the interaction picture to derive the Lindblad master equation with the decomposition $H_0 = H_S + H_R$ and $H_1(t) = V(t)$. Then $U_0(t) = e^{-iH_S t}\otimes e^{-iH_R t}$ and $\rho_I(t) = U_0^\dagger(t)\rho(t)U_0(t)$. According to Eq. (3.29), the density matrix of the composite system can be written as

$$\tilde{\rho}(t) = \tilde{\rho}(0) - i\int_0^t [H_I(s), \tilde{\rho}(s)]ds, \tag{3.77}$$

where the symbol ~ in the density matrix is used to indicate the interaction picture instead of the subscript I. Inserting Eq. (3.77) into Eq. (3.28) and taking the partial trace over the reservoir, we obtain

$$\frac{d}{dt}\tilde{\rho}_S(t) = -\int_0^t \mathrm{tr}_R \left\{[H_I(t), [H_I(s), \tilde{\rho}(s)]]\right\} ds. \tag{3.78}$$

Here, we have assumed that $\mathrm{tr}_R \left\{[H_I(t), \tilde{\rho}(0)]\right\} = 0$. In order to eliminate the term $\tilde{\rho}(s)$ in the right-hand side of Eq. (3.78), we perform the Born approximation, which assumes that the coupling between the system and the reservoir is weak and the state of the composite system can be approximated by a tensor product state, $\tilde{\rho}(t) \approx \tilde{\rho}_S(t) \otimes \tilde{\rho}_R$. Consequently, Eq. (3.78) becomes

$$\frac{d}{dt}\tilde{\rho}_S(t) = -\int_0^t \mathrm{tr}_R \left\{[H_I(t), [H_I(s), \tilde{\rho}_S(s) \otimes \tilde{\rho}_R]]\right\} ds. \tag{3.79}$$

Next, the Markov approximation is applied, which replaces $\tilde{\rho}_S(s)$ in the right-hand side of Eq. (3.79) by $\tilde{\rho}_S(t)$. Equation (3.79) now reads

$$\frac{d}{dt}\tilde{\rho}_S(t) = -\int_0^t \mathrm{tr}_R \left\{[H_I(t), [H_I(s), \tilde{\rho}_S(t) \otimes \tilde{\rho}_R]]\right\} ds, \tag{3.80}$$

which is known as the Redfield equation. Performing the variable transformation $s \to t - s$ in the integral and setting the upper limit to infinity, we further obtain

$$\frac{d}{dt}\tilde{\rho}_S(t) = -\int_0^\infty \mathrm{tr}_R \left\{[H_I(t), [H_I(t-s), \tilde{\rho}_S(t) \otimes \tilde{\rho}_R]]\right\} ds. \tag{3.81}$$

In general, the interaction Hamiltonian V can be written in the following form:

$$V = \sum_\alpha A_\alpha \otimes B_\alpha, \tag{3.82}$$

where A_α and B_α are Hermitians. We then define the operators

$$A_\alpha(\omega) := \sum_{\epsilon_m - \epsilon_n = \omega} \Pi_n A_\alpha \Pi_m, \tag{3.83}$$

where $\{\epsilon_n\}$ denote the eigenvalues of the system Hamiltonian H_S, and Π_n is the projection onto the eigenspace corresponding to the eigenvalue ϵ_n. From the equality $H_S\Pi_n = \Pi_n H_S = \epsilon_n \Pi_n$, one can easily verify the following relations:

$$[H_S, A_\alpha(\omega)] = -\omega A_\alpha(\omega), \tag{3.84}$$

$$[H_S, A_\alpha^\dagger(\omega)] = +\omega A_\alpha^\dagger(\omega). \tag{3.85}$$

Furthermore, the operators A_α in the interaction picture read

$$e^{iH_S t} A_\alpha(\omega) e^{-iH_S t} = e^{-i\omega t} A_\alpha(\omega), \tag{3.86}$$

$$e^{iH_S t} A_\alpha^\dagger(\omega) e^{-iH_S t} = e^{+i\omega t} A_\alpha^\dagger(\omega). \tag{3.87}$$

Note that $[H_S, A_\alpha^\dagger(\omega)A_{\alpha'}(\omega)] = 0$, $A_\alpha^\dagger(\omega) = A_\alpha(-\omega)$, and $\sum_\omega A_\alpha(\omega) = \sum_\omega A_\alpha^\dagger(\omega) = A_\alpha$. Hence, the interaction Hamiltonian V can be written as

$$V = \sum_{\alpha,\omega} A_\alpha(\omega) \otimes B_\alpha = \sum_{\alpha,\omega} A_\alpha^\dagger(\omega) \otimes B_\alpha^\dagger, \tag{3.88}$$

and its form in the interaction picture is given by

$$H_I(t) = e^{i(H_S+H_R)t} V e^{-i(H_S+H_R)t} = \sum_{\alpha,\omega} e^{-i\omega t} A_\alpha(\omega) \otimes B_\alpha(t) = \sum_{\alpha,\omega} e^{+i\omega t} A_\alpha^\dagger(\omega) \otimes B_\alpha^\dagger(t), \tag{3.89}$$

where $B_\alpha(t) = e^{iH_R t} B_\alpha e^{-iH_R t}$ is the interaction picture operator of B_α. Now, inserting Eq. (3.89) into Eq. (3.81), we obtain

$$\frac{d}{dt}\tilde{\rho}_S(t) = \int_0^\infty \mathrm{tr}_R \left\{ H_I(t-s)\tilde{\rho}_S(t) \otimes \tilde{\rho}_R H_I(t) - H_I(t) H_I(t-s)\tilde{\rho}_S(t) \otimes \tilde{\rho}_R \right\} ds + \text{h.c.} \tag{3.90}$$

$$= \sum_{\omega,\omega'} \sum_{\alpha,\alpha'} e^{i(\omega'-\omega)t} \Gamma_{\alpha\alpha'}(\omega) \left[A_{\alpha'}(\omega)\tilde{\rho}_S(t) A_\alpha^\dagger(\omega') - A_\alpha^\dagger(\omega') A_{\alpha'}(\omega)\tilde{\rho}_S(t) \right] + \text{h.c.} \tag{3.91}$$

Here, h.c. indicates the Hermitian conjugated terms and

$$\Gamma_{\alpha\alpha'}(\omega) \coloneqq \int_0^\infty e^{i\omega s} \mathrm{tr} \left\{ B_\alpha^\dagger(t) B_{\alpha'}(t-s)\tilde{\rho}_R \right\} ds. \tag{3.92}$$

Assuming that ρ_R is a stationary state of the reservoir, i.e., $[H_R, \rho_R] = 0$, then the reservoir correlation functions are homogeneous in time,

$$\mathrm{tr} \left\{ B_\alpha^\dagger(t) B_{\alpha'}(t-s)\tilde{\rho}_R \right\} = \mathrm{tr} \left\{ B_\alpha^\dagger(s) B_{\alpha'}(0)\tilde{\rho}_R \right\}. \tag{3.93}$$

This implies that the quantities $\Gamma_{\alpha\alpha'}(\omega)$ are time-independent. However, it is not the case when the reservoir is in a squeezed vacuum state. The time scale τ_S of the intrinsic evolution of the system can be defined as the typical value of $|\omega - \omega'|^{-1}$ for $\omega \neq \omega'$. When the time resolution of our interest is large compared to this intrinsic time scale (i.e., $t \gg \tau_S$), all the non-secular terms (i.e., the terms for which $\omega \neq \omega'$) oscillate rapidly and can be averaged out. This final approximation is known as the rotating wave approximation, which was conventionally applied to quantum optical systems. As a result, the following equation is obtained,

$$\frac{d}{dt}\tilde{\rho}_S(t) = \sum_{\omega} \sum_{\alpha,\alpha'} \Gamma_{\alpha\alpha'}(\omega) \left[A_{\alpha'}(\omega)\tilde{\rho}_S(t) A_\alpha^\dagger(\omega) - A_\alpha^\dagger(\omega) A_{\alpha'}(\omega)\tilde{\rho}_S(t) \right] + \text{h.c.} \tag{3.94}$$

To proceed further, it is convenient to divide $\Gamma_{\alpha\alpha'}(\omega)$ into Hermitian and non-Hermitian parts,

$$\Gamma_{\alpha\alpha'}(\omega) = \frac{1}{2}\gamma_{\alpha\alpha'}(\omega) + i\pi_{\alpha\alpha'}(\omega), \tag{3.95}$$

where $\gamma_{\alpha\alpha'}(\omega) = \Gamma_{\alpha\alpha'}(\omega) + \Gamma_{\alpha\alpha'}(\omega)^* = \int_{-\infty}^\infty e^{i\omega s} \mathrm{tr} \left\{ B_\alpha^\dagger(s) B_{\alpha'}(0)\tilde{\rho}_R \right\} ds$. Inserting the decomposition of $\Gamma_{\alpha\alpha'}(\omega)$ into Eq. (3.94) and transforming back to the Schrödinger picture via the

relation $\tilde{\rho}_S(t) = e^{iH_S t}\rho_S(t)e^{-iH_S t}$, we finally arrive at the master equation,

$$\frac{d}{dt}\rho_S(t) = -i[H_S+H_{\rm LS},\rho_S(t)]+\sum_{\omega}\sum_{\alpha,\alpha'}\gamma_{\alpha\alpha'}(\omega)\left[A_{\alpha'}(\omega)\rho_S(t)A^\dagger_\alpha(\omega)-\frac{1}{2}\left\{A^\dagger_\alpha(\omega)A_{\alpha'}(\omega),\rho_S(t)\right\}\right]. \tag{3.96}$$

Here, $H_{\rm LS} \coloneqq \sum_\omega\sum_{\alpha,\alpha'}\pi_{\alpha\alpha'}(\omega)A^\dagger_\alpha(\omega)A_{\alpha'}(\omega)$ is referred to as the Lamb shift Hamiltonian since it leads to a Lamb-type renormalization of the unperturbed energy levels induced by the system-reservoir coupling. Note that $H_{\rm LS}$ and H_S commute (i.e., $[H_{\rm LS},H] = 0$), and the matrix $[\gamma_{\alpha\alpha'}(\omega)]$ is positive since it is the Fourier transform of the positive matrix $\left[\mathrm{tr}\left\{B^\dagger_\alpha(s)B_{\alpha'}(0)\tilde{\rho}_R\right\}\right]$. Consequently, one can diagonalize the matrix $[\gamma_{\alpha\alpha'}(\omega)]$ and write the master equation in the diagonal form as

$$\begin{aligned}\frac{d}{dt}\rho_S(t) &= -i[H_S+H_{\rm LS},\rho_S(t)]+\sum_{\omega,k}\gamma_k(\omega)\left[L_k(\omega)\rho_S(t)L^\dagger_k(\omega)-\frac{1}{2}\left\{L^\dagger_k(\omega)L_k(\omega),\rho_S(t)\right\}\right],\\ &= -i[H_S+H_{\rm LS},\rho_S(t)]+\mathcal{D}(\rho_S(t)),\end{aligned} \tag{3.97}$$

where $\mathcal{D}(\rho) \coloneqq \sum_{\omega,k}\gamma_k(\omega)\left[L_k(\omega)\rho L^\dagger_k(\omega)-\frac{1}{2}\left\{L^\dagger_k(\omega)L_k(\omega),\rho\right\}\right]$ is usually called dissipator, which characterizes the non-unitary evolution of the density matrix. In practice, the non-Hermitian Lamb shift term $H_{\rm LS}$ is sometimes neglected for ease of analysis.

Relaxation to equilibrium and detailed balance condition.—Assuming that the reservoir is a thermal bath at the inverse temperature $\beta = 1/T$, then in the absence of the external control, the system is expected to relax to the Gibbs state irrespective of the initial state,

$$\rho^{\rm eq}_S \coloneqq \exp(-\beta H_S)/Z_S, \tag{3.98}$$

where $Z_S = \mathrm{tr}\{\exp(-\beta H_S)\}$ is the partition function. We can prove that if the system is ergodic and the coefficients $\gamma_k(\omega)$ satisfy the detailed balance condition, then the above expectation is met. The system is said to be ergodic if the relations

$$[X,L^\dagger_k(\omega)] = [X,L_k(\omega)] = 0\ \forall k,\omega \tag{3.99}$$

imply that X is proportional to the identity I_S. The detailed balance condition is analogous to the classical case, stating that

$$\gamma_k(\omega) = e^{\beta\omega}\gamma_k(-\omega). \tag{3.100}$$

3.4.2 Heat, work, and entropy production

Consider an open quantum system whose dynamics are described by the Lindblad master equation,

$$\frac{d}{dt}\rho_S(t) = -i[H_S(t),\rho_S(t)]+\sum_{\omega,k}\gamma_k(\omega)\left[L_k(\omega)\rho_S(t)L^\dagger_k(\omega)-\frac{1}{2}\left\{L^\dagger_k(\omega)L_k(\omega),\rho_S(t)\right\}\right], \tag{3.101}$$

where the Lamb shift term has been neglected. The system Hamiltonian is possibly time-dependent. Then, the internal energy, heat, and work can be defined as

$$E(t) \coloneqq \mathrm{tr}\left\{H_S(t)\rho_S(t)\right\}, \tag{3.102}$$

$$\dot{Q}(t) \coloneqq -\mathrm{tr}\left\{H_S(t)\dot{\rho}_S(t)\right\}, \tag{3.103}$$

$$\dot{W}(t) \coloneqq \mathrm{tr}\left\{\dot{H}_S(t)\rho_S(t)\right\}, \tag{3.104}$$

where the dot denotes the time derivative. The heat $\Delta Q = \int_0^\tau \dot{Q}(t)dt$ characterizes the energy loss of the system induced by the change of the density matrix due to the interaction with the reservoir. Thus, it can be regarded as the heat transferred from the system to the reservoir. On the other hand, the work $\Delta W = \int_0^\tau \dot{W}(t)dt$ expresses the energy change caused by the external agent acting on the Hamiltonian. With these definitions, the first law of thermodynamics can be established as

$$\mathrm{tr}\left\{H_S(\tau)\rho_S(\tau)\right\} - \mathrm{tr}\left\{H_S(0)\rho_S(0)\right\} = \Delta E = \Delta W - \Delta Q. \tag{3.105}$$

To define entropy production, we assume that the system has an instantaneous equilibrium state $\rho_S^{\mathrm{eq}}(t) \coloneqq \exp(-\beta H_S(t))/Z_S(t)$, i.e., $\mathcal{L}(\rho_S^{\mathrm{eq}}(t)) = 0$. Then, the total entropy production rate $\sigma_{\mathrm{tot}}(t)$ can be the sum of the system entropy production rate and the heat flow to the reservoir,

$$\sigma_{\mathrm{tot}}(t) = \dot{S}(t) + \beta\dot{Q}(t), \tag{3.106}$$

where $\dot{S}(t) = -\mathrm{tr}\left\{\dot{\rho}_S(t)\ln\rho_S(t)\right\}$ is the von Neumann entropy flux of the system. Plugging the expressions of $\dot{S}(t)$ and $\dot{Q}(t)$ into Eq. (3.106), we have

$$\sigma_{\mathrm{tot}}(t) = -\mathrm{tr}\left\{\dot{\rho}_S(t)\ln\rho_S(t)\right\} - \beta\mathrm{tr}\left\{H_S(t)\dot{\rho}_S(t)\right\} \tag{3.107}$$

$$= -\mathrm{tr}\left\{\dot{\rho}_S(t)[\ln\rho_S(t) - \ln\rho_S^{\mathrm{eq}}(t)]\right\} \tag{3.108}$$

$$= -\frac{d}{dt}S(\rho_S(t)||\rho_S^{\mathrm{eq}}(t)), \tag{3.109}$$

where the time derivative does not act on $\rho_S^{\mathrm{eq}}(t)$. The positivity of the entropy production rate can be proved using the monotonicity of the relative entropy under information processing,

$$\sigma_{\mathrm{tot}}(t) = -\frac{d}{dt}S(\rho_S(t)||\rho_S^{\mathrm{eq}}(t)) \tag{3.110}$$

$$= \lim_{\Delta t\to 0}\frac{S(\rho_S(t)||\rho_S^{\mathrm{eq}}(t)) - S(\rho_S(t+\Delta t)||\rho_S^{\mathrm{eq}}(t))}{\Delta t} \tag{3.111}$$

$$= \lim_{\Delta t\to 0}\frac{S(\rho_S(t)||\rho_S^{\mathrm{eq}}(t)) - S(\Lambda_*[\rho_S(t)]||\Lambda_*[\rho_S^{\mathrm{eq}}(t)])}{\Delta t} \geq 0. \tag{3.112}$$

Here, $\Lambda_* \coloneqq e^{\mathcal{L}\Delta t}$ is a Lindblad map satisfying $\Lambda_*[\rho_S(t)] = \rho_S(t+\Delta t)$ and $\Lambda_*[\rho_S^{\mathrm{eq}}(t)] = \rho_S^{\mathrm{eq}}(t)$. Since

$$S(\rho_1||\rho_2) \geq S(\Lambda[\rho_1]||\Lambda[\rho_2]) \tag{3.113}$$

for arbitrary density matrices ρ_1, ρ_2 and completely positive trace-preserving map Λ, we have

$$S(\rho_S(t)||\rho_S^{\rm eq}(t)) \geq S(\Lambda_*[\rho_S(t)]||\Lambda_*[\rho_S^{\rm eq}(t)]), \tag{3.114}$$

from which Eq. (3.112) is immediately obtained. For thermal relaxation processes (i.e., the Hamiltonian and jump operators are time-independent), the total entropy production can be explicitly calculated as

$$\Delta S_{\rm tot} = \int_0^\tau \sigma_{\rm tot}(t)dt = -\int_0^\tau \frac{d}{dt} S(\rho_S(t)||\rho_S^{\rm eq})dt \tag{3.115}$$

$$= S(\rho_S(0)||\rho_S^{\rm eq}) - S(\rho_S(\tau)||\rho_S^{\rm eq}) \geq 0. \tag{3.116}$$

Chapter 4

Thermodynamic uncertainty relations in Langevin systems

This chapter is devoted to investigating TURs for Langevin systems. It is of particular interest that the TUR is valid for overdamped Langevin systems [24, 83]. However, overdamped dynamics, which are only approximate descriptions of underdamped dynamics, can dramatically fail to capture thermodynamic quantities such as the entropy production [84–86]. Therefore, it is natural to ask whether the TUR is valid for underdamped systems; and more importantly, if not, whether there exists an analogous bound for such systems. We answer this question by numerically demonstrating that the TUR is actually violated; subsequently, we derive a new TUR which holds for finite observation times. Interestingly, the derived TUR indicates that the dynamical activity is on a par with entropy production to constrain the current fluctuation.

Physical systems used in experiments, such as heat engines, are often driven by external controllers. Nevertheless, in such non-stationary systems, the original TUR seems to be violated. This fact motivates us to derive TURs for Langevin systems under arbitrary control protocols. The derived TURs are applicable to both current and noncurrent observables that satisfy a scaling condition. The analytical and numerical results indicate that the observable fluctuation is constrained not only by entropy production but also by a kinetic term in both overdamped and underdamped systems.

4.1 Bounds for steady-state underdamped Langevin systems

In this section, we study TUR for steady-state underdamped Langevin dynamics, wherein damping does not suppress inertial effects. Regarding the validity of the TUR, we numerically found that it does not universally hold. Therefore, the original bound cannot be utilized for general underdamped systems. By applying information inequalities to systems, we derive new bounds for both scalar and vector currents in the steady state. Specifically, we prove that the relative fluctuation of a current is bounded from below by a quantity involving entropy production and the average dynamical activity. This activity term is a kinetic aspect of the system and plays a central role in characterizing its dynamics [87–92]. The results imply that

the current fluctuation is constrained not only by entropy production but also by dynamical activity. We empirically verify the derived bounds via numerical simulations. In addition, we show that our approach can be applied to the derivation of an uncertainty relation for active matter systems, which have recently attracted considerable interest [93–100].

4.1.1 Main results

We consider a general underdamped system of N particles, wherein the particle i is in contact with a heat reservoir in equilibrium at temperature T_i. The dynamics of the system are described by a set of coupled equations as follows:

$$\dot{r}_i = v_i, \;\; m_i \dot{v}_i = -\gamma_i v_i + F_i(\boldsymbol{r}) + \xi_i, \tag{4.1}$$

where the dots indicate time derivatives, $\boldsymbol{r} = [r_1, \ldots, r_N]^\top$ and $\boldsymbol{v} = [v_1, \ldots, v_N]^\top$ denote positions and velocities, respectively; m_i and γ_i are the mass and the damping coefficient of particle i, respectively; $F_i(\boldsymbol{r}) = -\partial_{r_i} U(\boldsymbol{r}) + f_i(\boldsymbol{r})$ is the total acting force with the potential $U(\boldsymbol{r})$; and the ξ_i's are zero-mean white Gaussian noises with variances $\langle \xi_i(t)\xi_j(t')\rangle = 2T_i\gamma_i\delta_{ij}\delta(t-t')$. Throughout this study, Boltzmann's constant is set to $k_\mathrm{B} = 1$. The time evolution of the phase-space probability distribution function, $P(\boldsymbol{r}, \boldsymbol{v}, t)$, can be described by the Kramers equation

$$\partial_t P(\boldsymbol{r}, \boldsymbol{v}, t) = \sum_{i=1}^{N} \left[-\partial_{r_i} J_{r_i}(\boldsymbol{r}, \boldsymbol{v}, t) - \partial_{v_i} J_{v_i}(\boldsymbol{r}, \boldsymbol{v}, t) \right], \tag{4.2}$$

where $J_{r_i}(\boldsymbol{r}, \boldsymbol{v}, t) = v_i P(\boldsymbol{r}, \boldsymbol{v}, t)$ and $J_{v_i}(\boldsymbol{r}, \boldsymbol{v}, t) = 1/m_i \left[-\gamma_i v_i + F_i(\boldsymbol{r}) - T_i\gamma_i/m_i \partial_{v_i} \right] P(\boldsymbol{r}, \boldsymbol{v}, t)$. Hereafter, we focus exclusively upon the steady state, in which the system has stationary distribution $P^{\mathrm{ss}}(\boldsymbol{r}, \boldsymbol{v})$ and probability currents $J^{\mathrm{ss}}_{r_i}(\boldsymbol{r}, \boldsymbol{v})$ and $J^{\mathrm{ss}}_{v_i}(\boldsymbol{r}, \boldsymbol{v})$.

Let $\boldsymbol{\Gamma} \equiv [\boldsymbol{r}(t), \boldsymbol{v}(t)]_{t=0}^{t=\mathcal{T}}$ denote a phase-space trajectory that starts at the point $(\boldsymbol{r}^0, \boldsymbol{v}^0) \equiv (\boldsymbol{r}(0), \boldsymbol{v}(0))$ and has length $\mathcal{T}$. The entropy production characterizes the irreversibility in the system and has been generalized to the level of stochastic trajectories [7]. Along the trajectory $\boldsymbol{\Gamma}$, the entropy production can be defined as $\Delta s_{\mathrm{tot}}[\boldsymbol{\Gamma}] \equiv \ln \left(\mathbb{P}[\boldsymbol{\Gamma}] / \mathbb{P}^\dagger[\boldsymbol{\Gamma}^\dagger] \right)$, which is a comparison of the probabilities of the forward path $\boldsymbol{\Gamma}$ and its time-reversed counterpart $\boldsymbol{\Gamma}^\dagger \equiv [\boldsymbol{r}(\mathcal{T}-t), -\boldsymbol{v}(\mathcal{T}-t)]_{t=0}^{t=\mathcal{T}}$ [101–103]. Here, $\mathbb{P}[\boldsymbol{\Gamma}]$ and $\mathbb{P}^\dagger[\boldsymbol{\Gamma}^\dagger]$ are the probabilities of observing the forward path $\boldsymbol{\Gamma}$ and its time-reversed path $\boldsymbol{\Gamma}^\dagger$, respectively. Because the initial distribution in the time-reversed process is $P(\boldsymbol{r}(\mathcal{T}), \boldsymbol{v}(\mathcal{T}), \mathcal{T})$, the entropy production can be decomposed as

$$\Delta s_{\mathrm{tot}}[\boldsymbol{\Gamma}] = -\ln \frac{P(\boldsymbol{r}(\mathcal{T}), \boldsymbol{v}(\mathcal{T}), \mathcal{T})}{P(\boldsymbol{r}(0), \boldsymbol{v}(0), 0)} + \ln \frac{\mathbb{P}[\boldsymbol{\Gamma}|\boldsymbol{r}(0), \boldsymbol{v}(0)]}{\mathbb{P}[\boldsymbol{\Gamma}^\dagger|\boldsymbol{r}(\mathcal{T}), -\boldsymbol{v}(\mathcal{T})]}, \tag{4.3}$$

where the first and second terms in the right-hand side of Eq. (4.3) correspond to the system entropy production and the medium entropy production, respectively. Using stochastic thermodynamics [3, 103], we can show that the entropy production rate, which includes changes

in the system entropy and the medium entropy, is as follows:

$$\sigma = \sum_{i=1}^{N} \iint d\boldsymbol{r}d\boldsymbol{v} \frac{m_i^2}{T_i\gamma_i} \frac{J_{v_i}^{\mathrm{ir}}(\boldsymbol{r},\boldsymbol{v})^2}{P^{\mathrm{ss}}(\boldsymbol{r},\boldsymbol{v})}, \tag{4.4}$$

where $J_{v_i}^{\mathrm{ir}}(\boldsymbol{r},\boldsymbol{v})$ is the irreversible current given by $J_{v_i}^{\mathrm{ir}}(\boldsymbol{r},\boldsymbol{v}) = -1/m_i \left[\gamma_i v_i + T_i\gamma_i/m_i \partial_{v_i}\right] P^{\mathrm{ss}}(\boldsymbol{r},\boldsymbol{v})$. The detailed calculation of σ is provided in Appendix A.1. For an arbitrary trajectory $\boldsymbol{\Gamma}$, we consider a generalized observable-type current, $\Theta[\boldsymbol{\Gamma}] = \int_0^{\mathcal{T}} dt\, \boldsymbol{\Lambda}(\boldsymbol{r})^{\top} \circ \dot{\boldsymbol{r}}$, where $\boldsymbol{\Lambda} \in \mathbb{R}^{N\times 1}$ is the projection function and $\circ$ denotes the Stratonovich product. Our aim is to derive a lower bound on the fluctuation of the current $\Theta[\boldsymbol{\Gamma}]$.

To derive our results, let us consider the auxiliary dynamics

$$\dot{r}_i = v_i, \;\; m_i\dot{v}_i = H_{i,\theta}(\boldsymbol{r},\boldsymbol{v}) + \xi_i, \tag{4.5}$$

where θ is a perturbation parameter and $H_{i,\theta}(\boldsymbol{r},\boldsymbol{v})$ is the force acting upon particle i. The detailed form of $H_{i,\theta}(\boldsymbol{r},\boldsymbol{v})$ will be determined later. For an arbitrary function $f[\boldsymbol{\Gamma}]$, let $\langle f\rangle_\theta \equiv \int \mathcal{D}\boldsymbol{\Gamma}\, f[\boldsymbol{\Gamma}]\mathbb{P}_\theta[\boldsymbol{\Gamma}]$ and $\mathrm{Var}_\theta[f] \equiv \langle (f - \langle f\rangle_\theta)^2\rangle_\theta$. Here, $\mathbb{P}_\theta[\boldsymbol{\Gamma}]$ is the probability of observing the trajectory $\boldsymbol{\Gamma}$ generated by the auxiliary dynamics. It can be expressed in a path-integral form as [104]

$$\mathbb{P}_\theta[\boldsymbol{\Gamma}] = \mathcal{N} P_\theta^{\mathrm{ss}}(\boldsymbol{r}^0,\boldsymbol{v}^0) \prod_{i=1}^{N} \exp\left(-\mathcal{A}_i[\boldsymbol{\Gamma}]\right), \tag{4.6}$$

where $\mathcal{A}_i[\boldsymbol{\Gamma}] \equiv \int_0^{\mathcal{T}} dt \left(m_i\dot{v}_i - H_{i,\theta}(\boldsymbol{r},\boldsymbol{v})\right)^2/(4T_i\gamma_i)$ is an Onsager–Machlup action functional, $P_\theta^{\mathrm{ss}}(\boldsymbol{r}^0,\boldsymbol{v}^0)$ is the stationary distribution of the auxiliary dynamics, and $\mathcal{N}$ is a term independent of θ. The integral in the action functional is interpreted as the continuum limit of an Ito sum with pre-point discretization. Note that writing the crossing term $\int dt\, \dot{v}_i H_{\theta,i}(\boldsymbol{r},\boldsymbol{v})$ in Stratonovich integral (i.e., mid-point discretization) results in a different form of the path integral. However, it can be shown that both pre- and mid-point discretization schemes reduce to the same path-integral representation in the case of additive noise (see Appendix A.2). Hereafter, the notations $\langle\cdot\cdot\rangle$ and $\langle\cdot\cdot\rangle_\theta$ imply averages taken over ensembles in the original and auxiliary dynamics, respectively. In the steady state, the average of the current becomes $\langle\Theta\rangle_\theta = \mathcal{T}\iint d\boldsymbol{r}d\boldsymbol{v}\, \boldsymbol{\Lambda}(\boldsymbol{r})^{\top}\boldsymbol{J}_{r,\theta}^{\mathrm{ss}}(\boldsymbol{r},\boldsymbol{v})$, where $\boldsymbol{J}_{r,\theta}^{\mathrm{ss}}(\boldsymbol{r},\boldsymbol{v}) = \boldsymbol{v}P_\theta^{\mathrm{ss}}(\boldsymbol{r},\boldsymbol{v})$ is the vector of probability currents in the auxiliary dynamics. Since $\langle\Theta\rangle_\theta$ is a function of θ, i.e., $\langle\Theta\rangle_\theta = \psi(\theta)$, we can consider Θ as an estimator of $\psi(\theta)$. The precision of this estimator is bounded from below by the reciprocal of the Fisher information as [33]

$$\frac{\mathrm{Var}_\theta[\Theta]}{(\partial_\theta\langle\Theta\rangle_\theta)^2} \geq \frac{1}{\mathcal{I}(\theta)}, \tag{4.7}$$

where $\mathcal{I}(\theta) \equiv -\left\langle\partial_\theta^2 \ln \mathbb{P}_\theta\right\rangle_\theta$ is the Fisher information, which can be calculated via the path integral in Eq. (4.6). Equation (4.7) is known as the Cramér–Rao inequality, and indicates a trade-off between the precision of an estimator and the Fisher information. The analogy between this inequality and the TUR has been utilized to derive the original bound [33, 105]. Next, we use the virtual-perturbation technique [44] and consider the auxiliary dynamics with

the following force:

$$H_{i,\theta}(\boldsymbol{r},\boldsymbol{v}) = -(1+\theta)\gamma_i v_i + (1+\theta)^2 F_i(\boldsymbol{r}) + \frac{T_i\gamma_i}{m_i}(1-(1+\theta)^3)\frac{\partial_{v_i}P^{\rm ss}(\boldsymbol{r},\boldsymbol{v}/(1+\theta))}{P^{\rm ss}(\boldsymbol{r},\boldsymbol{v}/(1+\theta))}. \tag{4.8}$$

When $\theta = 0$, $H_{i,\theta}(\boldsymbol{r},\boldsymbol{v}) = -\gamma_i v_i + F_i(\boldsymbol{r})$ and the auxiliary dynamics become the original ones. Verifying that these auxiliary dynamics have a stationary distribution $P^{\rm ss}_\theta(\boldsymbol{r},\boldsymbol{v}) = P^{\rm ss}(\boldsymbol{r},\boldsymbol{v}/(1+\theta))/(1+\theta)^N$ is easy. The average current in the auxiliary dynamics is related to that in the original dynamics as $\langle\Theta\rangle_\theta = (1+\theta)\langle\Theta\rangle$; thus, we have $\partial_\theta\langle\Theta\rangle_\theta = \langle\Theta\rangle$. By letting $\theta = 0$ in Eq. (4.7), we obtain the following inequality:

$$\frac{\mathrm{Var}[\Theta]}{\langle\Theta\rangle^2} \geq \frac{2}{\Sigma}, \tag{4.9}$$

where $\Sigma = 2\mathcal{I}(0) = \mathcal{T}(9\sigma + 4\Upsilon) + \Omega$ and

$$\Upsilon = \sum_{i=1}^{N}\Big(\frac{1}{T_i\gamma_i}\langle F_i(\boldsymbol{r})^2\rangle - 3\frac{\gamma_i}{T_i}\langle v_i^2\rangle + 4\frac{\gamma_i}{m_i}\Big), \tag{4.10}$$

$$\Omega = 2\Big\langle\Big(\sum_{i=1}^{N} v_i\partial_{v_i}P^{\rm ss}(\boldsymbol{r},\boldsymbol{v})/P^{\rm ss}(\boldsymbol{r},\boldsymbol{v})\Big)^2\Big\rangle - 2N^2. \tag{4.11}$$

Inequality (4.9) is the main result and holds for an arbitrary time scale and general underdamped systems. The detailed derivation is provided in Appendix A.3. As seen, the derived bound is not equal to the reciprocal of entropy production as is the original bound (which will be shown to be violated in underdamped systems). In addition to the entropy production, the derived bound also contains Υ, which involves the moments of the forces and velocities, and a boundary term Ω, which is always nonnegative, as $\Omega = 2\langle[\partial_\theta \ln P^{\rm ss}_\theta(\boldsymbol{r}^0,\boldsymbol{v}^0)]^2\rangle_{\theta=0}$. In the long-time limit, i.e., $\mathcal{T}\to\infty$, the boundary term can be neglected. Thus, our result reduces to a bound that was derived in Ref. [106] for a one-dimensional system using large deviation theory. Since the kinetic term Υ can be estimated from the experimental data, our bound can be applied to quantify the entropy production for underdamped systems as in Ref. [49], where the original bound has been used to infer a lower bound on entropy production for overdamped systems.

Considering the equality condition of the derived bound, the lower bound in Eq. (4.9) can be attained if and only if the equality condition in Eq. (4.7) is satisfied with $\theta = 0$. Equivalently, $\partial_\theta \ln \mathbb{P}_\theta[\boldsymbol{\Gamma}]|_{\theta=0} = \mu(\Theta[\boldsymbol{\Gamma}] - \psi(0))$ must hold for an arbitrary trajectory $\boldsymbol{\Gamma}$, where μ is a scaling coefficient. However, it can be proven that this lower bound cannot be attained (the detailed proof is provided in Appendix A.4).

So far, we have considered currents with projection functions involving only $\boldsymbol{r}$. Here, we derive a bound for a certain class of more general currents, $\Theta[\boldsymbol{\Gamma}] = \int_0^{\mathcal{T}} dt\, \boldsymbol{\Lambda}(\boldsymbol{r},\boldsymbol{v})^\top \circ \dot{\boldsymbol{r}}$, wherein the projection function involves the velocity variables. Suppose that $\boldsymbol{\Lambda}(\boldsymbol{r},\boldsymbol{v})$ satisfies $\boldsymbol{\Lambda}(\boldsymbol{r},(1+\theta)\boldsymbol{v}) = (1+\theta)^d\boldsymbol{\Lambda}(\boldsymbol{r},\boldsymbol{v})$ for all $\theta\in\mathbb{R}$ and for some nonnegative number d. For example, $\boldsymbol{\Lambda}(\boldsymbol{r},\boldsymbol{v})$ can be a vector of homogeneous polynomials of $\boldsymbol{v}$ (i.e., all nonzero terms have the same degree d with respect to $\boldsymbol{v}$). From the relationship $\langle\Theta\rangle_\theta = (1+\theta)^{d+1}\langle\Theta\rangle$, we have

$\partial_\theta \langle \Theta \rangle_\theta|_{\theta=0} = (d+1)\langle \Theta \rangle$. Consequently, we obtain the following bound:

$$\frac{\mathrm{Var}[\Theta]}{\langle \Theta \rangle^2} \geq \frac{2(d+1)^2}{\Sigma}. \tag{4.12}$$

When the projection function contains only $\boldsymbol{r}$, i.e., $d = 0$, Eq. (4.12) reduces to Eq. (4.9).

4.1.2 Physical interpretation of the bound

Now, we interpret the physical meaning of the term Υ in the bound. In the original dynamics, the action functional in the path integral with mid-point discretization is [107]

$$\mathcal{A}_i^{\mathrm{m}}[\boldsymbol{\Gamma}] \equiv \int_0^{\mathcal{T}} dt \left[\frac{1}{4T_i\gamma_i} \left(m_i \dot{v}_i + \gamma_i v_i - F_i \right)^2 - \frac{\gamma_i}{2m_i} \right]. \tag{4.13}$$

The functional $\mathcal{A}_i^{\mathrm{m}}$ can be decomposed into two contributions: the time-antisymmetric ($\mathcal{S}$) and time-symmetric ($\mathcal{K}_i$, $\mathcal{K}_i^*$) components as $-\mathcal{A}_i^{\mathrm{m}}[\boldsymbol{\Gamma}] = \mathcal{S}_i[\boldsymbol{\Gamma}] + \mathcal{K}_i[\boldsymbol{\Gamma}] + \mathcal{K}_i^*[\boldsymbol{\Gamma}]$ [108], where

$$\begin{aligned}
\mathcal{S}_i[\boldsymbol{\Gamma}] &= -\int_0^{\mathcal{T}} dt \, \frac{1}{2T_i} \left(m_i \dot{v}_i - F_i \right) \circ v_i, \\
\mathcal{K}_i[\boldsymbol{\Gamma}] &= \int_0^{\mathcal{T}} dt \left[\frac{1}{4T_i\gamma_i} \left(2m_i \dot{v}_i \circ F_i - \gamma_i^2 v_i^2 - F_i^2 \right) + \frac{\gamma_i}{2m_i} \right], \\
\mathcal{K}_i^*[\boldsymbol{\Gamma}] &= -\int_0^{\mathcal{T}} dt \, \frac{m_i^2 \dot{v}_i^2}{4T_i\gamma_i}.
\end{aligned} \tag{4.14}$$

The time-antisymmetric part corresponds to the integrated entropy flux from the system into the reservoirs and is thermodynamically consistent with the definition of medium entropy production $\Delta s_{\mathrm{m}}[\boldsymbol{\Gamma}] \equiv \sum_{i=1}^N \frac{1}{T_i} \int_0^{\mathcal{T}} dt \, (\gamma_i v_i - \xi_i) \circ v_i$. The kinetic term $\mathcal{K}_i^*$ relates to the mean square acceleration of the particles and may quantify an amount of activity. However, $\mathcal{K}_i^*$ should be interpreted as part of the functional measure; it determines the functional space over which to integrate [109]. In particular, $\mathcal{K}_i^*$ collects trajectories for which dv_i^2/dt remains finite when $dt \to 0$. The time-symmetric term $\mathcal{K}_i$ is identified as the dynamical activity, which has been introduced in the literature [110–114]. In discrete-state Markov-jump processes, the dynamical activity characterizes the time scale of the system and serves as an essential term in the speed-limit inequality [92] and the kinetic uncertainty relation [36]. Taking the average of $\mathcal{K}_i$, we explicitly obtain

$$\langle \mathcal{K}_i \rangle = \frac{\mathcal{T}}{4} \left(\frac{1}{T_i\gamma_i} \langle F_i(\boldsymbol{r})^2 \rangle - 3\frac{\gamma_i}{T_i} \langle v_i^2 \rangle + 4\frac{\gamma_i}{m_i} \right). \tag{4.15}$$

It can be easily confirmed that $\Upsilon = 4\sum_{i=1}^N \langle \mathcal{K}_i \rangle / \mathcal{T}$. Therefore, the term Υ in the derived bound is exactly the average dynamical activity. This implies that the current fluctuation in underdamped systems is not only constrained by the entropy production but also by its dynamical activity.

To clarify the role of dynamical activity in the bound, let us consider equilibrium systems (i.e., the external force $f_i(\boldsymbol{r}) = 0$ and the temperature $T_i = T$ for all $i = 1, \ldots, N$), where the

entropy production vanishes. The steady-state distribution is of a Maxwell–Boltzmann type,

$$P^{\mathrm{ss}}(\boldsymbol{r},\boldsymbol{v}) = C \exp\left[-\frac{1}{T}\left(\frac{1}{2}\sum_{i=1}^{N} m_i v_i^2 + U(\boldsymbol{r})\right)\right], \tag{4.16}$$

where C is the normalizing constant. The average dynamical activity is always positive, i.e., $\langle \mathcal{K}_i \rangle = \mathcal{T}\left(\langle F_i(\boldsymbol{r})^2\rangle/(T\gamma_i) + \gamma_i/m_i\right)/4 > 0$. The average current does not always vanish as in the equilibrium overdamped systems, for example, for $\boldsymbol{\Lambda}(\boldsymbol{r},\boldsymbol{v}) = \boldsymbol{v}$. Therefore, the fluctuation of a current in equilibrium is bounded only by the average dynamical activity.

In the following, we provide an explanation regarding why the dynamical activity appears in the lower bound of the current fluctuation in underdamped dynamics. For general Langevin systems, the probability currents can be decomposed into irreversible and reversible components [102]. In overdamped dynamics, which involves only the even variables, reversible currents are absent from the decomposition and the probability currents are irreversible. Both the entropy production and current fluctuation can be characterized via these probability currents. Therefore, the current fluctuation can be bounded solely by the associated entropy production. However, this is not the case for underdamped dynamics. Unlike in the case of overdamped dynamics, both irreversible and reversible currents exist in the decomposition of underdamped dynamics. Both types of currents jointly characterize the current fluctuation. Moreover, the entropy production is quantified via the irreversible currents, as in Eq. (4.4), and the dynamical activity is quantified via the reversible currents. Consequently, in underdamped dynamics, the current fluctuation is constrained not only by the entropy production but also by the dynamical activity.

4.1.3 Multidimensional TUR

Generally, there are correlations between currents in real-world systems. Simultaneously observing multiple currents is expected to yield more statistical information concerning the distribution. Therefore, the multidimensional TUR, which includes several currents in the observable, provides a tighter bound than does scalar TUR [105]. Such a bound can be applied to a study of the trade-off relationship between power and efficiency in steady-state heat engines [105, 115]. Here, we derive the multidimensional TUR for underdamped systems. We consider a vector observable $\boldsymbol{\Theta} \in \mathbb{R}^{M\times 1}$, defined by $\boldsymbol{\Theta}[\boldsymbol{\Gamma}] = \int_0^{\mathcal{T}} dt\, \boldsymbol{\Lambda}(\boldsymbol{r}) \circ \dot{\boldsymbol{r}}$, where $\boldsymbol{\Lambda} \in \mathbb{R}^{M\times N}$ is an arbitrary matrix-valued function of $\boldsymbol{r}$. By applying the information inequality for a multivariate estimator, we obtain (see Appendix A.5.1)

$$\mathrm{Cov}_\theta[\boldsymbol{\Theta}] \geq \mathcal{I}(\theta)^{-1} \partial_\theta \langle \boldsymbol{\Theta}\rangle_\theta \partial_\theta \langle \boldsymbol{\Theta}\rangle_\theta^{\top}, \tag{4.17}$$

where $\mathrm{Cov}_\theta[\boldsymbol{\Theta}] = [\mathrm{Cov}_\theta[\Theta_i;\Theta_j]] \in \mathbb{R}^{M\times M}$ is the covariance matrix of the estimator $\boldsymbol{\Theta}$ and the matrix inequality $\boldsymbol{X} \geq \boldsymbol{Y}$ indicates that $\boldsymbol{X}-\boldsymbol{Y}$ is positive semi-definite. Here, $\mathrm{Cov}_\theta[\Theta_i;\Theta_j] = \langle \Theta_i\Theta_j\rangle_\theta - \langle\Theta_i\rangle_\theta\langle\Theta_j\rangle_\theta$. Considering the same auxiliary dynamics as in Eq. (4.8), we obtain the multidimensional TUR as

$$\mathrm{Cov}[\boldsymbol{\Theta}] \geq \frac{2}{\Sigma}\langle\boldsymbol{\Theta}\rangle\langle\boldsymbol{\Theta}\rangle^{\top}. \tag{4.18}$$

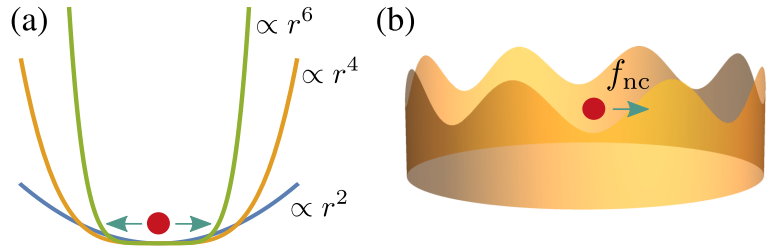

Figure 4.1: Schematic diagrams of systems used in simulations. (a) The particle is confined in a single-well potential $U(r) \propto r^{2n}$. There is no external force, and the system is in equilibrium. (b) The Brownian particle is driven out of equilibrium by a constant external force f_{nc} under a periodic potential $U(r) \propto \cos(2\pi n r/L)$.

From Eq. (4.18), one can derive various bounds for current fluctuation. For instance, in the case of two-dimensional currents, i.e., $\boldsymbol{\Theta} = [\Theta_1, \Theta_2]^\top$, the condition of the positive semi-definite matrix yields a tighter bound:

$$\mathrm{Var}[\Theta_1] \geq \frac{2}{\Sigma}\langle\Theta_1\rangle^2 + \sup_{\Theta_2} \frac{\left(\mathrm{Cov}[\Theta_1;\Theta_2] - \frac{2}{\Sigma}\langle\Theta_1\rangle\langle\Theta_2\rangle\right)^2}{\mathrm{Var}[\Theta_2] - \frac{2}{\Sigma}\langle\Theta_2\rangle^2}. \tag{4.19}$$

In addition to the variance of individual currents, this inequality also involves the correlation of two currents. A remarkable point in Eq. (4.19) is that, if a current Θ_1 satisfies $\mathrm{Var}[\Theta_1] = 2\langle\Theta_1\rangle^2/\Sigma$, then $\mathrm{Cov}[\Theta_1;\Theta_2] = 2\langle\Theta_1\rangle\langle\Theta_2\rangle/\Sigma$ holds for an arbitrary nonvanishing current Θ_2. Although the equality condition of the derived bound cannot be attained, inequalities like Eq. (4.19) provide insight into the correlation of currents. In particular, for overdamped dynamics, the current Θ_{tot} of stochastic total entropy production with a specific form of the drift function satisfies the equality condition [33]; thus, $\mathrm{Cov}[\Theta_{\mathrm{tot}};\Theta] = 2\langle\Theta\rangle$ for an arbitrary current Θ, which expresses a universal property of stochastic entropy production. Another direction is to derive an inequality directly from the definition of the positive semi-definite matrix, $\boldsymbol{x}^\top \left(\mathrm{Cov}[\boldsymbol{\Theta}] - 2\langle\boldsymbol{\Theta}\rangle\langle\boldsymbol{\Theta}\rangle^\top/\Sigma\right)^{-1}\boldsymbol{x} \geq 0$ for all $\boldsymbol{x} \in \mathbb{R}^{M\times 1}$ (if $\boldsymbol{X}$ is a non-singular, positive semi-definite matrix, then so is $\boldsymbol{X}^{-1}$). By choosing $\boldsymbol{x} = \langle\boldsymbol{\Theta}\rangle$, we obtain the following inequality (see Appendix A.5.2):

$$\langle\boldsymbol{\Theta}\rangle^\top \mathrm{Cov}[\boldsymbol{\Theta}]^{-1}\langle\boldsymbol{\Theta}\rangle \leq \frac{\Sigma}{2}, \tag{4.20}$$

which relates the means and covariances of multiple currents. For uncorrelated currents, i.e., $\mathrm{Cov}[\Theta_i;\Theta_j] = \delta_{ij}\mathrm{Var}[\Theta_i]$, one can obtain the following inequality from Eq. (4.20):

$$\sum_{i=1}^{M} \frac{\langle\Theta_i\rangle^2}{\mathrm{Var}[\Theta_i]} \leq \frac{\Sigma}{2}. \tag{4.21}$$

Equation (4.21) can be considered a generalization of Eq. (4.9). We note that inequalities analogous to Eqs. (4.20) and (4.21) have been derived for overdamped Langevin dynamics in Ref. [105]. However, they do not hold for general underdamped systems, although our derived bounds are always satisfied.

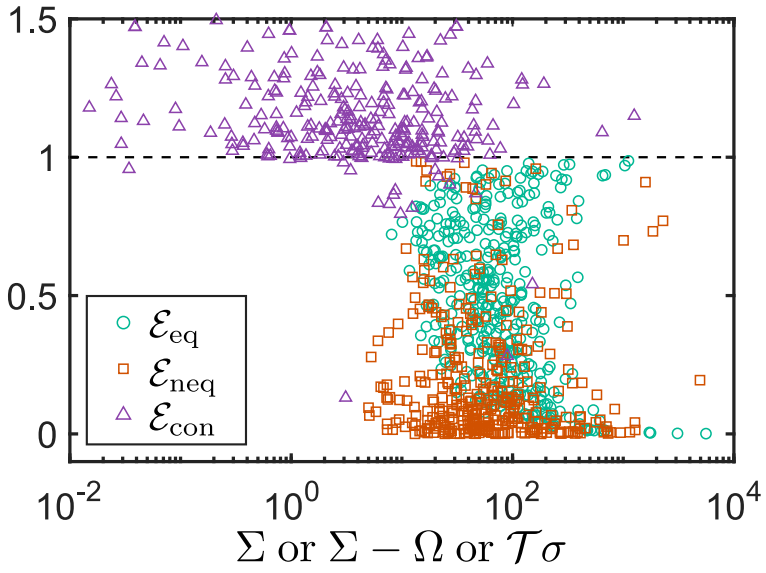

Figure 4.2: Numerical verification of the bounds. We randomly sample parameters and numerically solve the Langevin equation 10^6 times with the time step $\Delta t = 10^{-4}$. The parameter ranges are $m, \gamma, \alpha, T \in [0.1, 10]$ and $\mathcal{T} \in [1, 10]$. The dashed line depicts each saturated case of the bounds. For the single-well potential system, we calculate $\mathcal{E}_{\rm eq} \equiv 8\langle\Theta\rangle^2/(\Sigma\,{\rm Var}[\Theta])$, which should satisfy $\mathcal{E}_{\rm eq} \leq 1$, and plot $\mathcal{E}_{\rm eq}$ as a function of Σ with green circles. All circular points are located below the line, thus empirically verifying the derived bound [Eq. (4.12)]. Here, $n \in [1, 3]$. For the Brownian particle model, we evaluate $\mathcal{E}_{\rm neq} \equiv 2\langle\Theta\rangle^2/\{(\Sigma - \Omega)\,{\rm Var}[\Theta]\}$ since accurate calculation of Ω is difficult; $\mathcal{E}_{\rm neq}$ is plotted as a function of $\Sigma - \Omega$ with orange squares. Since Ω is nonnegative, the derived bound [Eq. (4.9)] is empirically verified if $\mathcal{E}_{\rm neq} \leq 1$ holds. It is possible that $\mathcal{E}_{\rm neq} > 1$ despite the derived bound being satisfied. We also simultaneously calculate $\mathcal{E}_{\rm con} \equiv 2\langle\Theta\rangle^2/(\mathcal{T}\sigma \cdot {\rm Var}[\Theta])$, which corresponds to the original bound [Eq. (1.4)], and plot it as a function of $\mathcal{T}\sigma$ with violet triangles. $\mathcal{E}_{\rm con} > 1$ indicates that the original bound is violated. As seen, all square points lie below the dashed line and the derived bound is empirically verified. By comparison, many triangular points are located above the line, thus implying that the original bound is violated. Here, $L = 1$, $f_{\rm nc} \in [0.1, 10]$ and $n \in [1, 10]$.

4.1.4 Numerical illustration

We illustrate our results [Eqs. (4.9) and (4.12)] with the aid of two systems. We first consider an equilibrium system under the symmetric single-well potential $U(r) = \alpha r^{2n}/(2n)$ with n as a positive integer, as illustrated in Fig. 4.1(a). The total force acting upon the particle is $F(r) = -\alpha r^{2n-1}$. For this system, the dynamical activity Υ and the boundary term Ω can be calculated analytically as

$$\Upsilon = \frac{\alpha^2}{T\gamma}\left(\frac{\alpha}{2nT}\right)^{-2+1/n}\frac{G(2-\frac{1}{2n})}{G(\frac{1}{2n})} + \frac{\gamma}{m},\ \Omega = 4, \tag{4.22}$$

where $G(z) = \int_0^\infty dx\, x^{z-1}e^{-x}$ is the gamma function. Since the entropy production vanishes, Σ can be expressed as $\Sigma = 4\mathcal{T}\Upsilon + 4$. We consider current $\Theta[\mathbf{\Gamma}] = \int_0^{\mathcal{T}} dt\, v^2$, which is proportional to the accumulated kinetic energy of the particle. According to Eq. (4.12), the bound on this current fluctuation reads $\mathrm{Var}[\Theta]/\langle\Theta\rangle^2 \geq 8/\Sigma$, which is illustrated in Fig. 4.2. We find that the bound is satisfied for all selected parameter settings.

Next, we study a Brownian particle circulating on a ring of circumference L under a periodic potential $U(r) = \alpha L/(2\pi n)\cos(2\pi n r/L)$, with integer $n > 0$ (see Fig. 4.1(b) for illustration). The total force acting upon the particle is $F(r) = -\partial_r U(r) + f_{\mathrm{nc}}$, where f_{nc} is a constant external force that drives the particle out of equilibrium. In the steady state, the entropy production rate becomes $\sigma = f_{\mathrm{nc}}\langle v\rangle/T$. We validate the derived bound for current $\Theta[\mathbf{\Gamma}] = \int_0^{\mathcal{T}} dt\, \dot{r}$, which corresponds to the accumulated distance traveled by the particle. According to Eq. (4.9), we have $\mathrm{Var}[\Theta]/\langle\Theta\rangle^2 \geq 2/\Sigma$. This and the original bound are illustrated in Fig. 4.2. We find that the original bound can be violated; thus, Eq. (1.4) does not hold for general underdamped systems. In comparison, our bound is always satisfied and, thus, Eq. (4.9) is empirically verified.

4.1.5 TUR for active matter systems

We consider a model system of active matter, namely, active Ornstein–Uhlenbeck particles (AOUPs), as has been studied in the literature [98, 99]. The system contains N self-propelled particles, which extract energy from the surrounding environment and exhibit self-induced motion. The dynamics of the particle i are governed by

$$\dot{r}_i = -\mu\partial_{r_i}\Phi(\boldsymbol{r}) + \eta_i,\ \tau\dot{\eta}_i = -\eta_i + \xi_i, \tag{4.23}$$

where μ is the mobility of particles, $\Phi(\boldsymbol{r})$ is an interaction potential, ξ_i's are zero-mean Gaussian white noises with properties $\langle\xi_i(t)\xi_j(t')\rangle = 2D_i\delta_{ij}\delta(t-t')$, and η_i's are Ornstein–Uhlenbeck processes with variances $\langle\eta_i(0)\eta_j(t)\rangle = D_i\delta_{ij}e^{-|t|/\tau}/\tau$. Here, τ is the persistent time. In the $\tau \to 0$ limit, η_i's become white noises with delta-function variances and r_i's become Markovian processes. It is interesting that the force that drives the system out of equilibrium arises from the nonequilibrium environment. To develop stochastic thermodynamics for the system, a mathematical mapping to an underdamped dynamics has been conducted by introducing velocity variables [98–100]. Specifically, taking the time derivative

of Eq. (4.23), the system dynamics can be mapped to the following underdamped dynamics:

$$\dot{r}_i = v_i, \;\; \tau\dot{v}_i = -v_i - \mu\left(1 + \tau\sum_{k=1}^{N} v_k\partial_{r_k}\right)\partial_{r_i}\Phi(\boldsymbol{r}) + \xi_i. \tag{4.24}$$

By applying our approach to these underdamped dynamics, an uncertainty relation for an arbitrary observable $\Theta[\boldsymbol{\Gamma}] = \int_0^{\mathcal{T}} dt\, \boldsymbol{\Lambda}(\boldsymbol{r})^\top \circ \dot{\boldsymbol{r}}$ can be obtained as follows:

$$\frac{\mathrm{Var}[\Theta]}{\langle\Theta\rangle^2} \geq \frac{2}{\Sigma}, \tag{4.25}$$

where $\Sigma = \mathcal{T}(9\sigma + 4\Upsilon_a) + \Omega$ and

$$\Upsilon_a = \sum_{i=1}^{N}\frac{1}{D_i}\left\langle \tau\mu\sum_{j=1}^{N} v_i v_j \partial^2_{r_i r_j}\Phi(\boldsymbol{r}) - 2\left(\sum_{j=1}^{N} v_j\left[\delta_{ij} + \tau\mu\partial^2_{r_i r_j}\Phi(\boldsymbol{r})\right]\right)^2 + \frac{3D_i}{\tau}\left(1 + \tau\mu\partial^2_{r_i}\Phi(\boldsymbol{r})\right)\right\rangle. \tag{4.26}$$

The detailed derivation of the bound is given in Appendix A.6. We note that the definition of the total entropy production in the AOUPs system is not unique and depends on the chosen coarse-grained model. The definition employed here is the same as in Ref. [98].

4.1.6 Concluding remarks and discussion

In summary, we have derived the bounds on the current fluctuation in underdamped Langevin dynamics using information inequalities. Our results indicated that the current fluctuation is constrained not only by the entropy production but also by the average dynamical activity. The derived bound can be used as a tool for estimating thermodynamic quantities from the experimental data. Deriving a bound for general currents of the form $\int dt\,[\boldsymbol{\Lambda}_1(\boldsymbol{r},\boldsymbol{v})^\top \circ \dot{\boldsymbol{r}} + \boldsymbol{\Lambda}_2(\boldsymbol{r},\boldsymbol{v})^\top \circ \dot{\boldsymbol{v}}]$ requires further investigation.

4.2 Bounds for systems driven by arbitrary control protocol

In this section, we focus on extending the applicability of TURs that have been derived for currents in steady-state systems. Considering general Langevin systems driven by an arbitrary time-dependent control protocol, we derive uncertainty relations for both current and noncurrent observables that satisfy a scaling condition. We prove for both overdamped and underdamped systems that the observable fluctuation is bounded by entropy production and a kinetic term. Notably, the derived bounds are not static; however, they are dynamic with respect to the observables and are tighter than the original for a broad class of observables. When the target system is unidirectionally affected by other systems, we prove a tighter bound for observables in the target system. That is, fluctuations of the observables are not constrained by the dissipation costs of other systems but by the information flows between them and the target system. Our results allow the investigation of arbitrary Langevin systems, ranging from relaxation processes to externally controlled systems such as stochastic

heat engines. We apply the results to investigate three systems: a dragged Brownian particle, a Brownian gyrator, and a stochastic underdamped heat engine.

4.2.1 Main results

For the sake of simplicity, we will describe our results with one-dimensional systems. The generalization to multidimensional systems is straight-forward. Unlike in most previous studies, where the system is assumed to be in a stationary or in a transient regime, here, the system starts from an arbitrary distribution at time $t = 0$ and is subsequently driven by an external control protocol λ up to time $t = \tau$. When λ is absent, it becomes a relaxation process. Let Γ denote the trajectory of system states during this time interval and $\phi(\Gamma)$ be a trajectory-dependent observable which can be time-symmetric. We aim to derive a bound on the relative fluctuation of $\phi(\Gamma)$.

We consider observables that satisfy the scaling condition: $\phi(\theta\Gamma) = \theta^\kappa \phi(\Gamma)$ for some constant $\kappa > 0$ and for all $\theta \in \mathbb{R}$. Given a trajectory $\Gamma = [x(t)]_{t=0}^{t=\tau}$, this can be satisfied with a current $\phi(\Gamma) = \int_0^\tau dt\, x^{\kappa-1} \circ \dot{x}$ or a noncurrent observable $\phi(\Gamma) = \int_0^\tau dt\, x^\kappa$. Here, $\circ$ denotes the Stratonovich product and the dot indicates the time derivative. Moreover, ϕ can be a discrete-time observable, e.g., $\phi(\Gamma) = \sum_i c_i x(t_i)^\kappa$, where $0 \le t_i \le \tau$ is the predetermined time and c_i is an arbitrary coefficient. From a practical perspective, measurements are discretely performed in most cases; thus, the acquisition of continuous-time observables may be difficult. Consequently, a bound on such discrete-time observables provides a useful tool with regard to thermodynamic inference problems. It is noteworthy that these noncurrent observables cannot be applied with the TURs previously reported. Hereafter, we consider these three types of observables.

Bounds for a full system

First, we consider a general overdamped Langevin system, whose dynamics are governed by the following equation:

$$\dot{x} = F(x, \lambda) + \xi, \tag{4.27}$$

where $F(x, \lambda)$ is the total force and ξ is a zero-mean Gaussian white noise with variance $\langle \xi(t)\xi(t') \rangle = 2D\delta(t - t')$. Here, $D > 0$ denotes the noise intensity. Throughout this chapter, Boltzmann's constant is set to $k_\mathrm{B} = 1$. Let $\rho(x, t)$ denote the probability distribution function of the system being in state x at time t. Then, its time evolution can be described using the Fokker–Planck equation as $\partial_t \rho(x, t) = -\partial_x j(x, t)$, where $j(x, t) = F(x, \lambda)\rho(x, t) - D\partial_x \rho(x, t)$ is the probability current. The dynamical solution of this differential equation is uniquely determined if the initial distribution $\rho(x, 0) = \rho_\mathrm{i}(x)$ is given.

As our first main result, we prove that the observable fluctuation is bounded as

$$\frac{\langle \phi \rangle^2}{\langle\langle \phi \rangle\rangle} \le \frac{1}{\kappa^2} \left(2\langle \sigma \rangle + \chi_\mathrm{o} + \psi_\mathrm{o} \right), \tag{4.28}$$

where $\chi_{\mathrm{o}} := \langle \int_0^\tau dt\, \Lambda_{\mathrm{o}}(x,t) \rangle$ is a kinetic term and $\psi_{\mathrm{o}} := \langle (x\partial_x \rho_{\mathrm{i}}/\rho_{\mathrm{i}})^2 \rangle_{\rho_{\mathrm{i}}} - 1$ is a nonnegative boundary value that can be neglected for long observation times. Here, $\Lambda_{\mathrm{o}} = [(\partial_x [xF])^2 - 4F\partial_x (xF) - 4D\partial_x^2 (xF)]/2D$ is a function in terms of force and position.

Next, we consider a general underdamped Langevin system, where inertial effects cannot be neglected. The system consists of a particle being in contact with an equilibrium heat bath. Its dynamics are described by the following equations:

$$\dot{x} = v, \;\; m\dot{v} = -\gamma v + F(x,\lambda) + \xi, \tag{4.29}$$

where m, γ are the mass and friction coefficient of the particle, respectively. Let $\rho(x,v,t)$ be the phase-space probability distribution function of the system at time t. Assuming that the system evolves from an initial distribution $\rho(x,v,0) = \rho_{\mathrm{i}}(x,v)$; then, $\rho(x,v,t)$ follows the Fokker–Planck equation, $\partial_t \rho(x,v,t) = -\partial_x j_x(x,v,t) - \partial_v j_v(x,v,t)$, where $j_x(x,v,t) = v\rho(x,v,t)$ and $j_v(x,v,t) = 1/m[-\gamma v + F(x,\lambda) - D/m\partial_v]\rho(x,v,t)$ are probability currents. Since the position x and the velocity v are the freedom degrees of the system, the trajectory can be written as $\Gamma = [x(t), v(t)]_{t=0}^{t=\tau}$.

For observables that satisfy the scaling condition, we prove that

$$\frac{\langle \phi \rangle^2}{\langle\langle \phi \rangle\rangle} \leq \frac{1}{\kappa^2} \left(2\langle \sigma \rangle + \chi_{\mathrm{u}} + \psi_{\mathrm{u}}\right), \tag{4.30}$$

where $\chi_{\mathrm{u}} := \langle \int_0^\tau dt\, \Lambda_{\mathrm{u}}(x,v,t) \rangle$ is a kinetic term and $\psi_{\mathrm{u}} := \langle [(x\partial_x \rho_{\mathrm{i}} + v\partial_v \rho_{\mathrm{i}})/\rho_{\mathrm{i}}]^2 \rangle_{\rho_{\mathrm{i}}} - 4$ is a nonnegative boundary term that can be neglected for large τ. Here, $\Lambda_{\mathrm{u}} = [(F - x\partial_x F)^2 - 4\gamma^2 v^2 + 8\gamma D/m]/2D$. Inequality (4.30) is our second main result. The detailed derivations of the bounds and the generalization to the multidimensional case are presented in Appendix B.1 and B.2, respectively.

We make several remarks about our main results [Eqs. (4.28) and (4.30)]. These inequalities hold for arbitrary protocol λ, arbitrary initial distribution ρ_{i}, and finite observation time τ; thus, they are also valid for steady-state systems. Interestingly, the derived bounds involve the scaling power κ; as κ is large enough, the bounds become tighter than the original [Eq. (1.4)]. Moreover, unlike the reported bounds, which deal only with currents, our bounds are applicable for current, noncurrent, and discrete-time observables, as well as for linear combinations of these observables with the same scaling power.

In addition to entropy production, the bounds contain kinetic terms $\chi_{\{\mathrm{o},\mathrm{u}\}}$. They are averages of observables, which can be calculated based on the observed trajectories. As will be shown later, these terms play an important role in the bounds, i.e., the observable fluctuation cannot be solely bounded by the entropy production, even with the exponential bound $(e^{\langle\sigma\rangle} - 1)/2$. Furthermore, the fluctuation of a noncurrent observable, $\langle \phi \rangle^2/\langle\langle \phi \rangle\rangle$, may not vanish in equilibrium, for example, for $\phi(\Gamma) = \int_0^\tau dt\, x^2$, while entropy production always does, i.e., $\langle \sigma \rangle = 0$. In this scenario, $\chi_{\{\mathrm{o},\mathrm{u}\}}$ are the key quantities that constrain fluctuations of such noncurrent observables.

We provide an intuitive explanation regarding why kinetic terms appear in the bounds. Entropy production, which is quantified via irreversible currents of probability density, characterizes the strength of the currents in the system. Zero entropy production implies that

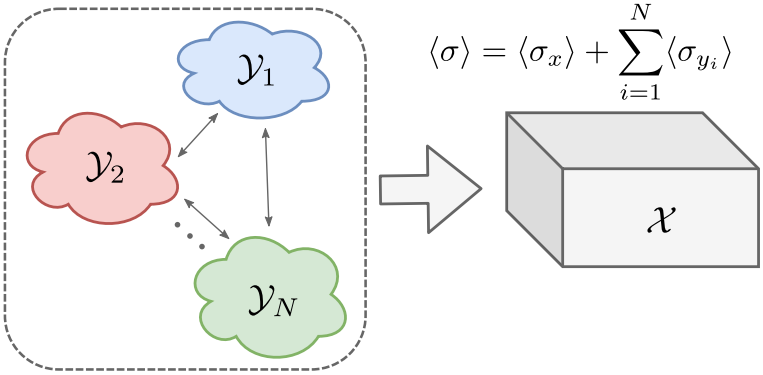

Figure 4.3: Illustration of multipartite interacting systems described by Langevin equations. The target system $\mathcal{X}$ is unidirectionally affected by other systems $\mathcal{Y}_1, \ldots, \mathcal{Y}_N$. The total entropy production $\langle\sigma\rangle$ of the full system (including $\mathcal{X}, \mathcal{Y}_1, \ldots, \mathcal{Y}_N$) can be decomposed into nonnegative components as $\langle\sigma\rangle = \langle\sigma_x\rangle + \sum_{i=1}^{N}\langle\sigma_{y_i}\rangle$, in which each component represents the contribution of the entropy production from each corresponding system.

there is no current in the system. Therefore, its genuine contribution to the bounds is the constraint on fluctuations of currents. To constrain fluctuations of noncurrent components (e.g., time-symmetric changes), another complement to entropy production, which is identified here as χ, is necessary [91].

With respect to attaining the derived bounds, one can show that the exact equality condition cannot be attained (from the equality condition of the Cauchy–Schwarz inequality) [53]. Unlike original TUR, which is saturated near equilibrium [33], attaining the derived bounds is not ensured in such regimes. As shown later, the bounds become tight for long observation times. For short observation times, a gap exists between the fluctuations of the observables and the derived bounds. This occurs due to the dominance of the boundary terms, $\psi_{\mathrm{o,u}}$.

Bounds for a subsystem

Let us consider a situation where the target system $\mathcal{X}$ undergoes unidirectional interactions with other systems $\mathcal{Y}_1, \ldots, \mathcal{Y}_N$. Each of these systems is coupled to a distinct thermal reservoir. We assume that $\mathcal{X}$ does not affect the dynamics of $\mathcal{Y}_i$ for all i, while each system $\mathcal{Y}_i$ can arbitrarily affect other systems (see Fig. 4.3 for the illustration). An example of this situation is a system that involves continuous-time imperfect measurement and feedback control. The systems $\{\mathcal{Y}_i\}$ correspond to the errors in the readout when performing measurements on $\mathcal{X}$. These errors instantly affect the system dynamics of $\mathcal{X}$ via feedback control. For simplicity, we consider the case $N = 1$, and the system states of $\mathcal{X}$ and $\mathcal{Y}$ are represented by variables x and y, respectively. The dynamics of $\mathcal{X}$ and $\mathcal{Y}$ are governed by the following equations:

$$\dot{x} = F_x(x, y, \lambda) + \xi_x, \tag{4.31}$$

$$\dot{y} = F_y(y, \lambda) + \xi_y, \tag{4.32}$$

where ξ_x and ξ_y are uncorrelated zero-mean Gaussian white noises satisfying $\langle\xi_z(t)\xi_z(t')\rangle = 2D_z\delta(t - t')$, for each $z \in \{x, y\}$. Let $\rho_{\mathrm{i}}(x, y) := \rho(x, y, 0)$ denote the distribution function at

time $t = 0$. The corresponding Fokker–Planck equation reads $\partial_t \rho(x, y, t) = -\sum_{z\in\{x,y\}} \partial_z j_z(x, y, t)$, where $j_z = F_z\rho - D_z\partial_z\rho$ is the probability current.

The entropy production of the full system (including both $\mathcal{X}$ and $\mathcal{Y}$) is given by

$$\langle\sigma\rangle = \int_0^\tau dt \int dxdy \left(\frac{j_x(x, y, t)^2}{D_x\rho(x, y, t)} + \frac{j_y(x, y, t)^2}{D_y\rho(x, y, t)}\right). \tag{4.33}$$

It can be rewritten as $\langle\sigma\rangle = \langle\sigma_x\rangle + \langle\sigma_y\rangle$, where $\langle\sigma_z\rangle = \int_0^\tau dt \int dxdy\, j_z(x, y, t)^2/D_z\rho(x, y, t) \geq 0$ is the entropy production contribution from $z \in \{x, y\}$. Moreover, $\langle\sigma_x\rangle$ can be further decomposed as $\langle\sigma_x\rangle = \langle\Delta s_x\rangle + \langle q_x\rangle/D_x + I_x$ [116], where $\langle\Delta s_x\rangle$ denotes the change in the Shannon entropy of $\mathcal{X}$, $\langle q_x\rangle$ denotes the heat flow from $\mathcal{X}$ to the reservoir, and I_x represents information flow into and out of $\mathcal{X}$. Note that because of information exchanged between $\mathcal{X}$ and $\mathcal{Y}$, $\langle\Delta s_x\rangle + \langle q_x\rangle/D_x$ can be negative.

For arbitrary observables involving only x and satisfying the scaling condition with the scaling power κ, we can prove that

$$\frac{\langle\phi\rangle^2}{\langle\langle\phi\rangle\rangle} \leq \frac{1}{\kappa^2}(2\langle\sigma_x\rangle + \chi_x + \psi_x), \tag{4.34}$$

where $\chi_x := \langle\int_0^\tau dt\, \Lambda_x(x, y, t)\rangle$ is a kinetic term and $\psi_x := \langle(x\partial_x\rho_{\rm i}/\rho_{\rm i})^2\rangle_{\rho_{\rm i}} - 1$ is a nonnegative boundary value. Here, $\Lambda_x = [(\partial_x[xF_x])^2 - 4F_x\partial_x(xF_x) - 4D_x\partial_x^2(xF_x)]/2D_x$. Inequality (4.34) is our third main result. Note that the bound in Eq. (4.28) also holds for this situation when we consider a full system that includes both $\mathcal{X}$ and $\mathcal{Y}$. The difference between these bounds [Eqs. (4.28) and (4.34)] is that the former contains terms that originate from all the systems, i.e., $\mathcal{X}$ and $\mathcal{Y}$, while the latter only involves contributions from $\mathcal{X}$. Focusing on the entropy production term, $\langle\sigma_x\rangle$, the bound in Eq. (4.34) implies that the fluctuations of the observables in $\mathcal{X}$ are not constrained by the dissipation in $\mathcal{Y}$ but by that in $\mathcal{X}$, $\langle\Delta s_x\rangle + \langle q_x\rangle/D_x$, and the information flow between $\mathcal{X}$ and $\mathcal{Y}$, I_x. This implication agrees with intuition. In general, the bound in Eq. (4.34) is tighter than that in Eq. (4.28) and reduces to the same one when there is no interaction between $\mathcal{X}$ and $\mathcal{Y}$. A bound for underdamped systems can be analogously derived. The derivation of Eq. (4.34) is provided in Appendix B.3.

4.2.2 Numerical illustration

In this section, we illustrate our results with the help of three systems, as follows.

Dragged Brownian particle

First, we investigate a dragged Brownian particle confined in a harmonic potential $U(x, \lambda) = c(x - \lambda)^2/2$, where $c > 0$ is a constant [see Fig. 4.4(a) for illustration]. The total force is $F(x, \lambda) = -\partial_x U(x, \lambda)$, and the particle position is governed by the following equation:

$$\dot{x} = c(\lambda - x) + \xi. \tag{4.35}$$

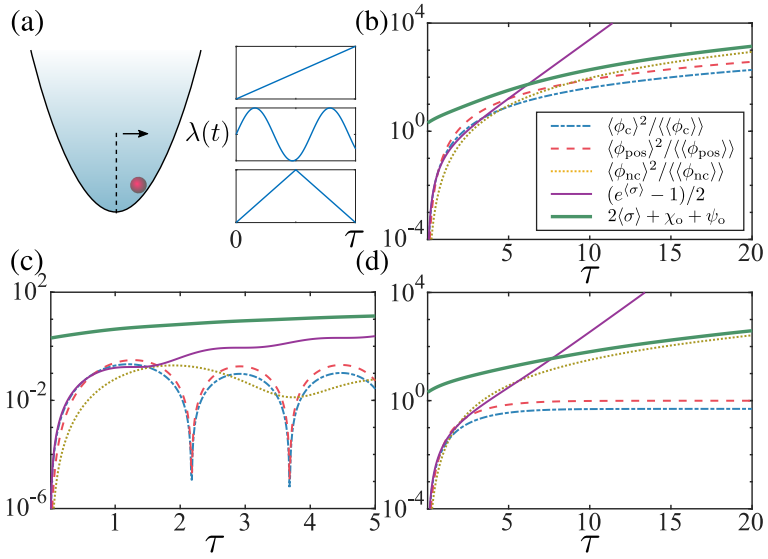

Figure 4.4: (a) Schematic diagram of the dragged Brownian particle with the control protocol λ. Bound on fluctuations of the observables under (b) time-linear, (c) time-periodic, and (d) time-symmetric protocols [Eq. (4.37)]. The dashed-dotted, dashed, dotted, thin, and thick solid lines represent the fluctuations $\langle\phi_{\rm c}\rangle^2/\langle\langle\phi_{\rm c}\rangle\rangle$, $\langle\phi_{\rm pos}\rangle^2/\langle\langle\phi_{\rm pos}\rangle\rangle$, $\langle\phi_{\rm nc}\rangle^2/\langle\langle\phi_{\rm nc}\rangle\rangle$, the exponential bound $(e^{\langle\sigma\rangle}-1)/2$, and the derived bound $2\langle\sigma\rangle+\chi_{\rm o}+\psi_{\rm o}$, respectively. The derived bound is always satisfied, while the exponential bound is violated for all three cases. The observation time τ is varied, while the remaining parameters are fixed as $c=1, \alpha=1, \beta=2$, and $D=1$.

We consider three cases: (a) a time-linear protocol $\lambda(t)=\alpha t$, (b) a time-periodic protocol $\lambda(t)=\alpha\sin(\beta t)$, and (c) a time-symmetric protocol

$$\lambda(t)=\begin{cases}\alpha t, & 0\le t\le \tau/2,\\ \alpha(\tau-t), & \tau/2<t\le\tau,\end{cases} \tag{4.36}$$

where α and β are positive constants. We assume that the system is initially in equilibrium with the distribution $\rho_{\rm i}(x)\propto\exp(-cx^2/2D)$. We consider three observables: a current representing the particle's displacement $\phi_{\rm c}(\Gamma)=x(\tau)-x(0)$, the final position $\phi_{\rm pos}(\Gamma)=x(\tau)$, and a noncurrent observable $\phi_{\rm nc}(\Gamma)=\int_0^\tau dt\,x$, which represents the area under the trajectory. These observables satisfy the scaling condition with $\kappa=1$, i.e., $\phi(\theta\Gamma)=\theta\phi(\Gamma)$. According to the derived bound [Eq. (4.28)], inequality

$$\frac{\langle\phi\rangle^2}{\langle\langle\phi\rangle\rangle}\le 2\langle\sigma\rangle+\chi_{\rm o}+\psi_{\rm o} \tag{4.37}$$

should be satisfied for all $\phi\in\{\phi_{\rm c},\phi_{\rm pos},\phi_{\rm nc}\}$. All the terms in this bound can be analytically calculated in the following.

Let $\rho(x,t)$ be the probability distribution function of x at time t. Since the force is linear, the distribution is Gaussian, i.e., $\rho(x,t)=\mathcal{N}(x;\mu(t),\vartheta(t))$, where $\mu(t)$ and $\vartheta(t)$ are the mean and variance, respectively. The initial conditions are $\mu(0)=0$, $\vartheta(0)=D/c$. From the

Fokker–Planck equation, we obtain

$$\dot{\mu}(t) = c\,[\lambda(t) - \mu(t)]\,, \quad \vartheta(t) = \frac{D}{c}. \tag{4.38}$$

Solving the differential equation [Eq. (4.38)] with respect to $\mu(t)$, we obtain

$$\mu(t) = c\int_0^t ds\, e^{-c(t-s)}\lambda(s). \tag{4.39}$$

Using the Laplace transform, the analytical solution of Eq. (4.35) can be expressed as

$$x(t) = \mu(t) + x_0 e^{-ct} + \int_0^t ds\, e^{-c(t-s)}\xi(s). \tag{4.40}$$

From Eq. (4.40), we obtain

$$\langle [x(t) - \mu(t)][x(t') - \mu(t')]\rangle = \frac{D}{c}e^{-c|t-t'|}. \tag{4.41}$$

The observable averages can be analytically calculated, i.e., $\langle \phi_{\rm c}\rangle = \langle \phi_{\rm pos}\rangle = \mu(\tau)$ and $\langle \phi_{\rm nc}\rangle = \int_0^\tau dt\,\mu(t)$. Analogously, the variances of the observables are obtained as $\langle\langle \phi_{\rm c}\rangle\rangle = 2D(1 - e^{-c\tau})/c$, $\langle\langle \phi_{\rm pos}\rangle\rangle = D/c$, and $\langle\langle \phi_{\rm nc}\rangle\rangle = 2D(e^{-c\tau} + c\tau - 1)/c^3$. The terms in the bound can be analytically calculated as

$$\langle\sigma\rangle = \frac{c^2}{D}\int_0^\tau dt\,(\lambda(t) - \mu(t))^2, \tag{4.42}$$

$$\chi_{\rm o} = 2c\tau - \frac{c^2}{2D}\int_0^\tau dt\left[4\mu(t)^2 + 3\lambda(t)^2 - 8\lambda(t)\mu(t)\right], \tag{4.43}$$

$$\psi_{\rm o} = 2. \tag{4.44}$$

We illustrate the bound [Eq. (4.37)] in Fig. 4.4(b)–(d), where the derived bound is always satisfied and the exponential bound is violated. As seen, for short observation times, a gap exists between the bound and the fluctuation. However, as τ is increased, the gap is reduced and the bound becomes tight.

Brownian gyrator

Next, we study a Brownian gyrator [117], which is a minimal microscopic heat engine that has recently been experimentally realized in an electronic and a colloidal system [118, 119]. The system consists of a particle with two degrees of freedom, $\boldsymbol{x} = [x_1, x_2]^\top$, trapped in an elliptical harmonic potential $U(\boldsymbol{x}) = [u_1\,(x_1\cos\alpha + x_2\sin\alpha)^2 + u_2\,(-x_1\sin\alpha + x_2\cos\alpha)^2]/2$, where $u_1, u_2 > 0$ are stiffnesses along its principal axes, and α is the rotation angle. The particle is simultaneously in contact with two heat baths at different temperatures acting in perpendicular directions [Fig. 4.5(a)]. The particle position follows overdamped Langevin equations,

$$\gamma_i \dot{x}_i = -\partial_{x_i} U(\boldsymbol{x}) + \xi_i,\ \ (i = 1, 2), \tag{4.45}$$

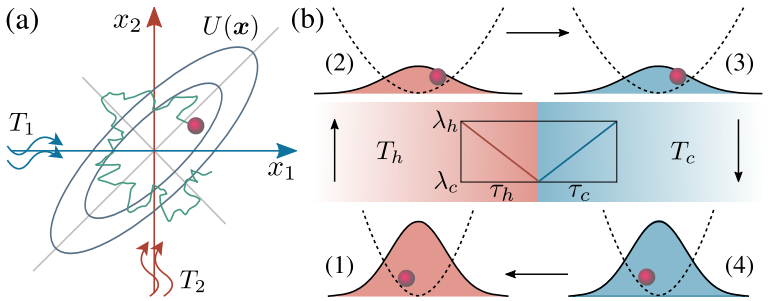

Figure 4.5: Schematic diagrams of (a) the Brownian gyrator and (b) the stochastic underdamped heat engine. A cyclic period consists of four steps: isothermal expansion for a time τ_h [(1) → (2)], instantaneously cooling the heat bath to temperature T_c [(2) → (3)], isothermal compression for a time τ_c [(3) → (4)], and instantaneously heating the heat bath to temperature T_h [(4) → (1)]. The solid and dashed lines represent the probability distribution $\rho(x,t)$ and the potential $U(x,\lambda)$, respectively.

where γ_i is the friction coefficient and ξ_i is the zero-mean Gaussian white noise with covariance $\langle \xi_i(t)\xi_j(t')\rangle = 2\delta_{ij}\gamma_i T_i \delta(t-t')$. Here, $T_1 \neq T_2$ are the temperatures of the heat baths. In generic cases, i.e., $u_1 \neq u_2$, the potential is asymmetric and a systematic gyrating motion of the particle around the potential minimum is induced due to the flow of heat. The interesting observable is the accumulated torque exerted by the particle on the potential

$$\phi_{\rm t}(\Gamma) = \int_0^\tau dt \left[x_1 \partial_{x_2} U(\boldsymbol{x}) - x_2 \partial_{x_1} U(\boldsymbol{x})\right]. \tag{4.46}$$

This observable is time-symmetric; thus, all TURs previously reported cannot be applied. Since $\phi_{\rm t}(\theta\Gamma) = \theta^2 \phi_{\rm t}(\Gamma)$, the following bound on torque fluctuation should be satisfied:

$$\frac{\langle \phi_{\rm t}\rangle^2}{\langle\langle \phi_{\rm t}\rangle\rangle} \leq \frac{\langle\sigma\rangle}{2} + \frac{\chi_{\rm o} + \psi_{\rm o}}{4}. \tag{4.47}$$

We illustrate Eq. (4.47) in Fig. 4.6(a). The fluctuation $\langle \phi_{\rm t}\rangle^2/\langle\langle \phi_{\rm t}\rangle\rangle$ is numerically evaluated, while $\langle\sigma\rangle$, $\chi_{\rm o}$, and $\psi_{\rm o}$ are analytically calculated. As seen, the bound is always satisfied when the observation time τ is varied. Positive entropy production is needed to generate a nonzero torque. However, the fluctuation cannot be bounded solely by entropy production, even with the exponential bound $(e^{\langle\sigma\rangle} - 1)/2$.

Stochastic underdamped heat engine

Lastly, we consider a stochastic underdamped heat engine comprising a particle trapped in a harmonic potential $U(x,\lambda) = \lambda x^2/2$ [120] [see Fig. 4.5(b)]. The particle is embedded in a heat bath, whose temperature T is cyclically varied to operate the system as a heat engine. Its dynamics are described using the Langevin equation,

$$m\dot{v} = -\gamma v - \lambda x + \xi, \tag{4.48}$$

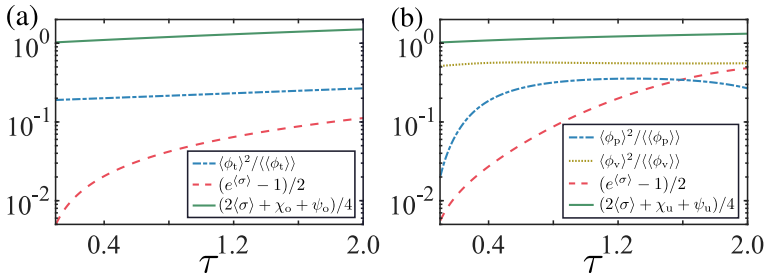

Figure 4.6: (a) Bound on the fluctuation of the accumulated torque [Eq. (4.47)]. The system is in steady state, wherein the distribution is Gaussian. The dashed-dotted, dashed, and solid lines represent the fluctuation $\langle\phi_t\rangle^2/\langle\langle\phi_t\rangle\rangle$, the exponential bound $(e^{\langle\sigma\rangle}-1)/2$, and the derived bound $(2\langle\sigma\rangle+\chi_o+\psi_o)/4$, respectively. The derived bound is always satisfied, while the exponential bound is not. The parameters are $\alpha=\pi/4$, $\gamma_1=\gamma_2=10$, $u_1=1$, $u_2=4$, $T_1=1$, and $T_2=4$. (b) Bound on fluctuations of the power output and the accumulated kinetic energy [Eq. (4.50)]. The fluctuations $\langle\phi_p\rangle^2/\langle\langle\phi_p\rangle\rangle, \langle\phi_v\rangle^2/\langle\langle\phi_v\rangle\rangle$, the exponential bound $(e^{\langle\sigma\rangle}-1)/2$, and the derived bound $(2\langle\sigma\rangle+\chi_u+\psi_u)/4$ are depicted by the dashed-dotted, dotted, dashed, and solid lines, respectively. The fluctuations exceed the exponential bound, while they are always smaller than the derived bound. The initial distribution ρ_i is a centered Gaussian with variances $\langle x^2\rangle=10, \langle v^2\rangle=1$, and $\langle xv\rangle=0$. The parameters are $m=1, \gamma_c=\gamma_h=0.1, T_c=1, T_h=4, \lambda_c=0.1, \lambda_h=2$, and $\tau_c=\tau_h=\tau/2$.

where the noise variance is $\langle\xi(t)\xi(t')\rangle=2\gamma T\delta(t-t')$. We employ a time-linear protocol [121]

$$\lambda(t)=\begin{cases}\lambda_h+(\lambda_c-\lambda_h)t/\tau_h, & 0\le t<\tau_h,\\ \lambda_c+(\lambda_h-\lambda_c)(t-\tau_h)/\tau_c, & \tau_h\le t<\tau,\end{cases} \tag{4.49}$$

where τ_h, τ_c are the coupling times to the hot and cold heat baths, respectively, and $\tau=\tau_h+\tau_c$ is the total observation time. The work w exerted on the particle during the period is equal to $w(\Gamma)=\int_0^\tau dt\,\partial_\lambda U(x,\lambda)\dot\lambda$. We consider two observables: the power output $\phi_p=-w/\tau$ and the accumulated kinetic energy $\phi_v=\int_0^\tau dt\,v^2$. Since $\phi(\theta\Gamma)=\theta^2\phi(\Gamma)$, fluctuations of these observables are bounded as

$$\frac{\langle\phi\rangle^2}{\langle\langle\phi\rangle\rangle}\le\frac{\langle\sigma\rangle}{2}+\frac{\chi_u+\psi_u}{4} \tag{4.50}$$

for $\phi\in\{\phi_p,\phi_v\}$. We assume that the initial distribution $\rho_i(x,v)$ is Gaussian and illustrate Eq. (4.50) in Fig. 4.6(b). As shown, the derived bound is always satisfied, while the fluctuations cannot be constrained by the exponential bound.

We illustrate the implication of our results for the power output of heat engines. The original TUR has been exploited to derive a bound on the fluctuation of power output in steady-state heat engines [115]. It indicates that a steady-state heat engine operating with Carnot's efficiency $\eta_C=1-T_c/T_h$ and delivering work with a finite fluctuation is impossible. However, our bound does not imply this consequence in the same manner as the original bound. It has been shown that one can construct a cyclic Brownian heat engine operating with efficiency asymptotically close to η_C at nonzero power output with vanishing fluctuations [122]. Our bound is applicable to such an engine and such arbitrary heat engines described

using Langevin dynamics.

4.2.3 Concluding remarks and discussion

Recent studies have made advances in generalizing TURs. It has been shown that a TUR is a direct consequence of the detailed fluctuation theorem, regardless of the underlying dynamics [39, 46, 56]. This bound is more applicable than the original, i.e., it holds for arbitrary currents and arbitrary dynamics as long as the fluctuation theorem is provided. However, it pays the cost of a weaker predictive power. A generalization to systems with a broken symmetry, known as the hysteretic TUR, has been conducted [43, 123]. This bound requires the evaluation of currents and entropy production in the backward process, having the following form:

$$\frac{(\langle\phi\rangle + \langle\phi\rangle_{\rm b})^2}{\langle\langle\phi\rangle\rangle + \langle\langle\phi\rangle\rangle_{\rm b}} \leq \exp\left(\frac{\langle\sigma\rangle + \langle\sigma\rangle_{\rm b}}{2}\right) - 1, \tag{4.51}$$

where $\langle\cdot\cdot\rangle_{\rm b}$ denotes averages taken over an ensemble in the backward experiment. Another extension that holds for arbitrary dynamics reads [45, 55]

$$\frac{\langle\phi\rangle^2}{\langle\langle\phi\rangle\rangle} \leq \frac{e^{\langle\tilde{\sigma}\rangle} - 1}{2}, \tag{4.52}$$

where $\langle\tilde{\sigma}\rangle$ is the Kullback–Leibler divergence between distributions of the forward path and its reversed counterpart in the system. However, $\langle\tilde{\sigma}\rangle$ is not equal to the entropy production $\langle\sigma\rangle$, except in steady-state systems with time-reversal symmetry. Despite the generalities of Eqs. (4.51) and (4.52), it is difficult to infer the entropy production from these bounds.

Based on information theory, we have derived bounds for both current and noncurrent observables in overdamped and underdamped regimes. These bounds universally hold for arbitrary protocols and arbitrary initial distributions. The results demonstrate that the fluctuations of observables are constrained not only by entropy production but also by a kinetic term. In all studied examples, we have shown that the exponential bound of entropy production, $(e^{\langle\sigma\rangle}-1)/2$, cannot constrain the fluctuation. For the case of multipartite systems where the dynamics of the target system are unidirectionally affected by other systems, we have proved a tighter bound. This bound reveals that the fluctuations of observables in the target system are not constrained by the dissipation costs of other systems but by the information flow between them and the target system.

Our results serve as a useful tool for estimation tasks in general Langevin systems. Information inequalities have successfully been applied to derive many important thermodynamic bounds, such as the sensitivity-precision trade-off [33], a quantum TUR [42], and the speed limit [124]. Extending our approach to other classical and quantum systems or finding a hyper-accurate observable [125] would be interesting.

Chapter 5

Thermodynamic uncertainty relations in non-Markovian systems

The TUR has been mainly investigated for Markovian systems. However, in the real world, "non-Markov is the rule, Markov is the exception," as remarked by N. G. van Kampen. For instance, the time delay that causes non-Markovian dynamical behavior inevitably exists in many real-world stochastic processes such as gene regulation [126, 127], biochemical reaction networks [128], and control systems involving a feedback protocol [129–131]. It is well-known that time delay can completely alter system dynamics, e.g., delay-induced oscillations [126]. Recently, Ref. [132] has shown that even a small delay time leads to finite heat flow in the system. Despite the importance of delay in many classical and quantum systems, thermodynamic analysis of such systems remains challenging [133, 134]. In addition, feedback control by an external protocol that depends on the measurement outcome is ubiquitous in both physics and biology and plays important roles in the study of nonequilibrium systems. The thermodynamics of feedback control [135–144] provides a crucial framework for analysing systems in the presence of Maxwell's demon, which can extract work from the system beyond the limit set by the conventional second law. The system performance can be significantly enhanced by applying the measured information about itself; moreover, such information could improve the precision of observables such as the displacement of a molecular motor [145, 146].

This chapter focuses on studying TURs in non-Markovian systems, such as time-delayed Langevin dynamics, systems involving measurement and feedback control, and semi-Markov processes. The obtained TURs reveal that the non-Markovian signatures such as information flow and memory effects play an important role in the suppression of current fluctuations.

5.1 Bounds for time-delayed Langevin systems

In this section, we study the TUR for general dynamical observables that are antisymmetric under conjugate operations such as time or position reversal. First, we define a trajectory-dependent quantity σ [cf. Eq. (5.5)], whose average is the Kullback–Leibler (KL) divergence between the distributions of the forward path and its conjugate counterpart. In the absence

of time delay and under time reversal, σ is identified as the trajectory-dependent total entropy production in Markovian systems. Starting from the point that the joint probability distribution of σ and the observable obeys the strong detailed fluctuation theorem, we prove that the relative fluctuation of the observable is lower bounded by $2/(e^{\langle\sigma\rangle}-1)$. This implies that the time irreversibility in the system constrains the fluctuation of observables that are odd under time reversal. For observables that are antisymmetric under position reversal, the bound reflects the degree of position-symmetry breaking in the system. The derived bound holds for arbitrary observation times and for a large class of time-delayed systems such as continuous- or discrete-time systems with multiple or distributed delays. We numerically verify the validity of the derived inequality in three systems wherein $\langle\sigma\rangle$ can be analytically obtained.

5.1.1 Model

To clearly illustrate the results, we consider here a single time-delayed system with dynamical variables $\boldsymbol{x}(t) = [x_1(t),\dots,x_N(t)]^\top$, as described by the following set of coupled Langevin equations:

$$\dot{\boldsymbol{x}} = \boldsymbol{F}(\boldsymbol{x},\boldsymbol{x}_\tau) + \boldsymbol{\xi}, \tag{5.1}$$

where $\boldsymbol{x}_\tau \equiv \boldsymbol{x}(t-\tau)$, $\boldsymbol{F}(\boldsymbol{x},\boldsymbol{x}_\tau) \in \mathbb{R}^N$ is a drift force, $\boldsymbol{\xi}(t) = [\xi_1(t),\dots,\xi_N(t)]^\top$ is zero-mean white Gaussian noise with covariance $\langle\xi_i(t)\xi_j(t')\rangle = 2D_i\delta_{ij}\delta(t-t')$, and $\tau \geq 0$ denotes the delay time in the system. Here, D_i's denote the noise intensity. Equation (5.1) is interpreted as Ito stochastic integration. Throughout this chapter, Boltzmann's constant is set to $k_\mathrm{B} = 1$. Let $P(\boldsymbol{x},t)$ be the probability distribution function for the system to be in state $\boldsymbol{x}$ at time t. Then, the corresponding Fokker–Planck equation (FPE) is expressed as [147, 148]

$$\partial_t P(\boldsymbol{x},t) = -\sum_{i=1}^{N} \partial_{x_i} J_i(\boldsymbol{x},t), \tag{5.2}$$

where

$$\begin{aligned} J_i(\boldsymbol{x},t) &= \int d\boldsymbol{y}\, F_i(\boldsymbol{x},\boldsymbol{y}) P(\boldsymbol{y},t-\tau;\boldsymbol{x},t) - D\partial_{x_i} P(\boldsymbol{x},t) \\ &= \overline{F}_i(\boldsymbol{x}) P(\boldsymbol{x},t) - D_i\partial_{x_i} P(\boldsymbol{x},t) \end{aligned} \tag{5.3}$$

is the probability current. Here,

$$\overline{F}_i(\boldsymbol{x}) = \int d\boldsymbol{y}\, F_i(\boldsymbol{x},\boldsymbol{y}) P(\boldsymbol{y},t-\tau|\boldsymbol{x},t) \tag{5.4}$$

is an effective force obtained by taking the delay-averaged integration of the variable $\boldsymbol{y}$ and $P(\boldsymbol{y},t-\tau;\boldsymbol{x},t)$ is a joint probability density for a system that takes value $\boldsymbol{x}$ at time t and $\boldsymbol{y}$ at time $t-\tau$. Generally, solving $P(\boldsymbol{y},t-\tau;\boldsymbol{x},t)$ results in an infinite hierarchy of equations, where n-time probability distribution depends on the $(n+1)$-time one. Therefore, it is difficult to analytically obtain the effective force $\overline{F}_i(\boldsymbol{x})$, except in linear systems.

We define $\mathcal{X}_{[s,e]} \equiv \{\boldsymbol{x}(t)\}_{t=s}^{t=e}$ as a trajectory that begins at $t=s$ and ends at $t=e$. Let $\mathcal{P}(\mathcal{X}_{[s,e]})$ be the probability of observing the trajectory $\mathcal{X}_{[s,e]}$. For each trajectory $\mathcal{X}_{[s,e]}$,

we consider a conjugate trajectory $\mathcal{X}^\dagger_{[s,e]}$ defined by $\mathcal{X}^\dagger_{[s,e]} \equiv \{\boldsymbol{x}^\dagger(t)\}_{t=s}^{t=e}$. Assuming that we observe the system during a time interval $[0,T]$, we then define a trajectory-dependent quantity $\sigma(\mathcal{X}_{[0,T]})$, which is the ratio of the probabilities of observing the forward path and its conjugate counterpart, as follows:

$$\sigma \equiv \ln \frac{\mathcal{P}(\mathcal{X}_{[0,T]})}{\mathcal{P}(\mathcal{X}^\dagger_{[0,T]})}. \tag{5.5}$$

For the sake of simplicity, we use the notation $\mathcal{X}$, omitting the time interval, to indicate $\mathcal{X}_{[0,T]}$. If the conjugate operation satisfies the property $(\mathcal{X}^\dagger)^\dagger = \mathcal{X}$, then σ is odd under it, i.e., $\sigma(\mathcal{X}^\dagger) = -\sigma(\mathcal{X})$. Hereafter, we consider conjugate operations that satisfy this property. Introducing the probability distribution $P(\sigma) = \int \mathcal{D}\mathcal{X}\, \delta(\sigma - \sigma(\mathcal{X}))\mathcal{P}(\mathcal{X})$, we show that $P(\sigma)$ satisfies the fluctuation theorem, i.e.,

$$\frac{P(\sigma)}{P(-\sigma)} = e^{\sigma}. \tag{5.6}$$

Equation (5.6) can be derived as follows:

$$\begin{aligned} P(\sigma) &= \int \mathcal{D}\mathcal{X}\, \delta(\sigma - \sigma(\mathcal{X}))\mathcal{P}(\mathcal{X}) \\ &= \int \mathcal{D}\mathcal{X}\, \delta(\sigma - \sigma(\mathcal{X}))e^{\sigma(\mathcal{X})}\mathcal{P}(\mathcal{X}^\dagger) \\ &= e^{\sigma} \int \mathcal{D}\mathcal{X}\, \delta(\sigma - \sigma(\mathcal{X}))\mathcal{P}(\mathcal{X}^\dagger) \\ &= e^{\sigma} \int \mathcal{D}\mathcal{X}^\dagger\, \delta(\sigma + \sigma(\mathcal{X}^\dagger))\mathcal{P}(\mathcal{X}^\dagger) \\ &= e^{\sigma} P(-\sigma). \end{aligned} \tag{5.7}$$

Equation (5.6) implies that σ satisfies the integral fluctuation theorem, i.e., $\langle e^{-\sigma}\rangle = 1$. By applying Jensen's inequality $\langle e^{-\sigma}\rangle \geq e^{-\langle\sigma\rangle}$, we have $\langle\sigma\rangle \geq 0$. The average value of σ can also be interpreted as the KL divergence between the distributions $\mathcal{P}$ and $\mathcal{P}^\dagger$

$$\langle\sigma\rangle = \mathcal{D}_{\mathrm{KL}}[\mathcal{P}||\mathcal{P}^\dagger] = \int \mathcal{D}\mathcal{X}\, \mathcal{P}(\mathcal{X}) \ln \frac{\mathcal{P}(\mathcal{X})}{\mathcal{P}^\dagger(\mathcal{X})}, \tag{5.8}$$

where $\mathcal{P}^\dagger(\mathcal{X}) \equiv \mathcal{P}(\mathcal{X}^\dagger)$. From Eq. (5.8), $\langle\sigma\rangle$ becomes zero only when $\mathcal{P}(\mathcal{X}) = \mathcal{P}(\mathcal{X}^\dagger)$ for all trajectories $\mathcal{X}$.

Let us discuss the conjugate operations that will be used here. The most conventional one is time reversal, i.e., $\boldsymbol{x}^\dagger(t) = \boldsymbol{\epsilon}\boldsymbol{x}(T-t)$. Here, $\epsilon_i = \pm 1$ for even and odd variables x_i, respectively. For systems where both even and odd variables exist, a reversed trajectory $\mathcal{X}^\dagger$ can be generated under forward dynamics. Therefore, σ is mathematically well defined. In this case, $\langle\sigma\rangle$ is a measure of the time-reversal symmetry breaking in the system. For steady-state systems involving only even variables, σ can be decomposed as

$$\sigma = -\ln \frac{P^{\mathrm{ss}}(\boldsymbol{x}(T))}{P^{\mathrm{ss}}(\boldsymbol{x}(0))} + \ln \frac{\mathcal{P}(\mathcal{X}|\boldsymbol{x}(0))}{\mathcal{P}(\mathcal{X}^\dagger|\boldsymbol{x}^\dagger(0))}, \tag{5.9}$$

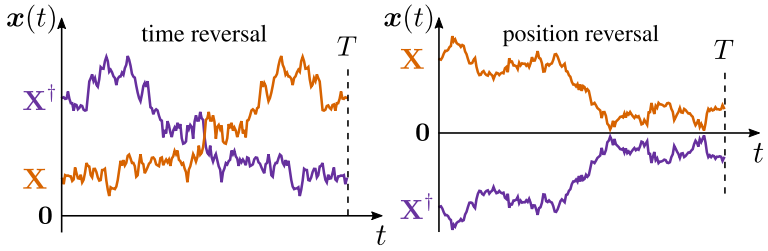

Figure 5.1: Illustration of the conjugate operations. For simplicity, we assume here that the system involves only even variables. For the trajectory $\mathcal{X} \equiv \{x(t)\}_{t=0}^{t=T}$, its reversed counterpart is $\mathcal{X}^\dagger \equiv \{x^\dagger(t)\}_{t=0}^{t=T}$, where $x^\dagger(t)$ is equal to $x(T-t)$ (or $-x(t)$) under time reversal (or position reversal). Here, T denotes the observation time.

where $P^{\rm ss}(\cdot)$ is the steady-state distribution and $\mathcal{P}(\cdot|\cdot)$ is the conditional path probability. When the time delay vanishes, σ is identified as the total entropy production along a trajectory in Markovian systems [3]; the first and second terms in the right-hand side of Eq. (5.9) correspond to the system and medium entropy production, respectively. Under time reversal, $\langle\sigma\rangle$ can be considered a generalization of total entropy production for time-delayed systems [149, 150]. It is worth noting that this generalization of entropy production is mathematical and that it is generally difficult to assess its relation to the thermodynamic notion of entropy production [151], except in Markovian processes where an explicit connection was established [7, 152]. Another possible conjugate operation is position reversal, i.e., $\boldsymbol{x}^\dagger(t) = \boldsymbol{\kappa} - \boldsymbol{x}(t)$. Here, $\boldsymbol{\kappa} \in \mathbb{R}^N$ is a constant that can basically take an arbitrary value, except in systems involving $n^{\rm th}$-time-derivative variables, where $n \in \mathbb{N}_{>0}$. For these systems, $\boldsymbol{\kappa}$ must be carefully chosen to ensure that a reversed trajectory can be generated by forward dynamics. In particular, $\boldsymbol{\kappa}$ must be set to $\kappa_i = 0$ for all such variables x_i. For example, if the system variables are the position and velocity of a particle, i.e., $\boldsymbol{x}(t) = [r(t), \dot{r}(t)]^\top$, where $r(t)$ is the particle's position, then the reversed trajectory $\{\boldsymbol{x}^\dagger(t)\} = \{\kappa_1 - r(t), \kappa_2 - \dot{r}(t)\}$ can be generated by the forward dynamics only if $\kappa_2 = 0$. Under this conjugate operation, $\langle\sigma\rangle$ reflects the degree of position-symmetry breaking with respect to the position $\boldsymbol{\kappa}/2$ in the system. In the remaining part of the section, we consider the $\boldsymbol{\kappa} = 0$ case. To distinguish when each operation is employed, we use subscripts t and p to refer time reversal and position reversal, respectively. The conjugate operations are illustrated in Fig. 5.1.

Because $\langle\sigma\rangle$ is the KL divergence between forward and reversed trajectories and trajectory-based quantities were previously measured [153–157], $\langle\sigma\rangle$ is in principle experimentally measurable. As will be shown in the examples, $\langle\sigma\rangle$ can be analytically calculated for several classes of systems. In what follows, we investigate a more detailed form of σ with respect to conjugate operations for the system defined in Eq. (5.1). For $T > \tau$, the path probability can be rewritten

$$\begin{aligned}\mathcal{P}(\mathcal{X}_{[0,T]}) &= \mathcal{P}(\mathcal{X}_{[\tau,T]}|\mathcal{X}_{[0,\tau]})\mathcal{P}(\mathcal{X}_{[0,\tau]}),\\ \mathcal{P}(\mathcal{X}^\dagger_{[0,T]}) &= \mathcal{P}(\mathcal{X}^\dagger_{[\tau,T]}|\mathcal{X}^\dagger_{[0,\tau]})\mathcal{P}(\mathcal{X}^\dagger_{[0,\tau]}),\end{aligned} \tag{5.10}$$

where $\mathcal{P}(\mathcal{X}_{[\tau,T]}|\mathcal{X}_{[0,\tau]})$ is the probability of observing $\mathcal{X}_{[\tau,T]}$, conditioned on $\mathcal{X}_{[0,\tau]}$. We note that under time reversal, $\mathcal{X}^\dagger_{[0,\tau]} = \{\boldsymbol{\epsilon}\boldsymbol{x}(T-t)\}_{t=0}^{t=\tau}$. The conditional probability can be calculated

via the path integral as

$$\mathcal{P}(\mathcal{X}_{[\tau,T]}|\mathcal{X}_{[0,\tau]}) = \mathcal{N}\exp\left(-\sum_{i=1}^{N}\mathcal{S}_i(\mathcal{X}_{[0,T]})\right), \tag{5.11}$$

where $\mathcal{S}_i(\mathcal{X}_{[0,T]})$ is the stochastic action given by

$$\mathcal{S}_i(\mathcal{X}_{[0,T]}) = \int_\tau^T dt\left[\frac{(\dot{x}_i - F_i(\boldsymbol{x},\boldsymbol{x}_\tau))^2}{4D_i} + \frac{\partial_{x_i}F_i(\boldsymbol{x},\boldsymbol{x}_\tau)}{2}\right], \tag{5.12}$$

and $\mathcal{N}$ is a positive term independent of the trajectory. Equation (5.11) can be obtained by discretizing the Langevin equation [cf. Eq. (5.1)] and evaluating the path probability via the occurrence probability of the noise trajectory [158]. The cross term $\int dt\, F_i(\boldsymbol{x},\boldsymbol{x}_\tau)\dot{x}_i$ in Eq. (5.12) should be interpreted as $\int dt\, F_i(\boldsymbol{x},\boldsymbol{x}_\tau)\circ\dot{x}_i$, where $\circ$ denotes the Stratonovich product. Using Eq. (5.10), the average of σ can be decomposed as

$$\langle\sigma\rangle = \left\langle \ln\frac{\mathcal{P}(\mathcal{X}_{[\tau,T]}|\mathcal{X}_{[0,\tau]})}{\mathcal{P}(\mathcal{X}^\dagger_{[\tau,T]}|\mathcal{X}^\dagger_{[0,\tau]})}\right\rangle + \left\langle \ln\frac{\mathcal{P}(\mathcal{X}_{[0,\tau]})}{\mathcal{P}(\mathcal{X}^\dagger_{[0,\tau]})}\right\rangle. \tag{5.13}$$

In the long-time limit, i.e., $T\to\infty$, the first term in the right-hand side of Eq. (5.13) becomes dominant as the second term is only a boundary value. Neglecting the contribution of this boundary term and plugging Eq. (5.11) into Eq. (5.13), $\langle\sigma_t\rangle$ and $\langle\sigma_p\rangle$ can be approximated as

$$\begin{aligned}
\langle\sigma_t\rangle &\approx \frac{1}{2}\sum_{i=1}^{N}\left\langle\int_0^{T-\tau} dt\left[\frac{(\dot{x}_i + F_i(\boldsymbol{x},\boldsymbol{x}_{-\tau}))^2}{2D_i} + \partial_{x_i}F_i(\boldsymbol{x},\boldsymbol{x}_{-\tau})\right] - \int_\tau^T dt\left[\frac{(\dot{x}_i - F_i(\boldsymbol{x},\boldsymbol{x}_\tau))^2}{2D_i} + \partial_{x_i}F_i(\boldsymbol{x},\boldsymbol{x}_\tau)\right]\right\rangle,\\
\langle\sigma_p\rangle &\approx \frac{1}{2}\sum_{i=1}^{N}\left\langle\int_\tau^T dt\left[\left(\frac{\dot{x}_i}{D_i} - \frac{F_i(\boldsymbol{x},\boldsymbol{x}_\tau) - F_i(-\boldsymbol{x},-\boldsymbol{x}_\tau)}{2D_i} - \partial_{x_i}\right)\circ(F_i(\boldsymbol{x},\boldsymbol{x}_\tau) + F_i(-\boldsymbol{x},-\boldsymbol{x}_\tau))\right]\right\rangle.
\end{aligned} \tag{5.14}$$

For general systems, it is difficult to obtain more detailed forms of $\langle\sigma_t\rangle$ and $\langle\sigma_p\rangle$ than those in Eq. (5.14), except in linear systems. $\langle\sigma_t\rangle$ becomes zero when the system is in equilibrium because $\langle\sigma_t\rangle$ characterizes the time reversibility of the system. Contrastingly, $\langle\sigma_p\rangle$ can be positive even in the equilibrium system so long as the symmetry with respect to position reversal is broken.

5.1.2 Main results

In this section, we derive the TUR for an arbitrary dynamical observable $\jmath(\mathcal{X})$, which is antisymmetric under the conjugate operation, i.e., $\jmath(\mathcal{X}^\dagger) = -\jmath(\mathcal{X})$. This antisymmetric property can be satisfied, e.g., for generalized currents of the form $\jmath(\mathcal{X}) = \int_0^T dt\,\boldsymbol{\Lambda}(\boldsymbol{x})^\top\circ\dot{\boldsymbol{x}}$ under time reversal, or for observables $\jmath(\mathcal{X}) = \int_0^T dt\,\Gamma_{\mathrm{o}}(\boldsymbol{x})$ or $\jmath(\mathcal{X}) = \int_0^T dt\,\boldsymbol{\Gamma}_{\mathrm{e}}(\boldsymbol{x})^\top\circ\dot{\boldsymbol{x}}$ under position reversal. Here, $\Gamma_{\mathrm{o}}(\boldsymbol{x})$ and $\boldsymbol{\Gamma}_{\mathrm{e}}(\boldsymbol{x})$ are arbitrary odd and even functions, respectively.

In Ref. [39], we derived a modified variant of the TUR using the fluctuation theorem for Markovian processes. Regardless of the underlying dynamics, the bound holds for as long as the fluctuation theorem is valid. Here, we apply the same technique and derive the TUR

for time-delayed systems. First, we show that the joint probability distribution of σ and $\jmath$, $P(\sigma,\jmath)$, obeys the fluctuation theorem; this can be proved analogously as follows:

$$\begin{aligned} P(\sigma,\jmath) &= \int \mathcal{D}\mathcal{X}\,\delta(\sigma-\sigma(\mathcal{X}))\delta(\jmath-\jmath(\mathcal{X}))\mathcal{P}(\mathcal{X}) \\ &= \int \mathcal{D}\mathcal{X}\,\delta(\sigma-\sigma(\mathcal{X}))\delta(\jmath-\jmath(\mathcal{X}))e^{\sigma(\mathcal{X})}\mathcal{P}(\mathcal{X}^\dagger) \\ &= e^{\sigma}\int \mathcal{D}\mathcal{X}\,\delta(\sigma-\sigma(\mathcal{X}))\delta(\jmath-\jmath(\mathcal{X}))\mathcal{P}(\mathcal{X}^\dagger) \\ &= e^{\sigma}\int \mathcal{D}\mathcal{X}^\dagger\,\delta(\sigma+\sigma(\mathcal{X}^\dagger))\delta(\jmath+\jmath(\mathcal{X}^\dagger))\mathcal{P}(\mathcal{X}^\dagger) \\ &= e^{\sigma}P(-\sigma,-\jmath). \end{aligned} \tag{5.15}$$

Inspired by Ref. [159], where the statistical properties of entropy production were obtained from the strong detailed fluctuation theorem, we derive the TUR solely from Eq. (5.15). Based on the following relation:

$$\begin{aligned} 1 &= \int_{-\infty}^{\infty} d\sigma \int_{-\infty}^{\infty} d\jmath\, P(\sigma,\jmath) \\ &= \int_{0}^{\infty} d\sigma \int_{-\infty}^{\infty} d\jmath\, (1+e^{-\sigma})P(\sigma,\jmath), \end{aligned} \tag{5.16}$$

we introduce a probability distribution $Q(\sigma,\jmath) \equiv (1+e^{-\sigma})P(\sigma,\jmath)$, defined over $[0,\infty)\times(-\infty,\infty)$. Using the distribution $Q(\sigma,\jmath)$, the moments of σ and $\jmath$ can be expressed in an alternative way as follows:

$$\begin{aligned} \langle\sigma^{2k}\rangle &= \left\langle\sigma^{2k}\right\rangle_Q, \\ \langle\jmath^{2k}\rangle &= \left\langle\jmath^{2k}\right\rangle_Q, \\ \langle\sigma^{2k+1}\rangle &= \left\langle\sigma^{2k+1}\tanh\left(\frac{\sigma}{2}\right)\right\rangle_Q, \\ \langle\jmath^{2k+1}\rangle &= \left\langle\jmath^{2k+1}\tanh\left(\frac{\sigma}{2}\right)\right\rangle_Q, \end{aligned} \tag{5.17}$$

where $\langle\cdot\cdot\rangle_Q$ denotes the expectation with respect to $Q(\sigma,\jmath)$. Applying the Cauchy–Schwarz inequality to $\langle\jmath\rangle$, we obtain

$$\langle\jmath\rangle^2 = \left\langle\jmath\tanh\left(\frac{\sigma}{2}\right)\right\rangle_Q^2 \le \langle\jmath^2\rangle_Q\left\langle\tanh\left(\frac{\sigma}{2}\right)^2\right\rangle_Q. \tag{5.18}$$

The last term in the right-hand side of Eq. (5.18) can be further upper bounded. We find that

$$\left\langle\tanh\left(\frac{\sigma}{2}\right)^2\right\rangle_Q \le \tanh\left(\frac{\langle\sigma\rangle}{2}\right). \tag{5.19}$$

Equation (5.19) is obtained by first noticing that $\tanh\left(\frac{\sigma}{2}\right)^2 \le \tanh\left[\frac{\sigma}{2}\tanh\left(\frac{\sigma}{2}\right)\right]$ for all $\sigma\ge 0$. Thereafter, by applying Jensen's inequality to the concave function $\tanh(x)$, we obtain

$$\left\langle\tanh\left[\frac{\sigma}{2}\tanh\left(\frac{\sigma}{2}\right)\right]\right\rangle_Q \le \tanh\left(\left\langle\frac{\sigma}{2}\tanh\left(\frac{\sigma}{2}\right)\right\rangle_Q\right)$$

$$= \tanh\left(\frac{\langle\sigma\rangle}{2}\right). \tag{5.20}$$

From Eqs. (5.18) and (5.19), we have

$$\langle \jmath \rangle^2 \leq \langle \jmath^2 \rangle \tanh\left(\frac{\langle\sigma\rangle}{2}\right). \tag{5.21}$$

By transforming Eq. (5.21), we obtain the following TUR for the observable $\jmath$:

$$\frac{\mathrm{Var}[\jmath]}{\langle j\rangle^2} = \frac{\langle \jmath^2\rangle - \langle \jmath\rangle^2}{\langle \jmath\rangle^2} \geq \frac{2}{e^{\langle\sigma\rangle} - 1}. \tag{5.22}$$

The inequality in Eq. (5.22) is the main result. For observables that are antisymmetric under time (or position) reversal, the term $\langle\sigma\rangle$ in the bound should be replaced by $\langle\sigma_t\rangle$ (or $\langle\sigma_p\rangle$).

In the limit $\tau \to 0$, the system [cf. Eq. (5.1)] becomes a continuous-time Markovian process, with the conventional TUR providing a lower bound on the current fluctuations as in Eq. (1.4). Since $e^{\langle\sigma\rangle} - 1 \geq \langle\sigma\rangle$, the derived bound is looser than the conventional bound. Regarding this difference, there are two possible explanations. Firstly, it is because there is no requirement on the details of the underlying dynamics of the system considered in the derivation. It was proven that the conventional bound does not hold for discrete-time Markovian processes [25, 160]. Contrastingly, the derived bound holds for both continuous- and discrete-time systems. The lower bound in Eq. (5.22) is the same as that in Ref. [25] in which the TUR was derived in the long-time limit for discrete-time Markovian processes. Secondly, the derived bound also holds for non-current observables, and differs from the conventional bound that holds only for current-type observables defined by $\jmath(\mathcal{X}) = \int_0^T dt\, \boldsymbol{\Lambda}(\boldsymbol{x})^\top \circ \dot{\boldsymbol{x}}$.

5.1.3 Numerical illustration

In this section, we study the derived bound with the help of three systems. The first two steady-state systems are embedded in a Markovian heat reservoir, whereas the third is in contact with a non-Markovian environment, i.e., a heat reservoir with memory effects. Unlike the conventional TUR, which was derived for steady-state systems, our bound holds even for non-steady-state systems. Therefore, in the last system, we focus on a non-steady state. For steady-state systems, $P^{\mathrm{ss}}(\boldsymbol{x})$ and $\boldsymbol{J}^{\mathrm{ss}}(\boldsymbol{x})$ denote the probability distribution and the probability current, respectively.

One-dimensional system

We study a one-dimensional linear system whose drift term is given by

$$F(x, x_\tau) = -ax - bx_\tau + f, \tag{5.23}$$

where a, b, and f are the given constants satisfying the conditions $a > b > 0$, $f > 0$. It is easy to see that $\langle x\rangle = \overline{f}$, where $\overline{f} = f/(a+b)$. The system has a Gaussian steady-state distribution that exists for arbitrary delay time τ because the force is linear, . We introduce

a new stochastic variable z, defined as $z = x - \overline{f}$. The FPE corresponding to z reads as

$$\partial_t P(z,t) = -\partial_z[\overline{G}(z)P(z,t)] + D\partial_z^2 P(z,t), \tag{5.24}$$

where $\overline{G}(z) = \int dy\,(-az - by)\,P(y, t-\tau|z,t)$. At the steady state, the probability current vanishes, i.e., $J^{\rm ss}(z) = \overline{G}(z)P^{\rm ss}(z) - D\partial_z P^{\rm ss}(z) = 0$. Here, $P^{\rm ss}(z)$ denotes the steady-state distribution. Let $\phi(t) = \langle z(0)z(t)\rangle$ be the time-correlation function of z; it was shown that $\phi(t) = A_+ e^{-c|t|} + A_- e^{c|t|}$ for all $|t| \le \tau$ [147, 161], where $c = \sqrt{a^2 - b^2}$, $A_\pm = 1/2\,[\phi(0) \pm D/c]$, and

$$\phi(0) = \langle z^2\rangle = \frac{D}{c}\frac{c + b\sinh(c\tau)}{a + b\cosh(c\tau)}. \tag{5.25}$$

First, we consider the TUR for observables that are antisymmetric under time reversal. According to Eq. (5.22), the following inequality should be satisfied:

$$\frac{\langle \jmath\rangle^2}{\mathrm{Var}[\jmath]} \le \frac{e^{\langle\sigma_t\rangle} - 1}{2}. \tag{5.26}$$

Since evaluating $\langle\sigma_t\rangle$ for $T > \tau$ necessitates complicated calculations, we consider only the case of $T \le \tau$ in which the path probability $\mathcal{P}(\mathcal{X}_{[0,T]})$ can be calculated analytically as [133]

$$\begin{aligned}\mathcal{P}(\mathcal{X}_{[0,T]}) \propto \exp\left[-\frac{1}{4D}\int_0^T dt\left(\dot{x} + cx - c\overline{f}\right)^2\right]\times \\ \exp\left(-\frac{c}{2D}\frac{\left[A_+e^{-cT}\left(x(0) - \overline{f}\right) - A_-\left(x(T) - \overline{f}\right)\right]^2}{A_+^2 e^{-2cT} - A_-^2}\right).\end{aligned} \tag{5.27}$$

It can be confirmed that $\mathcal{P}(\mathcal{X}) = \mathcal{P}(\mathcal{X}^\dagger)$; thus, $\langle\sigma_t\rangle = 0$. Consequently, Eq. (5.26) implies that an arbitrary observable that is antisymmetric under time reversal vanishes on average, i.e., $\langle\jmath\rangle = 0$. For the current-type observable defined by $\jmath(\mathcal{X}) = \int_0^T dt\,\Lambda(x)\circ\dot{x}(t)$, where $\Lambda(x)$ is an arbitrary projection function, one can easily check that $\langle\jmath\rangle = T\int_{-\infty}^{\infty} dz\,\Lambda(z+\overline{f})J^{\rm ss}(z) = 0$. Generally, this can be proven as

$$\begin{aligned}\langle\jmath\rangle &= \int \mathcal{D}\mathcal{X}\,\jmath(\mathcal{X})\mathcal{P}(\mathcal{X}) \\ &= \frac{1}{2}\left(\int \mathcal{D}\mathcal{X}\,\jmath(\mathcal{X})\mathcal{P}(\mathcal{X}) - \int \mathcal{D}\mathcal{X}^\dagger\,\jmath(\mathcal{X}^\dagger)\mathcal{P}(\mathcal{X}^\dagger)\right) = 0.\end{aligned} \tag{5.28}$$

Next, let us consider the TUR for non-current observables that are antisymmetric under position reversal. Specifically, we validate the TUR for the observable $\jmath(\mathcal{X}) = \int_0^T dt\,x$, representing the area under the trajectory. The average of the observable is $\langle\jmath\rangle = T\langle x\rangle = T\overline{f}$. For $T \le \tau$, using the path integral, σ_p can be calculated as

$$\begin{aligned}\sigma_p = \ln\frac{\mathcal{P}(\mathcal{X}_{[0,T]})}{\mathcal{P}(\mathcal{X}^\dagger_{[0,T]})} = \frac{c\overline{f}}{D}\int_0^T dt\;(\dot{x} + cx) \\ + \frac{2c\overline{f}}{D}\frac{A_+e^{-cT}x(0) - A_-x(T)}{A_+e^{-cT} + A_-}.\end{aligned} \tag{5.29}$$

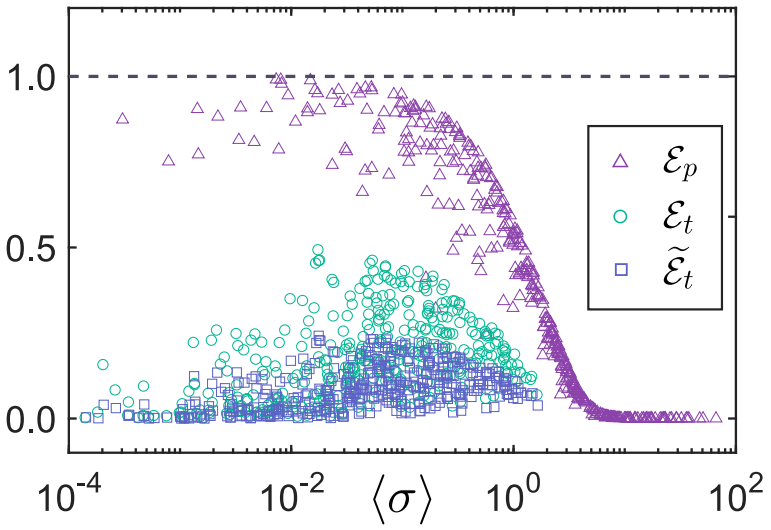

Figure 5.2: Numerical verification of the TUR in one- and two-dimensional systems. The dashed line represents the saturated TUR. In the one-dimensional system, $\mathcal{E}_p$ is plotted as a function of $\langle\sigma_p\rangle$ with triangular points. The parameter ranges are $a,\ f,\ D,\ \tau,\ T \in [0.01, 2]$, and $b \in (0, a)$. In the two-dimensional system, $\mathcal{E}_t$ and $\widetilde{\mathcal{E}}_t$ are plotted as functions of $\langle\sigma_t\rangle$ with circular and square points, respectively. The parameter ranges are the same as in the one-dimensional system, except $T \in [0.01, \tau]$. $\mathcal{E}_p \leq 1$, $\mathcal{E}_t \leq 1$, and $\widetilde{\mathcal{E}}_t \leq 1$ imply that the derived TUR is satisfied.

Because the system is in the steady state, we obtain

$$\langle\sigma_p\rangle = \left(cT + 2\frac{A_+e^{-cT} - A_-}{A_+e^{-cT} + A_-}\right)\frac{c\overline{f}^2}{D}. \tag{5.30}$$

The variance of the observable can also be obtained analytically as follows:

$$\begin{aligned}
\mathrm{Var}[J] &= \left\langle \int_0^T dt \int_0^T ds \left(x(t) - \overline{f}\right)\left(x(s) - \overline{f}\right)\right\rangle \\
&= \int_0^T dt \int_0^T ds\, \phi(t-s) \\
&= \int_0^T dt \int_0^T ds \left(A_+e^{-c|t-s|} + A_-e^{c|t-s|}\right) \\
&= \frac{2}{c^2}\left[A_+\left(e^{-cT} + cT - 1\right) + A_-\left(e^{cT} - cT - 1\right)\right].
\end{aligned} \tag{5.31}$$

We define

$$\mathcal{E}_p \equiv \frac{2\langle J\rangle^2}{\mathrm{Var}[J]\left(e^{\langle\sigma_p\rangle} - 1\right)}, \tag{5.32}$$

this should satisfy $\mathcal{E}_p \leq 1$. Using Eq. (5.30) and Eq. (5.31), one can numerically evaluate $\mathcal{E}_p$ and verify the TUR for $T \leq \tau$. For the $T > \tau$ case, one can calculate $\langle\sigma_p\rangle$ via Eq. (5.14) and obtain

$$\langle\sigma_p\rangle = \frac{Tf^2}{D} + \left(c\tau + 2\frac{A_+e^{-c\tau} - A_-}{A_+e^{-c\tau} + A_-}\right)\frac{c\overline{f}^2}{D}. \tag{5.33}$$

From Eq. (5.33), it can be concluded that decreasing the force f or increasing the noise intensity D both result in higher current fluctuation, which is consistent with our intuition. In the long-time limit $T \to \infty$, we have $\lim_{T\to\infty} T^{-1}\mathrm{Var}[J] = \chi_J''(0)$, where $\chi_J(k)$ is the scaled cumulant generating function defined by $\chi_J(k) = \lim_{T\to\infty} T^{-1} \ln\langle e^{kJ}\rangle$. Using discrete Fourier series, one can obtain $\chi_J(k) = k\overline{f} + Dk^2/(a+b)^2$ (see Appendix C.1). Therefore, the derived bound can be confirmed for $T \to \infty$ as

$$\frac{\mathrm{Var}[J]}{\langle J\rangle^2} = \frac{2D}{Tf^2} \geq \frac{2}{\langle\sigma_p\rangle} \geq \frac{2}{e^{\langle\sigma_p\rangle} - 1}. \tag{5.34}$$

Finally, we run numerical simulations to calculate $\mathrm{Var}[J]$ (for $T > \tau$) and verify the bound. We randomly select parameters (a, b, f, D, τ, T) and repeat the simulations 2×10^6 times for each selected parameter setting using time step $\Delta t = 10^{-4}$. We plot $\mathcal{E}_p$ as a function of $\langle\sigma_p\rangle$ as the triangular points in Fig. 5.2. The ranges of the parameters are given in the corresponding caption. As seen, all triangular points are located below the dashed line, which corresponds to the saturated case of the bound; thus, the derived TUR is empirically validated in this system.

Due to the presence of external force f, the position symmetry with respect to 0 is broken in the system. The degree of broken symmetry is reflected via the quantity $\langle\sigma_p\rangle$, which is always positive and is a monotonically increasing function of f. Therefore, the derived bound implies that increasing f results in a lower fluctuation. From a different point of view, since $J = T\overline{f} + \int_0^T dt\, z$, increasing f enlarges the mean $\langle J\rangle$ but keeps the variance $\mathrm{Var}[J]$ unchanged. Consequently, the fluctuation of the observable decreases when $f \to \infty$, which is consistent with the conclusion obtained from the TUR.

Two-dimensional system

Here, we consider a simple two-dimensional system with drift force

$$\boldsymbol{F}(\boldsymbol{x}, \boldsymbol{x}_\tau) = \begin{bmatrix} -ax_1 + bx_{2,\tau} \\ -ax_2 - bx_{1,\tau} \end{bmatrix}, \tag{5.35}$$

where $a > b > 0$ are the given constants and $x_{i,\tau} \equiv x_i(t-\tau)$. The noise intensities are set to $D_1 = D_2 = D$. This system is manipulated under a parabolic potential with linear delay feedback. The steady-state distribution $P^{\mathrm{ss}}(\boldsymbol{x})$ of the system is Gaussian, i.e., $P^{\mathrm{ss}}(\boldsymbol{x}) \propto \exp\left(-1/2\boldsymbol{x}^\top\boldsymbol{\Phi}^{-1}\boldsymbol{x}\right)$, because the force is linear. Here, $\boldsymbol{\Phi}$ is the covariance matrix with elements $\Phi_{ij} = \phi_{ij}(0)$, and $\phi_{ij}(z) = \langle x_i(t)x_j(t+z)\rangle$ denotes the time-correlation function. The analytical form of this function can be obtained for $|z| \leq \tau$ (see Appendix C.2.1). When $T \leq \tau$, $\langle\sigma_t\rangle$ can be calculated using a path integral (see Appendix C.2.2)

$$\langle\sigma_t\rangle = \frac{4A_{12}^2\left(1 - e^{-2cT}\right)}{\left[(A_{11}^+)^2 + A_{12}^2\right]e^{-2cT} - \left[(A_{11}^-)^2 + A_{12}^2\right]}, \tag{5.36}$$

where $c = \sqrt{a^2 - b^2}$ and

$$\begin{aligned} A_{11}^{\pm} &= \frac{D}{2c} \times \frac{(c \pm a)e^{\pm c\tau}}{a\cosh(c\tau) + c\sinh(c\tau)}, \\ A_{12} &= \frac{D}{2c} \times \frac{b}{a\cosh(c\tau) + c\sinh(c\tau)}. \end{aligned} \tag{5.37}$$

As seen, due to the time delay, $\langle \sigma_t \rangle$ is positive; this implies that the time-reversal symmetry in the system is broken.

Now, we validate the TUR for the following current-type observable

$$\jmath(\mathcal{X}) = \int_0^T dt\ \left[(-ax_1 + bx_2) \circ \dot{x}_1 + (-ax_2 - bx_1) \circ \dot{x}_2\right]. \tag{5.38}$$

We consider only the $T \leq \tau$ case, where $\langle \sigma_t \rangle$ can be analytically obtained. The effective forces are also linear and can be calculated explicitly (see Appendix C.2.3)

$$\overline{F}_1(\boldsymbol{x}) = -\overline{a}x_1 + \overline{b}x_2,\ \ \overline{F}_2(\boldsymbol{x}) = -\overline{a}x_2 - \overline{b}x_1, \tag{5.39}$$

where

$$\begin{aligned} \overline{a} &= \frac{c\,(a\cosh(c\tau) + c\sinh(c\tau))}{a\sinh(c\tau) + c\cosh(c\tau)}, \\ \overline{b} &= \frac{bc}{a\sinh(c\tau) + c\cosh(c\tau)}. \end{aligned} \tag{5.40}$$

The average of the observable is then obtained as

$$\begin{aligned} \langle \jmath \rangle &= T \int d\boldsymbol{x} \left[(-ax_1 + bx_2)J_1^{\mathrm{ss}}(\boldsymbol{x}) + (-ax_2 - bx_1)J_2^{\mathrm{ss}}(\boldsymbol{x})\right] \\ &= \frac{2DTb^2}{a\cosh(c\tau) + c\sinh(c\tau)}, \end{aligned} \tag{5.41}$$

which is always positive for an arbitrary delay time. Equation (5.41) reveals that increasing b, D, or T leads to a higher average current. We also consider a non-current observable $\widetilde{\jmath}(\mathcal{X}) = \mathrm{sign}[\jmath(\mathcal{X})]$, which represents the sign of the observable $\jmath$; this observable is obviously antisymmetric under time reversal. We define $\mathcal{E}_t \equiv 2\langle \jmath \rangle^2 / \left[\mathrm{Var}[\jmath]\left(e^{\langle \sigma_t \rangle} - 1\right)\right]$ and $\widetilde{\mathcal{E}}_t \equiv 2\langle \widetilde{\jmath} \rangle^2 / \left[\mathrm{Var}[\widetilde{\jmath}]\left(e^{\langle \sigma_t \rangle} - 1\right)\right]$, which should satisfy $\mathcal{E}_t \leq 1$ and $\widetilde{\mathcal{E}}_t \leq 1$. We run numerical simulations with the same settings as in the one-dimensional system, and plot $\mathcal{E}_t$ and $\widetilde{\mathcal{E}}_t$ as functions of $\langle \sigma_t \rangle$ with circular and square points, respectively, in Fig. 5.2. As seen, all circular and square points lie below the dashed line, thus empirically verifying the derived bound. During the simulation, we have not seen any violation of the inequality $\mathrm{Var}[\jmath]/\langle j \rangle^2 \geq 2/\langle \sigma_t \rangle$. We conjecture that for continuous-time systems, the fluctuation of arbitrary currents is lower bounded by $2/\langle \sigma_t \rangle$.

Now, we examine the relationship between the term $\langle \sigma_t \rangle$ and the heat dissipated from the system to the environment. The heat can be identified as the work done by the system on the environment [62, 133] and quantified as

$$\Delta Q = \int_0^T dt\ \left[F_1(\boldsymbol{x}, \boldsymbol{x}_\tau) \circ \dot{x}_1 + F_2(\boldsymbol{x}, \boldsymbol{x}_\tau) \circ \dot{x}_2\right]. \tag{5.42}$$

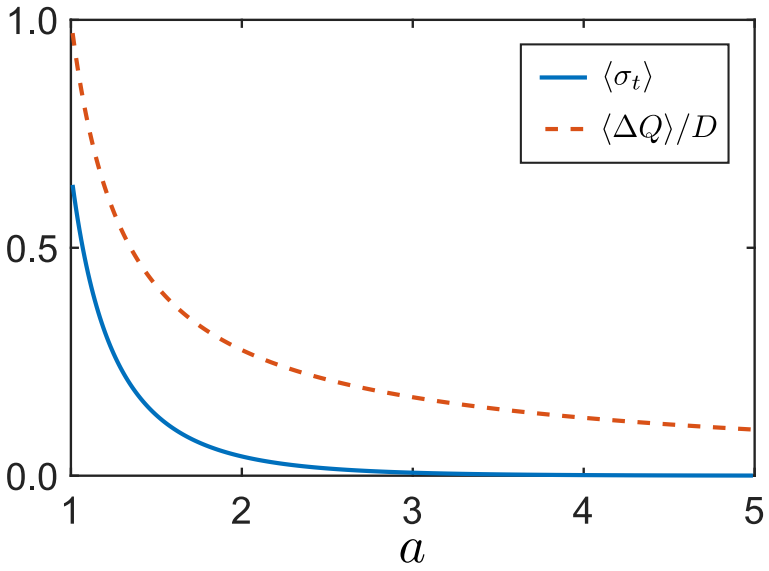

Figure 5.3: The quantity $\langle \sigma_t \rangle$ and the average dissipated heat $\langle \Delta Q \rangle$ in the two-dimensional system. Parameter a is varied from 1 to 5, while other parameters are fixed as $b = 1$, $D = 1$, $T = 0.5$, and $\tau = 1$.

Its average can be calculated analytically as

$$\begin{aligned} \langle \Delta Q \rangle &= T\langle (-ax_1 + bx_{2,\tau})^2 + (ax_2 + bx_{1,\tau})^2 - 2aD \rangle \\ &= T\left[2(a^2+b^2)\phi_{11}(0) + 4ab\phi_{12}(\tau) - 2aD\right] \\ &= 2DTb^2 \times \frac{\cosh(c\tau)}{a\cosh(c\tau) + c\sinh(c\tau)}. \end{aligned} \tag{5.43}$$

Equation (5.43) shows that the average dissipated heat is always nonnegative, i.e., $\langle \Delta Q \rangle \geq 0$. We plot $\langle \sigma_t \rangle$ and $\langle \Delta Q \rangle / D$ in Fig. 5.3 to illustrate how these quantities are related. We vary the value of a, while keeping other parameters unchanged. As seen, $\langle \sigma_t \rangle$ and $\langle \Delta Q \rangle$ show a strong correlation. When a is increased, both $\langle \sigma_t \rangle$ and $\langle \Delta Q \rangle$ decrease. In particular, $\langle \Delta Q \rangle$ decreases with order $O(a^{-1})$, while $\langle \sigma_t \rangle$ declines exponentially. Indeed, we can prove that $\langle \sigma_t \rangle \leq \langle \Delta Q \rangle / D$ (see Appendix C.2.4). Consequently, it can be concluded that

$$\frac{\mathrm{Var}[J]}{\langle J \rangle^2} \geq \frac{2}{e^{\langle \Delta Q \rangle / D} - 1}, \tag{5.44}$$

which is a direct consequence of the derived bound. In the region $a \geq 3$, $\langle \sigma_t \rangle$ is almost zero; this indicates that the system is near equilibrium. Nonetheless, $\langle \Delta Q \rangle$ slowly converges to zero due to the time delay. Therefore, the term $\langle \sigma_t \rangle$ characterizes the irreversibility in the system better than $\langle \Delta Q \rangle$ does.

Dragged particle in a non-Markovian heat reservoir

We study a harmonic oscillator of a unit-mass colloidal particle immersed in a heat reservoir at inverse temperature β with memory effects [162–165]. The center of the harmonic potential $U(x, \lambda(t)) = k/2(x - \lambda(t))^2$ is dragged by an external protocol $\lambda(t)$. The dynamics of the system

are governed by the following generalized Langevin equation:

$$\ddot{x}(t) = -\int_0^t ds\, \gamma(t-s)\dot{x}(s) - \partial_x U(x, \lambda(t)) + \eta(t), \tag{5.45}$$

where $\gamma(t) = (\gamma_0/\tau_c)e^{-|t|/\tau_c}$ is the friction memory kernel and $\eta(t)$ is the zero-mean Gaussian colored noise with variance $\langle \eta(t)\eta(t')\rangle = \beta^{-1}\gamma(t-t')$. Here, τ_c denotes the memory time of the heat reservoir and γ_0 is a positive constant. It is obvious that the system has distributed time delays.

Hereafter, we consider a time-symmetric protocol given by

$$\lambda(t) = \begin{cases} \alpha t, & \text{if } 0 \le t < T/2, \\ \alpha(T-t), & \text{if } T/2 \le t \le T, \end{cases} \tag{5.46}$$

where $\alpha > 0$ is a constant. This protocol satisfies the condition $\lambda(t) = \lambda(T-t)$. Suppose that the system is initially in equilibrium, i.e., the initial distribution is of a Maxwell–Boltzmann type, $P(x, v, 0) = C \exp\left(-\beta\left[v^2/2 + U(x, \lambda(0)\right]\right)$. Here, $v \equiv \dot{x}$ is the velocity and C is the normalization constant. Subsequently, the system is coupled with a non-Markovian heat reservoir and driven out of equilibrium by the protocol $\lambda(t)$ during the time interval $[0, T]$. The heat exchanged between the system and the heat reservoir is defined as

$$\begin{aligned} \Delta Q &= \int_0^T dt\, \left[\int_0^t ds\, \gamma(t-s)\dot{x}(s) - \eta(t)\right] \circ \dot{x}(t) \\ &= -\int_0^T dt\, \left[\ddot{x}(t) + k(x(t) - \lambda(t))\right] \circ \dot{x}(t). \end{aligned} \tag{5.47}$$

Because the trajectory $\mathcal{X}_{[0,T]}$ is uniquely specified if the noise trajectory $\boldsymbol{\eta} \equiv \{\eta(t)\}_{t=0}^{t=T}$ and the initial condition $\psi(0) \equiv [x(0), v(0)]$ are given, the path probability $\mathcal{P}(\mathcal{X}_{[0,T]}|\psi(0))$ can be expressed by the occurrence probability of the noise trajectory $\boldsymbol{\eta}$ as follows:

$$\mathcal{P}(\mathcal{X}|\psi(0))\mathcal{D}\mathcal{X} = \mathcal{P}(\boldsymbol{\eta})\mathcal{D}\boldsymbol{\eta}. \tag{5.48}$$

Since the noise is Gaussian, the probability of observing trajectory $\boldsymbol{\eta}$ is calculated as

$$\mathcal{P}(\boldsymbol{\eta}) \propto \exp\left(-\frac{1}{2}\int_0^T dt \int_0^T dt'\, \eta(t)G(t,t')\eta(t')\right), \tag{5.49}$$

where $G(t,t')$ is the inverse of the time-correlation function of the noise and defined as follows:

$$\int_0^T dt'\, G(t,t')\beta^{-1}\gamma(t'-t'') = \delta(t-t''). \tag{5.50}$$

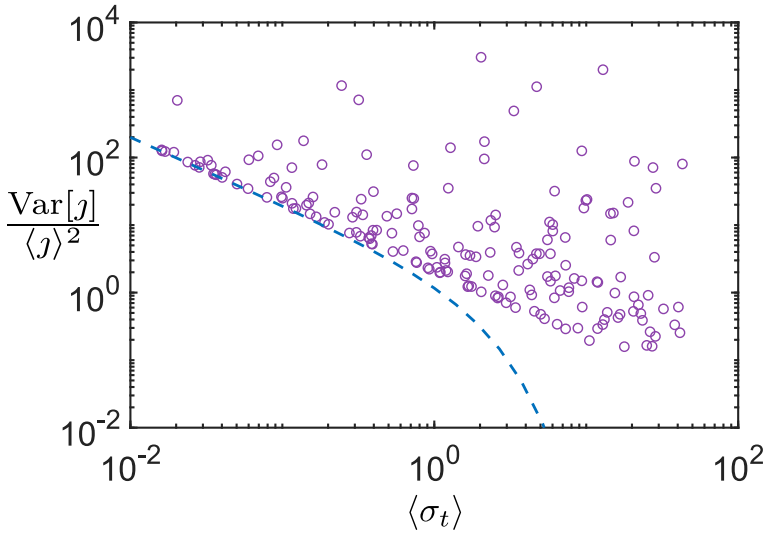

Figure 5.4: Numerical verification of the TUR in the system of a dragged colloidal particle. The parameter ranges are $\alpha, \beta, \gamma_0, \tau_c, k \in [0.1, 2]$, and $T \in [1, 10]$. $\mathrm{Var}[\jmath]/\langle \jmath \rangle^2$ is plotted as a function of $\langle \sigma_t \rangle$ with violet circles. The dashed line represents the derived bound $2/(e^{\langle \sigma_t \rangle} - 1)$. All circular points lie above the line; thus, the derived bound is empirically verified.

Plugging Eq. (5.49) into Eq. (5.48), the path probability can be readily obtained as

$$\begin{aligned} \mathcal{P}(\mathcal{X}_{[0,T]}|\psi(0)) = \mathcal{N} \exp\Bigg[&- \frac{1}{2} \int_0^T dt \int_0^T dt'\, G(t,t') \\ &\times \left\{ \ddot{x}(t) + \int_0^t ds\, \gamma(t-s)\dot{x}(s) + k(x(t) - \lambda(t)) \right\} \\ &\times \left\{ \ddot{x}(t') + \int_0^{t'} ds'\, \gamma(t'-s')\dot{x}(s') + k(x(t') - \lambda(t')) \right\} \Bigg], \end{aligned} \tag{5.51}$$

where $\mathcal{N}$ is a Jacobian term that is independent of the trajectories. The quantity σ_t can be expressed as

$$\sigma_t = \ln \frac{P(x(0), v(0), 0)}{P(x(T), -v(T), 0)} + \ln \frac{\mathcal{P}(\mathcal{X}_{[0,T]}|\psi(0))}{\mathcal{P}(\mathcal{X}^\dagger_{[0,T]}|\psi^\dagger(0))}. \tag{5.52}$$

Here, $\psi^\dagger(0) \equiv [x(T), -v(T)]$. Using the formula of the path probability in Eq. (5.51), we can prove that the second term in the right-hand side of Eq. (5.52) is equal to the dissipated heat [166]:

$$\ln \frac{\mathcal{P}(\mathcal{X}_{[0,T]}|\psi(0))}{\mathcal{P}(\mathcal{X}^\dagger_{[0,T]}|\psi^\dagger(0))} = \beta \Delta Q. \tag{5.53}$$

We now verify the derived TUR with the current $\jmath(\mathcal{X}) = \int_0^T dt\, \dot{x}(t) = x(T) - x(0)$, which expresses the displacement of the particle. Since this current is odd under time reversal, the inequality $\mathrm{Var}[\jmath]/\langle \jmath \rangle^2 \geq 2/(e^{\langle \sigma_t \rangle} - 1)$ should be satisfied. The fluctuation of this current and the derived bound can be calculated analytically. First, we have that $\langle x(0) \rangle = \langle v(0) \rangle = 0$, $\langle x(0)^2 \rangle = (k\beta)^{-1}$, and $\langle v(0)^2 \rangle = \beta^{-1}$. The average current is $\langle \jmath \rangle = \langle x(T) \rangle - \langle x(0) \rangle = \langle x(T) \rangle$.

The variance of the current becomes

$$\mathrm{Var}[J] = \langle x(T)^2\rangle - \langle x(T)\rangle^2 + \langle x(0)^2\rangle - 2\langle x(0)x(T)\rangle. \tag{5.54}$$

From Eq. (5.47), the average dissipated heat can be calculated as

$$\begin{aligned}\langle \Delta Q\rangle = \frac{1}{2}\langle v(0)^2 - v(T)^2\rangle + \frac{k}{2}\langle x(0)^2 - x(T)^2\rangle \\ + k\alpha\left\langle \int_{T/2}^{T} dt\, x(t) - \int_0^{T/2} dt\, x(t)\right\rangle.\end{aligned} \tag{5.55}$$

The average of the boundary term in Eq. (5.52) is

$$\begin{aligned}&\left\langle \ln \frac{P(x(0),v(0),0)}{P(x(T),-v(T),0)}\right\rangle \\ &= \frac{\beta}{2}\left\langle v(T)^2 - v(0)^2 + k\left(x(T)^2 - x(0)^2\right)\right\rangle.\end{aligned} \tag{5.56}$$

Combining Eqs. (5.55) and (5.56), we readily obtain

$$\langle \sigma_t\rangle = k\alpha\beta\left\langle \int_{T/2}^{T} dt\, x(t) - \int_0^{T/2} dt\, x(t)\right\rangle. \tag{5.57}$$

Using the Laplace transform, analytical forms of $\langle J\rangle$, $\mathrm{Var}[J]$, and $\langle\sigma_t\rangle$ can be obtained (see Appendix C.3 for detailed calculations). We randomly sample parameters $(\alpha,\beta,\gamma_0,\tau_c,k,T)$ and evaluate $\langle J\rangle$, $\mathrm{Var}[J]$, and $\langle\sigma_t\rangle$ using Eq. (C.59). The parameter ranges are given in the caption of Fig. 5.4. As seen in this figure, the derived bound is satisfied for all parameter settings. In the region $\langle\sigma_t\rangle < 1$, some circular points touch the line, which implies that the derived bound is attainable when the system is near equilibrium. As in the example of the two-dimensional system, we find that $\mathrm{Var}[J]/\langle J\rangle^2 \geq 2/\langle\sigma_t\rangle$ is satisfied for all selected parameters. This evidence strengthens the conjecture made in the preceding example.

We next consider a physical interpretation of the term $\langle\sigma_t\rangle$ in this system. From Eqs. (5.52) and (5.53), we have

$$\langle\sigma_t\rangle = \left\langle \ln \frac{P(\psi(0),0)}{P(\psi^\dagger(0),0)}\right\rangle + \beta\langle\Delta Q\rangle. \tag{5.58}$$

As seen, there are two contributions in $\langle\sigma_t\rangle$, the boundary term $\left\langle \ln P(\psi(0),0)/P(\psi^\dagger(0),0)\right\rangle$ and the dissipated heat $\beta\langle\Delta Q\rangle$. Neglecting this boundary value, one can approximate $\langle\sigma_t\rangle \approx \beta\langle\Delta Q\rangle$. This implies that $\langle\sigma_t\rangle$ can be interpreted as the average dissipated heat in the system. We note that for general cases, i.e., the protocol is time asymmetric, this is not the case.

5.1.4 Concluding remarks and discussion

In summary, we derived the TUR for the time-delayed systems. We provided two bounds on the relative fluctuations of general dynamical observables that are antisymmetric under conjugate operations. For observables that are antisymmetric under time reversal, the fluctuation is lower bounded by $2/(e^{\langle\sigma_t\rangle} - 1)$, where $\langle\sigma_t\rangle$ can be considered a generalization of the total entropy production. On the other hand, the fluctuation of observables that are odd

under position reversal is constrained by $\langle \sigma_p \rangle$, which reflects the degree of position-symmetry breaking in the system. These results hold for an arbitrary observation time. Because it is not necessary to know the underlying dynamics of the systems, the derived TUR holds for a large class of continuous- and discrete-time systems. The bound can be used as a tool to estimate a hidden thermodynamic quantity in real-world systems that involve time delays from finite-time experimental data.

From the results in the numerical experiment, we conjectured that the fluctuation of arbitrary time-integrated currents in continuous-time systems is bounded from below by the reciprocal of $\langle \sigma_t \rangle$. Proving this inequality would substantially improve the bound and requires further investigation.

5.2 Bounds for systems with measurement and feedback control

Here, we study TUR for steady-state systems involving repeated measurements and feedback control; in particular, we define a lower bound on the fluctuation of arbitrary dynamical observables that are antisymmetric under time reversal. We prove that $\mathrm{Var}[O]/\langle O \rangle^2$, where $\langle O \rangle$ and $\mathrm{Var}[O]$ are respectively the mean and the variance of the arbitrary observable O, is lower bounded by a function of $\langle \sigma \rangle$ [cf. Eq. (5.59)], which denotes a quantity reflecting the thermal cost and mutual entropy production. Due to the information flow, the observable fluctuation is bounded from below not only by the dissipated heat but also by the quantity of information obtained from the external controller. The inequality is valid for arbitrary observation times and for discrete- or continuous-time systems because the derivation does not require the underlying dynamics. In addition, for Langevin dynamics involving continuous measurement and feedback control, we provide a tighter bound on the fluctuation of time-integrated currents.

Then, we apply the results to the study of a flashing ratchet [167–170], in which the asymmetric potential is switched between on and off to induce a directed motion. The investigated device is a nonequilibrium Brownian ratchet, which has been applied for modeling biological processes such as actin polymerization [171] and ion transportation [172]. To analyze the observable uncertainty under feedback control, we consider a flashing ratchet using imperfect information about the system state to rectify the motion of a diffusive particle; the ratchet acts as a Maxwell's demon by utilizing the measured information to maximize the instant velocity. Besides the mean velocity, which is the most common quantity used for transport characterization, the relative fluctuation of the displacement, reflecting its precision, is another important attribute. We also empirically verify the derived bound for the displacement of both discrete- and continuous-state ratchets. To the best of our knowledge, this is the first time that a lower bound on the precision of an information ratchet is provided.

5.2.1 Model

We consider a classical Markovian system manipulated by repeated feedback, where an external controller uses the acquired information to evolve the system. The system state is

measured along a trajectory and the outcome is utilized to update the control protocol. The time and state space of the system can be discrete or continuous. We assume that every transition is reversible, i.e., if the transition probability from state x to state x' is nonzero, the reversed transition probability from x' to x is positive.

Suppose that we observe the system during a time interval $[0, \mathcal{T}]$. Let $\mathcal{X}$ and $\mathcal{M}$ be the trajectories of its states and measurement outcomes, respectively; their time-reversed counterparts are therefore denoted as $\mathcal{X}^\dagger$ and $\mathcal{M}^\dagger$. Then, we define the following trajectory-dependent quantity:

$$\sigma(\mathcal{X}, \mathcal{M}) \equiv \ln \frac{\mathcal{P}_{\rm F}(\mathcal{X}, \mathcal{M})}{\mathcal{P}_{\rm R}(\mathcal{X}^\dagger, \mathcal{M}^\dagger)}, \tag{5.59}$$

where $\mathcal{P}_{\rm F}(\mathcal{X}, \mathcal{M})$ and $\mathcal{P}_{\rm R}(\mathcal{X}^\dagger, \mathcal{M}^\dagger)$ are the joint probabilities of observing trajectories in the forward and time-reversed processes, respectively. As shown latter, the quantity $\langle\sigma\rangle$ constrains the fluctuation of the time-antisymmetric observables. We can easily confirm that σ satisfies the integral fluctuation theorem

$$\langle e^{-\sigma} \rangle = 1. \tag{5.60}$$

By applying the Jensen inequality to Eq. (5.60), we can readily obtain $\langle\sigma\rangle \geq 0$. This inequality can be considered as the second law of thermodynamics for a full system (e.g., system and controller), while σ can be identified as its total entropy production.

5.2.2 Main results

Discrete measurement and feedback control

Now, let us apply the measurement and feedback control to the system from time $t = 0$ up to the time $t = \mathcal{T}$. For simplicity, we define $t_0 \equiv 0$, $t_N \equiv \mathcal{T}$. Suppose that we perform measurements discretely at the predetermined times $t_0, t_1, \ldots, t_{N-1}$ and the measurement outcomes are $\mathcal{M} = \{m_0, m_1, \ldots, m_{N-1}\}$. The measurement times are $t_i = i\Delta t$ $(i = 0, \ldots, N)$, where $\Delta t = \mathcal{T}/N$ denotes the time gap between two consecutive measurements. Let $\mathcal{X} = \{x_0, x_1, \ldots, x_N\}$ be the system states during the control process, where x_i denotes the system state at time $t = t_i$ for each $i = 0, \ldots, N$; then, the measurement and feedback schemes are as follows. First, at the time $t = t_0$, the observable is measured with outcome m_0, and the system is then driven with the protocol $\lambda(m_0)$ from $t = t_0$ to $t = t_1$. At each subsequent time $t = t_i$ $(i = 1, \ldots, N-1)$, the measurement is performed and the corresponding outcome is m_i. The protocol is immediately changed from $\lambda(m_{i-1})$ to $\lambda(m_i)$, and it remains constant until the time t_{i+1}. The procedure is repeated up to the time $t = t_N$, which ends with the protocol $\lambda(m_{N-1})$. Herein, it is assumed that the time delay required for measuring and updating the protocol can be ignored. The measurement error is characterized using a conditional probability $p(m_k|x_k)$, where x_k denotes the actual system state, while m_k denotes the measurement outcome at time t_k. This implies that the outcome depends on only the system's state immediately before the measurement. In the sequel, we assume that the system is in the steady state under the measurement and feedback control.

Following Ref. [173], we consider a time-reversed process in which $\mathcal{X}^\dagger = \{x_N, \ldots, x_0\}, \mathcal{M}^\dagger = \{m_{N-1}, \ldots, m_0\}$ and the measurements are performed at times $t_i^\dagger = \mathcal{T} - t_{N-i}$ for each $i = 0, \ldots, N-1$. Since the control protocol is time-independent (i.e., it depends only on the measurement outcome), we have $\mathcal{P}_\mathrm{F} = \mathcal{P}_\mathrm{R} \equiv \mathcal{P}$. Taking the ratio of the probabilities of the forward path and its conjugate counterpart, we obtain [173]

$$\sigma = \ln \frac{\mathcal{P}(\mathcal{X}, \mathcal{M})}{\mathcal{P}(\mathcal{X}^\dagger, \mathcal{M}^\dagger)} = \Delta s + \Delta s_\mathrm{m} + \Delta s_\mathrm{i}, \tag{5.61}$$

where each term in the right-hand side of Eq. (5.61) is expressed as follows:

$$\begin{aligned} \Delta s &= \ln \frac{P^\mathrm{ss}(x_0)}{P^\mathrm{ss}(x_N)}, \\ \Delta s_\mathrm{m} &= \ln \left[\prod_{i=0}^{N-1} \frac{w(x_{i+1}, t_{i+1} | x_i, t_i, m_i)}{w(x_i, \mathcal{T} - t_i | x_{i+1}, \mathcal{T} - t_{i+1}, m_i)} \right], \\ \Delta s_\mathrm{i} &= \ln \left[\prod_{i=0}^{N-1} \frac{p(m_i|x_i)}{p(m_i|x_{i+1})} \right], \end{aligned} \tag{5.62}$$

where $P^\mathrm{ss}(x)$ denotes the steady-state distribution of the system and $w(x', t'|x, t, m)$ denotes the transition probability. The first term Δs and second term Δs_m denote the change in the system entropy and the medium entropy, respectively. The last term Δs_i involves the probability that characterizes the error in measurements; thus, it can be considered as an information quantity. When $p(m|x)$ is the same uniform distribution for all x, the measurement is completely random and does not provide any valuable information. In this case, $\Delta s_\mathrm{i} = 0$, which shows that the system does not obtain any information from measurements. Since $\langle \Delta s + \Delta s_\mathrm{m} + \Delta s_\mathrm{i} \rangle \geq 0$, we have $\langle \Delta s + \Delta s_\mathrm{m} \rangle \geq -\langle \Delta s_\mathrm{i} \rangle$. This implies that the entropy production of the system can be negative because of the effect of measurement and feedback control.

Next, we derive a lower bound on the fluctuation of the arbitrary dynamical observables that are antisymmetric under time reversal. In particular, we focus on a bound for $\mathrm{Var}[O]/\langle O \rangle^2$, where O satisfies the antisymmetric condition $O[\mathcal{X}^\dagger] = -O[\mathcal{X}]$. Current-type observables always satisfy this condition.

By considering $P(\sigma)$ as the probability distribution of σ, i.e., $P(\sigma) = \int \mathcal{D}\mathcal{X}\mathcal{D}\mathcal{M}\, \delta(\sigma - \sigma(\mathcal{X}, \mathcal{M}))\mathcal{P}(\mathcal{X}, \mathcal{M})$, we can show that σ satisfies the strong detailed fluctuation theorem

$$\frac{P(\sigma)}{P(-\sigma)} = e^\sigma. \tag{5.63}$$

We have previously demonstrated that a generalized TUR can be derived from the detailed fluctuation theorem (DFT) [39]. This derivation does not require detailed underlying dynamics and can be flexibly applied to other systems if the strong DFT is valid. Based on Ref. [39], we can prove that the observable fluctuation is bounded from below by a term involving $\langle \sigma \rangle$ as follows:

$$\frac{\mathrm{Var}[O]}{\langle O \rangle^2} \geq \mathrm{csch}^2 \left[f\left(\frac{\langle \sigma \rangle}{2} \right) \right] = \mathrm{csch}^2 \left[f\left(\frac{\langle \Delta s + \Delta s_\mathrm{m} \rangle + \langle \Delta s_\mathrm{i} \rangle}{2} \right) \right], \tag{5.64}$$

where $f(x)$ denotes the inverse function of $x \tanh(x)$. This lower bound is analogous to that utilized in Ref. [46], where the TUR was derived from exchange fluctuation theorems for

heat and particle exchange between multiple systems. In addition to the system entropy production $\langle \Delta s + \Delta s_{\mathrm{m}} \rangle$, the information term, $\langle \Delta s_{\mathrm{i}} \rangle$, also appears in the bound. Inequality (5.64) demonstrates that the precision of the arbitrary observables is constrained not only by the entropy production but also by the information obtained from the system measurement. Since $\mathrm{csch}^2(f(x))$ is a decreasing function of x, the fluctuation of observables is reduced when the information quantity increases. If we consider the limit $\Delta t \to 0$, i.e., the time gap between two consecutive measurements vanishes, the measurement and feedback control become continuous; therefore, this bound is also valid for the continuous-measurement case if $\langle \sigma \rangle$ is well defined in such limit (by properly constructing trajectories $\mathcal{X}$ and $\mathcal{M}$ and their corresponding time-reversed counterparts $\mathcal{X}^\dagger$ and $\mathcal{M}^\dagger$). The detailed derivation of Eq. (5.64) is provided in Appendix D.1.

Since $\mathrm{csch}^2[f(\langle \sigma \rangle/2)] \geq 2/(e^{\langle \sigma \rangle} - 1)$, the bound in Eq. (5.64) is tighter than that in Ref. [25], where the TUR is derived for discrete-time Markovian processes in the long-time limit. However, the derived bound is not as tight as the conventional bound $2/\langle \sigma \rangle$. This happens because the derived inequality holds for both continuous- and discrete-time systems, while the conventional bound is valid only for the formers [160]. In Section 5.2.3, we show that the conventional bound is actually violated for a discrete-time model.

Continuous measurement and feedback control

Here, we discuss systems involving continuous measurement and feedback control; in particular, we consider a Langevin system whose state variable is x. For simplicity, the system is assumed to be one-dimensional. The extension to multidimensional systems is straightforward. The system dynamics is governed by the following equation:

$$\dot{x} = f(x, m) + \xi, \tag{5.65}$$

where the dot indicates the time derivative and $f(x, m)$ is the force depending on x and the measurement outcome m. ξ is the zero-mean Gaussian white noise with variance $\langle \xi(t)\xi(t') \rangle = 2D_x \delta(t - t')$, where D_x denotes the noise intensity of ξ.

The measurement error is commonly incorporated by adding another zero-mean Gaussian noise, e, to the read-out of x, i.e., $m = x + e$. Since the white noise fluctuations are violent, we assume that e is a colored noise. Specifically, e is modeled by the Ornstein–Uhlenbeck (OU) process as

$$\dot{e} = -e + \eta, \tag{5.66}$$

where η is the zero-mean Gaussian white noise with variance $\langle \eta(t)\eta(t') \rangle = 2D_e \delta(t - t')$. D_e denotes the noise intensity of η and also reflects the magnitude of the measurement error. To ensure a clear illustration, we use the OU process to model the measurement error; however, another modeling of the noise does not affect the result as long as the noise is modeled by equilibrium overdamped Langevin dynamics (i.e., when the dynamics of e is described as $\dot{e} = g(e) + \eta$, where $g(e)$ denotes a proper function). In the sequel, we show that the analytical form of $\langle \sigma \rangle$ is independent of the form of $g(e)$.

Now, to investigate the analytical form of $\langle\sigma\rangle$, let us discretize the problem and take the continuous-time limit at the end. Let $\mathcal{X} = [x_0, x_1, \ldots, x_N]$ and $\mathcal{M} = [m_0, m_1, \ldots, m_{N-1}]$ be the trajectories of the system states and measurement outcomes, respectively, in the forward process. Here, $x_i \equiv x(i\Delta t)$, $m_i \equiv m(i\Delta t)$ and $\Delta t = \mathcal{T}/N$. Their time-reversed counterparts in the backward process are $\mathcal{X}^\dagger = [x_N, x_{N-1}, \ldots, x_0]$ and $\mathcal{M}^\dagger = [m_N, m_{N-1}, \ldots, m_1]$. Defining $e_i \equiv m_i - x_i$, the joint path probabilities, $\mathcal{P}(\mathcal{X}, \mathcal{M})$ and $\mathcal{P}(\mathcal{X}^\dagger, \mathcal{M}^\dagger)$, can be expressed as follows:

$$\begin{aligned}\mathcal{P}(\mathcal{X}, \mathcal{M}) \propto P^{\rm ss}(x_0, m_0) \exp\left(-\sum_{i=0}^{N-1} \frac{[x_{i+1} - x_i - f(x_i, m_i)\Delta t]^2}{4D_x \Delta t}\right) \\ \times \exp\left(-\sum_{i=1}^{N-1} \frac{[e_i - e_{i-1}(1-\Delta t)]^2}{4D_e \Delta t}\right),\end{aligned} \tag{5.67}$$

$$\begin{aligned}\mathcal{P}(\mathcal{X}^\dagger, \mathcal{M}^\dagger) \propto P^{\rm ss}(x_N, m_N) \exp\left(-\sum_{i=0}^{N-1} \frac{[x_i - x_{i+1} - f(x_{i+1}, m_{i+1})\Delta t]^2}{4D_x \Delta t}\right) \\ \times \exp\left(-\sum_{i=2}^{N} \frac{[e_{i-1} - e_i(1-\Delta t)]^2}{4D_e \Delta t}\right).\end{aligned} \tag{5.68}$$

Using Eqs. (5.67) and (5.68) and taking the $\Delta t \to 0$ limit, we then obtain

$$\langle\sigma\rangle = \left\langle \ln \frac{\mathcal{P}(\mathcal{X}, \mathcal{M})}{\mathcal{P}(\mathcal{X}^\dagger, \mathcal{M}^\dagger)} \right\rangle = \frac{1}{D_x} \left\langle \int_0^{\mathcal{T}} dt\, f(x, m) \circ \dot{x} \right\rangle, \tag{5.69}$$

where $\circ$ denotes the Stratonovich product. This expression can be used for the numerical evaluation of $\langle\sigma\rangle$. We note that $\langle\sigma\rangle$ is a limit of the discrete sum $1/D_x \sum_i (x_{i+1} - x_i)[f(x_{i+1}, m_{i+1}) + f(x_i, m_i)]/2$. When $f(x, m)$ is differentiable, $\langle\sigma\rangle$ is equivalent to the limit of the sum $1/D_x \sum_i (x_{i+1} - x_i) f((x_{i+1} + x_i)/2, (m_{i+1} + m_i)/2)$. However, when $f(x, m)$ is non-differentiable, it is not the case and the former should be employed.

Let us investigate the information contribution of $\langle\sigma\rangle = \mathcal{T}\bar{\sigma}$, where $\bar{\sigma}$ denotes the total entropy production rate. We can decompose $\bar{\sigma}$ into two positive terms as follows [116, 174]:

$$\bar{\sigma} = \bar{\sigma}_x + \bar{\sigma}_e, \tag{5.70}$$

where $\bar{\sigma}_z = \bar{S}_z + \bar{Q}_z/D_z \geq 0$ denotes the entropy production rate contributed from z, for each $z \in \{x, e\}$. Here, $\bar{S}_z = -\int dx de\, J_z(x, e) \partial_z \ln P^{\rm ss}(x, e)$ denotes the rate of change of the Shannon entropy, while $\bar{Q}_z = \int dx de\, J_z(x, e) F_z(x, e)$ denotes the heat flow from z into the environment. Note that $F_x(x, e) = f(x, x + e)$ and $F_e(x, e) = -e$ are the forces and $J_z(x, e) = F_z(x, e) P^{\rm ss}(x, e) - D_z \partial_z P^{\rm ss}(x, e)$ is the probability current in the corresponding Fokker–Planck equation. The flow of information from e to x,

$$\bar{I}_{e\to x} = -\int dx de\, J_e(x, e) \partial_e \ln \frac{P^{\rm ss}(x, e)}{P^{\rm ss}(x) P^{\rm ss}(e)}, \tag{5.71}$$

is (minus) the variation of the mutual information between x and e [175]

$$I(x; e) = \int dx de\, P^{\rm ss}(x, e) \ln \frac{P^{\rm ss}(x, e)}{P^{\rm ss}(x) P^{\rm ss}(e)}. \tag{5.72}$$

Since the noise is in equilibrium, we have that $\int dx\, J_e(x,e) = 0$. Consequently, we obtain that $\bar{Q}_e = 0$ and $\bar{I}_{e\to x} = \bar{S}_e$. Thus, $\bar{\sigma}_e = \bar{I}_{e\to x} \geq 0$ and $\bar{\sigma} = \bar{\sigma}_x + \bar{I}_{e\to x}$. This implies that, in addition to the system entropy production, $\bar{\sigma}_x$, there is a positive information flow, $\bar{I}_{e\to x}$, from the controller into the system, corresponding to the information contribution in $\langle\sigma\rangle$.

As regards Langevin systems [Eq. (5.65)] involving continuous measurements, a tighter bound can be obtained; more specifically, for arbitrary time-integrated currents being $\mathcal{O}[\mathcal{X}] = \int_0^{\mathcal{T}} dt\, \Lambda(x) \circ \dot{x}$, where $\Lambda(x)$ is an arbitrary projection function, we can prove that

$$\frac{\mathrm{Var}[\mathcal{O}]}{\langle\mathcal{O}\rangle^2} \geq \frac{2}{\langle\sigma\rangle} = \frac{2}{\mathcal{T}(\bar{\sigma}_x + \bar{I}_{e\to x})}. \tag{5.73}$$

This lower bound is analogous to the conventional one [Eq. (1.4)] and tighter than that in Eq. (5.64). The result implies that the fluctuation is bounded not only by entropy production, $\bar{\sigma}_x$, but also by information flow, $\bar{I}_{e\to x}$. The larger the information contribution is, the higher the precision of the observables. When there is no feedback to the system, $\bar{I}_{e\to x} = 0$, and $\langle\sigma\rangle$ becomes the system entropy production. The detailed derivation of Eq. (5.73) is provided in Appendix D.2.

5.2.3 Numerical illustration

We apply the derived uncertainty relation to study the precision of a flashing ratchet, which is a model of Brownian ratchet. First, we describe the conception of the flashing ratchet in the presence of external controller that utilizes information obtained from the measurements to rectify a directed motion. Afterward, we use both discrete- and continuous-state models of flashing ratchet to validate the derived bound. Both the continuous- and discrete-time ratchets are considered in the discrete-state system.

Let us introduce a flashing ratchet comprising of an overdamped Brownian particle in contact with an equilibrium heat bath at temperature T. The particle evolves under an external asymmetric potential $V(x)$, which can be either on or off depending on the feedback control. The dynamics of the particle can be described by the Langevin equation:

$$\gamma\dot{x} = \lambda(x)F(x) + \xi, \tag{5.74}$$

where x denotes the position of the particle, γ denotes the friction coefficient and ξ denotes white Gaussian noise with zero mean and time correlation $\langle\xi(t)\xi(t')\rangle = 2\gamma T\delta(t-t')$. The force is given by $F(x) = -\partial_x V(x)$, where $V(x)$ is periodic with $V(x+L) = V(x)$, and L denotes the period of the potential. The term $\lambda(x)$ denotes a control protocol that takes value 1 or 0, corresponding to switching on or off the potential.

In the previous conducted studies [169, 176], the protocol $\lambda(x)$ can be determined by $\lambda(x) = \Theta(F(x))$, where $\Theta(z)$ denotes the Heaviside function given by $\Theta(z) = 1$ if $z > 0$ and 0 otherwise. This indicates that the potential is turned on only when the net force applied to the particles is positive. The measurements in these studies were assumed to be perfect, i.e., there is no error in the measurement outcome of the sign of $F(x)$. This feedback control strategy was shown to be the best possible strategy for maximizing the average velocity of one

particle. However, it is not the best strategy for collective flashing ratchet, where more than one particle exists. Taking a more realistic model into account, Refs. [177, 178] studied the flashing ratchet with imperfect measurement. The error in the estimation of the sign of $F(x)$ occurs with a probability $r \in [0, 0.5]$. Equivalently, the potential is switched wrongly with probability r, i.e., the potential can be turned off when $F(x) > 0$ or turn on when $F(x) \leq 0$ with probability r.

Discrete-measurement and discrete-state case

In all the studies discussed so far, measurements are continuously executed, which is difficult to implement from the perspective of experimental realization. Moreover, there is a redundancy in the information that is obtained from continuous measurements; thus, leading to an inefficient implementation from the perspective of energetic cost. We consider a discrete-state flashing ratchet with discretely repeated measurements and feedback control in what follows.

Continuous-time model.—We consider a one-dimensional discrete-state flashing ratchet studied without using feedback control in Refs. [168, 179]. The ratchet comprises a Brownian particle and has discrete states n located at position $n\Delta x$ ($n \in \mathbb{Z}$), where Δx denotes the distance between neighboring states. The particle is only allowed to jump between adjacent states, i.e., the particle cannot instantly transit from state m to state n, for $|m - n| > 1$. The periodic potential is approximated by $\mathcal{N} = \mathcal{N}_1 + \mathcal{N}_2$ states, as illustrated in Fig. 5.5. For each $n \in \mathbb{Z}$, $\overline{n} \equiv n \pmod{\mathcal{N}}$ is defined as the remainder of the Euclidean division of n by $\mathcal{N}$. Suppose that the particle is in state n, then the potential should be turned off if $0 \leq \overline{n} < \mathcal{N}_1$ and turned on otherwise, i.e., if $\mathcal{N}_1 \leq \overline{n} < \mathcal{N}$. This is an ideal control protocol, which maximizes the instant velocity of the particle. Moreover, when the measurement is performed, there exists an error due to the noise and the potential is switched wrongly with a probability $r \in (0, 1)$. Particularly, the conditional probability that characterizes the measurement error is given as follows:

$$p(s|x) = \begin{cases} r, & \text{if } s = 1 \text{ and } 0 \leq \overline{x} < \mathcal{N}_1, \\ r, & \text{if } s = 0 \text{ and } \mathcal{N}_1 \leq \overline{x} < \mathcal{N}, \\ 1 - r, & \text{otherwise}, \end{cases} \tag{5.75}$$

where $s = 1$ and $s = 0$ show that the potential is switched on and off, respectively, while x denotes the system state when executing the measurement.

When the potential is on, the transition rate $\Gamma_{n,m}$ from state m to state n is given by

$$\begin{aligned} &\Gamma_{n+1,n} = \kappa_1, \ \Gamma_{n,n+1} = k_+\kappa_1^{-1}, \ \forall n : \overline{n} = 0, \ldots, \mathcal{N}_1 - 1, \\ &\Gamma_{n+1,n} = \kappa_2^{-1}, \ \Gamma_{n,n+1} = k_+\kappa_2, \ \forall n : \overline{n} = \mathcal{N}_1, \ldots, \mathcal{N} - 1, \\ &\Gamma_{n,m} = 0, \ \forall \ |m - n| > 1. \end{aligned} \tag{5.76}$$

Herein, $k_+ > 0$ reflects the asymmetry in transitions due to a load force, $V_{\max}$ denotes the peak of the potential, and

$$\kappa_1 = \exp\left[-\frac{V_{\max}}{2\mathcal{N}_1 k_{\mathrm{B}} T}\right], \ \kappa_2 = \exp\left[-\frac{V_{\max}}{2\mathcal{N}_2 k_{\mathrm{B}} T}\right]. \tag{5.77}$$

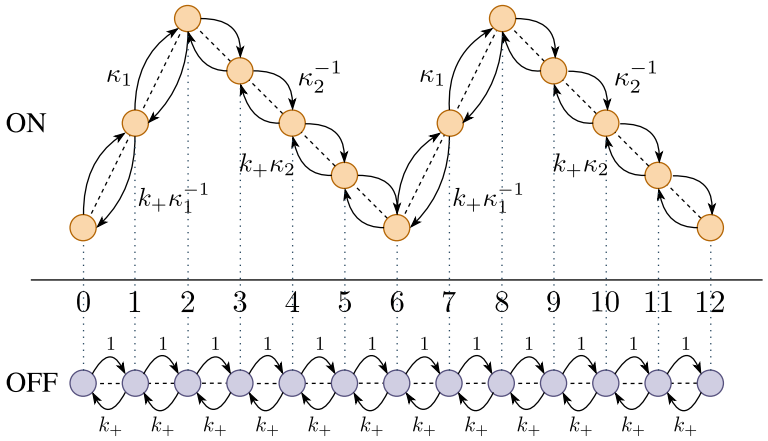

Figure 5.5: Illustration of discrete-state flashing ratchet, where $\mathcal{N} = 6$, $\mathcal{N}_1 = 2$ and $\mathcal{N}_2 = 4$. In the presence of the ratchet potential, the particle transits between adjacent states with predetermined rates. However, when the potential is off, the ratchet obeys a random walk with forward and backward transition rates equal to 1 and k_+, respectively.

When $k_+ = 1$, i.e., there is no load force, the transition rates satisfy the local detailed balance

$$\frac{\Gamma_{n+1,n}}{\Gamma_{n,n+1}} = \exp\left(\frac{V_n - V_{n+1}}{k_{\mathrm{B}}T}\right), \tag{5.78}$$

where V_n denotes the potential at state n, given by

$$V_n = \begin{cases} V_{\max}\overline{n}/\mathcal{N}_1, & \text{if } \overline{n} = 0, \dots, \mathcal{N}_1 - 1, \\ V_{\max}(\mathcal{N} - \overline{n})/\mathcal{N}_2, & \text{if } \overline{n} = \mathcal{N}_1, \dots, \mathcal{N} - 1. \end{cases} \tag{5.79}$$

Hereafter, we set $k_{\mathrm{B}}T = 1$. In the continuous limit, i.e., $\mathcal{N} \to \infty$, the discrete potential converges to the following continuous sawtooth potential:

$$V(x) = \begin{cases} V_{\max}x/(aL), & \text{if } 0 \le x \le aL, \\ V_{\max}(L - x)/[(1-a)L], & \text{if } aL < x \le L, \end{cases} \tag{5.80}$$

where $a = \lim_{\mathcal{N}\to\infty}(\mathcal{N}_1/\mathcal{N})$ is a given constant. Let $P_n(t)$ denote the probability of the system at state n and time t. Thus, the probability distribution is governed by the master equation

$$\partial_t P_n(t) = \sum_m \left[\Gamma_{n,m}P_m(t) - \Gamma_{m,n}P_n(t)\right]. \tag{5.81}$$

When the potential is off, the dynamics of the particle becomes a continuous-time random walk with forward and backward transition rates equal to 1 and k_+, respectively.

Let $\mathbb{P}(x_0, 0, s; x_1, \Delta t)$ denote the probability that the system is at state x_0 at time $t = 0$ with the measurement outcome s and being in state x_1 at time $t = \Delta t$. Since the system is periodic, we define the probability distribution $\mathbb{Q}(x_0, 0, s; x_1, \Delta t)$ for $x_0 \in [0, \mathcal{N}-1]$ and $x_1 \in \mathbb{Z}$

as follows:

$$\mathbb{Q}(x_0, 0, s; x_1, \Delta t) = \sum_{m,n} \mathbb{P}(n, 0, s; m, \Delta t)\delta_{\overline{n},x_0}\delta_{m-n,x_1-x_0}. \tag{5.82}$$

We note that $\mathbb{Q}(x_0, 0, s; x_1, \Delta t)$ is normalized, i.e., $\sum_{x_0=0}^{N-1}\sum_{x_1\in\mathbb{Z}}\sum_{s=0}^{1}\mathbb{Q}(x_0, 0, s; x_1, \Delta t) = 1$. The average of the system entropy production is equal to zero since the system is in the steady state. Therefore, the quantity $\langle\sigma\rangle$ can be evaluated as

$$\langle\sigma\rangle = N\left\langle \ln\frac{w(x_1, \Delta t|x_0, 0, s)}{w(x_0, \Delta t|x_1, 0, s)} + \ln\frac{p(s|x_0)}{p(s|x_1)}\right\rangle_{\mathbb{Q}}, \tag{5.83}$$

where the average is taken with respect to the probability distribution $\mathbb{Q}(x_0, 0, s; x_1, \Delta t)$.

Discrete-time model.—Let us consider a discrete-time model of flashing ratchet, where the control protocol is the same as that of the continuous-time model. Its dynamics is described by a Markov chain

$$P_n(t+\tau) = \sum_m \Lambda_{n,m}P_m(t), \tag{5.84}$$

where τ denotes the time step and $\Lambda_{n,m}$ denotes the transition probability from state m to n. To be consistent with the continuous-time model, the probability $\Lambda_{n,m}$ is set as follows. The ratchet transits between states with the following probabilities when the potential is on are given by

$$\Lambda_{n,m} = \begin{cases} \tau\Gamma_{n,m}, & \text{if } m \neq n, \\ 1 - \tau\left(\Gamma_{n+1,n} + \Gamma_{n-1,n}\right), & \text{if } m = n. \end{cases} \tag{5.85}$$

When the potential is off, the ratchet becomes a discrete-time random walk with the transition probabilities given by $\Lambda_{n,n-1} = \tau$, $\Lambda_{n,n+1} = \tau k_+$, $\Lambda_{n,n} = 1 - \tau(1 + k_+)$ and $\Lambda_{n,m} = 0$ for all $|m - n| > 1$. Moreover, the time step must be properly chosen to ensure the positivity of the transition probabilities, i.e.

$$\tau \leq \min\left\{\frac{1}{1+k_+}, \frac{1}{\max_n\left[\Gamma_{n+1,n} + \Gamma_{n-1,n}\right]}\right\}. \tag{5.86}$$

In addition, the gap time between two consecutive measurements should be a multiple of time step, i.e., $\Delta t/\tau \in \mathbb{N}$. The term $\langle\sigma\rangle$ can be evaluated analogously as in Eq. (5.83).

Bound on the precision of the discrete-state ratchet.—Now, we verify the derived bound for the following observable:

$$O[X] = x_N - x_0. \tag{5.87}$$

This observable is a current, which represents the distance travelled by the particle. The relative fluctuation, $\mathrm{Var}[O]/\langle O\rangle^2$, reflects the precision of the ratchet. According to Eq. (5.64), the inequality $\mathrm{Var}[O]/\langle O\rangle^2 \geq \mathrm{csch}^2[f(\langle\sigma\rangle/2)]$ should be satisfied. We conduct stochastic simulations for both the continuous- and discrete-time models and numerically evaluate the precision, $\mathrm{Var}[O]/\langle O\rangle^2$ and the bound term, $\langle\sigma\rangle$. For each random parameter setting, $(\mathcal{N}_1, \mathcal{N}, V_{\max}, k_+, r, \Delta t, \mathcal{T})$, we collect 10^7 realizations for the calculation. The ranges of the parameters are shown in the caption of Fig. 5.6. We plot $\mathrm{Var}[O]/\langle O\rangle^2$ as a function of $\langle\sigma\rangle$ in

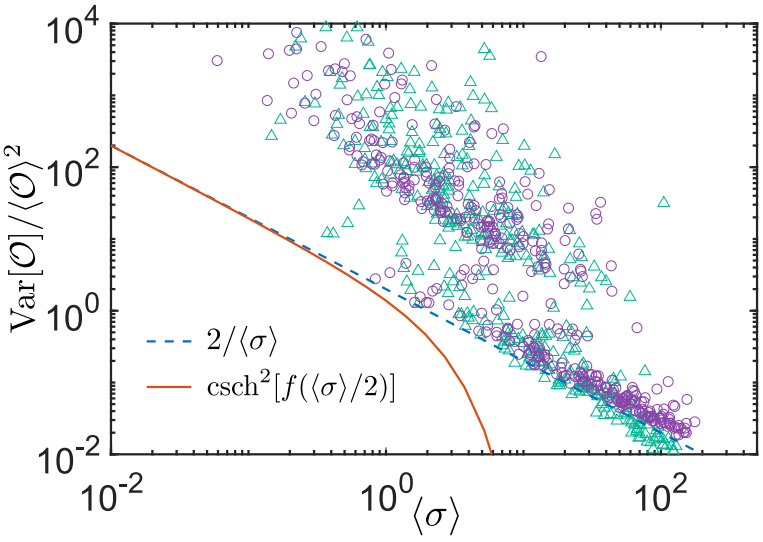

Figure 5.6: Numerical verification of the derived uncertainty relation in the discrete-state flashing ratchet system. The circular and triangular points denote the simulation results of the continuous- and discrete-time models, respectively. $\mathrm{csch}^2[f(\langle\sigma\rangle/2)]$ and $2/\langle\sigma\rangle$ are depicted by solid and dashed lines, respectively. The parameter ranges are $\mathcal{N} \in [3, 30]$, $\mathcal{N}_1 \in [1, \mathcal{N}/2]$, $V_{\max} \in [0.1, 10]$, $k_+ \in [0.1, 10]$ and $r \in (0, 0.5)$. The remaining parameters are $\Delta t \in [0.01, 1]$, $\mathcal{T} \in [2, 10]$ in continuous-time model, while $\tau \in [0.1, 0.5]$, $\Delta t/\tau \in [1, 10]$, $\mathcal{T}/\tau \in [10, 100]$ in discrete-time model.

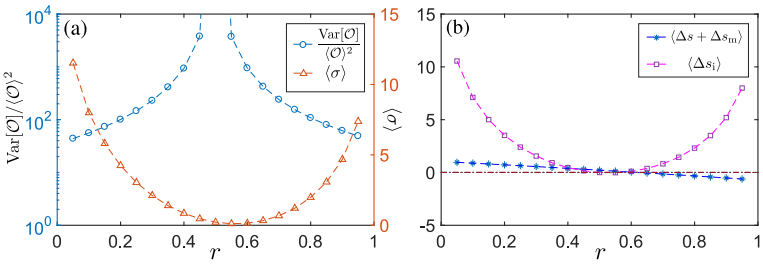

Figure 5.7: (a) The uncertainty and the total entropy production $\langle\sigma\rangle$ corresponding to the measurement error in the discrete-time model. Uncertainty and entropy production are depicted by circular and triangular points, respectively. (b) The entropy productions, $\langle\Delta s + \Delta s_{\mathrm{m}}\rangle$ and $\langle\Delta s_{\mathrm{i}}\rangle$, as functions of the measurement error. $\langle\Delta s + \Delta s_{\mathrm{m}}\rangle$ and $\langle\Delta s_{\mathrm{i}}\rangle$ are depicted by star and square points, respectively. The measurement error, r, is varied from 0.05 to 0.95, while the remaining parameters are fixed: $\mathcal{N} = 4$, $\mathcal{N}_1 = 2, V_{\max} = 1$, $k_+ = 1$, $\Delta t = 0.35$, $\mathcal{T} = 3.5$ and $\tau = 0.35$.

Fig. 5.6, where the circular and triangular points represent the results of the continuous- and discrete-time models, respectively. We depict the saturated case of the derived bound and the conventional bound by solid and dashed lines, respectively. As shown in Fig. 5.6, all the points are located above the solid line; thus, the validity of the derived bound is empirically verified. However, several triangular points lie below the dashed line, which implies that the conventional bound is violated.

We plot the uncertainty in the observable and the total entropy production as functions of measurement error parameter, r, in Fig. 5.7(a). When r decreases to 0 or increases to 1,

more information is obtained from measurement. Therefore, this results in higher entropy production and lower uncertainty. It is interesting that the uncertainty in observable declines exponentially when r is either decreased from 0.5 to 0 or increased from 0.5 to 1. When r is increased to 1, the error in the measurements leads to a reverse motion to the left side. In Fig. 5.7(b), we plot $\langle \Delta s + \Delta s_{\mathrm{m}} \rangle$ and $\langle \Delta s_{\mathrm{i}} \rangle$ as functions of r. As seen, $\langle \Delta s + \Delta s_{\mathrm{m}} \rangle$ becomes negative when $r \geq 0.65$, while $\langle \sigma \rangle$ is always positive. This implies that in this case, the controller works as a kind of Maxwell's demon.

Continuous-measurement and continuous-state case

Finally, we consider a continuous-state flashing ratchet under continuous measurement. Its dynamics is governed by the following equations:

$$\begin{aligned} \gamma \dot{x} &= \lambda(m) F(x) + \xi, \\ m &= x + e. \end{aligned} \tag{5.88}$$

Here, $F(x) = -\partial_x V(x)$ [the form of $V(x)$ is given in Eq. (5.80)], e is the OU process defined as in Eq. (5.66) and the protocol $\lambda(m)$ is a periodic function, i.e., $\lambda(m) = \lambda(m + L)$, defined as

$$\lambda(m) = \begin{cases} 0, & \text{if } 0 \leq m \leq aL, \\ 1, & \text{if } aL < m < L. \end{cases} \tag{5.89}$$

We verify the bound derived in Eq. (5.73) with the current $\mathcal{O}[\mathcal{X}] = \int_0^{\mathcal{T}} dt\, \dot{x} = x(\mathcal{T}) - x(0)$, which expresses the ratchet displacement. According to Eq. (5.73), the inequality $\mathrm{Var}[\mathcal{O}]/\langle \mathcal{O} \rangle^2 \geq 2/\langle \sigma \rangle$ should be satisfied. We randomly sample the parameters and run computer simulations to evaluate $\langle \mathcal{O} \rangle$, $\mathrm{Var}[\mathcal{O}]$ and $\langle \sigma \rangle$. For each parameter setting, we collect 10^7 trajectories by using the Euler–Maruyama method with the time step $\Delta t = 10^{-4}$. $\mathrm{Var}[\mathcal{O}]/\langle \mathcal{O} \rangle^2$ is plotted as a function of $\langle \sigma \rangle$ in Fig. 5.8. Since all the points are located above the line, the derived bound is empirically verified.

The ratchet precision is evaluated also by the Peclet number [168], which is defined as follows:

$$\mathrm{Pe} = \frac{\langle v \rangle}{\mathbb{D}}, \tag{5.90}$$

where $\langle v \rangle$ and $\mathbb{D}$ are, respectively, the mean velocity and the effective diffusion coefficient of the ratchet. Substituting

$$\langle v \rangle = \lim_{\mathcal{T} \to \infty} \frac{\langle \mathcal{O} \rangle}{\mathcal{T}}, \quad \mathbb{D} = \lim_{\mathcal{T} \to \infty} \frac{\mathrm{Var}[\mathcal{O}]}{2\mathcal{T}} \tag{5.91}$$

into Eq. (5.90), we obtain

$$\mathrm{Pe} = \lim_{\mathcal{T} \to \infty} \frac{2\langle \mathcal{O} \rangle}{\mathrm{Var}[\mathcal{O}]}, \tag{5.92}$$

which indicates that Pe is proportional to the inverse of the Fano factor: the larger Pe, the higher the ratchet precision. From the derived bound, we can readily obtain the following

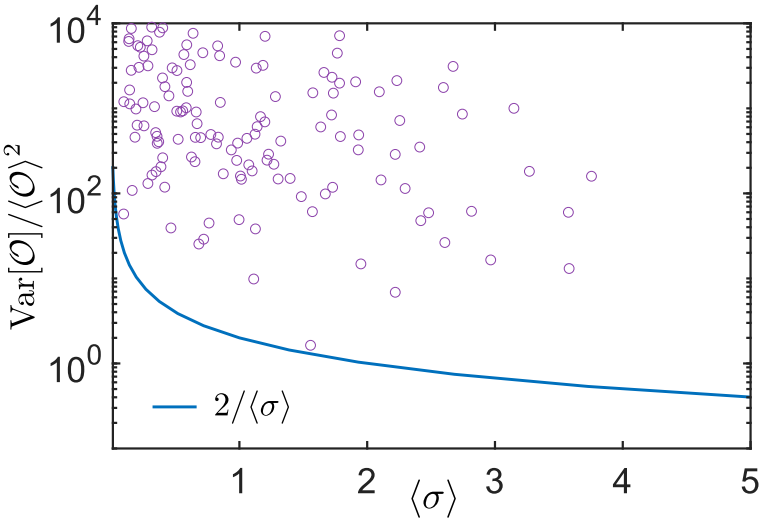

Figure 5.8: Numerical verification of the uncertainty relation in the continuous-state flashing ratchet. $\mathrm{Var}[\mathcal{O}]/\langle\mathcal{O}\rangle^2$ and $2/\langle\sigma\rangle$ are represented by the circles and the solid line, respectively. The parameter ranges are $V_{\max} \in [0.5, 2]$, $a \in [0.1, 0.5]$, $D_x, D_e \in [10^{-3}, 10^0]$ and $\mathcal{T} \in [0.1, 2]$. The remaining parameters are fixed: $\gamma = 1$ and $L = 1$.

upper bound on Pe:

$$\mathrm{Pe} \leq \frac{\langle\sigma\rangle}{\langle\mathcal{O}\rangle}. \tag{5.93}$$

This inequality can be rewritten as $\mathrm{Pe} \times \langle\mathcal{O}\rangle \leq \langle\sigma\rangle$, which implies a trade-off between the ratchet precision and the distance travelled, i.e., with a fixed energy cost $\langle\sigma\rangle$, a ratchet cannot attain both a high precision and a long displacement.

5.2.4 Concluding remarks and discussion

We derived the uncertainty relation for steady-state systems involving repeated measurements and feedback control. We showed that the relative fluctuation of arbitrary observables that are antisymmetric under time reversal is constrained from below by $\langle\sigma\rangle$, which is the sum of the entropy production and the mutual information. For Langevin dynamics involving continuous measurement, we also demonstrated a tighter bound from below on the fluctuation of time-integrated currents. Then, we empirically validated the derived bound for the displacement of a flashing ratchet.

The bound for the discrete-measurement case was derived from the fluctuation theorem, which holds for both continuous- and discrete-time systems. Although the measurements were performed discretely, we did not observe any violation of the conventional bound in the stochastic simulations for the continuous-time ratchet, i.e., $\mathrm{Var}[\mathcal{O}]/\langle\mathcal{O}\rangle^2 \geq 2/\langle\sigma\rangle$ held for all the parameter settings in the continuous-time model. We remark that proving this inequality could significantly improve the bound and, thus, requires further investigation.

We note that an independent related result has been obtained in Ref. [123], where the authors derive an uncertainty relation for systems involving measurement and feedback control. The relation holds even when the time-symmetry is broken (i.e., $\mathcal{P}_{\mathrm{F}} \neq \mathcal{P}_{\mathrm{R}}$) and includes

not only thermodynamic quantities in the forward experiment but also those in the backward experiment. When $\mathcal{P}_{\rm F} = \mathcal{P}_{\rm R}$, the lower bound reduces to $2/(e^{\langle\sigma\rangle} - 1)$, which is not tight as Eqs. (5.64) and (5.73).

5.3 Bounds for semi-Markov systems

It is well-known that Markov jump processes are memoryless, i.e., the jump probability is independent of the elapsed time since the last jump occurred. However, most processes in nature, ranging from physical [180–182] to biological [183, 184] systems, typically have memory effects due to hidden and unobserved variables. Therefore, Markov processes cannot provide reliable approximations for many stochastic dynamics. To effectively model such systems, semi-Markov processes may be required. In contrast to Markov processes, semi-Markov processes have a memory and have successfully been applied to study chemical and biological systems [185–187]. It is a fundamental question to ask how the fluctuation of observables is constrained in the presence of memory.

In this section, we generalize the uncertainty relations, TUR and KUR, for semi-Markov processes. Using the Cramér–Rao inequality, we prove that the fluctuation of observables is constrained not only by entropy production, either dynamical activity but also by memory terms characterized by waiting-time distributions. When the waiting-time distribution is Poissonian, the memory terms vanish, and our bounds reduce to the conventional ones. Therefore, the derived bounds can be regarded as generalizations of the TUR and the KUR. Our results also reveal whether the memory can cooperatively constrain the fluctuation of observables or not.

5.3.1 Semi-Markov processes

In this section, we give a brief introduction of semi-Markov processes, including the definition, statistic properties, and total entropy production. More details on the structure and the properties of semi-Markov processes can be found in Refs. [188, 189].

Definition and notions

Following Ref. [189], we describe here the definition and notions of semi-Markov processes. We consider continuous-time jump processes on a finite space Ω. Unlike in the Markov cases, semi-Markov processes have non-Poissonian waiting-time distributions. The probability of a jump from state x to y at a certain time depends only on the states x, y, and the time t since the last jump occurred. Specifically, transitions in the process are characterized by a density function $K(x, y, t)$. This function satisfies the normalization condition, i.e., $\sum_{y\in\Omega}\int_0^\infty dt\, K(x, y, t) = 1$ for all $x \in \Omega$. Using function $K(x, y, t)$, we define the waiting-time distribution at state x, $K(x, t)$, and the transition probability from x to y regardless of the waiting time, $p(x, y)$, as follows:

$$K(x,t) := \sum_{y\in\Omega} K(x,y,t), \quad p(x,y) := \int_0^\infty dt\, K(x,y,t). \tag{5.94}$$

It is obvious that $\int_0^\infty dt\, K(x,t) = 1$ and $\sum_{y\in\Omega} p(x,y) = 1$. The effective escape rate $\bar{\lambda}(x)$ is equal to the reciprocal of the average waiting time and can be calculated as

$$\bar{\lambda}(x) := \left(\int_0^\infty dt\, tK(x,t) \right)^{-1}. \tag{5.95}$$

When the waiting time does not depend on the future state, but depends only on the present state, i.e., $K(x,y,t) = p(x,y)K(x,t)$, we say that the semi-Markov process is time-direction independence. Hereafter, we exclusively focus on processes satisfying this condition. Note that, when $K(x,t) = \lambda(x)e^{-\lambda(x)t}$, the process becomes Markov.

In the stationary state, the probability distribution $\pi(x)$ satisfies the relation $\sum_{y\in\Omega} j(x,y) = 0$, where $j(x,y)$ is the probability current defined by

$$j(x,y) = \pi(x)\bar{\lambda}(x)p(x,y) - \pi(y)\bar{\lambda}(y)p(y,x). \tag{5.96}$$

Total entropy production

Let $\Gamma = [x_0, t_1, x_1, t_2, \ldots, x_{n-1}, t_n, x_n]$ be a trajectory observed during the time interval $[0,T]$. Here, t_i $(1 \le i \le n)$ denotes the time that a jump from state x_{i-1} to x_i occurred and $0 \le t_1 < t_2 < \cdots < t_n \le T$. At the start time $t = 0$, the system is already at state x_0, and its age is stationarily distributed. The probability distribution of path Γ has the following density:

$$\mathcal{P}[\Gamma] = \pi(x_0)\bar{\lambda}(x_0)\kappa(x_0,x_1,t_1)K(x_1,x_2,t_2-t_1)\ldots K(x_{n-1},x_n,t_n-t_{n-1})\kappa(x_n,T-t_n). \tag{5.97}$$

Here,

$$\kappa(x,y,t) := \int_t^\infty d\tau K(x,y,\tau), \quad \kappa(x,t) := \int_t^\infty d\tau K(x,\tau). \tag{5.98}$$

For each trajectory Γ, considering its time-reversed counterpart $\Gamma^\dagger = [x_n, T-t_n, x_{n-1}, T-t_{n-1}, \ldots, x_1, T-t_1, x_0]$. The total entropy production characterizes the irreversibility in the system and can be defined by the log-ratio of probabilities of observing forward and time-reversed trajectories as

$$\sigma[\Gamma] := \ln \frac{\mathcal{P}[\Gamma]}{\mathcal{P}[\Gamma^\dagger]}. \tag{5.99}$$

From the equality $\langle e^{-\sigma} \rangle = 1$, one can easily prove that $\langle \sigma \rangle \ge 0$, which represents the second law in thermodynamics. Using the formula of the path probability in Eq. (5.97), we obtain

$$\sigma = \ln \pi(x_0) - \ln \pi(x_n) + \sum_{i=1}^{n} \ln \frac{\bar{\lambda}(x_{i-1})p(x_{i-1},x_i)}{\bar{\lambda}(x_i)p(x_i,x_{i-1})}. \tag{5.100}$$

The first term in the right-hand side of Eq. (5.100), $\ln \pi(x_0) - \ln \pi(x_n)$, represents the change in the system entropy. The second term is interpreted as the entropy flux into the environment. In the stationary state, the average entropy production is equal to

$$\langle \sigma \rangle = \left\langle \sum_{i=1}^{n} \ln \frac{\pi(x_{i-1})\bar{\lambda}(x_{i-1})p(x_{i-1},x_i)}{\pi(x_i)\bar{\lambda}(x_i)p(x_i,x_{i-1})} \right\rangle = \frac{T}{2} \sum_{x,y} j(x,y) \ln \frac{\pi(x)\bar{\lambda}(x)p(x,y)}{\pi(y)\bar{\lambda}(y)p(y,x)}. \tag{5.101}$$

5.3.2 Main results

We consider a generic observable $O[\Gamma] = \sum_{i=0}^{n-1} \gamma(x_i, x_{i+1})$, where $\gamma : \Omega\times\Omega \mapsto \mathbb{R}$ is a real-valued function. When $\gamma(x, y)$ is asymmetric, i.e., $\gamma(x, y) = -\gamma(y, x)$, O is a time-antisymmetric observable and called a current. We modify the original dynamics by a perturbation parameter θ and obtain a modified dynamics. Let $\mathcal{P}_\theta[\Gamma]$ be the probability of observing the trajectory Γ in the modified dynamics, then by applying the Cauchy–Schwarz inequality to $(\partial_\theta\langle O\rangle_\theta)^2$, we obtain [33]

$$\frac{\langle\langle O\rangle\rangle_\theta}{(\partial_\theta\langle O\rangle_\theta)^2} \geq \frac{1}{\mathcal{I}(\theta)}, \tag{5.102}$$

where $\mathcal{I}(\theta) := \langle[\partial_\theta \ln \mathcal{P}_\theta(\Gamma)]^2\rangle = -\langle\partial_\theta^2 \ln \mathcal{P}_\theta(\Gamma)\rangle$ is the Fisher information, which places a lower bound on the precision of unbiased estimators. Here $\langle\cdot\cdot\rangle_\theta$ and $\langle\langle\cdot\cdot\rangle\rangle_\theta$ denote the mean and variance in the modified dynamics. Equation (5.102) is also known as the Cramér–Rao inequality in the context of estimation theory.

Thermodynamic bound on fluctuations of currents

Consider a modified process with the following waiting-time kernel:

$$K_\theta(x, t) = (1 + \alpha_x\theta)K(x, (1 + \alpha_x\theta)t), \quad p_\theta(x, y) = \frac{(1 + \alpha_{xy}\theta)p(x, y)}{1 + \alpha_x\theta}. \tag{5.103}$$

Here, α_{xy} and α_x are defined as follows:

$$\alpha_{xy} = 1 - \left(\frac{\pi(y)\bar{\lambda}(y)p(y, x)}{\pi(x)\bar{\lambda}(x)p(x, y)}\right)^{1/2}, \quad \alpha_x = \sum_{y\in\Omega} \alpha_{xy}p(x, y). \tag{5.104}$$

When $\theta = 0$, the modified dynamics become the original ones. Note that when $\theta \ll 1$, both $1 + \alpha_x\theta$ and $1 + \alpha_{xy}\theta$ are ensured to be positive; thus, $K_\theta(x, t)$ and $p_\theta(x, y)$ are well defined. It can be easily confirmed that they satisfy normalization conditions, i.e., $\int dt\, K_\theta(x, t) = 1$ and $\sum_{y\in\Omega} p_\theta(x, y) = 1$ for all x. This modified dynamics have the following properties: (i) the effective escape rates are scaled $\bar{\lambda}_\theta(x) = (1 + \alpha_x\theta)\bar{\lambda}(x)$, (ii) the stationary distribution remains unchanged $\pi_\theta(x) = \pi(x)$, and (iii) the probability currents are scaled $j_\theta(x, y) = (1+\theta)j(x, y)$. Since O is a current, its average can be expressed as $\langle O\rangle = T\sum_{x,y} \gamma(x, y)j(x, y)/2$. Consequently, the average of current O in the modified dynamics is scaled $\langle O\rangle_\theta = (1+\theta)\langle O\rangle$; thus, $\partial_\theta\langle O\rangle_\theta = \langle O\rangle$. The path probability density in the modified dynamics is expressed as

$$\begin{aligned}
\mathcal{P}_\theta[\Gamma] &= \pi_\theta(x_0)\bar{\lambda}_\theta(x_0)\kappa_\theta(x_0, x_1, t_1)K_\theta(x_1, x_2, t_2 - t_1)\dots K_\theta(x_{n-1}, x_n, t_n - t_{n-1})\kappa_\theta(x_n, T - t_n) \\
&= \pi(x_0)(1 + \alpha_{x_0}\theta)\bar{\lambda}(x_0)\prod_{i=0}^{n-1}(1 + \alpha_{x_i x_{i+1}}\theta)p(x_i, x_{i+1})\prod_{i=1}^{n-1}K(x_i, (1 + \alpha_{x_i}\theta)(t_{i+1} - t_i)) \\
&\quad\times\int_{t_1}^{\infty} d\tau K(x_0, (1 + \alpha_{x_0}\theta)\tau)(1 + \alpha_{x_n}\theta)\int_{T-t_n}^{\infty} d\tau K(x_n, (1 + \alpha_{x_n}\theta)\tau).
\end{aligned} \tag{5.105}$$

Using Eq. (5.105), the Fisher information $\mathcal{I}(0)$ can be calculated as

$$\mathcal{I}(0) = \left\langle \sum_{i=0}^{n-1} \alpha^2_{x_i x_{i+1}} \right\rangle - \left\langle \alpha^2_{x_0} f(x_0, t_1) + \alpha^2_{x_n} f(x_n, T - t_n) + \sum_{i=1}^{n-1} \alpha^2_{x_i} g(x_i, t_{i+1} - t_i) \right\rangle, \tag{5.106}$$

where $f(x,t) := t^2 \partial_t^2 \ln \int_t^\infty d\tau\, K(x,\tau)$ and $g(x,t) := t^2 \partial_t^2 \ln K(x,t)$. The first term in the right-hand side of Eq. (5.106) can be reduced to a closed form as

$$\begin{aligned} \left\langle \sum_{i=0}^{n-1} \alpha^2_{x_i x_{i+1}} \right\rangle &= T \sum_{x,y} \pi(x) \bar{\lambda}(x) p(x,y) \left[1 - \left(\frac{\pi(y)\bar{\lambda}(y)p(y,x)}{\pi(x)\bar{\lambda}(x)p(x,y)} \right)^{1/2} \right]^2 \\ &= T \sum_{x,y} \left(\sqrt{\pi(x)\bar{\lambda}(x)p(x,y)} - \sqrt{\pi(y)\bar{\lambda}(y)p(y,x)} \right)^2. \end{aligned} \tag{5.107}$$

Applying the inequality

$$\left(\sqrt{a} - \sqrt{b} \right)^2 \le \frac{1}{4}(a-b) \ln \frac{a}{b} \tag{5.108}$$

to Eq. (5.107), we obtain

$$\left\langle \sum_{i=0}^{n-1} \alpha^2_{x_i x_{i+1}} \right\rangle \le \frac{T}{4} \sum_{x,y} j(x,y) \ln \frac{\pi(x)\bar{\lambda}(x)p(x,y)}{\pi(y)\bar{\lambda}(y)p(y,x)} = \frac{\langle \sigma \rangle}{2}. \tag{5.109}$$

Finally, by letting $\theta = 0$ in Eq. (5.102), we obtain the following bound on the fluctuation of currents:

$$\frac{\langle\langle O \rangle\rangle}{\langle O \rangle^2} \ge \frac{2}{\langle \sigma \rangle + \chi_t}, \tag{5.110}$$

where χ_t is a memory term defined as

$$\chi_t := -2 \left\langle \alpha^2_{x_0} f(x_0, t_1) + \alpha^2_{x_n} f(x_n, T - t_n) + \sum_{i=1}^{n-1} \alpha^2_{x_i} g(x_i, t_{i+1} - t_i) \right\rangle. \tag{5.111}$$

Equation (5.110) is our first main result. When the process becomes Markov, $f(x,t) = g(x,t) = 0$, thus, $\chi_t = 0$, and the derived inequality reduces to the conventional TUR.

Kinetic bound on fluctuations of generic observables

Consider another modified semi-Markov process with the following waiting-time kernel:

$$K_\theta(x,t) = (1+\theta) K(x, (1+\theta)t), \quad p_\theta(x,y) = p(x,y). \tag{5.112}$$

Unlike in the previous modification, we change only the waiting-time distribution and keep the transition probabilities unchanged. When $\theta = 0$, the modified process becomes the original one. It can be easily confirmed that $\int dt\, K_\theta(x,t) = 1$ and $\sum_{y \in \Omega} p_\theta(x,y) = 1$ for all $x \in \Omega$. This modified dynamics have the following properties: (i) the effective escape rates are scaled $\bar{\lambda}_\theta(x) = (1+\theta)\bar{\lambda}(x)$, and (ii) the stationary distribution remains unchanged $\pi_\theta(x) = \pi(x)$. In the stationary state, the average of O can be calculated as $\langle O \rangle = T \sum_{x,y} \gamma(x,y) \pi(x) \bar{\lambda}(x) p(x,y)$.

It is easy to verify that $\langle O\rangle_\theta = (1+\theta)\langle O\rangle$; thus, $\partial_\theta\langle O\rangle_\theta = \langle O\rangle$. Since

$$\begin{aligned}\mathcal{P}_\theta[\Gamma] &= \pi_\theta(x_0)\bar{\lambda}_\theta(x_0)\kappa_\theta(x_0,x_1,t_1)K_\theta(x_1,x_2,t_2-t_1)\dots K_\theta(x_{n-1},x_n,t_n-t_{n-1})\kappa_\theta(x_n,T-t_n)\\ &= \pi(x_0)(1+\theta)\bar{\lambda}(x_0)\prod_{i=0}^{n-1}p(x_i,x_{i+1})\prod_{i=1}^{n-1}(1+\theta)K(x_i,(1+\theta)(t_{i+1}-t_i))\\ &\quad\times(1+\theta)\int_{t_1}^{\infty}d\tau K(x_0,(1+\theta)\tau)(1+\theta)\int_{T-t_n}^{\infty}d\tau K(x_n,(1+\theta)\tau).\end{aligned} \tag{5.113}$$

Using Eq. (5.113) and performing simple calculations, we obtain an expression of $\mathcal{I}(0)$

$$\mathcal{I}(0) = \langle n\rangle - \left\langle f(x_0,t_1) + f(x_n,T-t_n) + \sum_{i=1}^{n-1} g(x_i,t_{i+1}-t_i)\right\rangle. \tag{5.114}$$

The first term in the right-hand side of Eq. (5.114) is equal to the average number of jumps occurred during observation time and is identified as the dynamical activity of the system. It can be analytically calculated as

$$\langle n\rangle = T\sum_{x,y}\pi(x)\bar{\lambda}(x)p(x,y) = T\sum_{x}\pi(x)\bar{\lambda}(x). \tag{5.115}$$

Substituting $\theta = 0$ in Eq. (5.102), we obtain a kinetic bound on the fluctuation of observables

$$\frac{\langle\langle O\rangle\rangle}{\langle O\rangle^2} \geq \frac{1}{\langle n\rangle + \chi_k}, \tag{5.116}$$

where χ_k is a memory term defined by

$$\chi_k := -\left\langle f(x_0,t_1) + f(x_n,T-t_n) + \sum_{i=1}^{n-1} g(x_i,t_{i+1}-t_i)\right\rangle. \tag{5.117}$$

Equation (5.116) is our second main result. In the Markovian case, $\chi_k = 0$, and our result covers the conventional KUR derived for Markov processes.

We make several remarks about our main results, Eqs. (5.110) and (5.116). The derived bounds hold for arbitrary observation times and are generalizations of the conventional bounds [Eqs. (1.4) and (1.5)]. When the waiting-time distribution satisfies $f(x,t) \leq 0,\ g(x,t) \leq 0$ for all $x \in \Omega$, the memory terms are positive; thus, the bounds are lower than the conventional bounds. This implies that memory can reduce the fluctuation of observables in such cases; for example, when the waiting-time distributions are Gamma distributions,

$$K(x,t) = \frac{b_x^{a_x}t^{a_x-1}e^{-b_x t}}{G(a_x)}, \tag{5.118}$$

where $G(z)$ is the Gamma function and $a_x > 1, b_x > 0$ are constants. It is worth note that the bounds are tighter than the conventional ones when $\chi < 0$ (e.g., when $a_x < 1$).

5.3.3 Concluding remarks and discussion

In summary, we have derived finite-time bounds on the fluctuation of observables in steady-state semi-Markov processes. For observables that are antisymmetric under time reversal, we prove that the fluctuation is bounded not only by entropy production but also by the memory term χ_t. For generic observables, the memory term χ_k and dynamical activity simultaneously constrain the fluctuation. The memory terms can be positive or negative, depending on the form of the waiting-time distribution. The sign of the memory terms indicates whether memory can reduce the fluctuation of observables or not. Our results can be applied to study fluctuations in stochastic systems modeled by semi-Markov processes, such as dynamics of kinesin molecules [190] and biochemical reaction networks [191–193] where several reactions are unobserved, or the network topology is not fully revealed. Moreover, we anticipate that the derived bound [Eq. (5.110)] can be used to infer dissipation in living systems whose underlying dynamics are semi-Markov.

Chapter 6

Entropy production estimation with optimal current

Recent studies have made considerable advances in the entropy production inference based on the time-series data [49, 50, 194, 195]. Inference strategies can be generally classified into two classes: direct and indirect. The authors in Ref. [49] employed the former class to quantify dissipation for systems described by the additive-noise Langevin equations; the detailed dynamics of the system (e.g., drift terms and probability fluxes) were estimated, and the associated entropy production was subsequently approximated by either a spatial or a temporal average. However, with an increase in the dimensionality, this strategy becomes computationally costly, and prohibitive amount of data is required to accurately estimate the underlying dynamics. Furthermore, the direct strategy is not applicable to situations wherein the full freedom degrees of the system cannot be observed in the experiments (e.g., some hidden variables exist due to the resolution limit of the measuring instrument [196, 197]). Alternatively, an indirect strategy based on the TUR has been proposed [49, 50]. The TUR imposes the following bound for steady-state systems described by continuous-time Markov jump processes and overdamped Langevin dynamics:

$$\Sigma \geq \frac{2\langle \phi \rangle^2}{\tau \langle\langle \phi \rangle\rangle}, \tag{6.1}$$

where ϕ is an arbitrary time-integrated current, $\langle \phi \rangle$ and $\langle\langle \phi \rangle\rangle := \langle \phi^2 \rangle - \langle \phi \rangle^2$ are its mean and variance, respectively, τ is the observation time, and Σ is the entropy production rate. Theoretically, a lower bound of entropy production can be obtained using TUR. Specifically, when the equality in Eq. (6.1) is attained, the exact entropy production inference is possible [50]. TUR appears to be a powerful tool for entropy production inference; however, an efficient method is still in development from the practical perspective.

In this chapter, we propose a deterministic method of entropy production estimation that is based on the TUR for classical Markovian dynamics. We compute a current that maximizes the lower bound (i.e., minimizes its relative fluctuation) and is referred to as the optimal current. For overdamped Langevin dynamics, we rigorously prove that TUR can be saturated in the short-time limit with the current of entropy production, even when the system is arbitrarily far from equilibrium. Therefore, entropy production can be accurately

estimated via the fluctuation of the optimal current in the short-time limit. For Markov jump processes, we construct a counterexample in which TUR is unattainable with the current of entropy production. Accordingly, entropy production is not guaranteed to be exactly estimated as in the case of Langevin dynamics. In this case, our method provides the tightest possible lower bound on the entropy production. However, given that entropy production is the optimal current, exact estimate can be further obtained by combining our method with the fluctuation theorem. We illustrate our approach with the help of three systems: a four-state Markov jump process, a periodically driven nonlinear system, and a tractable bead-spring model. The results demonstrate that the proposed method produces accurate estimates of entropy production for Langevin systems, and the tightest lower bound for Markov jump processes. Notably, the computed optimal current accurately approximates the stochastic entropy production, which agrees with the theory that the entropy production is one of the optimal currents in the Langevin dynamics.

6.1 Proposed method

In this section, we describe our method of entropy production estimation for both Markov jump processes and Langevin dynamics. First, we discuss the strategy of entropy production estimation on the basis of TUR. Then, we explain in detail how to efficiently estimate entropy production in practice. The procedure of entropy production estimation is illustrated in Fig. 6.1.

6.1.1 Entropy production estimation on the basis of TUR

The lower bound of entropy production rate can be estimated from TUR [Eq. (6.1)] as

$$\Sigma \geq \widehat{\Sigma}_\tau := \max_{\phi} \frac{2\langle \phi \rangle^2}{\tau \langle\langle \phi \rangle\rangle}, \tag{6.2}$$

where the maximum is taken over all possible currents. The inequality (6.2) immediately suggests us a simple way to obtain the lower bound of entropy production rate as follows: (i) observing a variety of currents in the system and calculating the fluctuation of each current; (ii) setting the maximum of $\{2\langle \phi \rangle^2/\tau\langle\langle \phi \rangle\rangle\}$ as a lower bound on Σ. Despite its simplicity, there are several issues when employing this strategy. First, there is no theory that supports the number and the detailed forms of currents needed to yield a good estimate. Moreover, it is also difficult to assess whether the present maximum value is the tightest bound or not. Clearly, if the explicit form of the optimal current is known in advance, one can observe such current and readily obtain the tightest bound for the entropy production rate. Given the underlying dynamics, a recent study has proposed a method to analytically calculate the optimal current, which is called the hyper-accurate current [125]. Without accessibility to the details of dynamics, it is impossible to attain an exact form. In Ref. [49], the authors used the Monte Carlo method to randomly sample the optimal current. However, the resulted current is only sub-optimal when the system is strongly driven from equilibrium. In the next

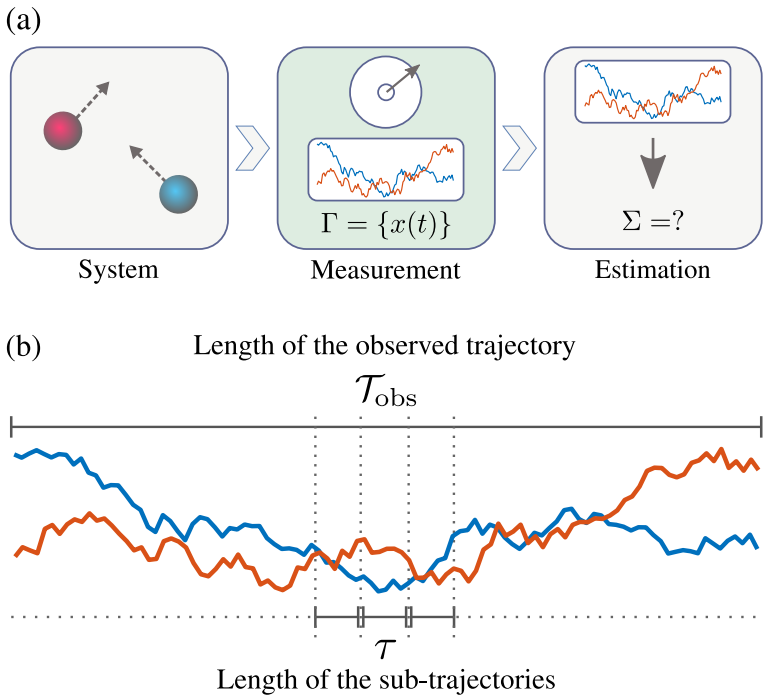

Figure 6.1: (a) Schematic diagram of entropy production estimation. A trajectory $\Gamma = \{x(t)\}_{t=0}^{t=\mathcal{T}_{\rm obs}}$ of the steady-state system is observed by a measuring instrument. Then, the entropy production rate Σ is estimated solely from this single trajectory. (b) Schematic diagram of the trajectory-split process. The observed trajectory of length $\mathcal{T}_{\rm obs}$ is split into multiple sub-trajectories of length τ ($\ll \mathcal{T}_{\rm obs}$). Note that the sub-trajectories can be overlapped in the splitting phase to increase the number of samples.

subsection, we propose a deterministic strategy to efficiently approximate the optimal current from a single trajectory.

To obtain an exact estimate of the entropy production rate, the saturation in Eq. (6.2) is required, i.e., $\widehat{\Sigma}_\tau = \Sigma$. Recently, the authors in Ref. [50] have stated that the equality can be attained in the short-time limit with the current σ of entropy production, i.e.,

$$\frac{2\langle\sigma\rangle^2}{\tau\langle\langle\sigma\rangle\rangle} \xrightarrow{\tau\to 0} \Sigma, \text{ or } \mathcal{F} := \frac{\langle\langle\sigma\rangle\rangle}{\langle\sigma\rangle} \xrightarrow{\tau\to 0} 2. \tag{6.3}$$

Here, we use the relation of $\langle\sigma\rangle = \tau\Sigma$, and $\mathcal{F}$ denotes the Fano factor of σ. Equation (6.3) implies that for short observation times, σ is the optimal current, and its Fano factor $\mathcal{F}$ converges to 2. However, we show that this statement holds for overdamped Langevin dynamics, but not for the Markov jump processes. As shown below, we rigorously prove that for systems described by overdamped Langevin equations, the Fano factor of entropy production always converges to 2 in the short-time limit. Regarding Markov jump processes, we construct a counterexample, in which $\mathcal{F}$ can be arbitrarily large even in the short-time limit. In conclusion, the entropy production rate can be accurately estimated for Langevin dynamics. However, only the tightest lower bound on the entropy production rate can be obtained for Markov jump processes.

Saturation of TUR for Langevin dynamics in the short-time limit

We prove that TUR is saturated with the current of entropy production in the $\tau \to 0$ limit. We consider a general multivariate Langevin system, whose dynamics are described by uncorrelated Ito stochastic differential equations,

$$\dot{x}_i = F_i(\boldsymbol{x}) + \sqrt{2D_i(\boldsymbol{x})}\xi_i(t), \tag{6.4}$$

where $\boldsymbol{x} = [x_1, \ldots, x_N]^\top$ is the vector of variables. The current of stochastic entropy production can be expanded up to the first order of τ as

$$\sigma(\Gamma) = \int_0^\tau dt\, \boldsymbol{\varphi}(\boldsymbol{x})^\top \circ \dot{\boldsymbol{x}} = \boldsymbol{\varphi}(\boldsymbol{x}_0)^\top(\boldsymbol{x}_\tau - \boldsymbol{x}_0) + O(\tau), \tag{6.5}$$

where $\boldsymbol{\varphi}(\boldsymbol{x}) := [D_i(\boldsymbol{x})^{-1} j_i^{\rm ss}(\boldsymbol{x})/p^{\rm ss}(\boldsymbol{x})]^\top \in \mathbb{R}^{N\times 1}$, and $j_i^{\rm ss}(\boldsymbol{x}) = F_i(\boldsymbol{x})p^{\rm ss}(\boldsymbol{x}) - \partial_{x_i}[D_i(\boldsymbol{x})p^{\rm ss}(\boldsymbol{x})]$ is the probability current. The average of entropy production is given by [102]

$$\langle\sigma\rangle = \tau \int d\boldsymbol{x} \sum_{i=1}^N \frac{j_i^{\rm ss}(\boldsymbol{x})^2}{D_i(\boldsymbol{x})p^{\rm ss}(\boldsymbol{x})}. \tag{6.6}$$

Using the short-time propagator [63], the transition probability can be written as

$$p(\boldsymbol{x}_\tau|\boldsymbol{x}_0) = \prod_{i=1}^N \frac{1}{\sqrt{4\pi D_i(\boldsymbol{x}_0)\tau}} \exp\left(-\frac{[x_{i,\tau} - x_{i,0} - \tau F_i(\boldsymbol{x}_0)]^2}{4D_i(\boldsymbol{x}_0)\tau}\right). \tag{6.7}$$

Here, $x_{i,0} := x_i(0)$, $x_{i,\tau} := x_i(\tau)$, and $p(\boldsymbol{x}_\tau|\boldsymbol{x}_0)$ denotes the conditional probability distribution that the system is in $\boldsymbol{x}_\tau$ at time $t = \tau$, given that the system is initially in $\boldsymbol{x}_0$ at time $t = 0$. Using Eqs. (6.5)–(6.7), the variance of entropy production can be analytically calculated as

$$\begin{aligned}
\langle\langle\sigma\rangle\rangle &= \langle\sigma^2\rangle - \langle\sigma\rangle^2 \\
&= \int d\boldsymbol{x}_0\, p^{\rm ss}(\boldsymbol{x}_0) \int d\boldsymbol{x}_\tau\, p(\boldsymbol{x}_\tau|\boldsymbol{x}_0) \\
&\quad \times \left[\boldsymbol{\varphi}(\boldsymbol{x}_0)^\top(\boldsymbol{x}_\tau - \boldsymbol{x}_0) + O(\tau)\right]^2 + O(\tau^2) \\
&= 2\tau \int d\boldsymbol{x} \sum_{i=1}^N \frac{j_i^{\rm ss}(\boldsymbol{x})^2}{D_i(\boldsymbol{x})p^{\rm ss}(\boldsymbol{x})} + O(\tau^2) \\
&= 2\langle\sigma\rangle + O(\tau^2).
\end{aligned} \tag{6.8}$$

Note that to obtain the third equality, means and covariances of $\boldsymbol{x}_\tau - \boldsymbol{x}_0$ are calculated by employing properties of the Gaussian distribution given in Eq. (6.7). Specifically, $\langle x_{i,\tau} - x_{i,0}\rangle = \tau F_i(\boldsymbol{x}_0)$ and $\langle (x_{i,\tau} - x_{i,0})(x_{j,\tau} - x_{j,0})\rangle = \delta_{ij}\left[\tau^2 F_i(\boldsymbol{x}_0)^2 + 2D_i(\boldsymbol{x}_0)\tau\right]$, where the average is taken over distribution $p(\boldsymbol{x}_\tau|\boldsymbol{x}_0)$ and $\boldsymbol{x}_0$ is fixed. Subsequently, the Fano factor can be written as

$$\mathcal{F} = \frac{\langle\langle\sigma\rangle\rangle}{\langle\sigma\rangle} = 2 + O(\tau). \tag{6.9}$$

Thus, one can easily confirm that the Fano factor of entropy production converges to 2 as $\tau \to 0$; equivalently, TUR is saturated in the short-time limit with the current of entropy

production.

Counterexample for the unattainability of TUR in Markov jump processes

We show an example of Markov jump processes, in which TUR is not saturated with the current of entropy production in the short-time limit. Explicitly, we consider a ring-type Markov chain with N states, $\{1, 2, \ldots, N\}$. For each $i = 1, \ldots, N$, a forward jump from state i to state $i+1$ occurs at the rate of $k_+ > 0$, and a backward jump from state $i+1$ to state i occurs at the rate of $k_- > 0$. Here, state $N+1$ is identical to state 1. There are no other transitions between nonconsecutive states. In the short-time limit, i.e., $\tau \to 0$, the mean and variance of entropy production can be calculated as

$$\langle \sigma \rangle = \tau(k_+ - k_-) \ln \frac{k_+}{k_-}, \tag{6.10}$$

$$\langle\langle \sigma \rangle\rangle = \tau(k_+ + k_-) \left(\ln \frac{k_+}{k_-} \right)^2 + O(\tau^2). \tag{6.11}$$

Subsequently, we can obtain the Fano factor $\mathcal{F}$ of entropy production

$$\mathcal{F} = \frac{\langle\langle \sigma \rangle\rangle}{\langle \sigma \rangle} \xrightarrow{\tau \to 0} \frac{k_+ + k_-}{k_+ - k_-} \ln \frac{k_+}{k_-}. \tag{6.12}$$

It is observed that $\mathcal{F}$ can be arbitrarily large and does not converge to 2 in the vanishing-time limit. Because

$$\ln \frac{k_+}{k_-} \geq 2 \frac{k_+ - k_-}{k_+ + k_-}, \ \forall k_+, k_- > 0, \tag{6.13}$$

we have $\mathcal{F} \geq 2$ as $\tau \to 0$. $\mathcal{F} \to 2$ only when $k_+/k_- \to 1$, which means that the system is near equilibrium. This agrees with the conclusion in previous studies [33, 83] that TUR is asymptotically saturated near equilibrium for the current of entropy production.

6.1.2 Approximation of the optimal current

Let $\mathcal{C} = \{\phi_i(\Gamma)\}_{i=1}^n$ be a set of predetermined basis currents such that an arbitrary current can be approximately formed as a linear combination of these currents. Here, Γ denotes a given trajectory, and n is the number of basis currents. The construction of $\mathcal{C}$ (i.e., how to define the detailed form of each basis current ϕ_i) will be described in the next subsection. We assume that the optimal current can be expressed in terms of basis currents as $\phi_{\mathrm{opt}}(\Gamma) = \sum_{i=1}^n c_i \phi_i(\Gamma)$, where $\boldsymbol{c} = [c_1, \ldots, c_n]^\top \in \mathbb{R}^{n \times 1}$ is the coefficient vector. Then, the mean and variance of ϕ_{opt} can be analytically calculated via the basis currents as

$$\langle \phi_{\mathrm{opt}} \rangle = \boldsymbol{c}^\top \boldsymbol{\mu}, \tag{6.14}$$

$$\langle\langle \phi_{\mathrm{opt}} \rangle\rangle = \boldsymbol{c}^\top \Xi \boldsymbol{c}, \tag{6.15}$$

where $\boldsymbol{\mu} := [\langle \phi_1 \rangle, \ldots, \langle \phi_n \rangle]^\top \in \mathbb{R}^{n \times 1}$ and $\Xi := [\langle \phi_i \phi_j \rangle - \langle \phi_i \rangle \langle \phi_j \rangle] \in \mathbb{R}^{n \times n}$ denote the means and the covariance matrix of basis currents, respectively. The computation of ϕ_{opt} is equivalent

to finding the optimal value of $\boldsymbol{c}$ that maximizes the following function:

$$\mathcal{J}(\boldsymbol{c}) = \frac{\langle \phi_{\mathrm{opt}} \rangle^2}{\langle\langle \phi_{\mathrm{opt}} \rangle\rangle} = \frac{\mathcal{E}(\boldsymbol{c})^2}{\mathcal{V}(\boldsymbol{c})}, \tag{6.16}$$

where $\mathcal{E}(\boldsymbol{c}) = \boldsymbol{c}^\top \boldsymbol{\mu}$ and $\mathcal{V}(\boldsymbol{c}) = \boldsymbol{c}^\top \Xi \boldsymbol{c}$. Fortunately, this optimization problem can be solved analytically. Since $\mathcal{J}(\boldsymbol{c})$ is scale-invariant with respect to $\boldsymbol{c}$, i.e., $\mathcal{J}(\kappa \boldsymbol{c}) = \mathcal{J}(\boldsymbol{c})\ \forall \kappa \neq 0$, we can add an equality constraint, $\mathcal{E}(\boldsymbol{c}) = 1$. Consequently, the maximizing $\mathcal{J}(\boldsymbol{c})$ and minimizing $\mathcal{V}(\boldsymbol{c})$ optimizations are equivalent. The latter optimization can be exactly solved using the Lagrange multipliers method. We consider the Lagrangian function

$$\mathcal{L}(\boldsymbol{c}, \lambda) = \frac{1}{2}\mathcal{V}(\boldsymbol{c}) - \lambda(\mathcal{E}(\boldsymbol{c}) - 1). \tag{6.17}$$

Taking the partial derivative of $\mathcal{L}$ with respect to c_i $(i = 1, \ldots, n)$ and λ, we obtain

$$0 = \partial_{c_i} \mathcal{L}(\boldsymbol{c}, \lambda) = \sum_{j=1}^{n} c_j \Xi_{ij} - \lambda \mu_i, \ \ (i = 1, \ldots, n), \tag{6.18}$$

$$0 = \partial_{\lambda} \mathcal{L}(\boldsymbol{c}, \lambda) = 1 - \sum_{i=1}^{n} c_i \mu_i. \tag{6.19}$$

By solving Eqs. (6.18) and (6.19), the explicit solution is obtained

$$\lambda = (\boldsymbol{\mu}^\top \Xi^{-1} \boldsymbol{\mu})^{-1}, \ \ \boldsymbol{c} = (\boldsymbol{\mu}^\top \Xi^{-1} \boldsymbol{\mu})^{-1} \Xi^{-1} \boldsymbol{\mu}. \tag{6.20}$$

Thus, the maximum value of $\mathcal{J}(\boldsymbol{c})$ is

$$\mathcal{J}_{\max} := \max_{\boldsymbol{c}} \mathcal{J}(\boldsymbol{c}) = \boldsymbol{\mu}^\top \Xi^{-1} \boldsymbol{\mu}. \tag{6.21}$$

Since the fluctuation of the optimal current ϕ_{opt} obeys TUR, we have

$$\frac{2\langle \phi_{\mathrm{opt}} \rangle^2}{\tau \langle\langle \phi_{\mathrm{opt}} \rangle\rangle} = \frac{2\mathcal{J}_{\max}}{\tau} = \frac{2\boldsymbol{\mu}^\top \Xi^{-1} \boldsymbol{\mu}}{\tau} \leq \Sigma. \tag{6.22}$$

Equation (6.22) implies that $\widehat{\Sigma}_\tau = 2\mathcal{J}_{\max}/\tau$ is the tightest lower bound for the entropy production rate Σ for the given set of basis currents $\mathcal{C}$. Because TUR can be saturated in the short-time limit for Langevin dynamics, this lower bound is expected to be exactly the entropy production rate. Moreover, as shown later, an arbitrary current in the Markov jump process can always be exactly expressed in the form of a linear combination of basis currents; thus, $2\mathcal{J}_{\max}/\tau$ is the tightest lower bound on entropy production rate for arbitrary observation times. Using the coefficient vector $\boldsymbol{c}$ obtained in Eq. (6.20), the optimal current can be readily calculated as $\phi_{\mathrm{opt}} = \sum_{i=1}^{n} c_i \phi_i$. The inequality $\boldsymbol{\mu}^\top \Xi^{-1} \boldsymbol{\mu} \leq \tau\Sigma/2$ is also a consequence of the multidimensional TUR [53, 105], which provides a tighter bound than that of the scalar TUR [Eq. (6.1)]. Here, our analysis indicates that the multidimensional TUR has a remarkable application in entropy production estimation, which was not revealed until now.

We summarize the procedure of estimating entropy production rate in the following.

Algorithm 1 Estimation of the entropy production rate

Require: a given trajectory of system states $\Gamma = \{x(t)\}_{t=0}^{t=\mathcal{T}_{\rm obs}}$
Ensure: the estimated entropy production rate $\widehat{\Sigma}_\tau$
1: Define a set of basis currents $C = \{\phi_1, \ldots, \phi_n\}$
2: Split Γ into sub-trajectories $\{\Gamma_k\}$ of length τ as [see Fig. 6.1(b)]
3: Compute $\mu_i = \langle\phi_i\rangle, \Xi_{ij} = \langle\phi_i\phi_j\rangle - \langle\phi_i\rangle\langle\phi_j\rangle$ using $\{\Gamma_k\}$
4: Calculate optimal coefficients $\boldsymbol{c} = (\boldsymbol{\mu}^\top \Xi^{-1} \boldsymbol{\mu})^{-1} \Xi^{-1} \boldsymbol{\mu}$
5: Return $\widehat{\Sigma}_\tau = 2\boldsymbol{\mu}^\top \Xi^{-1} \boldsymbol{\mu}/\tau$

The statistical values of ϕ_i can be numerically approximated from sub-trajectories as

$$\langle\phi_i\rangle = \frac{1}{\mathcal{N}_\Gamma} \sum_k \phi_i(\Gamma_k), \tag{6.23}$$

$$\langle\phi_i\phi_j\rangle = \frac{1}{\mathcal{N}_\Gamma} \sum_k \phi_i(\Gamma_k)\phi_j(\Gamma_k), \tag{6.24}$$

where $\mathcal{N}_\Gamma := |\{\Gamma_k\}|$ denotes the number of sub-trajectories.

6.1.3 Construction of basis currents

Here, we describe the construction of basis currents for continuous-time Markov jump processes and overdamped Langevin dynamics.

Markov jump process

We consider a system modeled by the continuous-time Markov jump process on a finite countable state space Ω. Its dynamics are governed by the master equation

$$\partial_t p(y,t) = \sum_{z\in\Omega} \left[p(z,t) w_{zy} - p(y,t) w_{yz} \right], \tag{6.25}$$

where $p(y,t)$ denotes the probability distribution at time t, and w_{yz} denotes the transition rate from state y to state z. We assume that $w_{zy} > 0$ whenever $w_{yz} > 0$, and the system always relaxes to a unique steady state in the long-time limit. Let $p^{\rm ss}(y)$ denote the steady-state distribution, which satisfies $\sum_{z\in\Omega} \left[w_{zy} p^{\rm ss}(z) - w_{yz} p^{\rm ss}(y) \right] = 0, \ \forall y \in \Omega$.

Given a trajectory $\Gamma = [x(t)]_{t=0}^{\tau}$, a generic current in the system can be represented as

$$\phi(\Gamma) = \sum_{y<z} \gamma_{yz} \int_0^\tau dt \, (\delta_{x(t^-),y}\delta_{x(t^+),z} - \delta_{x(t^-),z}\delta_{x(t^+),y}), \tag{6.26}$$

where γ_{yz}'s are arbitrary real numbers, and $x(t^-)$ and $x(t^+)$ denote the state of the system immediately before and after a jump, respectively. Defining the set of basis currents as $C = \{\phi_{yz}\}_{y<z}$, where $\phi_{yz}(\Gamma) = \int_0^\tau dt \, (\delta_{x(t^-),y}\delta_{x(t^+),z} - \delta_{x(t^-),z}\delta_{x(t^+),y})$ is a current that counts the net number of jumps between y and z. Then, arbitrary current ϕ can be written in terms of basis currents $\{\phi_{yz}\}$ as $\phi(\Gamma) = \sum_{y<z} \gamma_{yz}\phi_{yz}(\Gamma)$. For example, the current of stochastic

entropy production has the form [3]

$$\sigma(\Gamma) = \sum_{y<z} \ln \frac{p^{\rm ss}(y)w_{yz}}{p^{\rm ss}(z)w_{zy}} \phi_{yz}(\Gamma), \tag{6.27}$$

which corresponds to the case $\gamma_{yz} = \ln p^{\rm ss}(y)w_{yz}/p^{\rm ss}(z)w_{zy}$. Because arbitrary currents can always be expressed as a linear combination of basis currents $\{\phi_{yz}\}$, the optimal current $\phi_{\rm opt}$ can be accurately computed. Equivalently, the tightest lower bound on entropy production rate can be always obtained.

In special cases, the entropy production rate can, in principle, be accurately estimated using additional steps, even when the optimal current does not saturate the TUR. If the entropy production is the optimal current, i.e., $\sigma = \alpha\phi_{\rm opt}$, where α is an unknown scaling factor, then Σ can be estimated by employing the integral fluctuation theorem as follows. First, α can be determined by examining whether the relation $\langle e^{-\sigma}\rangle = 1$ holds or not. Specifically, this is equivalent to solving equation $\Psi(\alpha) = \mathcal{N}_\Gamma$, where $\Psi(\alpha) = \sum_k e^{-\alpha\phi_{\rm opt}(\Gamma_k)}$. Here, we consider the case that the trajectory Γ is well sampled, i.e., both negative and positive values are contained in $\{\phi_{\rm opt}(\Gamma_k)\}_k$. Since $\Psi(\alpha)$ is a convex function and $\Psi(0) = \mathcal{N}_\Gamma$, $\Psi(-\infty) = \Psi(\infty) = \infty$, this equation has at most one nonzero solution, which can be, if exists, efficiently computed using the Newton–Raphson method. After obtaining α, the entropy production rate can be readily estimated as $\widehat{\Sigma}_\tau = \alpha\langle\phi_{\rm opt}\rangle/\tau$. It was proved that the entropy production is the optimal current for the long-time limit [22]. However, the stochastic entropy production tends to be positive in this limit and the negative samples are rare. Thus, the equation $\Psi(\alpha) = \mathcal{N}_\Gamma$ may have only the trivial solution $\alpha = 0$, which means that the entropy production rate cannot be further estimated.

Langevin dynamics

For simplicity, we consider a one-dimensional system, whose dynamics are described by the Langevin equation,

$$\dot{x} = F(x) + \sqrt{2D(x)}\xi(t), \tag{6.28}$$

where $F(x)$ is the force, $D(x) > 0$ is the diffusion term, and ξ is the zero-mean Gaussian white noise with a variance of $\langle\xi(t)\xi(t')\rangle = \delta(t-t')$. The noise term in Eq. (6.28), $\sqrt{2D(x)}\xi$, is interpreted in the Ito sense. Boltzmann's constant and the friction coefficient are set to unity throughout this study. Let $p(x,t)$ denote the probability distribution function of the system state at time t. Then, the corresponding Fokker–Planck equation is written as

$$\partial_t p(x,t) = -\partial_x j(x,t), \tag{6.29}$$

where $j(x,t) = F(x)p(x,t) - \partial_x[D(x)p(x,t)]$ is the probability current. Again, we focus exclusively on the steady state, where $p(x,t) = p^{\rm ss}(x)$ and $j(x,t) = j^{\rm ss}$. The current of stochastic entropy production is expressed as [102]

$$\sigma(\Gamma) = \int_0^\tau dt\, \varphi(x) \circ \dot{x}, \tag{6.30}$$

where $\varphi(x) := j^{\rm ss}/D(x)p^{\rm ss}(x)$ and $\circ$ denotes the Stratonovich product.

A generic time-integrated current takes the form of $\phi(\Gamma) = \int_0^\tau dt\, f(x) \circ \dot{x}$, where $f(x)$ is the projection function. The entropy production current corresponds to the case of $f(x) = \varphi(x)$. We consider a finite set of basis currents defined as $\phi_i(\Gamma) = \int_0^\tau dt\, f_i(x) \circ \dot{x}$, where $f_i(x)$ is the basis function. We seek basis functions that have a rich representation, i.e., an arbitrary function $f(x)$ can be well approximated by a linear combination of $\{f_i(x)\}_{i=1}^n$ for the certain region of x. For example, $\{f_i(x)\}$ can be trigonometric functions of the Fourier basis, $\{\sin(ix), \cos(ix)\}$, or Gaussian radial basis function kernels, $\exp\left[-(x-x_i)^2/2\vartheta_i^2\right]$, where x_i and ϑ_i are the center and the bandwidth of the kernel, respectively. As other choices, $\{f_i(x)\}$ can be orthogonal polynomials such as Legendre or Chebyshev polynomials [198]. In all examples, we employ trigonometric functions and Gaussian kernels and determine that they provide excellent approximations. Theoretically, increasing the number of basis currents will enhance the representation ability. However, as shown later, the truncation of n to some order is sufficient to obtain good estimates.

Once the basis functions $\{f_i(x)\}$ are determined, the corresponding set of basis currents is $\mathcal{C} = \{\phi_i\}$, where $\phi_i(\Gamma) = \int_0^\tau dt\, f_i(x) \circ \dot{x}$. Using the coefficient vector, which is calculated via means and covariances of basis currents using Eq. (6.20), one can construct the optimal current as $\phi_{\rm opt}(\Gamma) = \int_0^\tau dt\, f_{\rm opt}(x) \circ \dot{x}$, where $f_{\rm opt}(x) = \sum_i c_i f_i(x)$.

6.2 Applications

In this section, we apply the proposed method to three systems: the four-state Markov jump process, the periodically driven particle, and the bead-spring model. For each system, we run a simulation and obtain a single trajectory of length $\mathcal{T}_{\rm obs}$, from which we estimate the entropy production rate. Specifically, for Langevin systems, we use the Euler method to numerically solve system dynamics with a time step of $\Delta t = 10^{-4}$. To examine the stability of the proposed method, we independently perform 20 estimations and calculate the mean and standard deviation of the estimates for each parameter setting.

6.2.1 Four-state Markov jump process

We consider the four-state Markov jump process [22], whose transition rates are given as follows:

$$[w_{yz}] = \begin{bmatrix} 0 & k_+ & k_+ & k_- \\ k_- & 0 & k_+ & k_+ \\ k_- & k_- & 0 & k_+ \\ k_+ & k_- & k_- & 0 \end{bmatrix}, \tag{6.31}$$

where k_+ and k_- are positive parameters [see Fig. 6.2(a) for illustration]. When $k_+ = k_-$, the system relaxes to an equilibrium after a long period of time. By solving the master equation,

one can readily obtain the steady-state distribution

$$[p^{\rm ss}(y)] = \frac{1}{10k_-^2 + 12k_-k_+ + 10k_+^2} \begin{bmatrix} 4k_-^2 + 2k_-k_+ + 2k_+^2 \\ 3k_-^2 + 4k_-k_+ + k_+^2 \\ k_-^2 + 4k_-k_+ + 3k_+^2 \\ 2k_-^2 + 2k_-k_+ + 4k_+^2 \end{bmatrix}. \tag{6.32}$$

Using $[p^{\rm ss}(y)]$, the entropy production rate can be immediately calculated

$$\Sigma = \sum_{y<z} \left[p^{\rm ss}(y)w_{yz} - p^{\rm ss}(z)w_{zy}\right] \ln \frac{p^{\rm ss}(y)w_{yz}}{p^{\rm ss}(z)w_{zy}}. \tag{6.33}$$

We apply the proposed method to estimate the tightest lower bound on the entropy production rate from the single trajectory Γ of length $\mathcal{T}_{\rm obs} = 10^4$, which is obtained from the simulation using the Gillespie algorithm [199]. The value of k_- is fixed to 1, while k_+ is varied in the range of $[1, 5]$. We illustrate the estimated results in Fig. 6.2(b). As seen, the estimated lower bound on Σ is tight and coincides with the actual entropy production rate when the system is close to equilibrium, i.e., when $k_+/k_- \to 1$. When $k_+/k_- \gg 1$, the gap between the estimate value and the actual value increases, which implies that TUR cannot be saturated in this regime even with the short-time limit. We also generate random coefficients $\gamma_{yz} \in [-1, 1]$ and form random currents $\phi_{\rm r} = \sum_{y<z} \gamma_{yz}\phi_{yz}$. We evaluate the fluctuation of each random current, $2\langle\phi_{\rm r}\rangle^2/\tau\langle\langle\phi_{\rm r}\rangle\rangle$ (which is a lower bound on Σ), and plot the result in the same figure. Clearly, the estimated lower bound $\widehat{\Sigma}_\tau$, which is based on the optimal current, is always better than the one that is based on each individual random current.

We investigate the form of the computed optimal current by measuring the distance between the coefficients of $\phi_{\rm opt}$ and those of the entropy production σ. Specifically, we normalize the coefficient vectors, $\widehat{\gamma} = \gamma/\|\gamma\|_2$, and calculate their inner product. Here, $\|\cdot\|_2$ denotes the Euclidean norm. We vary k_+ and plot the cosine similarities in Fig. 6.2(c). The cosine similarity between γ_1 and γ_2 is defined as $\widehat{\gamma}_1 \cdot \widehat{\gamma}_2$, where $\cdot$ denotes the inner product of two vectors. Interestingly, the inner products are always approximately equal to 1, which implies that $\phi_{\rm opt}$ is identical to the current of entropy production (by ignoring the scaling factor). Thus, $\sigma = \alpha\phi_{\rm opt}$, where $\alpha \in \mathbb{R}$ is the unknown scaling factor. Therefore, we use the fluctuation theorem to further estimate the entropy production rate, as demonstrated in the previous section (i.e., not the lower bound but the exact value of Σ). We solve equation $\Psi(\alpha) = \mathcal{N}_\Gamma$ using the Newton–Raphson method to find the nontrivial solution $\alpha \neq 0$. Then, we estimate the entropy production rate as $\widehat{\Sigma}_\tau = \alpha\langle\phi_{\rm opt}\rangle/\tau$. We plot the estimated results in Fig. 6.2(b). As illustrated, the method in combination with the fluctuation theorem produces accurate estimates even when the system is far from equilibrium.

6.2.2 Periodically driven particle

Next, we consider a Brownian particle that circulates on a ring with a circumference of 2π [33], and its dynamics are governed by the Langevin equation with $F(x) = [a + \sin(x)][b + \cos(x)]$ and $D(x) = [a + \sin(x)]^2$, where $a > 1$ and $b \geq 0$ are the parameters. The effective potential

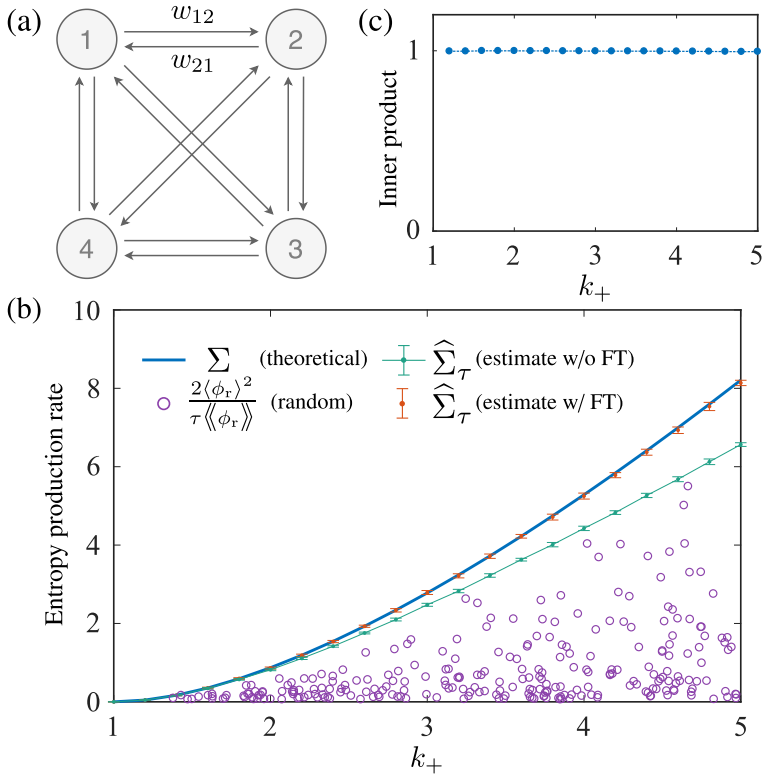

Figure 6.2: (a) Schematic diagram of the four-state Markov jump process whose states are fully connected. (b) Estimation of the entropy production rate. The blue solid line represents the actual entropy production rate, while the green solid line with dots represents its estimated tightest lower bound. The error bar depicts the standard deviation of the estimated values. The violet circles denote the lower bound on the basis of individual random currents. The orange dots with error bars represent the estimated values by combining the proposed method with the fluctuation theorem. When the entropy production is the optimal current, Σ can be accurately estimated with the help of the fluctuation theorem. (c) Cosine similarities between the coefficients of the computed optimal current and those of the entropy production current. As shown, all inner products are close to 1 for all $k_+ \in [1, 5]$, which empirically indicates that the entropy production is the optimal current. Parameter k_+ is varied while the remaining parameters are fixed as $k_- = 1, \mathcal{T}_{\rm obs} = 10^4$, and $\tau = 10^{-2}$.

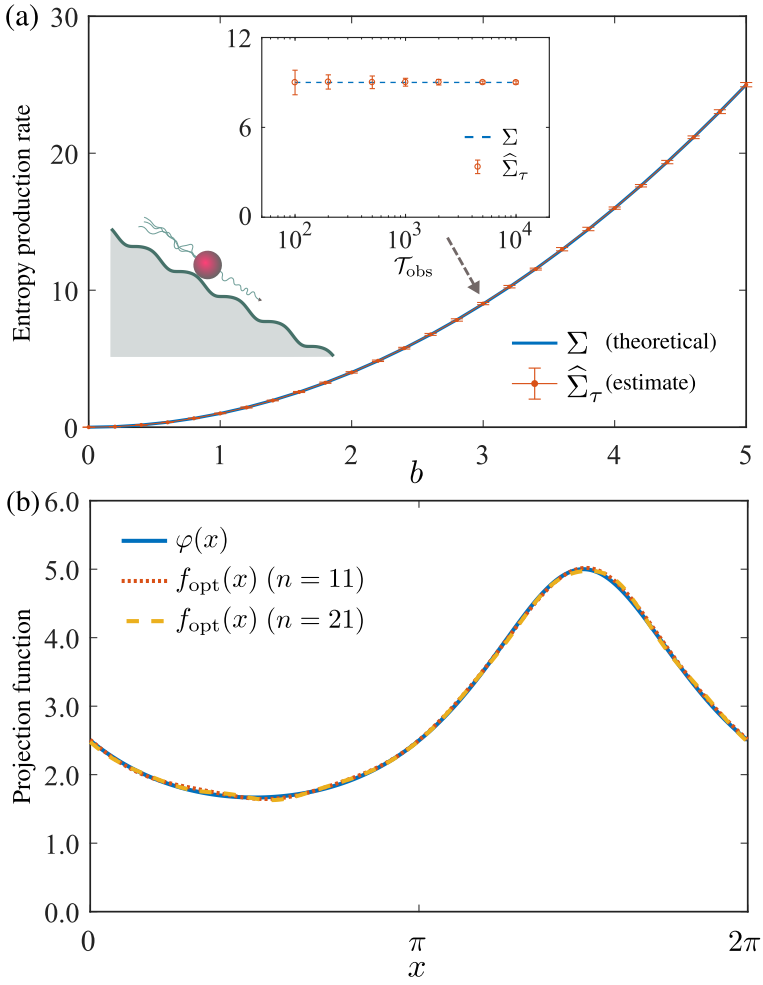

Figure 6.3: (a) Estimation of the entropy production rate Σ in the periodically driven particle system. The blue solid line depicts the theoretical entropy production rate. The orange solid line with dots represents the mean of the estimates of Σ, and the error bars represent the standard errors. The inset shows how the estimation results are affected when the length $\mathcal{T}_{\mathrm{obs}}$ is changed (at $b = 3$). (b) Comparison between the projection function of the computed optimal current, $f_{\mathrm{opt}}(x)$, and that of the entropy production current (which is theoretically the optimal one), $\varphi(x)$, in two cases: $n = 11$ and $n = 21$ basis currents, when $b = 5$. The solid, dotted, and dashed lines represent $\varphi(x)$, $f_{\mathrm{opt}}(x)$ $(n = 11)$, and $f_{\mathrm{opt}}(x)$ $(n = 21)$, respectively. The result shows that the optimal current is well approximated in both cases. The parameters are fixed as $a = 2, \mathcal{T}_{\mathrm{obs}} = 10^4$, and $\tau = 10^{-2}$.

is

$$U(x) = -\frac{1}{2}[a + \sin(x)]^2 - b[ax - \cos(x)], \tag{6.34}$$

which is illustrated in Fig. 6.3(a). Although the system is nonlinear, the steady-state distribution can be analytically calculated

$$p^{\mathrm{ss}}(x) = \frac{c}{a + \sin(x)}, \tag{6.35}$$

where $c > 0$ is the normalization constant such that $\int_0^{2\pi} dx\, p^{\mathrm{ss}}(x) = 1$. The entropy production rate is given by

$$\Sigma = \int_0^{2\pi} dx \frac{(j^{\mathrm{ss}})^2}{D(x)p^{\mathrm{ss}}(x)} = b^2, \tag{6.36}$$

where $j^{\mathrm{ss}} = bc$ is the probability current. It has been shown that the equality of TUR can be exactly attained with the current of entropy production [33]

$$\sigma(\Gamma) = \int_0^{\tau} dt\, \varphi(x) \circ \dot{x} \tag{6.37}$$

for arbitrary observation time τ, where $\varphi(x) = b/[a + \sin(x)]$.

To compute the optimal current, we employ basis currents with the following projection functions:

$$f_i(x) = \begin{cases} 1 + \cos(mx), & \text{if } i = 2m + 1, \\ 1 + \sin(mx), & \text{if } i = 2m, \end{cases} \tag{6.38}$$

for $i = 1, \ldots, n$. Here, 1 is added to each projection function to avoid vanishing currents. We fix $a = 2$ and vary b in the range of $[0, 5]$. For each parameter setting, we use $n = 21$ basis currents to approximate the optimal current. We plot the mean and the standard error of the estimated results over 20 independent trajectories in Fig. 6.3(a). It is observed that the estimated value $\widehat{\Sigma}_\tau$ and the actual entropy production rate Σ agree well for all b. The errors are always small even when Σ increases, which confirms the stability of our method. We also investigate the effect of the length of the trajectory on the estimation result. We vary the value of $\mathcal{T}_{\mathrm{obs}}$ in the range of $[10^2, 10^4]$ and plot the results in the inset of the same figure. As illustrated, the estimator is unbiased for all finite lengths of the trajectory. The mean of the estimated values is always approximately equal to the actual entropy production rate, even when the trajectory is not long. Compared to when $\mathcal{T}_{\mathrm{obs}}$ is large, the standard error tends to increase when $\mathcal{T}_{\mathrm{obs}}$ is small. This occurs due to the limited length of the trajectory (i.e., there are statistical errors in the calculation of moments of basis currents).

We define

$$f_{\mathrm{opt}}(x) := \sum_{i=1}^{n} c_i f_i(x), \tag{6.39}$$

which is the projection function of the computed optimal current. We plot $f_{\mathrm{opt}}(x)$ and $\varphi(x)$ in Fig. 6.3(b) to examine whether the computed function is close to the optimal one or not. We consider two cases: using $n = 11$ and $n = 21$ basis currents. We find that $f_{\mathrm{opt}}(x)$ and $\varphi(x)$ are almost identical in both cases, which implies that the theoretically optimal current is approximated well by our method, even when using a small number of basis currents, $n = 11$.

6.2.3 Bead-spring model

Finally, we consider a nonequilibrium system that consists of N beads that are coupled in one dimension [49]. Each bead is in contact with a thermal reservoir at different temperature. The dynamics of the system are described by the multivariate Langevin equation

$$\dot{\boldsymbol{x}} = \mathsf{A}\boldsymbol{x} + \sqrt{2\mathsf{D}}\boldsymbol{\xi}, \tag{6.40}$$

where $\boldsymbol{x} = [x_1, \ldots, x_N]^\top$ denotes the positions of the beads, and $\mathsf{A} \in \mathbb{R}^{N\times N}$ and $\mathsf{D} \in \mathbb{R}^{N\times N}$ are the drift and diffusion terms, respectively. Note that $\mathsf{D} = \mathrm{diag}(D_1, \ldots, D_N)$ is a diagonal matrix, and the noises that affects each bead are uncorrelated. Because the forces are linear, the steady-state distribution is Gaussian,

$$p^{\mathrm{ss}}(\boldsymbol{x}) = \frac{1}{\sqrt{(2\pi)^N |\mathsf{C}|}} \exp\left(-\frac{1}{2}\boldsymbol{x}^\top \mathsf{C}^{-1}\boldsymbol{x}\right). \tag{6.41}$$

Here, C is the covariance matrix of $\boldsymbol{x}$, given by $\mathsf{C}_{ij} = \langle x_i x_j\rangle - \langle x_i\rangle\langle x_j\rangle$. The probability current in the Fokker–Planck equation is

$$\boldsymbol{j}^{\mathrm{ss}}(\boldsymbol{x}) = (\mathsf{A}\boldsymbol{x} - \mathsf{D}\boldsymbol{\nabla}_{\boldsymbol{x}})\, p^{\mathrm{ss}}(\boldsymbol{x}) = (\mathsf{A} + \mathsf{D}\mathsf{C}^{-1})\boldsymbol{x} p^{\mathrm{ss}}(\boldsymbol{x}). \tag{6.42}$$

The current of stochastic entropy production reads $\sigma(\Gamma) = \int dt\, \boldsymbol{\varphi}(\boldsymbol{x})^\top \circ \dot{\boldsymbol{x}}$, where

$$\boldsymbol{\varphi}(\boldsymbol{x}) = \mathsf{D}^{-1}\boldsymbol{j}^{\mathrm{ss}}(\boldsymbol{x})/p^{\mathrm{ss}}(\boldsymbol{x}) = (\mathsf{D}^{-1}\mathsf{A} + \mathsf{C}^{-1})\boldsymbol{x}. \tag{6.43}$$

Then, the entropy production rate is analytically obtained

$$\Sigma = \int d\boldsymbol{x}\, \boldsymbol{j}^{\mathrm{ss}}(\boldsymbol{x})^\top \boldsymbol{\varphi}(\boldsymbol{x}) = \mathrm{Tr}\left[\mathsf{D}^{-1}\mathsf{A}\mathsf{C}\mathsf{A}^\top - \mathsf{C}^{-1}\mathsf{D}\right], \tag{6.44}$$

where $\mathrm{Tr}[\cdot]$ is the trace operator that calculates the sum of elements on the main diagonal.

First, we consider the case of $N = 2$ beads with the drift and diffusion terms given by

$$\mathsf{A} = \begin{bmatrix} -2k & k \\ k & -2k \end{bmatrix}, \quad \mathsf{D} = \begin{bmatrix} T_h & 0 \\ 0 & T_c \end{bmatrix}. \tag{6.45}$$

Here, $k > 0$ is the stiffness of the springs, and $T_h \geq T_c > 0$ are the temperatures of the thermal reservoirs that are coupled to each bead. From Eq. (6.44), the entropy production rate can be analytically calculated

$$\Sigma = \frac{k(T_h - T_c)^2}{4T_h T_c}. \tag{6.46}$$

We use m^2 Gaussian kernels to approximate the optimal current. Specifically, for each $i = 1, \ldots, m^2$, we define

$$f_i(\boldsymbol{x}) = \exp\left[-\frac{(\boldsymbol{x} - \boldsymbol{x}_i)^\top \mathsf{B}^{-1}(\boldsymbol{x} - \boldsymbol{x}_i)}{2}\right], \tag{6.47}$$

where $\boldsymbol{x}_i$ is the kernel center and B is the kernel bandwidth. From the given trajectory, we

calculate $\overline{\boldsymbol{x}} = [\overline{x}_1, \overline{x}_2]^\top$, where $\overline{x}_\nu := 10 + \max_t \{|x_\nu(t)|\}$. Then, $\boldsymbol{x}_i$ and B are determined as follows:

$$\boldsymbol{x}_i = \begin{bmatrix} (0.5 + (i-1)\%m)\,\Delta x_1 - \overline{x}_1 \\ (0.5 + \lfloor (i-1)/m \rfloor)\,\Delta x_2 - \overline{x}_2 \end{bmatrix}, \tag{6.48}$$

$$\mathsf{B} = \begin{bmatrix} \Delta x_1^2 & 0 \\ 0 & \Delta x_2^2 \end{bmatrix}, \tag{6.49}$$

where $\Delta x_\nu = 2\overline{x}_\nu/m$ $(\nu = 1, 2)$, $\%$ denotes the remainder of the Euclidean division, and $\lfloor \cdot \rfloor$ denotes the floor function. Equation (6.48) indicates that the kernel centers are uniformly sampled over the region of interest, $[-\overline{x}_1, \overline{x}_1] \times [-\overline{x}_2, \overline{x}_2]$. The optimal current is approximated using $n = 2m^2$ basis currents as

$$\begin{aligned} \phi_{\mathrm{opt}}(\Gamma) &= \int dt \sum_{i=1}^{m^2} \left[c_{i,1} f_i(\boldsymbol{x}) \circ \dot{x}_1 + c_{i,2} f_i(\boldsymbol{x}) \circ \dot{x}_2 \right], \\ &= \int dt\, \boldsymbol{f}_{\mathrm{opt}}(\boldsymbol{x})^\top \circ \dot{\boldsymbol{x}}. \end{aligned} \tag{6.50}$$

Here, $\boldsymbol{f}_{\mathrm{opt}}(\boldsymbol{x}) := \mathsf{C}\boldsymbol{f}_{\mathrm{b}}(\boldsymbol{x})$, C is the matrix of coefficients given by

$$\mathsf{C} := \begin{bmatrix} c_{1,1} & c_{2,1} & \dots & c_{m^2,1} \\ c_{1,2} & c_{2,2} & \dots & c_{m^2,2} \end{bmatrix}, \tag{6.51}$$

and $\boldsymbol{f}_{\mathrm{b}}(\boldsymbol{x}) := [f_1(\boldsymbol{x}), \dots, f_{m^2}(\boldsymbol{x})]^\top$.

We vary the temperature ratio T_c/T_h in the range of $[0.1, 1]$ and test the effectiveness of our method using $n = 50$ basis currents (i.e., $m = 5$). For each parameter setting, we collect a trajectory of length $\mathcal{T}_{\mathrm{obs}} = 10^4$, from which we estimate the entropy production rate. We independently perform 20 estimations and obtain the mean and standard error of the estimated values. As illustrated in Fig. 6.4(a), on average, the estimator always produces an exact estimate of the entropy production rate, even when the system is far from equilibrium. The inset shows the performance of the estimator when the length of the trajectory is changed. Although the estimated values are biased for finite lengths, they converge to the exact values when $\mathcal{T}_{\mathrm{obs}}$ is increased. In addition, the standard errors also decrease when the length $\mathcal{T}_{\mathrm{obs}}$ is sufficiently long.

We investigate whether the projection function of the computed optimal current, $\boldsymbol{f}_{\mathrm{opt}}(\boldsymbol{x})$, is close to that of the entropy production current, $\boldsymbol{\varphi}(\boldsymbol{x})$. We plot $\boldsymbol{f}_{\mathrm{opt}}(\boldsymbol{x})$ and $\boldsymbol{\varphi}(\boldsymbol{x})$ as vector fields in Fig. 6.4(b). It is observed that these vector fields are in an excellent agreement in both direction and magnitude. This implies that $\sigma(\Gamma)$ (which is the theoretically optimal current in the short-time limit) is well approximated by the linear combination of the constructed basis currents.

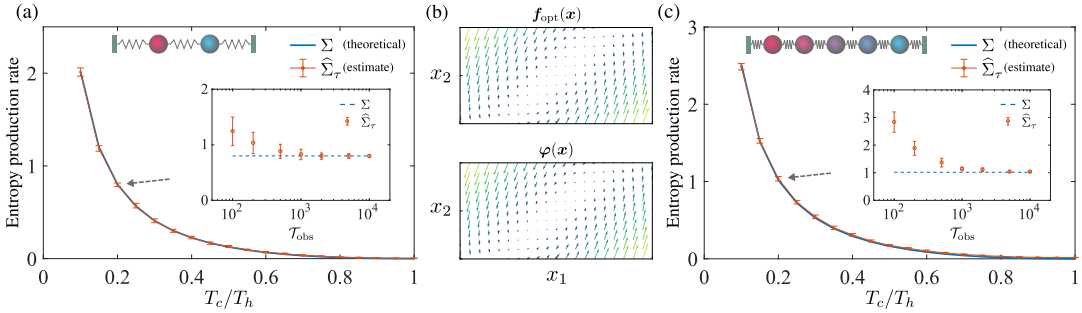

Figure 6.4: (a) Estimation of the entropy production rate in the two-bead system. The blue solid line represents the actual entropy production rate Σ. The orange solid line with dots depicts the estimated values $\widehat{\Sigma}_\tau$, while the error bars indicate standard deviations. Blue and orange solid lines almost overlap, which implies that Σ is accurately estimated. The inset shows the performance of the estimator when the length of the trajectory is changed. With an increase in $\mathcal{T}_{\rm obs}$, the estimated value converges to the exact value of Σ with high stability. (b) Comparison between the projection function of the computed optimal current, $\boldsymbol{f}_{\rm opt}(\boldsymbol{x})$ (upper panel), and that of the entropy production current, $\boldsymbol{\varphi}(\boldsymbol{x})$ (lower panel). Two vector fields show the same behavior in both direction and magnitude, which empirically verifies that the optimal current is approximated well. (c) Estimation of the entropy production rate in the five-bead system. The blue and orange solid lines represent the actual entropy production rate Σ and the estimate $\widehat{\Sigma}_\tau$, respectively. The error bars depict the standard deviations of the estimated values. The inset shows the estimation performance when the length $\mathcal{T}_{\rm obs}$ of the trajectory is varied. Parameter T_h is varied while the remaining parameters are fixed as $k = 1$ (two-bead) and 4 (five-bead), $T_c = 10, \mathcal{T}_{\rm obs} = 10^4$, and $\tau = 10^{-2}$.

Next, we consider a five-bead system, whose drift and diffusion terms are

$$\mathsf{A} = \begin{bmatrix} -2k & k & 0 & 0 & 0 \\ k & -2k & k & 0 & 0 \\ 0 & k & -2k & k & 0 \\ 0 & 0 & k & -2k & k \\ 0 & 0 & 0 & k & -2k \end{bmatrix}, \tag{6.52}$$

$$\mathsf{D} = \frac{1}{4}\begin{bmatrix} 4T_h & 0 & 0 & 0 & 0 \\ 0 & 3T_h + T_c & 0 & 0 & 0 \\ 0 & 0 & 2T_h + 2T_c & 0 & 0 \\ 0 & 0 & 0 & T_h + 3T_c & 0 \\ 0 & 0 & 0 & 0 & 4T_c \end{bmatrix}. \tag{6.53}$$

For this system, the entropy production rate is equal to

$$\Sigma = \frac{k(T_h - T_c)^2(111T_h^2 + 430T_hT_c + 111T_c^2)}{495T_hT_c(3T_h + T_c)(T_h + 3T_c)}. \tag{6.54}$$

Again, we employ Gaussian kernels, whose centers and bandwidth are analogously determined as in the two-bead case. We use $n = 160$ basis currents to approximate the optimal current and plot the estimated results in Fig. 6.4(c). As shown, the estimator is unbiased for all temperature ratios T_c/T_h even when the dynamics are strongly driven from equilibrium. The inset in the same figure illustrates the statistics of the estimated values when the length $\mathcal{T}_{\rm obs}$ is changed. The estimator is biased for small $\mathcal{T}_{\rm obs}$ but rapidly converges to the exact value when $\mathcal{T}_{\rm obs}$ is increased, which is analogous to the two-bead case.

In the end, we compare the performance of our estimator, $\widehat{\Sigma}_\tau$, with that of the two estimators proposed in Ref. [49], $\widehat{\Sigma}_{\rm TUR}$ and $\widehat{\Sigma}_{\rm temp}$. Herein, we will briefly describe these two estimators (see Ref. [49] for details). The thermodynamic force of the entropy production is estimated as $\widehat{\boldsymbol{\varphi}}(\boldsymbol{x}) = \mathsf{D}^{-1}\widehat{\boldsymbol{j}}^{\rm ss}(\boldsymbol{x})/\widehat{p}^{\rm ss}(\boldsymbol{x})$, where $\widehat{\boldsymbol{j}}^{\rm ss}(\boldsymbol{x})$ and $\widehat{p}^{\rm ss}(\boldsymbol{x})$ are estimators of $\boldsymbol{j}^{\rm ss}(\boldsymbol{x})$ and $p^{\rm ss}(\boldsymbol{x})$, respectively. Subsequently, $\widehat{\Sigma}_{\rm TUR}$ estimates the lower bound of the entropy production rate by utilizing the TUR with the current $\int dt\, \widehat{\boldsymbol{\varphi}}(\boldsymbol{x})^\top \circ \dot{\boldsymbol{x}}$. On the other hand, $\widehat{\Sigma}_{\rm temp}$ directly estimates the entropy production rate via its temporal average, $\widehat{\Sigma}_{\rm temp} = \mathcal{T}_{\rm obs}^{-1}\int_0^{\mathcal{T}_{\rm obs}} dt\, \widehat{\boldsymbol{\varphi}}(\boldsymbol{x})^\top \circ \dot{\boldsymbol{x}}$. It is worth noting that these two estimators require knowledge of the diffusion matrix D, while our estimator does not rely on such information.

To evaluate the performance of the estimators, we vary the trajectory length $\mathcal{T}_{\rm obs} = 1.2 \times 10^l$ $(1 \le l \le 4)$ and focus on the convergence of each estimator. We examine two temperature ratios, $T_c/T_h = 0.1$ and $T_c/T_h = 0.5$, using both the two and five-bead models. The parameter values and experimental settings are the same as used in Ref. [49]. We calculate the mean and standard deviation of the ratio $\widehat{\Sigma}/\Sigma$ using 10 independent estimations and plot them in Fig. 6.5. As illustrated, our estimator shows the best convergence in all cases. When the trajectory length $\mathcal{T}_{\rm obs}$ is short, $\widehat{\Sigma}_\tau$ is prone to overestimating the actual entropy production rate because the trajectory does not provide sufficient information to accurately calculate the mean and variance of each basis current. However, when $\mathcal{T}_{\rm obs}$ is sufficiently long, $\widehat{\Sigma}_\tau$ always obtains accurate estimates. Notably, for the five-bead model with $T_c/T_h = 0.5$, estimators

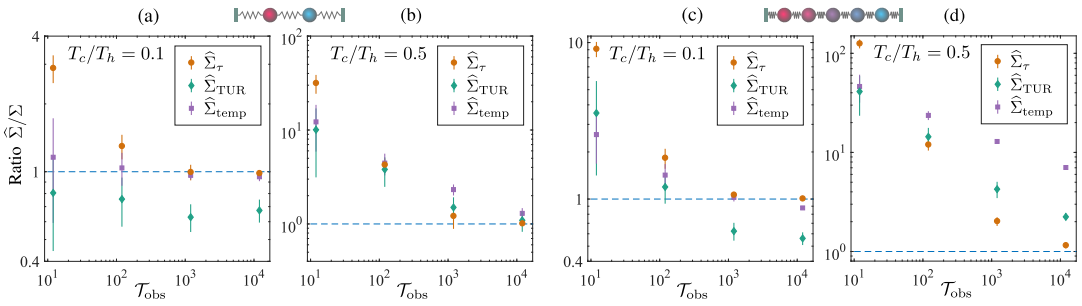

Figure 6.5: Performance of the different estimators. We compare our estimator herein, $\widehat{\Sigma}_\tau$, with the two estimators used in Ref. [49], $\widehat{\Sigma}_{\rm TUR}$ and $\widehat{\Sigma}_{\rm temp}$. The mean and standard deviation of each ratio $\widehat{\Sigma}/\Sigma$ are calculated using 10 independent estimations via the two-bead model with (a) T_c/T_h = 0.1, (b) T_c/T_h = 0.5, and via the five-bead model with (c) T_c/T_h = 0.1, (d) T_c/T_h = 0.5. The results of the estimators $\widehat{\Sigma}_\tau$, $\widehat{\Sigma}_{\rm TUR}$, and $\widehat{\Sigma}_{\rm temp}$ are depicted using circles, diamonds, and squares, respectively. The dashed line represents the actual ratio, which equals 1. Our estimator shows the best convergence and always provides accurate estimates when $\mathcal{T}_{\rm obs}$ is sufficiently long. Notably, for the five-bead model with T_c/T_h = 0.5, estimators $\widehat{\Sigma}_{\rm TUR}$ and $\widehat{\Sigma}_{\rm temp}$ show slow convergence, while $\widehat{\Sigma}_\tau$ rapidly converges to the actual entropy production rate. The length $\mathcal{T}_{\rm obs}$ of the observed trajectory is varied, while the remaining parameters are fixed to k = 1 (two-bead) and ≈ 3.215 (five-bead), T_c = 25, $\Delta t = 10^{-3}$, and $\tau = 10^{-2}$.

$\widehat{\Sigma}_{\rm TUR}$ and $\widehat{\Sigma}_{\rm temp}$ slowly converge and return inaccurate estimates even when $\mathcal{T}_{\rm obs}$ is long. In contrast, our estimator rapidly converges to the actual entropy production rate and provides the best estimate.

6.3 Concluding remarks and discussion

Indirect inference on the basis of the TUR has several advantages over the direct one. First, it can robustly estimate a lower bound on entropy production even in the presence of hidden variables, while the direct strategy cannot. This situation is common in the biological context, where the full degrees of freedom are often inaccessible. Second, for Langevin dynamics involving multiplicative noises, the accurate estimation of both the drift and diffusion terms is not a simple task, especially in the high-dimensional case. Moreover, the errors that occurred in the estimation of these quantities can be accumulated in the phase of calculating entropy production, which potentially affects the accuracy of estimate. In contrast, inference that is based on the TUR does not require to know the underlying dynamics, e.g., whether the noises are additive or multiplicative.

In summary, the method for estimating entropy production based on the TUR was proposed. Three examples, including Markov jump processes and Langevin dynamics, were studied to illustrate the effectiveness of the proposed method. It was shown that the entropy production rate can be accurately estimated for Langevin dynamics using the short-time limit. The results demonstrate that the estimates are significantly consistent with the theoretical entropy production rates, even when the system is far from equilibrium. The proposed

method always effectively performs, regardless of whether the noise is additive or multiplicative. Further, it was empirically confirmed that the optimal current, which is proportional to the entropy production in the short-time limit, can be successfully approximated by the linear combination of predetermined basis currents. Thus, the entropy production current can be accurately inferred by integrating our method with the fluctuation theorem. Namely, one can infer not only the average of entropy production but also its probability distribution. For Markov jump processes, our method provides the tightest lower bound for the entropy production rate. If the condition that the entropy production current is the optimal one is given, then an exact estimate can be obtained through the combination with the integral fluctuation theorem.

From a practical perspective, the proposed algorithm can be easily implemented and is computationally efficient (i.e., all numerical computations can be performed in parallel). The Monte Carlo sampling utilized in Ref. [49] suffers from a local optimum when the dynamics are strongly driven; thus, it can be replaced by our method, which always produces a global optimum. Unlike in Ref. [50], where the details of underlying dynamics (e.g., the system entropy, heat, and work) are required to form the optimal current, the proposed method does not require such prior knowledge of the dynamics.

We discuss some possible future research directions. This study focused on estimating entropy production; however, the proposed method should also apply to the estimation of the Fisher information, which is lower bounded by means and covariances of multiple observables [124]. Moreover, it is of interest to test our method with the experimental data. For example, one can estimate the dissipation cost in the motor protein F_1-adenosine triphosphatase [200] from the trajectory of the rotational angles, whose dynamics are governed by the Langevin equation. Along with studies of applications, further research on theoretical guarantees of the proposed method is desirable. Basically, the longer the input trajectory is, the more accurate estimate can be obtained. However, a full investigation regarding the relationship between the error of estimate and the trajectory length is beyond the scope of this study. The development of theoretical bounds on the error with respect to the length needs to be addressed. Besides, overcoming the curse of dimensionality in entropy production estimation remains an open problem. Although our proposed method works well in the five-dimensional model, it is still challenging to handle genuinely high-dimensional Langevin systems. A considerable number of basis functions may be required to obtain an accurate approximation of the optimal current, which leads to a substantial computational cost. As an alternative solution, one can estimate with multiple sets, whose number of basis currents is limited, and assigns the largest estimated value as the lower bound of the entropy production rate.

Chapter 7

Bounds on irreversibility in Markovian systems

In recent years, many studies have characterized the dissipation of thermodynamic processes using information geometry [201–211], which is the application of techniques from differential geometry to the manifolds of probability distributions and density matrices [212]. Reference [213] showed that entropy production in a closed driven quantum system is bounded from below by the Bures length between the final state and the corresponding equilibrium state. Following a similar approach, Ref. [214] determined a geometrical upper bound for the equilibration processes of open quantum systems. As is well known, in classical systems near equilibrium, irreversible entropy production is related to the distance between thermodynamic states [215, 216]. Meanwhile, a lower bound on dissipation in terms of the Wasserstein distance [217] has been defined for nonequilibrium Markovian systems described by Langevin equations [218–220]. Information geometry is useful for deriving other important relations, such as speed limits [124, 221–223], quantum work fluctuation-dissipation relations [224], and the efficiency-power trade-off in microscopic heat engines [225].

In this chapter, we enlarge the family of these universal relations by investigating quantum and classical open systems that satisfy the detailed balance condition. These systems obey reversible Markovian dynamics and can be modeled as coupled to an infinite thermal reservoir. Examples include equilibration processes, which have received considerable interest in nonequilibrium physics [8, 226–228]. Specifically, we derive geometrical lower bounds on the entropy production in reversible Markovian systems described by master equations. The spaces of quantum states and discrete distributions are treated as Riemannian manifolds, on which the time evolution of a system state is described by a smooth curve. By defining a modified Wasserstein metric, we prove that the entropy production is bounded from below by the square of the geodesic distance between the initial and final states divided by the process time [cf. Eqs. (7.55) and (7.64)]. The derived bounds strengthen the Clausius inequality of the second law for reversible Markovian systems. They can also be regarded as generalizations of the bounds reported in Refs. [218, 220] to the discrete-state quantum and classical systems. The equality of these bounds is attained only when the system dynamics follow the shortest paths. Our modified metric is a quantum generalization of the Wasserstein metric,

which measures the distance between two distributions and is widely used in optimal transport problems [217]. Interestingly, the obtained inequalities can be interpreted as speed limits [92, 229–235], which establish the trade-off relations between the speed and dissipation cost of a state transformation. We numerically illustrate the results on a quantum Otto engine and a classical two-level system.

7.1 Differential geometry and information geometry

Differential geometry studies (smooth) manifolds, and it aims to characterize the global properties of manifolds. A smooth manifold is, in general, a multi-dimensional space that is locally *flat* and on which one can perform calculus. Information geometry applies techniques in differential geometry to study the geometrical structure of the manifolds of classical and quantum states. Here, the classical and quantum states are the probability distributions over the classical phase space and the density matrices over the quantum Hilbert space, respectively. The set of these states can be treated as a smooth Riemannian manifold equipped with a proper metric. Geometrically studying thermodynamic quantities such as heat, work, and entropy production not only allows us to discover new thermodynamic relations but also opens up new avenues for solving optimization problems.

To understand the results presented in this chapter, we briefly describe only some relevant concepts of information geometry. The interested reader should refer to the book [212] for a detailed explanation of other important concepts such as the Riemannian connection and dual connections.

7.1.1 Smooth manifolds

Following a great description in Ref. [236], we briefly explain the concept of smooth manifolds. First, we start with a formal definition of topological manifolds — the most basic type of manifolds — in the following.

Definition 7.1. *M is a topological manifold of dimension n if it satisfies the following properties:*

1. *M is a Hausdorff space: for every pair of distinct points $p, q \in M$, there are disjoint open subset $U, V \subseteq M$ such that $p \in U$ and $q \in V$.*
2. *M is second-countable: there exists a countable basis for the topology of M.*
3. *M is locally Euclidean of dimension n: each point of M has a neighborhood that is homeomorphic to an open subset of $\mathbb{R}^n$.*

The second property says that there exists a countable set B of open subsets of M such that every open subset of M can be written as a union of elements of some subsets of B. For example, the Euclidean space $\mathbb{R}^n$ is second-countable because the set of the open balls $B_x(\epsilon)$ with radius $\epsilon \in \mathbb{Q}_{\geq 0}$ and center points $x \in \mathbb{Q}^n$ is a countable basis. The third property means

that for each point $p \in M$, one can find an open subset $U \subseteq M$ containing p, and open subset $\widehat{U}$ of $\mathbb{R}^n$, and a homeomorphism[1] $\varphi : U \to \widehat{U}$.

Coordinate charts

A coordinate chart on M is a pair (U, φ) where U is an open subset of M and $\varphi : U \to \widehat{U}$ is a homeomorphism from U to an open subset $\widehat{U} = \varphi(U) \subseteq \mathbb{R}^n$. By definition of a topological manifold, each point $p \in M$ is contained in the domain of some chart (U, φ). Given a chart (U, φ), we call the set U a coordinate domain and the map φ a (local) coordinate map, and the component functions $(x_1, \ldots, x_n)$ of φ, defined by $\varphi(p) = [x_1(p), \ldots, x_n(p)]$, are called local coordinates on U. If (U, φ) and (V, ψ) are two charts such that $U \cap V \neq \emptyset$, the composite map $\psi \circ \varphi^{-1} : \varphi(U \cap V) \to \psi(U \cap V)$ is called the transition map from φ to ψ. Two charts (U, φ) and (V, ψ) are said to be smoothly compatible if either $U \cap V = \emptyset$ or the transition map $\psi \circ \varphi^{-1}$ is a diffeomorphism[2]. A collection of charts whose domains cover M is called an atlas for M. An atlas A is called a smooth atlas if any two charts in A are smoothly compatible with each other.

Definition 7.2. *A smooth atlas is a set of charts $A = \{(U_i, \varphi_i)\}_{i \in I}$ such that*

1. *$M = \cup_{i \in I} U_i$.*
2. *The transition maps $\varphi_{ij} = \varphi_j \circ \varphi_i^{-1}$ are diffeomorphisms.*

In general, there are many possible atlases that give the same smooth structure. Nonetheless, a smooth structure can be defined as an equivalence class of smooth atlases. An equivalence relation on smooth atlases can be defined in the following manner. Two smooth atlases A and A' are equivalent if $A \cup A'$ is again a smooth atlas. A smooth atlas A on M is maximal if it is not properly contained in any larger smooth atlas. An equivalence class of this equivalence relation is called a smooth structure D on M, and the maximal atlas associated with D is denoted by A_D.

With the above definitions in place, we can then define a smooth manifold as the following.

Definition 7.3. *Let M and D be, respectively, a topological manifold and a smooth structure on M with maximal atlas A_D. Then the pair (M, A_D) is called a smooth manifold.*

Let us examine some examples of smooth manifolds.

Example 7.1. (Euclidean spaces) For each positive integer number n, the Euclidean space $\mathbb{R}^n$ is a smooth manifold with the smooth structure determined by the atlas consisting of the single chart $(\mathbb{R}^n, \mathrm{id}_{\mathbb{R}^n})$, where id_M denotes the identity function from M to M.

Example 7.2. (Spaces of matrices) Let $M_{n\times n}(\mathbb{R})$ denote the set of $n \times n$ matrices with real entries. Since an arbitrary matrix in $M_{n\times n}(\mathbb{R})$ can be represented as a real vector of length n^2, $M_{n\times n}(\mathbb{R})$ is a smooth manifold of dimension n^2. Analogously, the space $M_{n\times n}(\mathbb{C})$ of $n \times n$ complex matrices is a smooth manifold of dimension $2n^2$.

[1] A homeomorphism is a continuous bijective map whose inverse is also continuous.
[2] A diffeomorphism is a differentiable bijective map whose inverse is also differentiable.

Example 7.3. (Unit spheres) For an integer $n > 0$, let us consider the unit n-sphere

$$\mathbb{S}^n := \left\{(x_1, \ldots, x_{n+1}) \in \mathbb{R}^{n+1} \mid \sum_{i=1}^{n+1} x_i^2 = 1\right\}. \tag{7.1}$$

We will show that $\mathbb{S}^n$ is a smooth manifold of dimension n. Let $\mathbb{B}^n$ denote the n-dimensional open unit ball,

$$\mathbb{B}^n := \left\{(x_1, \ldots, x_n) \in \mathbb{R}^n \mid \sum_{i=1}^{n} x_i^2 < 1\right\}. \tag{7.2}$$

For each index $i = 1, \ldots, n+1$, let U_i^+ denote the subset of $\mathbb{R}^{n+1}$ where the i-th coordinate is positive,

$$U_i^+ := \left\{(x_1, \ldots, x_{n+1}) \in \mathbb{R}^{n+1} \mid x_i > 0\right\}. \tag{7.3}$$

It is easy to check that the set $U_i^+ \cap \mathbb{S}^n$ is the graph of the function

$$x_i = \sqrt{1 - (x_1^2 + \cdots + x_{i-1}^2 + x_{i+1}^2 + \cdots + x_n^2)}. \tag{7.4}$$

Similarly, U_i^- is the set where $x_i < 0$, and $U_i^- \cap \mathbb{S}^n$ is the graph of

$$x_i = -\sqrt{1 - (x_1^2 + \cdots + x_{i-1}^2 + x_{i+1}^2 + \cdots + x_n^2)}. \tag{7.5}$$

Thus, each subset $U_i^\pm \cap \mathbb{S}^n$ is locally an Euclidean space of dimension n, and $\varphi_i^\pm : U_i^\pm \cap \mathbb{S}^n \to \mathbb{B}^n$ are local coordinate maps for $\mathbb{S}^n$. Since each point of $\mathbb{S}^n$ is included in some chart of the atlas $A := \{(U_i^+ \cap \mathbb{S}^n, \varphi_i^+), (U_i^- \cap \mathbb{S}^n, \varphi_i^-)\}_{i=1}^{n+1}$, $\mathbb{S}^n$ is a topological manifold of dimension n. Moreover, one can easily confirm that for any $1 \le i, j \le n+1$, the transition map $\varphi_i^\pm \circ \varphi_j^\pm$ is a diffeomorphism; thus, A is a smooth atlas. Subsequently, $\mathbb{S}^n$ is a smooth manifold of dimension n.

Throughout this chapter, we consider only smooth manifolds that have a global coordinate system. In the quantum case, M can be the space of density operators ρ, which are positive (i.e., $\rho \ge 0$) and have unit trace (i.e., $\operatorname{tr}\rho = 1$). Meanwhile, in classical discrete-state systems, M can be the collection of discrete distributions $\boldsymbol{p} = [p_1, \ldots, p_N]^\top$, where $p_n \ge 0$ and $\sum_{n=1}^N p_n = 1$. We use the standard notation $\langle \cdot, \cdot \rangle$ of the scalar inner product, i.e., $\langle \boldsymbol{x}, \boldsymbol{y} \rangle = \boldsymbol{x}^\top \boldsymbol{y}$ and $\langle f(x), g(x) \rangle = \int_{\mathbb{R}^N} f(x)^\top g(x) dx$ for the classical case and $\langle X, Y \rangle = \operatorname{tr}\left\{X^\dagger Y\right\}$ for the quantum case.

In order to define geometric notions such as lengths and angles on a vector space, we have to introduce a proper metric (which is an inner product between two tangent vectors). The most suitable metrics for smooth manifolds are Riemannian metrics, which will be discussed in the following.

7.1.2 Riemannian metrics

In the Euclidean space, the inner product between two vectors can be defined in a conventional way, $\langle \boldsymbol{u}, \boldsymbol{v} \rangle = \sum_{n=1}^N u_n v_n$. This inner product allows us to define lengths of vectors and angles between them in the Euclidean geometry. Transferring these ideas to manifolds, a Riemannian

metric can be defined as a smooth symmetric covariant 2-tensor field that is positive definite at each point.

Definition 7.4. *Given a smooth manifold M, a Riemannian metric g_p is an inner product on the tangent space T_pM at each point p on the manifold, which satisfies the following conditions:*

1. *Bilinearity: $g_p(u,v) : T_pM \times T_pM \to \mathbb{R}$ is a bilinear function, i.e., $u \mapsto g_p(u,v)$ and $v \mapsto g_p(u,v)$ are both linear functions.*
2. *Symmetry: $g_p(u,v) = g_p(v,u)$.*
3. *Positive-definiteness: $g_p(u,u) > 0$ for all $u \neq 0$.*

A smooth manifold equipped with a Riemannian metric is called a Riemannian manifold. For smooth manifolds involving complex numbers, the properties of bilinearity and symmetry should be properly modified since the inner product g_p could be a complex number. To provide a better understanding of the concept of metrics, let us review some Riemannian metrics in the following.

Example 7.4. (The Euclidean metric) One simplest example of a Riemannian metric is the Euclidean metric on $\mathbb{R}^n$. Given two tangent vectors $\boldsymbol{u}, \boldsymbol{v} \in T_pM$, the Euclidean metric is defined as

$$g_p(\boldsymbol{u}, \boldsymbol{v}) \coloneqq u_1 v_1 + \cdots + u_n v_n = \langle \boldsymbol{u}, \boldsymbol{v} \rangle. \tag{7.6}$$

It is obvious that the Euclidean metric satisfies the three above conditions of a Riemannian metric.

Example 7.5. (Product metrics) If (M_1, g^1) and (M_2, g^2) be Riemannian manifolds, then the product manifold $M_1 \times M_2$ has a natural product metric $g = g^1 \oplus g^2$, given by

$$g_p((\boldsymbol{u}_1, \boldsymbol{u}_2), (\boldsymbol{v}_1, \boldsymbol{v}_2)) \coloneqq g^1_{p_1}(\boldsymbol{u}_1, \boldsymbol{v}_1) + g^2_{p_2}(\boldsymbol{u}_2, \boldsymbol{v}_2), \tag{7.7}$$

where $\boldsymbol{u}_i, \boldsymbol{v}_i \in T_{p_i}M_i$.

A Riemannian metric allows us to define the length of a curve. The length of an arbitrary smooth curve $\gamma(t) : [0, \tau] \to M$ with respect to the metric g can be defined as

$$\ell(\gamma) \coloneqq \int_0^\tau \sqrt{g_\gamma(\dot{\gamma}(t), \dot{\gamma}(t))}dt. \tag{7.8}$$

It is easy to check that this definition is independent of parameterization. The distance between two points p and q on the manifold can then be defined as the length of the shortest path that connects two points,

$$d(p,q) \coloneqq \inf_\gamma \{\ell(\gamma) \mid \gamma(0) = p, \gamma(\tau) = q\}. \tag{7.9}$$

$d(p,q)$ is called the geodesic distance between points p and q. Note that except some particular cases, obtaining the analytical form of $d(p,q)$ is, in general, difficult.

Another important quantity is the divergence of the path, given by

$$\mathcal{J}(\gamma) \coloneqq \tau \int_0^\tau g_\gamma(\dot{\gamma}(t), \dot{\gamma}(t))dt. \tag{7.10}$$

Applying the Cauchy–Schwarz inequality, a relation between ℓ and $\mathcal{J}$ can be obtained,

$$\ell(\gamma)^2 = \left(\int_0^\tau \sqrt{g_\gamma(\dot{\gamma}(t), \dot{\gamma}(t))}dt\right)^2 \leq \int_0^\tau dt \int_0^\tau g_\gamma(\dot{\gamma}(t), \dot{\gamma}(t))dt = \mathcal{J}(\gamma), \tag{7.11}$$

or equivalently $\ell(\gamma) \leq \mathcal{J}(\gamma)^{1/2}$. The divergence $\mathcal{J}(\gamma)$ is also called the energy or action along the path. In the thermodynamics context, $\ell(\gamma)$ and $\mathcal{J}(\gamma)$ are referred to as the thermodynamic length and the thermodynamic divergence, respectively. An important connection between the geodesic distance and the divergence is stated in the following theorem.

Theorem 7.1. *The geodesic distance between two points is equal to the infimum of square root of the divergence taken over all possible paths,*

$$d(p, q) = \inf_\gamma \left\{\mathcal{J}(\gamma)^{1/2} \mid \gamma(0) = p, \gamma(\tau) = q\right\}. \tag{7.12}$$

Proof. We broadly follow the approach used in Theorem 5.4 of Ref. [237]. In order to prove the theorem, we will show that $d(p, q) \leq \inf_\gamma \left\{\mathcal{J}(\gamma)^{1/2}\right\}$ and $d(p, q) \geq \inf_\gamma \left\{\mathcal{J}(\gamma)^{1/2}\right\}$. The former is obvious since $d(p, q) = \inf_\gamma \{\ell(\gamma)\} \leq \inf_\gamma \left\{\mathcal{J}(\gamma)^{1/2}\right\}$. Thus, we need only prove the latter. For an arbitrary positive number $\epsilon > 0$ and a smooth curve $\{\gamma(t)\}$ connecting p and q, we define

$$\kappa_\epsilon(t) \coloneqq \int_0^t \left(\epsilon + g_\gamma(\dot{\gamma}(s), \dot{\gamma}(s))\right)^{1/2} ds, \; t \in [0, \tau]. \tag{7.13}$$

One can easily see that κ_ϵ is strictly increasing with $\kappa_\epsilon(\tau) =: S_\epsilon > 0$; thus, its inverse map $\upsilon_\epsilon : [0, S_\epsilon] \to [0, \tau]$ is well defined, with

$$\frac{d}{dz}\upsilon_\epsilon = (\epsilon + g_\gamma(\dot{\gamma}(t), \dot{\gamma}(t)))^{-1/2}, \tag{7.14}$$

where $z = \kappa_\epsilon(t)$. Set $\gamma_\epsilon = \gamma \circ \upsilon_\epsilon$, then γ_ϵ is a curve connecting p and q with $\gamma_\epsilon(0) = p$ and $\gamma_\epsilon(S_\epsilon) = q$. Thus, we have

$$\inf_\gamma \{\mathcal{J}(\gamma)\} \leq S_\epsilon \int_0^{S_\epsilon} g_{\gamma_\epsilon}(\dot{\gamma}_\epsilon(z), \dot{\gamma}_\epsilon(z)))dz \tag{7.15a}$$

$$= S_\epsilon \int_0^\tau \frac{g_\gamma(\dot{\gamma}(t), \dot{\gamma}(t)))}{\epsilon + g_\gamma(\dot{\gamma}(t), \dot{\gamma}(t))}(\epsilon + g_\gamma(\dot{\gamma}(t), \dot{\gamma}(t)))^{1/2}dt \tag{7.15b}$$

$$\leq S_\epsilon \int_0^\tau (\epsilon + g_\gamma(\dot{\gamma}(t), \dot{\gamma}(t)))^{1/2}dt = S_\epsilon^2. \tag{7.15c}$$

Here we have used the variable transformation $z = \kappa_\epsilon(t)$ to obtain Eq. (7.15b) and the inequality $g_\gamma(\dot{\gamma}(t), \dot{\gamma}(t))) \leq \epsilon + g_\gamma(\dot{\gamma}(t), \dot{\gamma}(t))$ to obtain Eq. (7.15c). Taking the $\epsilon \to 0$ limit, we get

$$\inf_\gamma \{\mathcal{J}(\gamma)\} \leq \ell(\gamma)^2. \tag{7.16}$$

Consequently, we obtain $\inf_\gamma \left\{\mathcal{J}(\gamma)^{1/2}\right\} \leq \inf_\gamma\{\ell(\gamma)\} = d(p,q)$, which completes the proof. □

We can see that the equality in Eq. (7.12) is attained with a constant-speed path $\{\gamma(t)\}$, i.e., $g_\gamma(\dot\gamma(t),\dot\gamma(t)) \equiv \text{const}$ for all $t \in [0,\tau]$, which can be derived from the equality condition of the Cauchy–Schwarz inequality.

Note that there is an infinite number of metrics on a smooth manifold, as long as the linearity, symmetry, and positive-definite conditions are met. Notably, there exists a family of monotone metrics that are contractive under physical maps [238–240], and a representative of which is the Fisher information metric [241, 242]. In the following, we briefly introduce the class of monotone metrics.

7.1.3 Monotone metrics

For the sake of generality, we consider the manifold M of quantum states on the N-dimensional Hilbert space. The tangent space $\{T_\rho M\}_\rho$ is then the collection of traceless Hermitian operators. A Riemannian metric g_ρ is said to be monotone if $g_\rho(X,X) \geq g_{\Lambda(\rho)}(\Lambda(X),\Lambda(X))$ for an arbitrary $X \in T_\rho M$ and an arbitrary completely positive trace-preserving map Λ. It should be noted that the corresponding geodesic distance $d(\cdot,\cdot)$ of a monotone metric is contractive under Λ, i.e.,

$$d(\rho,\sigma) \geq d(\Lambda(\rho),\Lambda(\sigma)), \tag{7.17}$$

for any density matrices $\rho,\sigma \in M$. Considering $d(\cdot,\cdot)$ as a measure of distinguishability, Eq. (7.17) implies that the distinguishability between two states always decreases under information processing. The monotone metrics thus provide a Riemannian geometric measure of distinguishability within the classical and quantum settings. The family of such monotone metrics is completely characterized by the Morozova, Čencov, and Petz theorem [238]. A function $f(x) : \mathbb{R}_+ \to \mathbb{R}_+$ which is operator monotone (i.e., $f(X) \leq f(Y)$ for any positive semi-definite operators $X \leq Y$) and self-inverse (i.e., $f(x) = xf(1/x)$ and $f(1) = 1$) is called the Morozova-Čencov (MC) function. Then, any monotone metric can be written in the following form up to a constant factor,

$$g_\rho(X,Y) = \frac{1}{4}\mathrm{tr}\left\{Xc^f(\mathcal{L}_\rho,\mathcal{R}_\rho)Y\right\}, \tag{7.18}$$

where $X,Y \in T_\rho M$, $\mathcal{L}_\rho$ and $\mathcal{R}_\rho$ are two linear superoperators defined as $\mathcal{L}_\rho X = \rho X$ and $\mathcal{R}_\rho X = X\rho$, and

$$c^f(x,y) \coloneqq \frac{1}{yf(x/y)} \tag{7.19}$$

is a symmetric function, $c^f(x,y) = c^f(y,x)$. Using the spectral decomposition of the density operator $\rho = \sum_{j=1}^N p_j|j\rangle\langle j|$, the metric can be explicitly written as

$$g_\rho(\partial_\theta\rho,\partial_\theta\rho) = \frac{1}{4}\left[\sum_{j=1}^N \frac{|\langle j|\partial_\theta\rho|j\rangle|^2}{p_j} + 2\sum_{j<l} c^f(p_j,p_l)|\langle j|\partial_\theta\rho|l\rangle|^2\right], \tag{7.20}$$

where θ is a parameter (which can be time t). As can be seen in Eq. (7.20), there are two separate contributions in the metric g_ρ. The first contribution in terms of populations $\{p_j\}$ of ρ corresponds to the classical Fisher information metric at the probability distribution $\{p_j\}_{j=1}^N$. The second contribution is purely a quantum term, which is due to the coherence between $\dot{\rho}$ and ρ with respect to the eigenbasis of ρ.

It has been shown [243] that any MC function must satisfy $f_{\min}(x) \leq f(x) \leq f_{\max}(x)$, where $f_{\min}(x) = 2x/(1+x)$ and $f_{\max}(x) = (1+x)/2$ are the minimal and maximal functions, respectively. The maximal one corresponds to the quantum Fisher information metric, whereas the Wigner-Yanase information metric is characterized by an intermediate MC function, $f_{\mathrm{WY}}(x) = (1+\sqrt{x})^2/4$. As mentioned above, obtaining the analytical expression for the geodesic distance of a metric is a difficult task. Fortunately, the geodesic distance induced by the quantum Fisher information metric can be explicitly calculated as [244]

$$d_{\mathrm{QF}}(\rho,\sigma) = \arccos\left[\sqrt{F(\rho,\sigma)}\right], \tag{7.21}$$

where $F(\rho,\sigma) = \mathrm{tr}\left\{\sqrt{\sqrt{\rho}\sigma\sqrt{\rho}}\right\}^2$ is the Uhlmann fidelity, and that induced by the Wigner-Yanase information metric is [245]

$$d_{\mathrm{WY}}(\rho,\sigma) = \arccos\left[A(\rho,\sigma)\right], \tag{7.22}$$

where $A(\rho,\sigma) = \mathrm{tr}\left\{\sqrt{\rho}\sqrt{\sigma}\right\}$ is the quantum affinity. In the classical setting (i.e., all off-diagonal elements are zero), all monotone metrics reduce exactly to the classical Fisher information metric,

$$g_p(\partial_\theta \boldsymbol{p}, \partial_\theta \boldsymbol{p}) = \frac{1}{4}\sum_{n=1}^{N}\frac{(\partial_\theta p_n)^2}{p_n}, \tag{7.23}$$

and the corresponding geodesic distance is given by $d_{\mathrm{CF}}(\boldsymbol{p},\boldsymbol{q}) = \arccos\left(\sum_{n=1}^N \sqrt{p_n q_n}\right)$.

In the following, we will exclusively focus on the (quantum) Fisher information metric and explain its important properties.

Fisher information and Fisher information metric

Let us consider an estimation problem of an unknown parameter θ, which is embedded in the state ρ_θ of a physical system. The information of the parameter θ is extracted by means of positive operator-valued measure (POVM) Π_x satisfying $\sum_x \Pi_x = \mathbb{I}$. The conditional probability of obtaining a measurement outcome x_i, given a certain value of the parameter θ, is determined by the Born rule:

$$p(x_i|\theta) = \mathrm{tr}\left\{\rho_\theta \Pi_{x_i}\right\}. \tag{7.24}$$

An unbiased[3] estimator Λ_θ then provides an estimate $\Lambda(x)$ based on the measurement outcome x. According to the Cramér–Rao inequality, the accuracy of the unbiased estimator Λ_θ

[3] An estimator is said *unbiased* if its mean value coincides with the unknown parameter, i.e., $\langle \Lambda_\theta \rangle = \sum_x p(x|\theta)\Lambda_\theta(x) = \theta$.

is bounded from below by the classical Fisher information,

$$\langle\langle \Lambda_\theta \rangle\rangle \geq \frac{1}{\mathcal{I}(\theta)}, \tag{7.25}$$

where $\langle\langle \Lambda_\theta \rangle\rangle \coloneqq \langle \Lambda_\theta^2 \rangle - \langle \Lambda_\theta \rangle^2$ is the variance of Λ_θ and $\mathcal{I}(\theta)$ is the classical Fisher information, given by

$$\mathcal{I}(\theta) = \left\langle [\partial_\theta \ln p(x|\theta)]^2 \right\rangle = \sum_x \frac{[\partial_\theta p(x|\theta)]^2}{p(x|\theta)}. \tag{7.26}$$

By introducing the symmetric logarithmic derivative (SLD) L_θ, defined as the self-adjoint operator satisfying the equation

$$\partial_\theta \rho_\theta = \frac{1}{2}\left(\rho_\theta L_\theta + L_\theta \rho_\theta\right), \tag{7.27}$$

the Fisher information can be expressed in terms of L_θ as

$$\mathcal{I}(\theta) = \sum_x \frac{\mathfrak{R}(\mathrm{tr}\{\rho_\theta \Pi_x L_\theta\})^2}{\mathrm{tr}\{\rho_\theta \Pi_x\}}. \tag{7.28}$$

Here, we have used the relation $\partial_\theta p(x|\theta) = \mathrm{tr}\{\partial_\theta \rho_\theta \Pi_x\} = \mathfrak{R}(\mathrm{tr}\{\rho_\theta \Pi_x L_\theta\})$, and $\mathfrak{R}(z)$ denotes the real part of a complex number z.

Given a state ρ_θ, the Fisher information can be maximized over all possible POVMs $\{\Pi_x\}$. Applying the inequality $|\mathrm{tr}\left\{X^\dagger Y\right\}|^2 \leq \mathrm{tr}\left\{X^\dagger X\right\} \mathrm{tr}\left\{Y^\dagger Y\right\}$, one can prove that [246]

$$\mathcal{I}(\theta) \leq \sum_x \left| \frac{\mathrm{tr}\{\rho_\theta \Pi_x L_\theta\}}{\sqrt{\mathrm{tr}\{\rho_\theta \Pi_x\}}} \right|^2 = \sum_x \left| \mathrm{tr}\left\{ \frac{\sqrt{\rho_\theta}\sqrt{\Pi_x}}{\sqrt{\mathrm{tr}\{\rho_\theta \Pi_x\}}} \sqrt{\Pi_x} L_\theta \sqrt{\rho_\theta} \right\} \right|^2 \tag{7.29a}$$

$$\leq \sum_x \mathrm{tr}\{\Pi_x L_\theta \rho_\theta L_\theta\} = \mathrm{tr}\{L_\theta \rho_\theta L_\theta\} = \mathrm{tr}\left\{\rho_\theta L_\theta^2\right\} =: \mathcal{I}_{\mathrm{QF}}(\theta). \tag{7.29b}$$

The quantity $\mathcal{I}_{\mathrm{QF}}(\theta)$ is known as the quantum Fisher information, which constrains the precision of unbiased estimators as

$$\langle\langle \Lambda_\theta \rangle\rangle \geq \frac{1}{\mathcal{I}_{\mathrm{QF}}(\theta)}. \tag{7.30}$$

Equation (7.30) is the quantum Cramér–Rao bound. The SLD L_θ can be written as

$$L_\theta = 2\int_0^\infty \exp(-\rho_\theta t)\partial_\theta \rho_\theta \exp(-\rho_\theta t). \tag{7.31}$$

In terms of the eigenbasis of ρ_θ, L_θ reads

$$L_\theta = 2\sum_{j,l} \frac{\langle j|\partial_\theta \rho_\theta|l\rangle}{p_j + p_l} |j\rangle\langle l|. \tag{7.32}$$

Inserting Eq. (7.32) into $\mathcal{I}_{\mathrm{QF}} = \mathrm{tr}\left\{\rho_\theta L_\theta^2\right\}$, we obtain an explicit form of the quantum Fisher information as

$$\mathcal{I}_{\mathrm{QF}}(\theta) = \sum_j \frac{|\langle j|\partial_\theta \rho_\theta|j\rangle|^2}{p_j} + 4\sum_{j<l} \frac{|\langle j|\partial_\theta \rho_\theta|l\rangle|^2}{p_j + p_l}. \tag{7.33}$$

On the other hand, substituting the MC function $f_{\max}(x) = (1+x)/2$ into Eq. (7.20) gives an explicit expression of the quantum Fisher information metric,

$$g_{\rho_\theta}(\partial_\theta \rho_\theta, \partial_\theta \rho_\theta) = \frac{1}{4}\left[\sum_{j=1}^{N} \frac{|\langle j|\partial_\theta \rho_\theta|j\rangle|^2}{p_j} + 4\sum_{j<l} \frac{|\langle j|\partial_\theta \rho_\theta|l\rangle|^2}{p_j + p_l}\right]. \tag{7.34}$$

Combining Eqs. (7.33) and (7.34) derives the following relation:

$$\mathcal{I}_{\mathrm{QF}}(\theta) = 4g_{\rho_\theta}(\partial_\theta \rho_\theta, \partial_\theta \rho_\theta). \tag{7.35}$$

7.1.4 Wasserstein distance

The Wasserstein distance is a metric on probability distributions and is closely connected to the concept of optimal transport. Roughly speaking, it measures the minimal cost to transform a distribution $p(x)$ of a mass into another distribution $q(x)$ on the same space. The problem of optimal transport — how to optimally transport a pile of earth into another pile that is the same in volume but may be different in shape — was originally initiated by Monge. Subsequently, it was reformulated by Kantorovich to a more well-defined problem in terms of transport planning via the coupling of probability measures. The Wasserstein distance is exactly a special case of Kantorovich's problem where the cost function is L^n-norm. Interestingly, from the fluid mechanics point of view, a variational formula for the L^2-Wasserstein distance was developed by Benamou and Brenier, allowing us to interpret the Wasserstein distance as a Riemannian distance on the infinite-dimensional manifold of probability distribution functions.

In the following, we present a brief description of the Wasserstein distance and discuss it in the context of thermodynamics. For details of the optimal transport problem and a full history and description of the Wasserstein distance, see the excellent book [217]. For simplicity, we consider only probability distributions on a continuous-state space.

Imagine that we have two probability distribution functions p and q on the space $\mathbb{R}^N$ and each of the functions is associated with a distribution of a mass. Monge's optimal transport problem is to find a one-to-one map $\varphi : \mathbb{R}^N \to \mathbb{R}^N$ that minimizes the objective function,

$$\mathcal{W}_n(p,q)^n = \inf_{\varphi} \int_{\mathbb{R}^N} \|\boldsymbol{x} - \varphi(\boldsymbol{x})\|^n p(\boldsymbol{x}) d\boldsymbol{x}, \tag{7.36}$$

where the infimum is over all φ satisfying $p(\boldsymbol{x}) = q(\varphi(\boldsymbol{x}))|\det(\nabla\varphi(\boldsymbol{x}))|$. Intuitively, the quantity $\mathcal{W}_n(p,q)$ measures the minimal cost one needs to transform the mass of distribution p to that of distribution q with respect to the transport cost $\|\cdot\|^n$. However, there is an issue in this formulation regarding the non-existence of transport maps, i.e., the map φ might not exist in the discrete case. Fortunately, this issue was resolved by the relaxation of Kantorovich, which led to the following definition.

Definition 7.5. *Let $p(\boldsymbol{x})$ and $q(\boldsymbol{x})$ be the probability distribution functions with finite n-th moments over the space $\mathbb{R}^N$, the L^n-Wasserstein distance is defined as*

$$\mathcal{W}_n(p,q)^n = \inf_{\pi}\left\{\int_{\mathbb{R}^N\times\mathbb{R}^N} \|\boldsymbol{x}-\boldsymbol{y}\|^n \pi(\boldsymbol{x},\boldsymbol{y})d\boldsymbol{x}d\boldsymbol{y} \;\middle|\; \pi\in\Pi(p,q)\right\}.$$

Here, $\Pi(p,q)$ denotes the set of joint probability distributions whose marginal distributions coincide with p and q, respectively.

The Wasserstein distance is indeed a measure of distance and satisfies the triangle inequality, $\mathcal{W}_n(p_1,p_3) \le \mathcal{W}_n(p_1,p_2)+\mathcal{W}_n(p_2,p_3)$ for arbitrary probability distribution functions p_i $(i=1,2,3)$ with finite n-th moments. In Kantorovich's problem, the L^n-norm cost function $\|\boldsymbol{x}-\boldsymbol{y}\|^n$ is replaced by a generic cost function $c(\boldsymbol{x},\boldsymbol{y}):\mathbb{R}^N\times\mathbb{R}^N\to\mathbb{R}$. A dual formulation for the Wasserstein distance can also be obtained

$$\mathcal{W}_n(p,q)^n = \sup_{\phi,\psi}\left\{\int_{\mathbb{R}^N}\phi(\boldsymbol{x})p(\boldsymbol{x})d\boldsymbol{x} - \int_{\mathbb{R}^N}\psi(\boldsymbol{y})q(\boldsymbol{y})d\boldsymbol{y} \;\middle|\; \phi(\boldsymbol{x})-\psi(\boldsymbol{y})\le\|\boldsymbol{x}-\boldsymbol{y}\|^n, \forall\boldsymbol{x},\boldsymbol{y}\right\}, \tag{7.37}$$

where $\psi,\phi:\mathbb{R}^N\to\mathbb{R}$ are integrable functions. In the case of $n=1$, a more simple representation for the L^1-Wasserstein distance known as the Kantorovich-Rubinstein duality was derived,

$$\mathcal{W}_1(p,q) = \sup_{\phi}\left\{\int \phi(\boldsymbol{x})[p(\boldsymbol{x})-q(\boldsymbol{x})]d\boldsymbol{x} \;\middle|\; |\phi(\boldsymbol{x})-\phi(\boldsymbol{y})|\le\|\boldsymbol{x}-\boldsymbol{y}\|, \forall\boldsymbol{x},\boldsymbol{y}\right\}. \tag{7.38}$$

In general, it is difficult to obtain a closed form for $\mathcal{W}_n(p,q)$, except the case where $n=2$ and p,q are both normal distributions. Specifically, if $p\sim\mathcal{N}(\boldsymbol{\mu}_p,\Sigma_p)$ and $q\sim\mathcal{N}(\boldsymbol{\mu}_q,\Sigma_q)$, then

$$\mathcal{W}_2(p,q)^2 = \|\boldsymbol{\mu}_p-\boldsymbol{\mu}_q\|^2 + \mathrm{tr}\left\{\Sigma_p+\Sigma_q-2\sqrt{\sqrt{\Sigma_p}\Sigma_q\sqrt{\Sigma_p}}\right\}. \tag{7.39}$$

Due to the difficulty in computing the L^2-Wasserstein distance, a lower bound is often taken into consideration. It was proven that $\mathcal{W}_2(p,q)^2$ can be bounded from below in terms of means and variances of p and q as [247]

$$\mathcal{W}_2(p,q)^2 \ge \|\boldsymbol{\mu}_p-\boldsymbol{\mu}_q\|^2 + \mathrm{tr}\left\{\Sigma_p+\Sigma_q-2\sqrt{\sqrt{\Sigma_p}\Sigma_q\sqrt{\Sigma_p}}\right\}, \tag{7.40}$$

where $\boldsymbol{\mu}_p,\Sigma_p$ $(\boldsymbol{\mu}_q,\Sigma_q)$ are mean and covariance matrices of the distribution p (q).

Importantly, the L^2-Wasserstein distance can be cast in the setting of fluid mechanics.

Theorem 7.2. *(Benamou-Brenier formula) Given two probability distribution functions $p(\boldsymbol{x})$ and $q(\boldsymbol{x})$, the L^2-Wasserstein distance can be written as*

$$\mathcal{W}_2(p,q)^2 = \inf\left\{\tau\int_0^\tau\int_{\mathbb{R}^N}\|\boldsymbol{\nu}(\boldsymbol{x},t)\|^2\mu(\boldsymbol{x},t)d\boldsymbol{x}dt \;\middle|\; \partial_t\mu+\nabla_x\cdot(\boldsymbol{\nu}\mu)=0, \mu(\cdot,0)=p, \mu(\cdot,\tau)=q\right\}.$$

For details of a proof, see Proposition 1.1 in Ref. [248]. This reformulation enables us to find a numerical scheme for computing the L^2-Wasserstein distance. In the following, we make some remarks regarding the relevance of the Benamou-Brenier formula.

First, with this formulation the distance $\mathcal{W}_2(p,q)$ can be interpreted as a Riemannian distance on the infinite-dimensional Riemannian manifold of probability distribution functions. For each distribution function $\mu(\boldsymbol{x})$, the tangent space $T_\mu M$ can be defined as

$$T_\mu M \coloneqq \left\{ u(\boldsymbol{x}) : \mathbb{R}^N \to \mathbb{R} \;\middle|\; \exists \boldsymbol{w}(\boldsymbol{x}) : \mathbb{R}^N \to \mathbb{R}^N \text{ s.t. } u + \nabla_x \cdot (\boldsymbol{w}\mu) = 0 \right\}. \tag{7.41}$$

Then, a Riemannian metric $g_\mu : T_\mu M \times T_\mu M \to \mathbb{R}$ can be defined as

$$g_\mu(u_1, u_2) \coloneqq \langle \boldsymbol{w}_1(\boldsymbol{x})\mu(\boldsymbol{x})^{1/2}, \boldsymbol{w}_2(\boldsymbol{x})\mu(\boldsymbol{x})^{1/2} \rangle. \tag{7.42}$$

With this defined metric, one can see that $\mathcal{W}_2(p,q)$ is exactly the geodesic distance between p and q,

$$\mathcal{W}_2(p,q)^2 = \inf_\mu \left\{ \tau \int_0^\tau g_\mu(\partial_t \mu, \partial_t \mu) dt \right\}. \tag{7.43}$$

Second, from the Benamou-Brenier formula, a lower bound on dissipation for Langevin dynamics can be derived [218–220]. Here we show a sketch proof of the bound using the Benamou-Brenier formula. For simplicity, let us consider a one-dimensional system described by the overdamped Langevin equation

$$\dot{x} = \alpha f(x,t) + \sqrt{2\alpha T}\xi, \tag{7.44}$$

where α is the particle mobility, $f(x,t)$ is the drift term, T is the bath temperature, and ξ is the white Gaussian noise satisfying $\langle \xi(t) \rangle = 0$ and $\langle \xi(t)\xi(t') \rangle = \delta(t-t')$. The total entropy production during period τ can be explicitly expressed as

$$\Delta S_{\text{tot}} = \frac{1}{\alpha T} \int_0^\tau \int_{\mathbb{R}} v(x,t)^2 p(x,t) dx dt, \tag{7.45}$$

where $v(x,t) = \alpha \left[f(x,t) - T\partial_x \ln p(x,t) \right]$ is the probability current satisfying the Fokker–Planck equation $\partial_t p(x,t) + \partial_x [v(x,t)p(x,t)] = 0$. Let $\{p(x,t)\}_{0 \le t \le \tau}$ be the curve described by the system dynamics, then the total entropy production can be written in terms of thermodynamic divergence along the curve as

$$\Delta S_{\text{tot}} = \frac{1}{\alpha T} \int_0^\tau g_p(\partial_t p, \partial_t p) dt = \frac{1}{\alpha T \tau} \mathcal{J}(p). \tag{7.46}$$

Consequently, the following bound can be immediately obtained by noticing from Eq. (7.43) that $\mathcal{W}_2 = \inf_\mu \{\mathcal{J}(\mu)^{1/2}\}$,

$$\Delta S_{\text{tot}} \ge \frac{\mathcal{W}_2(p(x,0), p(x,\tau))^2}{\alpha T \tau}. \tag{7.47}$$

The inequality (7.47) implies that given the initial and final distribution functions, the dissipation required to transform $p(x,0)$ to $p(x,\tau)$ is always bounded from below by the L^2-Wasserstein distance between these distribution functions. This implication sheds light on the problem of finding the optimal control protocol that minimizes the dissipation in overdamped Langevin systems [218]. The universality and the significance of the bound in Eq. (7.47) actually motivate us to generalize the result to discrete-state quantum and classical systems.

7.1.5 Gradient flow

Given a functional $\mathcal{E}(p)$ and a Riemannian metric g_p on the manifold M, the gradient flow under metric g_p of $\mathcal{E}$ equals the flow associated with the dynamics of $p(t)$ if

$$g_p(\partial_t p, u) = -\langle \nabla_p \mathcal{E}(p), u\rangle, \ \forall u \in T_p M. \tag{7.48}$$

An important implication of the gradient-flow structure is that the time derivative of the functional $\mathcal{E}$ can be expressed in terms of the Riemannian metric. Specifically, inserting $u = \partial_t p$ into Eq. (7.48), we readily obtain

$$\frac{d\mathcal{E}(p)}{dt} = -g_p(\partial_t p, \partial_t p). \tag{7.49}$$

Taking the time integral over $[0, \tau]$, the decrease in $\mathcal{E}$ can be related to the divergence along the path described by the dynamics of $p(t)$ as

$$\Delta\mathcal{E} \coloneqq \mathcal{E}(p(0)) - \mathcal{E}(p(\tau)) = \int_0^\tau g_p(\partial_t p, \partial_t p)dt = \mathcal{J}(p)/\tau. \tag{7.50}$$

For the relaxation process of an overdamped Langevin system, we can show that the gradient flow of free energy $\mathcal{E}(p) = \alpha T D(p||p^{\mathrm{eq}})$ under the Wasserstein metric is associated with its Fokker–Planck dynamics. Here, $p^{\mathrm{eq}}(x) = \exp\left[(F - U(x))/T\right]$ is the equilibrium distribution and $U(x)$ is the potential energy. Note that the drift term is obtained from the potential energy as $f(x) = -\partial_x U(x)$. In order to prove the above relation, we need only verify Eq. (7.48) with g_p defined in Eq. (7.42). Noticing that an arbitrary tangent vector $u(x) \in T_p M$ can be written as $u(x) = -\partial_x[w(x)p(x)]$ for some $w(x)$ and $\nabla_p \mathcal{E}(p) = \alpha T\left[\ln(p/p^{\mathrm{eq}}) - 1\right]$, one can calculate the inner product as follows:

$$\begin{aligned}
-\langle \nabla_p \mathcal{E}(p), u\rangle &= \langle \nabla_p \mathcal{E}(p), \partial_x[w(x)p(x)]\rangle && \text{(7.51a)}\\
&= \alpha T \int_{\mathbb{R}} \left(\ln \frac{p(x)}{p^{\mathrm{eq}}(x)} - 1\right) \partial_x[w(x)p(x)]dx && \text{(7.51b)}\\
&= -\alpha T \int_{\mathbb{R}} w(x)p(x)\partial_x \left(\ln \frac{p(x)}{p^{\mathrm{eq}}(x)} - 1\right) dx && \text{(7.51c)}\\
&= \alpha T \int_{\mathbb{R}} w(x)p(x)\left[f(x)/T - \partial_x \ln p(x)\right] dx && \text{(7.51d)}\\
&= \int_{\mathbb{R}} v(x)w(x)p(x)dx && \text{(7.51e)}\\
&= \langle v(x)p(x)^{1/2}, w(x)p(x)^{1/2}\rangle && \text{(7.51f)}\\
&= g_p(\partial_t p, u). && \text{(7.51g)}
\end{aligned}$$

Thus, the relation $g_p(\partial_t p, u) = -\langle \nabla_p \mathcal{E}(p), u\rangle$ is proved.

7.2 Main results

7.2.1 Bounds for open quantum systems

We first consider an open quantum system that is weakly coupled to a heat bath at the inverse temperature β. The time evolution of the density operator $\rho(t)$ of this system is described by the Lindblad master equation [82, 249]:

$$\dot{\rho} = \mathcal{L}(\rho) := -i[H(t), \rho] + \mathcal{D}(\rho), \tag{7.52}$$

where $\mathcal{L}$ is the Lindblad operator, $H(t)$ is the Hamiltonian, and $\mathcal{D}(\rho)$ is the dissipator given by $\mathcal{D}(\rho) := \sum_{\mu,\omega} \alpha_\mu(\omega) \left[2L_\mu(\omega)\rho L_\mu^\dagger(\omega) - \left\{L_\mu^\dagger(\omega)L_\mu(\omega), \rho\right\}\right]$. Here, $\{\cdot,\cdot\}$ is the anti-commutator and $L_\mu(\omega)$ is a jump operator that satisfies $L_\mu^\dagger(\omega) = L_\mu(-\omega)$ and $[L_\mu(\omega), H] = \omega L_\mu(\omega)$. Note that jump operators and coupling coefficients can be time-dependent, but we omit the time notation for simplicity. We also assume that the detailed balance condition $\alpha_\mu(\omega) = e^{\beta\omega}\alpha_\mu(-\omega)$ is satisfied and the system is ergodic [250] (i.e., $[L_\mu(\omega), X] = 0$ for all μ, ω if and only if X is proportional to the identity operator). These assumptions are sufficient conditions for the Gibbs state $\rho^{\mathrm{eq}}(t) := e^{-\beta H(t)}/Z_\beta(t)$ to be the instantaneous stationary state of the Lindblad master equation, i.e., $\mathcal{L}[\rho^{\mathrm{eq}}(t)] = 0$ [251, 252], where $Z_\beta(t)$ is the partition function.

The entropy growth of the open system during time period τ is $\Delta S_{\mathrm{tot}} = \int_0^\tau \sigma_{\mathrm{tot}}(t)dt$, where $\sigma_{\mathrm{tot}}(t) = \dot{S} + \beta\dot{Q}$ is the entropy production rate [80]. Here, $\dot{S} = -\mathrm{tr}\{\dot{\rho}(t)\ln\rho(t)\}$ denotes the von Neumann entropy flux of the system and $\dot{Q} = -\mathrm{tr}\{H(t)\dot{\rho}(t)\}$ denotes the heat flux dissipated from the system to the bath. The entropy production rate can be rewritten as $\sigma_{\mathrm{tot}}(t) = -\langle \ln\rho(t) - \ln\rho^{\mathrm{eq}}(t), \dot{\rho}(t)\rangle = -\frac{d}{dt}S(\rho(t)||\rho^{\mathrm{eq}}(t))$, where $S(\rho_1||\rho_2) := \mathrm{tr}\{\rho_1(\ln\rho_1 - \ln\rho_2)\}$ is the relative entropy of ρ_1 with respect to ρ_2, and the time derivative does not act on $\rho^{\mathrm{eq}}(t)$. $\sigma_{\mathrm{tot}}(t)$ is non-negative because the relative entropy is monotonic under completely positive trace-preserving maps; thereby, one can obtain the Clausius inequality $\Delta S_{\mathrm{tot}} \geq 0$.

We now construct an operator $\mathcal{K}_\rho$, and alternatively express the Lindblad master equation [Eq. (7.52)] in the form $\dot{\rho} = \mathcal{K}_\rho(-\ln\rho + \ln\rho^{\mathrm{eq}})$ (see Appendix E.1.1). For an arbitrary density operator ρ, we define a tilted operator $[\rho]_\theta(X) := e^{-\theta/2}\int_0^1 e^{s\theta}\rho^s X \rho^{1-s} ds$, where θ is a real number. Using this operator, $\mathcal{K}_\rho$ can be explicitly constructed as $\mathcal{K}_\rho(\psi) := i\beta^{-1}[\psi, \rho] + \mathcal{O}_\rho(\psi)$. Here,

$$\mathcal{O}_\rho(\psi) := \sum_{\mu,\omega} e^{-\beta\omega/2}\alpha_\mu(\omega)[L_\mu(\omega), [\rho]_{\beta\omega}([L_\mu^\dagger(\omega), \psi])] \tag{7.53}$$

is a self-adjoint positive operator, which can be interpreted as a quantum analog of the Onsager matrix. For an arbitrary smooth curve $\{\gamma(t)\}_{0\leq t\leq\tau}$, there exists a unique vector field of traceless self-adjoint operators $\{\nu(t)\}_{0\leq t\leq\tau}$ such that $\dot{\gamma}(t) = \mathcal{K}_\gamma[\nu(t)]$ for all t. Exploiting this representation, one can define a metric g under which the gradient flow of the instantaneous relative entropy equals the flow associated with the system dynamics [253–256]. Specifically, we define the metric $g_\gamma(\dot{\gamma}, \dot{\gamma}) = \langle \nu, \mathcal{K}_\gamma(\nu)\rangle$, which is always non-negative because $\langle \nu, \mathcal{K}_\gamma(\nu)\rangle = \langle \nu, \mathcal{O}_\gamma(\nu)\rangle \geq 0$. Although the operator $\nu(t)$ is implicitly obtained from $\dot{\gamma}(t)$, it can be regarded as the generalized thermodynamic force, and $g_\gamma(\dot{\gamma}, \dot{\gamma})$ is the quantum dissipation function [6]. This can be clarified as considering the path generated by the system dynamics, i.e., $\dot{\rho} = \mathcal{K}_\rho(\phi)$ and $g_\rho(\dot{\rho}, \dot{\rho}) = \sigma_{\mathrm{tot}}(t)$, where $\phi = -(\ln\rho - \ln\rho^{\mathrm{eq}}) + c$ is a traceless self-adjoint

operator. In addition to the thermodynamic length $\ell(\gamma)$, the thermodynamic divergence of a path, defined as [215]

$$\ell_{\mathrm{q}}(\gamma)^2 \coloneqq \tau \int_0^\tau g_\gamma(\dot{\gamma},\dot{\gamma})dt, \tag{7.54}$$

is a measure of the dissipation along the path. Note that by the Cauchy–Schwarz inequality, $\ell_{\mathrm{q}}(\gamma) \geq \ell(\gamma)$. A modified Wasserstein distance between two states ρ_0 and ρ_τ can be defined as $\mathcal{W}_{\mathrm{q}}(\rho_0,\rho_\tau) \coloneqq \inf_\gamma\{\ell_{\mathrm{q}}(\gamma)\}$, where the infimum is taken over smooth curves with end points ρ_0 and ρ_τ. For relaxation processes, $\mathcal{W}_{\mathrm{q}}$ is exactly the geodesic distance induced by the defined metric[4]. It has been shown that a clear-cut definition of the quantum Wasserstein distance, by the direct generalization of the classical one, is not achievable [257]. Our generalization here is based on the Benamou–Brenier flow formulation of the original L^2-Wasserstein [248, 255, 256]. Other generalized metrics based on quantum couplings [257–259] and the Kantorovich–Rubinstein duality [260] have also been proposed in the literature. From the definition of $\mathcal{W}_{\mathrm{q}}$, the first main result is a geometrical lower bound of the entropy production:

$$\Delta S_{\mathrm{tot}} \geq \frac{\mathcal{W}_{\mathrm{q}}(\rho(0),\rho(\tau))^2}{\tau}. \tag{7.55}$$

Inequality (7.55) indicates that the irreversible entropy production is lower bounded by the distance between the initial and final states. This bound is stronger than the conventional second law of thermodynamics; it can also be interpreted as a quantum speed limit, as it limits the time required to transform the system state. The limit is governed by dissipation and the geometrical distance between states. To generalize the result to the infinite-dimensional Hilbert space, the existence and the construction of the operator $\nu(t)$ in the definition of the metric must be clarified. Since the distance $\mathcal{W}_{\mathrm{q}}$ is usually difficult to compute explicitly, we provide a lower bound of $\mathcal{W}_{\mathrm{q}}$ in terms of the trace-like distance $\mathsf{d}_{\mathrm{T}}(\rho_0,\rho_\tau) = \sum_{n=1}^N |a_n - b_n|$, where $\{a_n\}$ and $\{b_n\}$ are increasing eigenvalues of ρ_0 and ρ_τ, respectively. Specifically, we prove that $\mathcal{W}_{\mathrm{q}}(\rho_0,\rho_\tau)^2 \geq \mathsf{d}_{\mathrm{T}}(\rho_0,\rho_\tau)^2/4\mathcal{A}_{\mathrm{T}}$ (see Appendix E.1.3) , where $\mathcal{A}_{\mathrm{T}} \coloneqq \tau^{-1}\int_0^\tau \sum_{\mu,\omega}\alpha_\mu(\omega)\|L_\mu(\omega)\|_\infty^2 dt$ characterizes the time scale of the quantum system and $\|X\|_\infty$ denotes the spectral norm of the operator X. Note that this lower bound on $\mathcal{W}_{\mathrm{q}}$ is not invariant under the well-known unitary transformation of jump operators, because the conditions of jump operators uniquely determine the parameterization of the dynamics. Consequently, the entropy production is also bounded from below by the trace-like distance between the initial and final states, given by

$$\Delta S_{\mathrm{tot}} \geq \frac{\mathsf{d}_{\mathrm{T}}(\rho(0),\rho(\tau))^2}{4\tau\mathcal{A}_{\mathrm{T}}}. \tag{7.56}$$

The Hamiltonian and jump operators of a system must be time-independent in order to equilibrate with the environment and reach a steady state. Thus, during equilibration, the entropy production can be bounded by the distance $\mathsf{d}_{\mathrm{E}}(\rho_0,\rho_\tau) = |\mathrm{tr}\{H(\rho_0-\rho_\tau)\}|$ of the

[4]Since $\ell_{\mathrm{q}}(\gamma) \geq \ell(\gamma)$, we have $\mathcal{W}_{\mathrm{q}}(\rho_0,\rho_\tau) \geq \inf_\gamma\{\ell(\gamma)\}$ in the general case. However, for relaxation processes (i.e., the operator $\mathcal{K}_\gamma$ is time-independent), it can be shown that $\mathcal{W}_{\mathrm{q}}(\rho_0,\rho_\tau) = \inf_\gamma\{\ell(\gamma)\}$, where the equality is attained with a constant-speed path [237].

average energy change (see Appendix E.1.4),

$$\Delta S_{\rm tot} \geq \frac{\mathsf{d}_{\rm E}(\rho(0),\rho(\tau))^2}{\tau \mathcal{A}_{\rm E}}, \tag{7.57}$$

where $\mathcal{A}_{\rm E} \coloneqq \sum_{\mu,\omega} \alpha_\mu(\omega)\omega^2 \|L_\mu(\omega)\|_\infty^2$. A tighter bound in terms of the square of the heat current to the reservoir [261],

$$\Delta S_{\rm tot} \geq \frac{\left(\int_0^\tau |\dot{Q}| dt\right)^2}{\tau \mathcal{A}_{\rm E}}, \tag{7.58}$$

and another bound in terms of the change in entropy of the system,

$$\Delta S_{\rm tot} \geq \frac{|\Delta S|^2}{\Upsilon}, \tag{7.59}$$

can also be obtained. Here, $\Upsilon \coloneqq \int_0^\tau \langle \ln\rho, \mathcal{O}_\rho(\ln\rho)\rangle dt$ is a system-dependent quantity. However, these bounds are not tight in the zero-temperature limit, as compared to the bound reported in Ref. [13]. Inequalities (7.56) and (7.57) provide lower bounds not only on the entropy production, but also on the equilibration time, which is an essential quantity in quantum-state preparation [262], and which aids our understanding of thermalization [8]. In applications, the equilibration time can be approximated without solving the Lindblad master equation, which may be time-consuming in the weak coupling limit. The dissipation-current trade-off relation [263], which unveils the role of coherence between energy eigenstates in realizing a dissipation-less heat current, can also be derived using our geometrical approach (see Appendix E.1.5).

The system becomes classical when the initial density matrix has no coherence in the energy eigenbasis of the Hamiltonian. In what follows, we present the analysis for classical systems.

7.2.2 Bounds for classical systems

Next, we consider a discrete-state system in contact with a heat bath at the inverse temperature β. During a time period τ, stochastic transitions between the states are induced by interactions with the heat bath. The dynamics obey a time-continuous Markov jump process and are described by the master equation:

$$\dot{p}_n(t) = \sum_{m(\neq n)} \left[R_{nm}(t)p_m(t) - R_{mn}(t)p_n(t)\right], \tag{7.60}$$

where $p_n(t)$ is the probability of finding the system in state n at time t, and $R_{mn}(t)$ is the (possibly time-dependent) transition rate from state n to state m ($1 \leq n \neq m \leq N$). We assume an irreducible system in which the transition rates satisfy the detailed balance condition $R_{nm}(t)e^{-\beta\mathcal{E}_m(t)} = R_{mn}(t)e^{-\beta\mathcal{E}_n(t)}$ for all $m \neq n$, where $\mathcal{E}_n(t)$ is the instantaneous energy of state n at time t. When the transition rates are time-independent, the system always relaxes to a unique equilibrium state after a sufficiently long time, irrespective of its initial state. Herein, we define the instantaneous equilibrium state $\boldsymbol{p}^{\rm eq}(t)$ as $p_n^{\rm eq}(t) \propto e^{-\beta\mathcal{E}_n(t)}$.

Within the stochastic thermodynamics framework [3], the irreversible entropy production $\Delta S_{\rm tot}$ is quantified by the change in the system's Shannon entropy and the heat flow dissipated into the environment. Specifically, $\Delta S_{\rm tot} = \int_0^\tau \sigma_{\rm tot}(t)dt$, where $\sigma_{\rm tot}(t) = \sigma(t) + \sigma_{\rm M}(t)$ is the total entropy production rate. The terms $\sigma(t) = \sum_{m,n} R_{mn}p_n \ln(p_n/p_m)$ and $\sigma_{\rm M}(t) = \sum_{m,n} R_{mn}p_n \ln(R_{mn}/R_{nm})$ define the entropy production rates of the system and medium, respectively. Under the detailed balance condition, the entropy production rate can be explicitly calculated as $\sigma_{\rm tot}(t) = \langle \boldsymbol{f}(t), \dot{\boldsymbol{p}}(t)\rangle = -\frac{d}{dt}D(\boldsymbol{p}(t)||\boldsymbol{p}^{\rm eq}(t))$, where $\boldsymbol{f}(t) \coloneqq -\nabla_p D(\boldsymbol{p}(t)||\boldsymbol{p}^{\rm eq}(t))$ is a vector of thermodynamic forces, and the time derivative does not act on $\boldsymbol{p}^{\rm eq}(t)$. Here, $D(\boldsymbol{p}||\boldsymbol{q}) = \sum_n p_n \ln(p_n/q_n)$ is the relative entropy between the distributions $\boldsymbol{p}$ and $\boldsymbol{q}$, and $\nabla_p \coloneqq [\partial_{p_1}, \dots, \partial_{p_N}]^\top$ denotes the gradient with respect to $\boldsymbol{p}$. The second law of thermodynamics, $\Delta S_{\rm tot} \geq 0$, is affirmed from the positivity of the entropy production rate $\sigma_{\rm tot}(t)$. In the following analysis, we will sharpen the lower bound of $\Delta S_{\rm tot}$ using the geometrical distance between the initial state $\boldsymbol{p}(0)$ and the final state $\boldsymbol{p}(\tau)$.

The master equation [Eq. (7.60)] can be alternatively written as $\dot{\boldsymbol{p}}(t) = \mathsf{K}_p(t)\boldsymbol{f}(t)$ (see Appendix E.2.1), where $\mathsf{K}_p(t)$ is a symmetric positive semi-definite matrix, given by

$$\mathsf{K}_p(t) \coloneqq \sum_{n<m} R_{nm}(t)p_m^{\rm eq}(t)\Phi\left(\frac{p_n(t)}{p_n^{\rm eq}(t)}, \frac{p_m(t)}{p_m^{\rm eq}(t)}\right)\mathsf{E}_{nm}. \tag{7.61}$$

Here, $\Phi(x,y) = (x-y)/[\ln(x) - \ln(y)]$ is the logarithmic mean of $x, y > 0$ and $\mathsf{E}_{nm} = [e_{ij}] \in \mathbb{R}^{N\times N}$ is a matrix with $e_{nn} = e_{mm} = 1$, $e_{nm} = e_{mn} = -1$, and zeros in all other elements. The symmetric matrix K_p is actually the Onsager matrix [6], which linearly relates the thermodynamic forces to the probability currents. For an arbitrary smooth curve $\{\boldsymbol{\gamma}(t)\}_{0\leq t\leq\tau}$, there exists a unique vector field $\{\boldsymbol{v}(t)\}_{0\leq t\leq\tau}$ such that $\dot{\boldsymbol{\gamma}}(t) = \mathsf{K}_\gamma(t)\boldsymbol{v}(t)$ and $\langle \mathbf{1}, \boldsymbol{v}(t)\rangle = 0$, where $\mathbf{1} \coloneqq [1, \dots, 1]^\top$ is an all-ones vector. We can thus define the Riemannian metric $g_\gamma(\dot{\boldsymbol{\gamma}}, \dot{\boldsymbol{\gamma}}) = \langle \boldsymbol{v}, \mathsf{K}_\gamma \boldsymbol{v}\rangle$, which is always non-negative. Using this metric, the thermodynamic divergence of a curve can be defined as

$$\ell_{\rm c}(\boldsymbol{\gamma})^2 \coloneqq \tau \int_0^\tau g_\gamma(\dot{\boldsymbol{\gamma}}, \dot{\boldsymbol{\gamma}})dt. \tag{7.62}$$

The modified Wasserstein distance between two points $\boldsymbol{p}_0$ and $\boldsymbol{p}_\tau$ is then defined as $\mathcal{W}_{\rm c}(\boldsymbol{p}_0, \boldsymbol{p}_\tau) \coloneqq \inf_\gamma \{\ell_{\rm c}(\boldsymbol{\gamma})\}$, where the infimum is taken over all smooth curves connecting $\boldsymbol{p}_0$ and $\boldsymbol{p}_\tau$ on the manifold. Notably, this distance is bounded from below by the total variation distance (see Appendix E.2.4),

$$\mathcal{W}_{\rm c}(\boldsymbol{p}_0, \boldsymbol{p}_\tau)^2 \geq \frac{\mathsf{d}_{\rm V}(\boldsymbol{p}_0, \boldsymbol{p}_\tau)^2}{2\mathcal{A}_{\rm V}}, \tag{7.63}$$

where $\mathcal{A}_{\rm V} \coloneqq \tau^{-1}\int_0^\tau \sum_{m\neq n} R_{mn}(t)\gamma_n(t)dt$ is the average dynamical activity along the geodesic path $\{\boldsymbol{\gamma}(t)\}_{0\leq t\leq\tau}$. The dynamical activity $\mathcal{A}_{\rm V}$ characterizes the time scale of the system. The bound in Eq. (7.63) can be further refined by replacing the dynamical activity $\mathcal{A}_{\rm V}$ by a smaller term called the partial dynamical activity (see Appendix E.2.4 for details of the derivation). It is worth noting that the defined metric is not equivalent to the traditional discrete version of the classical Wasserstein metric. In practice, $\mathcal{W}_{\rm c}$ can be numerically calculated by the geodesic equation (see Appendix E.2.3), which computes the shortest path between two points. Defining $\boldsymbol{h}(t) \coloneqq \boldsymbol{f}(t) - N^{-1}\langle \mathbf{1}, \boldsymbol{f}(t)\rangle \mathbf{1}$, one observes that $\dot{\boldsymbol{p}}(t) = \mathsf{K}_p(t)\boldsymbol{h}(t)$ and $\langle \mathbf{1}, \boldsymbol{h}(t)\rangle = 0$.

As $\sigma_{\rm tot}(t) = \langle \boldsymbol{h}(t), \mathsf{K}_p(t)\boldsymbol{h}(t)\rangle$, $\tau\Delta S_{\rm tot}$ is exactly the thermodynamic divergence of the path described by the system dynamics. As the second main result, we obtain the following bound:

$$\Delta S_{\rm tot} \geq \frac{\mathcal{W}_{\rm c}(\boldsymbol{p}(0), \boldsymbol{p}(\tau))^2}{\tau}. \tag{7.64}$$

Inequality (7.64) provides a stronger bound than the Clausius inequality of the second law, and is valid as long as the transition rates satisfy the detailed balance condition. Geometrically, Eq. (7.64) can be considered as a discrete-state generalization of the relation between dissipation and the Wasserstein distance, which has been studied in continuous-state Markovian dynamics governed by Langevin equations [218, 220]. Concretely, Eq. (21) in Ref. [218] and Eq. (2) in Ref. [220] are referred to as the continuum analogs of Eq. (7.64). Our generalization newly and appropriately connects these thermodynamic and geometric quantities in the discrete case. Therefore, it is applicable to the many discrete physical phenomena in biological and quantum physics.

Tighter speed limit

All the derived bounds above can be interpreted as speed limits. The authors in Ref. [92] proved the following classical speed limit:

$$\tau \geq \tau_{\rm tot} := \frac{\mathsf{d}_{\rm V}(\boldsymbol{p}(0), \boldsymbol{p}(\tau))^2}{2\Delta S_{\rm tot}\mathcal{A}}, \tag{7.65}$$

where $\mathcal{A} := \tau^{-1}\int_0^\tau \sum_{m\neq n} R_{mn}(t)p_n(t)dt$ is the average dynamical activity along the path described by the master equation of the distribution $\boldsymbol{p}(t)$. With our geometrical approach, we can prove a tighter bound defined as

$$\tau \geq \frac{\mathsf{d}_{\rm V}(\boldsymbol{p}(0), \boldsymbol{p}(\tau))^2}{2\Delta S_{\rm tot}\mathcal{A}^{\rm par}} =: \tau_{\rm par} \geq \tau_{\rm tot}, \tag{7.66}$$

where $\mathcal{A}^{\rm par} := \tau^{-1}\int_0^\tau \sum_{{\rm par}(m)\neq{\rm par}(n)} R_{mn}(t)p_n(t)dt \leq \mathcal{A}$ is the *partial* dynamical activity. Here, ${\rm par}(n) = 1$ if $p_n(0) > p_n(\tau)$ and ${\rm par}(n) = -1$ if $p_n(0) \leq p_n(\tau)$. This new bound indicates that the transformation time is not constrained by the total dynamical activity, but by the partial dynamical activity induced by transitions between states in $\mathcal{X}_-$ and $\mathcal{X}_+$, where

$$\mathcal{X}_- := \{n \mid 1 \leq n \leq N,\ p_n(0) \leq p_n(\tau)\},$$
$$\mathcal{X}_+ := \{n \mid 1 \leq n \leq N,\ p_n(0) > p_n(\tau)\}.$$

Here, the subset $\mathcal{X}_-$ ($\mathcal{X}_+$) includes states whose probability must be increased (decreased). The conclusion agrees well with our intuition from the viewpoint of optimal transport, that is, in transforming $\boldsymbol{p}(0)$ to $\boldsymbol{p}(\tau)$, transitions between states in different subsets $\mathcal{X}_-$ and $\mathcal{X}_+$ are more essential than those between states in the same subset $\mathcal{X}_-$ or $\mathcal{X}_+$. The details of the derivation can be found in Appendix E.2.4.

7.3 Numerical illustration

First, we illustrate the bounds derived in Eqs. (7.56) and (7.57) on a quantum Otto heat engine [264–266], which consists of a two-level atom with the Hamiltonian $H(t) = \omega(t)\sigma_z/2$. This system is alternatively coupled to two heat baths at different inverse temperatures [one hot, one cold, $\beta_k = 1/T_k$ $(k = h, c)$], and is cyclically operated through four steps as demonstrated in Fig. 7.1(a). During adiabatic expansion (compression), the isolated system unitarily evolves during time τ_a, and its frequency changes from $\omega_h \to \omega_c$ $(\omega_c \to \omega_h)$. The dynamics in each isochoric process $k = h, c$ are described by the Lindblad master equation [80]:

$$\begin{aligned}\dot{\rho} = -i[H_k, \rho] + \alpha_k \bar{n}(\omega_k)(2\sigma_+\rho\sigma_- - \{\sigma_-\sigma_+, \rho\}) \\ +\alpha_k(\bar{n}(\omega_k)+1)(2\sigma_-\rho\sigma_+ - \{\sigma_+\sigma_-, \rho\}),\end{aligned} \tag{7.67}$$

where the frequency is fixed at ω_k, $\sigma_\pm = (\sigma_x \pm i\sigma_y)/2$, α_k is a positive damping rate, and $\bar{n}(\omega_k) = (e^{\beta_k\omega_k} - 1)^{-1}$ is the Planck distribution. The density operator ρ in this thermalization process is analytically solvable [267] and the total entropy production can be explicitly evaluated as $\Delta S^k_{\rm tot} = S(\rho(0)||\rho^{\rm eq}) - S(\rho(\tau_k)||\rho^{\rm eq})$, where τ_k denotes the process time. Equations (7.56) and (7.57) constrain $\Delta S^k_{\rm tot}$ within the distances $\mathsf{d}_{\rm T}$ and $\mathsf{d}_{\rm E}$, as numerically verified in Fig. 7.1(b). Note that unlike the classical case [228], $\Delta S^k_{\rm tot}$ in generic thermalization processes is not bounded by the relative entropy $S(\rho(0)||\rho(\tau_k))$.

The total entropy production in each cycle is the sum of those in the hot and cold isochoric processes; that is, $\Delta S_{\rm tot} = \Delta S^h_{\rm tot} + \Delta S^c_{\rm tot}$. Assuming a stationary-state system, let Q_h and Q_c denote the heat taken from the hot bath and the heat transferred to the cold bath, respectively. From the inequality $\Delta S_{\rm tot} = \beta_h Q_h - \beta_c Q_c \geq 0$ imposed by the second law, one can prove that the engine efficiency cannot exceed the Carnot efficiency $\eta := 1 - \frac{Q_c}{Q_h} \leq 1 - \frac{\beta_h}{\beta_c} =: \eta_{\rm C}$. From the derived bounds, we can tighten the bound on the efficiency of the quantum Otto engine. Applying Eqs. (7.56) and (7.57) to isochoric processes, one readily obtains $\beta_h Q_h - \beta_c Q_c \geq \mathfrak{g}$, where

$$\begin{aligned}\mathfrak{g} := \max\left\{\mathsf{d}_{\rm T}(\rho_1,\rho_4)^2/4\tau_h\mathcal{A}^h_{\rm T}, \mathsf{d}_{\rm E}(\rho_1,\rho_4)^2/\tau_h\mathcal{A}^h_{\rm E}\right\} \\ +\max\left\{\mathsf{d}_{\rm T}(\rho_2,\rho_3)^2/4\tau_c\mathcal{A}^c_{\rm T}, \mathsf{d}_{\rm E}(\rho_2,\rho_3)^2/\tau_c\mathcal{A}^c_{\rm E}\right\}.\end{aligned} \tag{7.68}$$

Here, ρ_i denotes the density operator at the beginning of process i $(1 \leq i \leq 4)$, $\mathcal{A}^k_{\rm T} := \alpha_k(2\bar{n}(\omega_k)+1)$, and $\mathcal{A}^k_{\rm E} := \omega_k^2\alpha_k(2\bar{n}(\omega_k)+1)$ for each $k = h, c$. Consequently, the efficiency can be bounded from above as $\eta \leq \eta_{\rm C} - \frac{\mathfrak{g}}{\beta_c Q_h} =: \eta_{\rm G}$. This bound is numerically verified in Fig. 7.1(c), which plots the efficiency against the ω_c/ω_h ratio.

Next, we numerically verify the bound derived in Eq. (7.64) in a time-driven two-level classical system. The instantaneous energies of states 1 and 2 are $\mathcal{E}_1(t) = \beta^{-1}\ln[(1-a+b(t+1)/\tau)/(a-bt/\tau)]$ and $\mathcal{E}_2(t) = 0$, respectively, where $0 < b < a < 1$ are constants. Their respective transition rates are $R_{12}(t) = 1, R_{21}(t) = e^{\beta\mathcal{E}_1(t)}$. The probability distribution and entropy production are analytically calculated as $p_1(t) = a - bt/\tau$ and $\Delta S_{\rm tot} = b\tau^{-1}\int_0^\tau \ln[(1-a+b(t+1)/\tau)/(1-a+bt/\tau)]dt$, respectively. The entropy production and modified Wasserstein distance are plotted as functions of time τ in Fig. 7.1(d). The entropy production at all

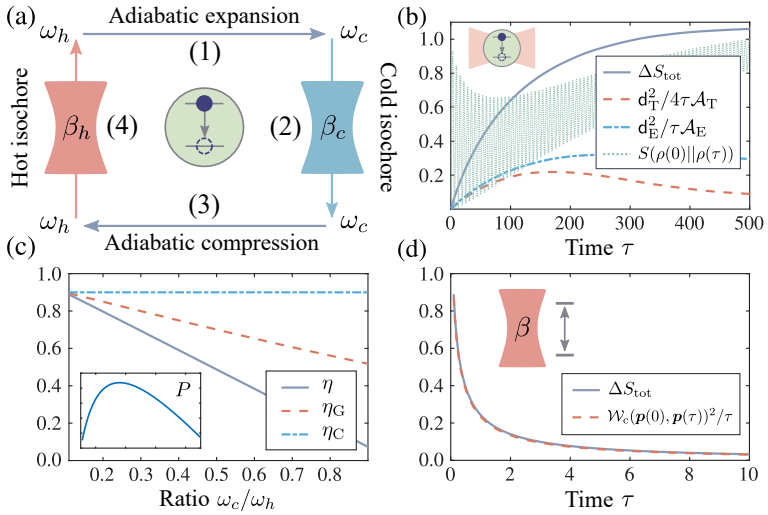

Figure 7.1: Numerical verification. (a) Quantum Otto engine: A two-level atom undergoes two isochoric and two adiabatic processes. (b) Thermalization process of the two-level atom. Plotted are $\Delta S_{\rm tot}$ (solid line), $\mathsf{d}_{\rm T}^2/4\tau\mathcal{A}_{\rm T}$ (dashed line), $\mathsf{d}_{\rm E}^2/\tau\mathcal{A}_{\rm E}$ (dash-dotted line), and $S(\rho(0)||\rho(\tau))$ (dotted line). Parameters are $\beta_k = 1, \omega_k = 1, \alpha_k = 10^{-3}$, and $\rho(0) = (\mathbb{I}_2 + 0.1\sigma_x - 0.5\sigma_y + 0.8\sigma_z)/2$. Here, $\mathbb{I}_2$ denotes the 2×2 identity matrix and $\{\sigma_x, \sigma_y, \sigma_z\}$ is a set of Pauli matrices. (c) Engine efficiency η (solid line), Carnot efficiency $\eta_{\rm C}$ (dash-dotted line), and the derived efficiency bound $\eta_{\rm G}$ (dashed line), as functions of the cold-to-hot ratio of operating frequency. The inset plots the power output P of the engine over the same frequency-ratio range. Parameters are $\beta_c = 1, \beta_h = 0.1, \alpha_h = \alpha_c = 10^{-3}$, and $\tau_a = \tau_c = \tau_h = 1$. (d) Classical two-level system. Plotted are $\Delta S_{\rm tot}$ (solid line) and $\mathcal{W}_{\rm c}(\boldsymbol{p}(0), \boldsymbol{p}(\tau))^2/\tau$ (dashed line). Parameters are fixed as $a = 0.7, b = 0.4$.

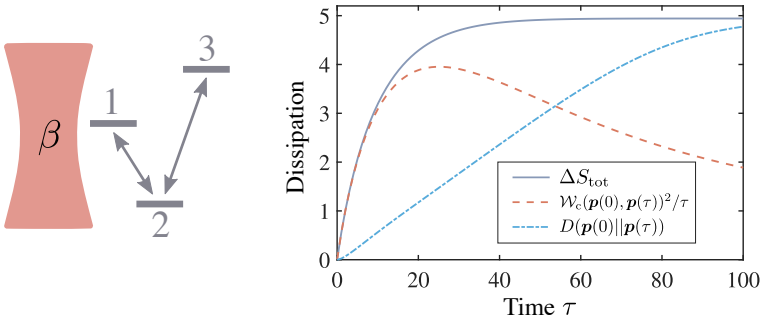

Figure 7.2: Numerical verification of the derived bound on the three-level classical system. $\Delta S_{\rm tot}$ (solid line), $\mathcal{W}_{\rm c}(\boldsymbol{p}(0),\boldsymbol{p}(\tau))^2/\tau$ (dashed line), and $D(\boldsymbol{p}(0)||\boldsymbol{p}(\tau))$ (dash-dotted line) during the thermalization process of a three-level system. Parameters are set as $\beta = 1, w_{12} = 1, w_{23} = 2, w_{13} = 0, \mathcal{E}_1 = 3, \mathcal{E}_2 = -0.5, \mathcal{E}_3 = 6$, and $\boldsymbol{p}(0) = [0.1, 0.1, 0.8]^{\top}$.

times was tightly bounded from below by the distance $\mathcal{W}_{\rm c}$. This result numerically verifies Eq. (7.64).

Finally, we illustrate the derived bound on the thermalization process of a three-level system. The transition rates are time-independent and equal to

$$R_{mn} = w_{mn} e^{\beta(\mathcal{E}_n - \mathcal{E}_m)/2} \mathrm{sech}[\beta(\mathcal{E}_n - \mathcal{E}_m)/2], \tag{7.69}$$

where $w_{mn} = w_{nm}$ are nonnegative constants. Evidently, the transition rates satisfy the detailed balance conditions $R_{mn} p_n^{\rm eq} = R_{nm} p_m^{\rm eq}$. According to Eq. (7.64) in the main text, the entropy production is bounded from below by the modified Wasserstein distance as

$$\Delta S_{\rm tot} \geq \frac{\mathcal{W}_{\rm c}(\boldsymbol{p}(0),\boldsymbol{p}(\tau))^2}{\tau}. \tag{7.70}$$

The total entropy production can be explicitly expressed as $\Delta S_{\rm tot} = D(\boldsymbol{p}(0)||\boldsymbol{p}^{\rm eq}) - D(\boldsymbol{p}(\tau)||\boldsymbol{p}^{\rm eq})$. In thermalization processes satisfying the detailed balance conditions, Ref. [228] proved that the relative entropy satisfies the reverse triangle inequality:

$$D(\boldsymbol{p}(0)||\boldsymbol{p}^{\rm eq}) \geq D(\boldsymbol{p}(0)||\boldsymbol{p}(\tau)) + D(\boldsymbol{p}(\tau)||\boldsymbol{p}^{\rm eq}). \tag{7.71}$$

Subsequently, the entropy production during thermalization processes is bounded from below by an information-theoretical quantity of the initial and final states, $\Delta S_{\rm tot} \geq D(\boldsymbol{p}(0)||\boldsymbol{p}(\tau))$. For fixed transition rates, Fig. 7.2 plots the entropy production, modified Wasserstein distance, and relative entropy as functions of time τ. In this figure, the distance term $\mathcal{W}_{\rm c}^2(\boldsymbol{p}(0),\boldsymbol{p}(\tau))/\tau$ and the relative entropy always lie below the entropy production $\Delta S_{\rm tot}$. The modified Wasserstein distance is tight in the short-time regime, whereas the relative entropy saturates in the long-time limit. Therefore, these two bounds complementarily characterize the irreversibility in thermalization processes.

7.4 Concluding remarks and discussion

In this chapter, we derived the geometrical bounds of irreversibility in both quantum and classical open systems, thus strengthening the Clausius inequality of the second law of thermodynamics. These bounds are significant, because they constrain the total entropy production from below by the distance between the initial and final states on the manifold. Furthermore, the study results elucidate that, beyond the linear response regime, the entropy production can be geometrically characterized. This finding sheds light on the problem of minimizing dissipation in discrete-state systems by methods of optimal control [218]. Interpreting the bounds as speed limits shows that the state-transformation speed is constrained by dissipation in quantum systems. By investigating the information-geometrical structure underlying the system dynamics, we lay the foundations for obtaining useful thermodynamic relations. Exploring analogous bounds in generic systems, which violate the detailed balance condition, and for higher cumulants of dissipation [268, 269], would be promising research directions.

Chapter 8

Conclusion

This chapter concludes with the research results presented in the thesis and a prospect in future research directions.

In this thesis, we elucidated thermodynamic relations on irreversibility in nonequilibrium systems. In the first part, we derived novel TURs for various stochastic dynamics that cannot be covered by the original one. Notably, we derived the bounds for steady-state underdamped dynamics and Langevin systems driven by arbitrary control protocols in both overdamped and underdamped regimes (chapter 4). We also obtained TURs for non-Markovian systems involving time delay, measurement and feedback control, and semi-Markov processes (chapter 5). Our findings revealed that other quantities such as dynamical activity, information flow, and memory terms are on par with entropy production in constraining fluctuations of finite-time observables. In addition to the theoretical approach, we proposed a TUR-based method to accurately infer entropy production without knowing details of microscopic dynamics (chapter 6). In the second part, we refined the conventional second law of thermodynamics for Markovian systems satisfying the detailed balance condition. We showed that the entropy production is lower bounded by a geometrical distance between the initial and final states (chapter 7). This study result has two important implications. First, beyond the linear response regime, entropy production can be associated with the thermodynamic divergence of the path described by the system dynamics with an appropriate Riemannian metric. Second, entropy production constrains the time required to transform the state of an open quantum system.

Some open questions remain to be addressed. First, although the TUR does not, in general, hold for finite-time currents in underdamped Langevin systems, it seems that the TUR is still valid in a long observation time. Proving the validity of the TUR or finding a counterexample for long-time underdamped dynamics would be significant progress. Second, the TUR has been mainly investigated for classical systems. Several attempts to extend the uncertainty relations to the quantum regime have been made. These bounds can be regarded as quantum analogs of the KUR, which relate the dynamical activity and counting observables in open quantum systems subject to continuous measurement. A genuine generalization of the TUR for quantum systems thus remains veiled. Last, it has been shown that irreversibility in the thermal relaxation of classical open systems is bounded from below by the relative entropy between the initial and final distributions. However, a straightforward extension to the quantum case does not work, i.e., the relative entropy between the initial and final states

cannot be a lower bound on irreversibility. This suggests that an appropriate modification of the bound may be needed. Revealing such information-theoretical bounds not only improves our understanding of irreversibility but also provides an efficient way to estimate entropy production.

Appendix A

Appendix A

For the sake of convenience, we consider a more general system whose dynamics are described by

$$\dot{r}_i = v_i,\ m_i\dot{v}_i = H_i(\boldsymbol{r},\boldsymbol{v}) + \xi_i, \tag{A.1}$$

where $H_i(\boldsymbol{r},\boldsymbol{v}) = \sum_{j=1}^{N} v_j G_{ij}(\boldsymbol{r}) + F_i(\boldsymbol{r})$ and $\langle \xi_i(t)\xi_j(t')\rangle = 2D_i\delta_{ij}\delta(t-t')$. The system employed in the paper can be obtained by substituting

$$G_{ij}(\boldsymbol{r}) \leftarrow -\delta_{ij}\gamma_i,\ D_i \leftarrow T_i\gamma_i. \tag{A.2}$$

A.1 Calculation of entropy production rate

Following Ref. [102], we calculate the entropy production rate. Let us consider an infinitesimal time interval $[t, t+dt]$, in which $\boldsymbol{r} \equiv \boldsymbol{r}(t), \boldsymbol{v} \equiv \boldsymbol{v}(t), \boldsymbol{r}' \equiv \boldsymbol{r}(t+dt)$, and $\boldsymbol{v}' \equiv \boldsymbol{v}(t+dt)$. From the definition of the entropy production in Eq. (4.3), the entropy production in this time interval is given by

$$d\Delta s_{\mathrm{tot}} = -d(\ln P(\boldsymbol{r},\boldsymbol{v},t)) + \ln \frac{\mathbb{P}[\boldsymbol{r}',\boldsymbol{v}',t+dt|\boldsymbol{r},\boldsymbol{v},t]}{\mathbb{P}[\boldsymbol{r},-\boldsymbol{v},t+dt|\boldsymbol{r}',-\boldsymbol{v}',t]}. \tag{A.3}$$

By using the short time propagator, we can express the transition probability as

$$\mathbb{P}[\boldsymbol{r}',\boldsymbol{v}',t+dt|\boldsymbol{r},\boldsymbol{v},t] = \prod_{i=1}^{N} \frac{m_i}{\sqrt{4\pi D_i dt}} \exp\left[-\frac{(m_i dv_i - H_i(\boldsymbol{r},\boldsymbol{v})dt)^2}{4D_i dt}\right], \tag{A.4}$$

where $dv_i = v_i' - v_i$. The force $H_i(\boldsymbol{r},\boldsymbol{v})$ can be decomposed into reversible and irreversible parts as $H_i(\boldsymbol{r},\boldsymbol{v}) = H_i^{\mathrm{ir}}(\boldsymbol{r},\boldsymbol{v}) + H_i^{\mathrm{rev}}(\boldsymbol{r},\boldsymbol{v})$, where $H_i^{\mathrm{ir}}(\boldsymbol{r},\boldsymbol{v}) = \sum_{j=1}^{N} v_j G_{ij}(\boldsymbol{r})$ and $H_i^{\mathrm{rev}}(\boldsymbol{r},\boldsymbol{v}) = F_i(\boldsymbol{r})$. Analogously, we also have

$$\mathbb{P}[\boldsymbol{r},-\boldsymbol{v},t+dt|\boldsymbol{r}',-\boldsymbol{v}',t] = \prod_{i=1}^{N} \frac{m_i}{\sqrt{4\pi D_i dt}} \exp\left[-\frac{\left(m_i dv_i - \left[-H_i^{\mathrm{ir}}(\boldsymbol{r},\boldsymbol{v}) + H_i^{\mathrm{rev}}(\boldsymbol{r},\boldsymbol{v})\right]dt\right)^2}{4D_i dt} - \frac{1}{m_i}\partial_{v_i} H_i^{\mathrm{ir}}(\boldsymbol{r},\boldsymbol{v})dt\right]. \tag{A.5}$$

We note that in the case of additive noise, the discretization schemes in the forward and backward paths are independent. However, for multiplicative noise, there is a constraint on the discretization. That is, if the evaluation points in the forward path are $a\boldsymbol{r}' + (1-a)\boldsymbol{r}$ and

$a\boldsymbol{v}' + (1-a)\boldsymbol{v}$, then in the backward path, they should be $b\boldsymbol{r} + (1-b)\boldsymbol{r}'$ and $b\boldsymbol{v} + (1-b)\boldsymbol{v}'$, where $b = 1 - a$. Here, we have employed the discretization with $a = 0$ and $b = 1$. Using Eqs. (A.4) and (A.5), we obtain

$$\ln \frac{\mathbb{P}[\boldsymbol{r}', \boldsymbol{v}', t+dt|\boldsymbol{r}, \boldsymbol{v}, t]}{\mathbb{P}[\boldsymbol{r}, -\boldsymbol{v}, t+dt|\boldsymbol{r}', -\boldsymbol{v}', t]} = \sum_{i=1}^{N} \left[\frac{m_i}{D_i} H_i^{\mathrm{ir}}(\boldsymbol{r}, \boldsymbol{v}) dv_i - \frac{1}{D_i} H_i^{\mathrm{ir}}(\boldsymbol{r}, \boldsymbol{v}) H_i^{\mathrm{rev}}(\boldsymbol{r}, \boldsymbol{v}) dt + \frac{1}{m_i} \partial_{v_i} H_i^{\mathrm{ir}}(\boldsymbol{r}, \boldsymbol{v}) dt \right]. \tag{A.6}$$

The change in the system entropy is written in Ito rules as

$$\begin{aligned} -d(\ln P(\boldsymbol{r}, \boldsymbol{v}, t)) = &- \frac{1}{P(\boldsymbol{r}, \boldsymbol{v}, t)} \partial_t P(\boldsymbol{r}, \boldsymbol{v}, t) dt - \frac{1}{P(\boldsymbol{r}, \boldsymbol{v}, t)} \sum_{i=1}^{N} \partial_{r_i} P(\boldsymbol{r}, \boldsymbol{v}, t) dr_i - \frac{1}{P(\boldsymbol{r}, \boldsymbol{v}, t)} \sum_{i=1}^{N} \partial_{v_i} P(\boldsymbol{r}, \boldsymbol{v}, t) dv_i \\ &- \sum_{i=1}^{N} \frac{D_i}{m_i^2 P(\boldsymbol{r}, \boldsymbol{v}, t)} \left[\partial_{v_i}^2 P(\boldsymbol{r}, \boldsymbol{v}, t) - \frac{1}{P(\boldsymbol{r}, \boldsymbol{v}, t)} \left(\partial_{v_i} P(\boldsymbol{r}, \boldsymbol{v}, t) \right)^2 \right]. \end{aligned} \tag{A.7}$$

Plugging Eqs. (A.6) and (A.7) into Eq. (A.3), we obtain

$$\begin{aligned} d\Delta s_{\mathrm{tot}} = &\sum_{i=1}^{N} \left[\frac{m_i}{D_i} H_i^{\mathrm{ir}}(\boldsymbol{r}, \boldsymbol{v}) dv_i - \frac{1}{D_i} H_i^{\mathrm{ir}}(\boldsymbol{r}, \boldsymbol{v}) H_i^{\mathrm{rev}}(\boldsymbol{r}, \boldsymbol{v}) dt + \frac{1}{m_i} \partial_{v_i} H_i^{\mathrm{ir}}(\boldsymbol{r}, \boldsymbol{v}) dt \right] \\ &- \frac{1}{P(\boldsymbol{r}, \boldsymbol{v}, t)} \partial_t P(\boldsymbol{r}, \boldsymbol{v}, t) dt - \frac{1}{P(\boldsymbol{r}, \boldsymbol{v}, t)} \sum_{i=1}^{N} \partial_{r_i} P(\boldsymbol{r}, \boldsymbol{v}, t) dr_i - \frac{1}{P(\boldsymbol{r}, \boldsymbol{v}, t)} \sum_{i=1}^{N} \partial_{v_i} P(\boldsymbol{r}, \boldsymbol{v}, t) dv_i \\ &- \sum_{i=1}^{N} \frac{D_i}{m_i^2 P(\boldsymbol{r}, \boldsymbol{v}, t)} \left[\partial_{v_i}^2 P(\boldsymbol{r}, \boldsymbol{v}, t) - \frac{1}{P(\boldsymbol{r}, \boldsymbol{v}, t)} \left(\partial_{v_i} P(\boldsymbol{r}, \boldsymbol{v}, t) \right)^2 \right]. \end{aligned} \tag{A.8}$$

In the steady state, i.e., $P(\boldsymbol{r}, \boldsymbol{v}, t) = P^{\mathrm{ss}}(\boldsymbol{r}, \boldsymbol{v})$, the average entropy production can be calculated as

$$\langle d\Delta s_{\mathrm{tot}} \rangle = \iint d\boldsymbol{r} d\boldsymbol{v} P^{\mathrm{ss}}(\boldsymbol{r}, \boldsymbol{v}) \langle d\Delta s_{\mathrm{tot}} | \boldsymbol{r}, \boldsymbol{v} \rangle, \tag{A.9}$$

where $\langle d\Delta s_{\mathrm{tot}} | \boldsymbol{r}, \boldsymbol{v} \rangle$ can be evaluated by replacing terms in $d\Delta s_{\mathrm{tot}}$ such that $dr_i = v_i dt$ and $m_i dv_i = H_i(\boldsymbol{r}, \boldsymbol{v}) dt$. Then, we obtain

$$\begin{aligned} \langle d\Delta s_{\mathrm{tot}} \rangle &= \sum_{i=1}^{N} \iint d\boldsymbol{r} d\boldsymbol{v} \left[\frac{1}{D_i} P^{\mathrm{ss}}(\boldsymbol{r}, \boldsymbol{v}) H_i^{\mathrm{ir}}(\boldsymbol{r}, \boldsymbol{v})^2 + \frac{P^{\mathrm{ss}}(\boldsymbol{r}, \boldsymbol{v})}{m_i} \partial_{v_i} H_i^{\mathrm{ir}}(\boldsymbol{r}, \boldsymbol{v}) - v_i \partial_{r_i} P^{\mathrm{ss}}(\boldsymbol{r}, \boldsymbol{v}) \right. \\ &\quad \left. - \frac{H_i(\boldsymbol{r}, \boldsymbol{v})}{m_i} \partial_{v_i} P^{\mathrm{ss}}(\boldsymbol{r}, \boldsymbol{v}) - \frac{D_i}{m_i^2} \partial_{v_i}^2 P^{\mathrm{ss}}(\boldsymbol{r}, \boldsymbol{v}) + \frac{D_i}{m_i^2 P^{\mathrm{ss}}(\boldsymbol{r}, \boldsymbol{v})} \left(\partial_{v_i} P^{\mathrm{ss}}(\boldsymbol{r}, \boldsymbol{v}) \right)^2 \right] dt \\ &= \sum_{i=1}^{N} \iint d\boldsymbol{r} d\boldsymbol{v} \frac{\left(H_i^{\mathrm{ir}}(\boldsymbol{r}, \boldsymbol{v}) P^{\mathrm{ss}}(\boldsymbol{r}, \boldsymbol{v}) - D_i / m_i \partial_{v_i} P^{\mathrm{ss}}(\boldsymbol{r}, \boldsymbol{v}) \right)^2}{D_i P^{\mathrm{ss}}(\boldsymbol{r}, \boldsymbol{v})} dt \\ &= \sum_{i=1}^{N} \iint d\boldsymbol{r} d\boldsymbol{v} \frac{m_i^2}{D_i} \frac{J_{v_i}^{\mathrm{ir}}(\boldsymbol{r}, \boldsymbol{v})^2}{P^{\mathrm{ss}}(\boldsymbol{r}, \boldsymbol{v})} dt, \end{aligned} \tag{A.10}$$

where $J_{v_i}^{\mathrm{ir}}(\boldsymbol{r}, \boldsymbol{v}) = 1/m_i \left[H_i^{\mathrm{ir}}(\boldsymbol{r}, \boldsymbol{v}) - D_i / m_i \partial_{v_i} \right] P^{\mathrm{ss}}(\boldsymbol{r}, \boldsymbol{v})$. Finally, the entropy production rate is given by

$$\sigma \equiv \frac{\langle d\Delta s_{\mathrm{tot}} \rangle}{dt} = \sum_{i=1}^{N} \iint d\boldsymbol{r} d\boldsymbol{v} \frac{m_i^2}{D_i} \frac{J_{v_i}^{\mathrm{ir}}(\boldsymbol{r}, \boldsymbol{v})^2}{P^{\mathrm{ss}}(\boldsymbol{r}, \boldsymbol{v})}. \tag{A.11}$$

Now, by setting

$$G_{ij}(\boldsymbol{r}) \leftarrow -\delta_{ij}\gamma_i, \quad D_i \leftarrow T_i\gamma_i, \tag{A.12}$$

the irreversible current becomes $J^{\mathrm{ir}}_{v_i}(\boldsymbol{r},\boldsymbol{v}) = -1/m_i\left[\gamma_i v_i + T_i\gamma_i/m_i\partial_{v_i}\right]P^{\mathrm{ss}}(\boldsymbol{r},\boldsymbol{v})$, and the entropy production rate reads

$$\sigma = \sum_{i=1}^{N}\iint d\boldsymbol{r}d\boldsymbol{v}\frac{m_i^2}{T_i\gamma_i}\frac{J^{\mathrm{ir}}_{v_i}(\boldsymbol{r},\boldsymbol{v})^2}{P^{\mathrm{ss}}(\boldsymbol{r},\boldsymbol{v})}. \tag{A.13}$$

A.2 Path integral

We discretize time by dividing the interval $[0,\mathcal{T}]$ into K equipartitioned intervals with a time step Δt, where $\mathcal{T} = K\Delta t$, $t^k \equiv k\Delta t$, $r_i^k \equiv r_i(t^k)$, and $v_i^k \equiv v_i(t^k)$ (superscripts denote points in a temporal sequence). Discretization of Eq. (A.1) yields

$$\begin{aligned} r_i^{k+1} - r_i^k &= v_i^k\Delta t, \\ m_i(v_i^{k+1} - v_i^k) &= H_i(r_i^k, v_i^k)\Delta t + \Delta w_i^k, \end{aligned} \tag{A.14}$$

where $\Delta w_i^k \equiv w_i^{k+1} - w_i^k = w_i(t^{k+1}) - w_i(t^k)$ is a Wiener process with the following properties:

$$\langle \Delta w_i^k\rangle = 0, \quad \langle \Delta w_i^k \Delta w_{i'}^{k'}\rangle = 2\delta_{ii'}\delta_{kk'}D_i\Delta t. \tag{A.15}$$

A stochastic trajectory $\boldsymbol{\Gamma} \equiv \left[\boldsymbol{r}^0,\boldsymbol{v}^0,\boldsymbol{r}^1,\boldsymbol{v}^1,\boldsymbol{r}^2,\boldsymbol{v}^2,\ldots,\boldsymbol{r}^K,\boldsymbol{v}^K\right]$ is specified given $\boldsymbol{\mathcal{W}} \equiv [\Delta\boldsymbol{w}^0,\Delta\boldsymbol{w}^1,\ldots,\Delta\boldsymbol{w}^{K-1}]$ and $(\boldsymbol{r}^0,\boldsymbol{v}^0)$. The probability density function of the Wiener processes $\Delta\boldsymbol{w}^k$ is given by Eq. (A.16):

$$\mathbb{P}[\boldsymbol{\mathcal{W}}] = \prod_{i=1}^{N}\prod_{k=0}^{K-1}P(\Delta w_i^k) = \prod_{i=1}^{N}\prod_{k=0}^{K-1}\frac{1}{\sqrt{4\pi D_i\Delta t}}\exp\left[-\frac{(\Delta w_i^k)^2}{4D_i\Delta t}\right]. \tag{A.16}$$

Let us change the variables in Eq. (A.16) from $\boldsymbol{\mathcal{W}} = \left[\Delta\boldsymbol{w}^0,\Delta\boldsymbol{w}^1,\ldots,\Delta\boldsymbol{w}^{K-1}\right]$ to $\boldsymbol{\mathcal{V}} = [\boldsymbol{v}^1,\boldsymbol{v}^2,\ldots,\boldsymbol{v}^K]$. From Eq. (A.14), the determinant of the Jacobian matrix is

$$\left|\frac{\partial(\boldsymbol{v}^1,\ldots,\boldsymbol{v}^K)}{\partial(\Delta\boldsymbol{w}^0,\ldots,\Delta\boldsymbol{w}^{K-1})}\right| = \prod_{i=1}^{N}\prod_{k=0}^{K-1}\frac{1}{m_i}, \tag{A.17}$$

given that the determinant of triangular matrices is a product of their diagonal elements. Using Eqs. (A.14), (A.16), and (A.17), we obtain

$$\mathbb{P}[\boldsymbol{\Gamma}|\boldsymbol{r}^0,\boldsymbol{v}^0] = \left(\prod_{i=1}^{N}\prod_{k=0}^{K-1}\frac{m_i}{\sqrt{4\pi D_i\Delta t}}\right)\exp\left[-\sum_{i=1}^{N}\frac{\Delta t}{4D_i}\sum_{k=0}^{K-1}\left(\frac{m_i(v_i^{k+1}-v_i^k)}{\Delta t} - H_i(r_i^k,v_i^k)\right)^2\right]. \tag{A.18}$$

In the limit $K\to\infty$, we obtain the path integral in Eq. (A.19).

$$\mathbb{P}[\boldsymbol{\Gamma}|\boldsymbol{r}^0,\boldsymbol{v}^0] = \mathcal{N}\prod_{i=1}^{N}\exp\left[-\frac{1}{4D_i}\int_0^{\mathcal{T}}dt\,(m_i\dot{v}_i - H_i(\boldsymbol{r},\boldsymbol{v}))^2\right] \tag{A.19}$$

By substituting such that $D_i = T_i\gamma_i$ and $H_i(\boldsymbol{r},\boldsymbol{v}) = -\gamma_i v_i + F_i(\boldsymbol{r})$, we have

$$\mathbb{P}[\boldsymbol{\Gamma}|\boldsymbol{r}^0,\boldsymbol{v}^0] = \mathcal{N}\prod_{i=1}^{N}\exp\left[-\frac{1}{4T_i\gamma_i}\int_0^{\mathcal{T}} dt\,(m_i\dot{v}_i + \gamma_i v_i - F_i(\boldsymbol{r}))^2\right]. \tag{A.20}$$

The path integral in Eq. (A.19) is a continuous limit of the Ito sum, which can be transformed to a Stratonovich integral via the following rule:

$$\int_0^{\mathcal{T}} dt\ \dot{v}_i \cdot H_i(\boldsymbol{r},\boldsymbol{v}) = \int_0^{\mathcal{T}} dt\ \dot{v}_i \circ H_i(\boldsymbol{r},\boldsymbol{v}) - \frac{D_i}{m_i^2}\int_0^{\mathcal{T}} dt\ \partial_{v_i}H_i(\boldsymbol{r},\boldsymbol{v}), \tag{A.21}$$

where $\cdot$ and $\circ$ denote the Ito and Stratonovich products, respectively. The path integral using the mid-point discretization is then expressed as

$$\mathbb{P}[\boldsymbol{\Gamma}|\boldsymbol{r}^0,\boldsymbol{v}^0] = \mathcal{N}\prod_{i=1}^{N}\exp\left[-\frac{1}{4D_i}\int_0^{\mathcal{T}} dt\left\{(m_i\dot{v}_i - H_i(\boldsymbol{r},\boldsymbol{v}))^2 + \frac{2D_i}{m_i}\partial_{v_i}H_i(\boldsymbol{r},\boldsymbol{v})\right\}\right]. \tag{A.22}$$

For one-dimensional underdamped dynamics

$$\dot{r} = v, \quad m\dot{v} = -\gamma v + F(r) + \xi(t), \tag{A.23}$$

the path probability written as the Stratonovich integral becomes

$$\mathbb{P}[\boldsymbol{\Gamma}|r^0,v^0] = \mathcal{N}\exp\left(\frac{\mathcal{T}\gamma}{2m}\right)\exp\left[-\frac{1}{4T\gamma}\int_0^{\mathcal{T}} dt\,(m\dot{v} + \gamma v - F(r))^2\right], \tag{A.24}$$

which is consistent with the result in Ref. [107].

A.3 Bound on the fluctuation of currents

Let $P^{\rm ss}(\boldsymbol{r},\boldsymbol{v})$ be the steady-state distribution of the original dynamics. Now, we consider the following auxiliary dynamics

$$\dot{r}_i = v_i,\ m_i\dot{v}_i = H_{i,\theta}(\boldsymbol{r},\boldsymbol{v}) + \xi_i, \tag{A.25}$$

where

$$H_{i,\theta}(\boldsymbol{r},\boldsymbol{v}) = (1+\theta)\sum_{j=1}^{N} v_j G_{ij}(\boldsymbol{r}) + (1+\theta)^2 F_i(\boldsymbol{r}) + \frac{D_i}{m_i}(1-(1+\theta)^3)\frac{\partial_{v_i}P^{\rm ss}(\boldsymbol{r},\boldsymbol{v}/(1+\theta))}{P^{\rm ss}(\boldsymbol{r},\boldsymbol{v}/(1+\theta))}. \tag{A.26}$$

We note that when $\theta = 0$, $H_{i,\theta}(\boldsymbol{r},\boldsymbol{v}) = \sum_{j=1}^{N} v_j G_{ij}(\boldsymbol{r}) + F_i(\boldsymbol{r})$ and the auxiliary dynamics become the original ones. The corresponding Kramers equation of this dynamics is

$$\partial_t P_\theta(\boldsymbol{r},\boldsymbol{v},t) = \sum_{i=1}^{N}\left[-\partial_{r_i}J_{r_i,\theta}(\boldsymbol{r},\boldsymbol{v},t) - \partial_{v_i}J_{v_i,\theta}(\boldsymbol{r},\boldsymbol{v},t)\right], \tag{A.27}$$

where

$$J_{r_i,\theta}(\boldsymbol{r},\boldsymbol{v},t) = v_i P_\theta(\boldsymbol{r},\boldsymbol{v},t),\ J_{v_i,\theta}(\boldsymbol{r},\boldsymbol{v},t) = 1/m_i \left[H_{i,\theta}(\boldsymbol{r},\boldsymbol{v}) - D_i/m_i \partial_{v_i}\right] P_\theta(\boldsymbol{r},\boldsymbol{v},t). \quad \text{(A.28)}$$

It can be easily proven that the steady-state distribution of the auxiliary dynamics is $P^{\rm ss}_\theta(\boldsymbol{r},\boldsymbol{v}) = P^{\rm ss}(\boldsymbol{r},\boldsymbol{v}/(1+\theta))/(1+\theta)^N$. Since $\langle\Theta\rangle_\theta = (1+\theta)\langle\Theta\rangle \Rightarrow \partial_\theta\langle\Theta\rangle_\theta = \langle\Theta\rangle$, the Cramér-Rao inequality when letting $\theta = 0$ reads

$$\frac{\mathrm{Var}[\Theta]}{\langle\Theta\rangle^2} \geq \frac{1}{\mathcal{I}(0)}. \quad \text{(A.29)}$$

The Fisher information can be calculated as

$$\mathcal{I}(0) = -\left\langle \partial_\theta^2 \ln P^{\rm ss}_\theta(\boldsymbol{r}^0,\boldsymbol{v}^0)\right\rangle_{\theta=0} + \frac{1}{2}\left\langle \int_0^{\mathcal{T}} dt \sum_{i=1}^N \frac{1}{D_i}\left(\partial_\theta H_{i,\theta}(\boldsymbol{r},\boldsymbol{v})\right)^2\right\rangle_{\theta=0} \quad \text{(A.30)}$$

$$= \left\langle \left[\partial_\theta \ln P^{\rm ss}_\theta(\boldsymbol{r}^0,\boldsymbol{v}^0)\right]^2\right\rangle_{\theta=0} + \frac{\mathcal{T}}{2}\sum_{i=1}^N \frac{1}{D_i}\left\langle \left(\partial_\theta H_{i,\theta}(\boldsymbol{r},\boldsymbol{v})\right)^2\right\rangle_{\theta=0} \quad \text{(A.31)}$$

$$= \left\langle \left[\partial_\theta \ln P^{\rm ss}_\theta(\boldsymbol{r}^0,\boldsymbol{v}^0)\right]^2\right\rangle_{\theta=0} + \frac{\mathcal{T}}{2}\sum_{i=1}^N \frac{1}{D_i}\left\langle \left(\sum_{j=1}^N v_j G_{ij}(\boldsymbol{r}) + 2F_i(\boldsymbol{r}) - 3\frac{D_i}{m_i}\frac{\partial_{v_i}P^{\rm ss}(\boldsymbol{r},\boldsymbol{v})}{P^{\rm ss}(\boldsymbol{r},\boldsymbol{v})}\right)^2\right\rangle \quad \text{(A.32)}$$

$$= \left\langle \left[\partial_\theta \ln P^{\rm ss}_\theta(\boldsymbol{r}^0,\boldsymbol{v}^0)\right]^2\right\rangle_{\theta=0} + \frac{\mathcal{T}}{2}\sum_{i=1}^N \frac{1}{D_i}\left\langle 4\left(F_i(\boldsymbol{r}) - \sum_{j=1}^N v_j G_{ij}(\boldsymbol{r})\right)^2 + 9m_i^2\left(\frac{J^{\rm ir}_{v_i}(\boldsymbol{r},\boldsymbol{v})}{P^{\rm ss}(\boldsymbol{r},\boldsymbol{v})}\right)^2 + 12 m_i \frac{J^{\rm ir}_{v_i}(\boldsymbol{r},\boldsymbol{v})}{P^{\rm ss}(\boldsymbol{r},\boldsymbol{v})}\left(F_i(\boldsymbol{r}) - \sum_{j=1}^N v_j G_{ij}(\boldsymbol{r})\right)\right\rangle. \quad \text{(A.33)}$$

In Eq. (A.33), we used the relation that $J^{\rm ir}_{v_i}(\boldsymbol{r},\boldsymbol{v}) = 1/m_i\left[\sum_{j=1}^N v_j G_{ij}(\boldsymbol{r}) P^{\rm ss}(\boldsymbol{r},\boldsymbol{v}) - D_i/m_i \partial_{v_i} P^{\rm ss}(\boldsymbol{r},\boldsymbol{v})\right]$. Now, we transform each term in $\mathcal{I}(0)$. The first term, which is a boundary value, can be evaluated as

$$\left\langle \left[\partial_\theta \ln P^{\rm ss}_\theta(\boldsymbol{r}^0,\boldsymbol{v}^0)\right]^2\right\rangle_{\theta=0} = \left\langle \left(\sum_{i=1}^N v_i \partial_{v_i} P^{\rm ss}(\boldsymbol{r},\boldsymbol{v})/P^{\rm ss}(\boldsymbol{r},\boldsymbol{v})\right)^2\right\rangle - N^2. \quad \text{(A.34)}$$

The second term in $\mathcal{I}(0)$ can be transformed as

$$\left\langle \left(F_i(\boldsymbol{r}) - \sum_{j=1}^N v_j G_{ij}(\boldsymbol{r})\right)^2\right\rangle = \langle F_i(\boldsymbol{r})^2\rangle + \left\langle \left(\sum_{j=1}^N v_j G_{ij}(\boldsymbol{r})\right)^2\right\rangle - 2\sum_{j=1}^N \langle v_j F_i(\boldsymbol{r}) G_{ij}(\boldsymbol{r})\rangle. \quad \text{(A.35)}$$

The third term is equal to the entropy production rate

$$\sum_{i=1}^N \frac{m_i^2}{D_i}\left\langle \left(\frac{J^{\rm ir}_{v_i}(\boldsymbol{r},\boldsymbol{v})}{P^{\rm ss}(\boldsymbol{r},\boldsymbol{v})}\right)^2\right\rangle = \sum_{i=1}^N \iint d\boldsymbol{r}d\boldsymbol{v}\frac{m_i^2}{D_i}\frac{J^{\rm ir}_{v_i}(\boldsymbol{r},\boldsymbol{v})^2}{P^{\rm ss}(\boldsymbol{r},\boldsymbol{v})} = \sigma. \quad \text{(A.36)}$$

The last term can be calculated as

$$\left\langle \frac{m_i J_{v_i}^{\mathrm{ir}}(\boldsymbol{r},\boldsymbol{v})}{P^{\mathrm{ss}}(\boldsymbol{r},\boldsymbol{v})}\left(F_i(\boldsymbol{r})-\sum_{j=1}^{N} v_j G_{ij}(\boldsymbol{r})\right)\right\rangle = \sum_{j=1}^{N}\langle v_j F_i(\boldsymbol{r}) G_{ij}(\boldsymbol{r})\rangle - \left\langle\left(\sum_{j=1}^{N} v_j G_{ij}(\boldsymbol{r})\right)^2\right\rangle - \frac{D_i}{m_i}\langle G_{ii}(\boldsymbol{r})\rangle. \tag{A.37}$$

Collecting the terms in Eqs. (A.34)–(A.37), we can rewritte $\mathcal{I}(0)$ as

$$\mathcal{I}(0) = \frac{1}{2}\left[\mathcal{T}(9\sigma + 4\Upsilon) + \Omega\right], \tag{A.38}$$

where

$$\Upsilon = \sum_{i=1}^{N}\frac{1}{D_i}\left(\langle F_i(\boldsymbol{r})^2\rangle - 2\left\langle\left(\sum_{j=1}^{N} v_j G_{ij}(\boldsymbol{r})\right)^2\right\rangle + \sum_{j=1}^{N}\langle v_j F_i(\boldsymbol{r}) G_{ij}(\boldsymbol{r})\rangle - \frac{3D_i}{m_i}\langle G_{ii}(\boldsymbol{r})\rangle\right), \tag{A.39}$$

$$\Omega = 2\left\langle\left(\sum_{i=1}^{N} v_i \partial_{v_i} P^{\mathrm{ss}}(\boldsymbol{r},\boldsymbol{v})/P^{\mathrm{ss}}(\boldsymbol{r},\boldsymbol{v})\right)^2\right\rangle - 2N^2. \tag{A.40}$$

The bound in Eq. (A.29) then becomes

$$\frac{\mathrm{Var}[\Theta]}{\langle\Theta\rangle^2} \geq \frac{2}{\mathcal{T}(9\sigma + 4\Upsilon) + \Omega}. \tag{A.41}$$

Now, by substituting $G_{ij}(\boldsymbol{r}) = -\delta_{ij}\gamma_i$ and $D_i = T_i\gamma_i$ into Υ, we have

$$\Upsilon = \sum_{i=1}^{N}\frac{1}{T_i\gamma_i}\left(\langle F_i(\boldsymbol{r})^2\rangle - 2\gamma_i^2\langle v_i^2\rangle - \gamma_i\langle v_i F_i(\boldsymbol{r})\rangle + \frac{3T_i\gamma_i^2}{m_i}\right). \tag{A.42}$$

Since

$$\langle v_i F_i(\boldsymbol{r})\rangle = \gamma_i\langle v_i^2\rangle - \frac{T_i\gamma_i}{m_i}, \tag{A.43}$$

Υ can be further simplified as

$$\Upsilon = \sum_{i=1}^{N}\left(\frac{1}{T_i\gamma_i}\langle F_i(\boldsymbol{r})^2\rangle - 3\frac{\gamma_i}{T_i}\langle v_i^2\rangle + 4\frac{\gamma_i}{m_i}\right). \tag{A.44}$$

Finally, we obtain the bound

$$\frac{\mathrm{Var}[\Theta]}{\langle\Theta\rangle^2} \geq \frac{2}{\Sigma}, \tag{A.45}$$

where $\Sigma = \mathcal{T}(9\sigma + 4\Upsilon) + \Omega$.

A.4 Equality condition of the derived bound

The equality condition of the derived bound is that the following relation,

$$\partial_\theta \ln \mathbb{P}_\theta[\boldsymbol{\Gamma}]|_{\theta=0} = \mu\left[\Theta[\boldsymbol{\Gamma}] - \psi(0)\right], \tag{A.46}$$

holds for an arbitrary trajectory $\mathbf{\Gamma}$. Using the formula of the path integral, we have

$$\begin{aligned}
\partial_\theta \ln \mathbb{P}_\theta[\mathbf{\Gamma}]|_{\theta=0} &= \partial_\theta \ln P^{\mathrm{ss}}_\theta(\boldsymbol{r}^0,\boldsymbol{v}^0)\big|_{\theta=0} + \sum_{i=1}^N \frac{1}{2D_i}\int_0^{\mathcal{T}} dt\, \partial_\theta H_{i,\theta}\left(\dot{v}_i - H_{i,\theta}\right)\Big|_{\theta=0} \\
&= -N - \sum_{i=1}^N \frac{v_i^0 \partial_{v_i} P^{\mathrm{ss}}(\boldsymbol{r}^0,\boldsymbol{v}^0)}{P^{\mathrm{ss}}(\boldsymbol{r}^0,\boldsymbol{v}^0)} \\
&\quad + \sum_{i=1}^N \frac{1}{2D_i}\int_0^{\mathcal{T}} dt \left(-\gamma_i v_i + 2F_i(\boldsymbol{r}) - \frac{3D_i}{m_i}\frac{\partial_{v_i} P^{\mathrm{ss}}(\boldsymbol{r},\boldsymbol{v})}{P^{\mathrm{ss}}(\boldsymbol{r},\boldsymbol{v})}\right)\cdot\left(m_i\dot{v}_i + \gamma_i v_i - F_i(\boldsymbol{r})\right) \\
&= -N - \sum_{i=1}^N \frac{v_i^0 \partial_{v_i} P^{\mathrm{ss}}(\boldsymbol{r}^0,\boldsymbol{v}^0)}{P^{\mathrm{ss}}(\boldsymbol{r}^0,\boldsymbol{v}^0)} + \sum_{i=1}^N \frac{1}{2m_i}\int_0^{\mathcal{T}} dt \left(\gamma_i + \frac{3D_i}{m_i}\partial_{v_i}\left(\frac{\partial_{v_i} P^{\mathrm{ss}}(\boldsymbol{r},\boldsymbol{v})}{P^{\mathrm{ss}}(\boldsymbol{r},\boldsymbol{v})}\right)\right) \\
&\quad + \sum_{i=1}^N \frac{1}{2D_i}\int_0^{\mathcal{T}} dt \left(-\gamma_i v_i + 2F_i(\boldsymbol{r}) - \frac{3D_i}{m_i}\frac{\partial_{v_i} P^{\mathrm{ss}}(\boldsymbol{r},\boldsymbol{v})}{P^{\mathrm{ss}}(\boldsymbol{r},\boldsymbol{v})}\right)\circ\left(m_i\dot{v}_i + \gamma_i v_i - F_i(\boldsymbol{r})\right).
\end{aligned} \tag{A.47}$$

Therefore, Eq. (A.46) is equivalent with

$$\begin{aligned}
&-N - \sum_{i=1}^N \frac{v_i^0 \partial_{v_i} P^{\mathrm{ss}}(\boldsymbol{r}^0,\boldsymbol{v}^0)}{P^{\mathrm{ss}}(\boldsymbol{r}^0,\boldsymbol{v}^0)} + \sum_{i=1}^N \frac{1}{2D_i}\int_0^{\mathcal{T}} dt \left(-\gamma_i v_i + 2F_i(\boldsymbol{r}) - \frac{3D_i}{m_i}\frac{\partial_{v_i} P^{\mathrm{ss}}(\boldsymbol{r},\boldsymbol{v})}{P^{\mathrm{ss}}(\boldsymbol{r},\boldsymbol{v})}\right)\circ\left(m_i\dot{v}_i + \gamma_i v_i - F_i(\boldsymbol{r})\right) \\
&= \mu\left[\int_0^{\mathcal{T}} dt\, \mathbf{\Lambda}(\boldsymbol{r})^\top \circ \dot{\boldsymbol{r}} - \psi(0)\right] - \sum_{i=1}^N \frac{1}{2m_i}\int_0^{\mathcal{T}} dt \left(\gamma_i + \frac{3D_i}{m_i}\partial_{v_i}\left(\frac{\partial_{v_i} P^{\mathrm{ss}}(\boldsymbol{r},\boldsymbol{v})}{P^{\mathrm{ss}}(\boldsymbol{r},\boldsymbol{v})}\right)\right).
\end{aligned} \tag{A.48}$$

Since the left-hand side of Eq. (A.48) contains $\dot{\boldsymbol{v}}$ while the right-hand side does not, Eq. (A.48) only holds for all trajectories when the term $\dot{\boldsymbol{v}}$ disappears, i.e., when

$$-\gamma_i v_i + 2F_i(\boldsymbol{r}) - 3\frac{D_i}{m_i}\frac{\partial_{v_i} P^{\mathrm{ss}}(\boldsymbol{r},\boldsymbol{v})}{P^{\mathrm{ss}}(\boldsymbol{r},\boldsymbol{v})} = 0 \tag{A.49}$$

for all $\boldsymbol{r},\boldsymbol{v}$. Consequently, Eq. (A.48) becomes

$$-N - \sum_{i=1}^N \frac{v_i^0 \partial_{v_i} P^{\mathrm{ss}}(\boldsymbol{r}^0,\boldsymbol{v}^0)}{P^{\mathrm{ss}}(\boldsymbol{r}^0,\boldsymbol{v}^0)} = \mu\left[\int_0^{\mathcal{T}} dt\, \mathbf{\Lambda}(\boldsymbol{r})^\top \circ \dot{\boldsymbol{r}} - \psi(0)\right] - \sum_{i=1}^N \frac{1}{2m_i}\int_0^{\mathcal{T}} dt \left(\gamma_i + \frac{3D_i}{m_i}\partial_{v_i}\left(\frac{\partial_{v_i} P^{\mathrm{ss}}(\boldsymbol{r},\boldsymbol{v})}{P^{\mathrm{ss}}(\boldsymbol{r},\boldsymbol{v})}\right)\right). \tag{A.50}$$

Now, we take the partial derivative of both sides of Eq. (A.49) with respect to v_i to obtain

$$\gamma_i + \frac{3D_i}{m_i}\partial_{v_i}\left(\frac{\partial_{v_i} P^{\mathrm{ss}}(\boldsymbol{r},\boldsymbol{v})}{P^{\mathrm{ss}}(\boldsymbol{r},\boldsymbol{v})}\right) = 0. \tag{A.51}$$

Using Eq. (A.51), we can simplify Eq. (A.50) to be

$$-N - \sum_{i=1}^N \frac{m_i}{3D_i} v_i^0\left(-\gamma_i v_i^0 + 2F_i(\boldsymbol{r}^0)\right) = \mu\left[\int_0^{\mathcal{T}} dt\, \mathbf{\Lambda}(\boldsymbol{r})^\top \circ \dot{\boldsymbol{r}} - \psi(0)\right]. \tag{A.52}$$

As can be seen, the term in the left-hand side of Eq. (A.52) is only dependent on the initial point of the trajectory, $[\boldsymbol{r}^0,\boldsymbol{v}^0]$, while the term in the right-hand side depends entirely on the trajectory $\mathbf{\Gamma}$. Therefore, Eq. (A.52) does not hold for all trajectories, thus implying that the equality condition of the derived bound cannot be attained.

A.5 Multidimensional TUR

A.5.1 Derivation of Eq. (4.17)

Following Ref. [270], here we show a proof of Eq. (4.17). First, noticing that

$$\partial_\theta \langle \boldsymbol{\Theta} \rangle_\theta = \partial_\theta \int \mathcal{D}\boldsymbol{\Gamma}\, \mathbb{P}_\theta[\boldsymbol{\Gamma}]\boldsymbol{\Theta}[\boldsymbol{\Gamma}] = \int \mathcal{D}\boldsymbol{\Gamma}\, \mathbb{P}_\theta[\boldsymbol{\Gamma}]\boldsymbol{\Theta}[\boldsymbol{\Gamma}]\partial_\theta \ln \mathbb{P}_\theta[\boldsymbol{\Gamma}] = \mathbb{E}[\boldsymbol{\Theta}[\boldsymbol{\Gamma}]\partial_\theta \ln \mathbb{P}_\theta[\boldsymbol{\Gamma}]], \tag{A.53}$$

where $\mathbb{E}[\cdot]$ denotes the average taken over all possible trajectories. Since $\mathbb{E}[\partial_\theta \ln \mathbb{P}_\theta[\boldsymbol{\Gamma}]] = \partial_\theta \int \mathcal{D}\boldsymbol{\Gamma}\, \mathbb{P}_\theta[\boldsymbol{\Gamma}] = 0$, Eq. (A.53) can be written

$$\partial_\theta \langle \boldsymbol{\Theta} \rangle_\theta = \mathrm{Cov}[\boldsymbol{\Theta};\, \partial_\theta \ln \mathbb{P}_\theta]. \tag{A.54}$$

Now, consider the following vector:

$$\begin{pmatrix} \boldsymbol{\Theta}[\boldsymbol{\Gamma}] \\ \partial_\theta \ln \mathbb{P}_\theta[\boldsymbol{\Gamma}] \end{pmatrix} \in \mathbb{R}^{(M+1)\times 1}, \tag{A.55}$$

whose covariance matrix,

$$\begin{pmatrix} \mathrm{Cov}[\boldsymbol{\Theta}] & \mathrm{Cov}[\boldsymbol{\Theta};\, \partial_\theta \ln \mathbb{P}_\theta] \\ \mathrm{Cov}[\boldsymbol{\Theta};\, \partial_\theta \ln \mathbb{P}_\theta]^\top & \mathrm{Cov}[\partial_\theta \ln \mathbb{P}_\theta] \end{pmatrix}, \tag{A.56}$$

is positive semi-definte and is equal to

$$\begin{pmatrix} \mathrm{Cov}[\boldsymbol{\Theta}] & \partial_\theta \langle \boldsymbol{\Theta} \rangle_\theta \\ \partial_\theta \langle \boldsymbol{\Theta} \rangle_\theta^\top & \mathcal{I}(\theta) \end{pmatrix}. \tag{A.57}$$

Using the fact that if a matrix $\boldsymbol{X}$ is positive semi-definte, then so is $\boldsymbol{Y}^\top \boldsymbol{X} \boldsymbol{Y}$, we have that

$$\begin{pmatrix} \boldsymbol{I} & -\mathcal{I}(\theta)^{-1}\partial_\theta \langle \boldsymbol{\Theta} \rangle_\theta \end{pmatrix} \begin{pmatrix} \mathrm{Cov}[\boldsymbol{\Theta}] & \partial_\theta \langle \boldsymbol{\Theta} \rangle_\theta \\ \partial_\theta \langle \boldsymbol{\Theta} \rangle_\theta^\top & \mathcal{I}(\theta) \end{pmatrix} \begin{pmatrix} \boldsymbol{I} \\ -\mathcal{I}(\theta)^{-1}\partial_\theta \langle \boldsymbol{\Theta} \rangle_\theta^\top \end{pmatrix} \tag{A.58}$$

is also positive semi-definite, where $\boldsymbol{I} \in \mathbb{R}^{M\times M}$ is the identity matrix. After performing some matrix multiplications in Eq. (A.58), we obtain that the matrix

$$\mathrm{Cov}[\boldsymbol{\Theta}] - \mathcal{I}(\theta)^{-1}\partial_\theta \langle \boldsymbol{\Theta} \rangle_\theta \partial_\theta \langle \boldsymbol{\Theta} \rangle_\theta^\top \tag{A.59}$$

is positive semi-definite, i.e., $\mathrm{Cov}[\boldsymbol{\Theta}] \geq \mathcal{I}(\theta)^{-1}\partial_\theta \langle \boldsymbol{\Theta} \rangle_\theta \partial_\theta \langle \boldsymbol{\Theta} \rangle_\theta^\top$.

A.5.2 Derivation of Eq. (4.20)

By substituting $\boldsymbol{x} = \langle \boldsymbol{\Theta} \rangle$ into $\boldsymbol{x}^\top \left(\mathrm{Cov}[\boldsymbol{\Theta}] - 2\langle \boldsymbol{\Theta} \rangle \langle \boldsymbol{\Theta} \rangle^\top / \Sigma\right)^{-1} \boldsymbol{x} \geq 0$, we have

$$\langle \boldsymbol{\Theta} \rangle^\top \left(\mathrm{Cov}[\boldsymbol{\Theta}] - 2\langle \boldsymbol{\Theta} \rangle \langle \boldsymbol{\Theta} \rangle^\top / \Sigma\right)^{-1} \langle \boldsymbol{\Theta} \rangle \geq 0. \tag{A.60}$$

Using the Sherman–Morrison formula,

$$(\boldsymbol{A}+\boldsymbol{u}\boldsymbol{v}^{\top})^{-1}=\boldsymbol{A}^{-1}-\frac{\boldsymbol{A}^{-1}\boldsymbol{u}\boldsymbol{v}^{\top}\boldsymbol{A}^{-1}}{1+\boldsymbol{v}^{\top}\boldsymbol{A}^{-1}\boldsymbol{u}}, \tag{A.61}$$

where $\boldsymbol{A}\in\mathbb{R}^{n\times n}$ and $\boldsymbol{u},\boldsymbol{v}\in\mathbb{R}^{n}$, Eq. (A.60) can be transformed as follows:

$$\begin{aligned}\langle\boldsymbol{\Theta}\rangle^{\top}\left(\mathrm{Cov}[\boldsymbol{\Theta}]-2\langle\boldsymbol{\Theta}\rangle\langle\boldsymbol{\Theta}\rangle^{\top}/\Sigma\right)^{-1}\langle\boldsymbol{\Theta}\rangle=&\langle\boldsymbol{\Theta}\rangle^{\top}\left(\mathrm{Cov}[\boldsymbol{\Theta}]^{-1}+\frac{2\mathrm{Cov}[\boldsymbol{\Theta}]^{-1}\langle\boldsymbol{\Theta}\rangle\langle\boldsymbol{\Theta}\rangle^{\top}\mathrm{Cov}[\boldsymbol{\Theta}]^{-1}/\Sigma}{1-2\langle\boldsymbol{\Theta}\rangle^{\top}\mathrm{Cov}[\boldsymbol{\Theta}]^{-1}\langle\boldsymbol{\Theta}\rangle/\Sigma}\right)\langle\boldsymbol{\Theta}\rangle\\ =&z+\frac{2z^{2}/\Sigma}{1-2z/\Sigma}\geq 0,\quad \left(z=\langle\boldsymbol{\Theta}\rangle^{\top}\mathrm{Cov}[\boldsymbol{\Theta}]^{-1}\langle\boldsymbol{\Theta}\rangle\geq 0\right)\\ \Leftrightarrow&\ 1-2z/\Sigma\geq 0\\ \Leftrightarrow&\ \langle\boldsymbol{\Theta}\rangle^{\top}\mathrm{Cov}[\boldsymbol{\Theta}]^{-1}\langle\boldsymbol{\Theta}\rangle\leq\frac{\Sigma}{2}.\end{aligned} \tag{A.62}$$

A.6 TUR for active matter systems

The dynamics in Eq. (4.24) can be obtained from Eq. (A.1) by plugging $m_i\leftarrow\tau$, $G_{ij}(\boldsymbol{r})\leftarrow-\delta_{ij}-\tau\mu\partial^{2}_{r_ir_j}\Phi(\boldsymbol{r})$, $F_i(\boldsymbol{r})\leftarrow-\mu\partial_{r_i}\Phi(\boldsymbol{r})$. According to Eq. (A.41), we have

$$\frac{\mathrm{Var}[\Theta]}{\langle\Theta\rangle^{2}}\geq\frac{2}{\mathcal{T}(9\sigma+4\Upsilon_a)+\Omega}, \tag{A.63}$$

where Ω is defined as in Eq. (A.40) and Υ_a is given by

$$\Upsilon_a=\sum_{i=1}^{N}\frac{1}{D_i}\left(\langle F_i(\boldsymbol{r})^{2}\rangle-2\left\langle\left(\sum_{j=1}^{N}v_jG_{ij}(\boldsymbol{r})\right)^{2}\right\rangle+\sum_{j=1}^{N}\langle v_jF_i(\boldsymbol{r})G_{ij}(\boldsymbol{r})\rangle-\frac{3D_i}{m_i}\langle G_{ii}(\boldsymbol{r})\rangle\right). \tag{A.64}$$

In the steady state, we have

$$\begin{aligned}0=&\sum_{i=1}^{N}\left[\partial_{r_i}J^{\mathrm{ss}}_{r_i}(\boldsymbol{r},\boldsymbol{v})+\partial_{v_i}J^{\mathrm{ss}}_{v_i}(\boldsymbol{r},\boldsymbol{v})\right]\\ =&\sum_{i=1}^{N}\left[\partial_{r_i}\left[v_iP^{\mathrm{ss}}(\boldsymbol{r},\boldsymbol{v})\right]+\frac{1}{m_i}\partial_{v_i}\left[\sum_{j=1}^{N}v_jG_{ij}(\boldsymbol{r})P^{\mathrm{ss}}(\boldsymbol{r},\boldsymbol{v})\right]+\frac{1}{m_i}\partial_{v_i}\left[F_i(\boldsymbol{r})P^{\mathrm{ss}}(\boldsymbol{r},\boldsymbol{v})\right]-\frac{D_i}{m_i^{2}}\partial^{2}_{v_i}P^{\mathrm{ss}}(\boldsymbol{r},\boldsymbol{v})\right].\end{aligned} \tag{A.65}$$

Using the relation in Eq. (A.65) and taking integration by parts, we obtain for $i\neq j$

$$\langle v_jF_i(\boldsymbol{r})G_{ij}(\boldsymbol{r})\rangle=-m_i\sum_{k}\left\langle v_iv_k\partial_{r_k}F_i(\boldsymbol{r})\right\rangle-\sum_{l\neq j}\langle v_lF_i(\boldsymbol{r})G_{il}(\boldsymbol{r})\rangle-\langle F_i(\boldsymbol{r})^{2}\rangle. \tag{A.66}$$

Hence,

$$\sum_{j=1}^{N}\langle v_jF_i(\boldsymbol{r})G_{ij}(\boldsymbol{r})\rangle=-\langle F_i(\boldsymbol{r})^{2}\rangle-m_i\sum_{j=1}^{N}\left\langle v_iv_j\partial_{r_j}F_i(\boldsymbol{r})\right\rangle. \tag{A.67}$$

By plugging Eq. (A.67) into Eq. (A.64), we have

$$\Upsilon_a = -\sum_{i=1}^{N} \frac{1}{D_i}\left(m_i \sum_{j=1}^{N} \left\langle v_i v_j \partial_{r_j} F_i(\boldsymbol{r}) \right\rangle + 2\left\langle \left(\sum_{j=1}^{N} v_j G_{ij}(\boldsymbol{r}) \right)^2 \right\rangle + \frac{3D_i}{m_i} \langle G_{ii}(\boldsymbol{r}) \rangle \right). \tag{A.68}$$

Next, substituting $m_i \leftarrow \tau,\ G_{ij}(\boldsymbol{r}) \leftarrow -\delta_{ij} - \tau\mu\partial^2_{r_i r_j}\Phi(\boldsymbol{r}),\ F_i(\boldsymbol{r}) \leftarrow -\mu\partial_{r_i}\Phi(\boldsymbol{r})$ into Eq. (A.68), we obtain

$$\Upsilon_a = \sum_{i=1}^{N} \frac{1}{D_i}\left\langle \tau\mu \sum_{j=1}^{N} v_i v_j \partial^2_{r_i r_j}\Phi(\boldsymbol{r}) - 2\left(\sum_{j=1}^{N} v_j \left[\delta_{ij} + \tau\mu\partial^2_{r_i r_j}\Phi(\boldsymbol{r}) \right] \right)^2 + \frac{3D_i}{\tau}\left(1 + \tau\mu\partial^2_{r_i}\Phi(\boldsymbol{r})\right) \right\rangle. \tag{A.69}$$

The TUR for the active matter system is then given as follows:

$$\frac{\mathrm{Var}[\Theta]}{\langle\Theta\rangle^2} \geq \frac{2}{\Sigma}, \tag{A.70}$$

where $\Sigma = \mathcal{T}(9\sigma + 4\Upsilon_a) + \Omega$.

Appendix B

Appendix B

B.1 Derivation of the bounds for a full system

To obtain Eqs. (4.28) and (4.30), we employ information-theoretic inequality with the perturbation technique [24]. We modify the force in the original system with a perturbation parameter θ and obtain new auxiliary dynamics. For a given trajectory Γ, let $\mathcal{P}_\theta(\Gamma)$ denote the path probability of observing Γ in the auxiliary dynamics. According to the Cramér–Rao inequality [33], the precision of the observable ϕ is bounded by the Fisher information as

$$\frac{(\partial_\theta \langle \phi \rangle_\theta)^2}{\langle\langle \phi \rangle\rangle_\theta} \leq \mathcal{I}(\theta). \tag{B.1}$$

Here, $\mathcal{I}(\theta) := \langle (\partial_\theta \ln \mathcal{P}_\theta(\Gamma))^2 \rangle_\theta = -\langle \partial_\theta^2 \ln \mathcal{P}_\theta(\Gamma) \rangle_\theta$ is the Fisher information. Inequality (B.1) can be proven by applying the Cauchy–Schwarz inequality to $(\partial_\theta \langle \phi \rangle_\theta)^2$ as follows:

$$\begin{aligned}
(\partial_\theta \langle \phi \rangle_\theta)^2 &= \left(\partial_\theta \int \mathcal{D}\Gamma \, \mathcal{P}_\theta(\Gamma) \phi(\Gamma) \right)^2 \\
&= \left(\int \mathcal{D}\Gamma \, \mathcal{P}_\theta(\Gamma) (\phi(\Gamma) - \langle \phi \rangle_\theta) \partial_\theta \ln \mathcal{P}_\theta(\Gamma) \right)^2 \\
&\leq \langle\langle \phi \rangle\rangle_\theta \, \mathcal{I}(\theta).
\end{aligned} \tag{B.2}$$

For overdamped systems, we consider the auxiliary dynamics, $\dot{x} = H_\theta(x,t) + \xi$, where

$$H_\theta(x,t) = \theta F(x/\theta, \lambda) + D(1-\theta^2) \frac{\partial_x \rho(x/\theta, t)}{\rho(x/\theta, t)}. \tag{B.3}$$

Analogously, for underdamped systems, the dynamics are modified as $m\dot{v} = H_\theta(x,v,t) + \xi$, where

$$H_\theta(x,v,t) = -\gamma v + \theta F(x/\theta, \lambda) + \frac{D}{m}(1-\theta^2) \frac{\partial_v \rho(x/\theta, v/\theta, t)}{\rho(x/\theta, v/\theta, t)}. \tag{B.4}$$

When $\theta = 1$, these auxiliary dynamics become the original ones. The distributions of auxiliary dynamics in the overdamped and underdamped cases are $\rho_\theta(x,t) = \rho(x/\theta, t)/\theta$ and $\rho_\theta(x,v,t) = \rho(x/\theta, v/\theta, t)/\theta^2$, respectively. In both cases, the observable average is scaled as $\langle \phi \rangle_\theta = \theta^\kappa \langle \phi \rangle$; thus, $\partial_\theta \langle \phi \rangle_\theta |_{\theta=1} = \kappa \langle \phi \rangle$. The path probability using the pre-point discretization

can be expressed via the path-integral representation as

$$\mathcal{P}_\theta(\Gamma) = \mathcal{N}_\mathrm{o}\rho_\theta(x(0),0)\exp\left(-\int_0^\tau dt\frac{(\dot{x}-H_\theta(x,t))^2}{4D}\right) \tag{B.5}$$

for the overdamped case and

$$\mathcal{P}_\theta(\Gamma) = \mathcal{N}_\mathrm{u}\rho_\theta(x(0),v(0),0)\exp\left(-\int_0^\tau dt\frac{(m\dot{v}-H_\theta(x,v,t))^2}{4D}\right) \tag{B.6}$$

for the underdamped case. Here, $\mathcal{N}_\mathrm{o}$ and $\mathcal{N}_\mathrm{u}$ are terms independent of θ. Note that entropy production $\langle\sigma\rangle$ is $\int_0^\tau dt\int dx\, j(x,t)^2/D\rho(x,t)$ in overdamped systems and $\int_0^\tau dt\int dxdv\, j^\mathrm{ir}(x,v,t)^2/D\rho(x,v,t)$ in underdamped systems. Here, $j^\mathrm{ir}(x,v,t) = -1/m[\gamma v + D/m\partial_v]\rho(x,v,t)$ is the irreversible probability current. Consequently, performing simple algebraic calculations, one can show that $\mathcal{I}(1)$ is equal to $2\langle\sigma\rangle+\chi_\mathrm{o}+\psi_\mathrm{o}$ for the overdamped case and to $2\langle\sigma\rangle+\chi_\mathrm{u}+\psi_\mathrm{u}$ for the underdamped case. By letting $\theta = 1$ in Eq. (B.1), we obtain the uncertainty relations given in Eqs. (4.28) and (4.30).

B.2 Bounds for multidimensional systems

We consider n-dimensional systems with variables $\boldsymbol{x} = [x_1, x_2, \ldots, x_n]^\top$. We consider observables that satisfy the scaling condition: $\phi(\theta\Gamma) = \theta^\kappa\phi(\Gamma)$, where $\kappa > 0$ is a real constant. Specifically, we focus on three types of observables: a current observable $\phi(\Gamma) = \int_0^\tau dt\,\boldsymbol{\Lambda}_\mathrm{c}(\boldsymbol{x})^\top\circ\dot{\boldsymbol{x}}$, a noncurrent observable $\phi(\Gamma) = \int_0^\tau dt\,\Lambda_\mathrm{nc}(\boldsymbol{x})$, and a discrete-time observable $\phi(\Gamma) = \sum_i c_i\Lambda_\mathrm{nc}(\boldsymbol{x}(t_i))$, where $\boldsymbol{\Lambda}_\mathrm{c}(\boldsymbol{x})$ and $\Lambda_\mathrm{nc}(\boldsymbol{x})$ satisfy that $\boldsymbol{\Lambda}_\mathrm{c}(\theta\boldsymbol{x}) = \theta^{\kappa-1}\boldsymbol{\Lambda}_\mathrm{c}(\boldsymbol{x})$ and $\Lambda_\mathrm{nc}(\theta\boldsymbol{x}) = \theta^\kappa\Lambda_\mathrm{nc}(\boldsymbol{x})$. By employing the same modified dynamics as in Appendix B.1, one can show that the probability currents and distribution function in the auxiliary dynamics are scaled as $\rho_\theta(\boldsymbol{x},t) = \rho(\boldsymbol{x}/\theta,t)/\theta^n$, $j_\theta(\boldsymbol{x},t) = j(\boldsymbol{x}/\theta,t)/\theta^{n-1}$ for overdamped cases and $\rho_\theta(\boldsymbol{x},\boldsymbol{v},t) = \rho(\boldsymbol{x}/\theta,\boldsymbol{v}/\theta,t)/\theta^{2n}$, $j_\theta(\boldsymbol{x},\boldsymbol{v},t) = j(\boldsymbol{x}/\theta,\boldsymbol{v}/\theta,t)/\theta^{2n-1}$ for underdamped cases. Consequently, it is easy to verify that $\langle\phi\rangle_\theta = \theta^\kappa\langle\phi\rangle$. For n-dimensional overdamped systems described as

$$\dot{x}_i = F_i(\boldsymbol{x},\lambda)+\xi_i,\ \ (i=1,\ldots,n), \tag{B.7}$$

the uncertainty relation reads

$$\frac{\langle\phi\rangle^2}{\langle\langle\phi\rangle\rangle} \le \frac{1}{\kappa^2}\left(2\langle\sigma\rangle+\chi_\mathrm{o}+\psi_\mathrm{o}\right), \tag{B.8}$$

where the terms in the right-hand side of Eq. (B.8) are defined by

$$\chi_\mathrm{o} := \int_0^\tau dt\int d\boldsymbol{x}\,\Lambda_\mathrm{o}(\boldsymbol{x},t)\rho(\boldsymbol{x},t), \tag{B.9}$$

$$\psi_\mathrm{o} := \left\langle\left(\sum_{i=1}^n x_i\partial_{x_i}\rho_\mathrm{i}/\rho_\mathrm{i}\right)^2\right\rangle_{\rho_\mathrm{i}} - n^2. \tag{B.10}$$

Here, $\Lambda_{\rm o} = \sum_{i=1}^{n} \left(G_i^2 - 4F_iG_i - 4D_i\partial_{x_i}G_i\right)/2D_i$ and $G_i = F_i + \sum_{j=1}^{n} x_j\partial_{x_j}F_i$. Analogously, for n-dimensional underdamped systems described as

$$\dot{x}_i = v_i,\ m\dot{v}_i = -\gamma_i v_i + F_i(\boldsymbol{x},\lambda) + \xi_i,\ (i = 1,\ldots,n), \tag{B.11}$$

the bound has the following form:

$$\frac{\langle\phi\rangle^2}{\langle\langle\phi\rangle\rangle} \leq \frac{1}{\kappa^2}\left(2\langle\sigma\rangle + \chi_{\rm u} + \psi_{\rm u}\right), \tag{B.12}$$

where the terms in the right-hand side of Eq. (B.12) are defined by

$$\chi_{\rm u} := \int_0^\tau dt \int d\boldsymbol{x}d\boldsymbol{v}\,\Lambda_{\rm u}(\boldsymbol{x},\boldsymbol{v},t)\rho(\boldsymbol{x},\boldsymbol{v},t), \tag{B.13}$$

$$\psi_{\rm u} := \left\langle \left[\sum_{i=1}^{n}\left(x_i\partial_{x_i}\rho_{\rm i} + v_i\partial_{v_i}\rho_{\rm i}\right)/\rho_{\rm i}\right]^2\right\rangle_{\rho_{\rm i}} - 4n^2. \tag{B.14}$$

Here, $\Lambda_{\rm u} = \sum_{i=1}^{n}[(F_i - \sum_{j=1}^{n} x_j\partial_{x_j}F_i)^2 - 4\gamma_i^2 v_i^2 + 8\gamma_i D_i/m_i]/2D_i$.

B.3 Derivation of the bound for a subsystem

We consider the following auxiliary dynamics:

$$\dot{x} = \theta F_x(x/\theta,y,\lambda) + D_x(1-\theta^2)\frac{\partial_x\rho(x/\theta,y,t)}{\rho(x/\theta,y,t)} + \xi_x, \tag{B.15}$$

$$\dot{y} = F_y(y,\lambda) + \xi_y, \tag{B.16}$$

Unlike the previous modifications, we change only the dynamics of the target system, $\mathcal{X}$, and keep those of other systems, $\mathcal{Y}$, unchanged. It can be verified that the distribution of this dynamics is scaled as $\rho_\theta(x,y,t) = \rho(x/\theta,y,t)/\theta$, while the probability currents are scaled as $j_{x,\theta}(x,y,t) = j_x(x/\theta,y,t)$ and $j_{y,\theta}(x,y,t) = j_y(x/\theta,y,t)/\theta$. Subsequently, by applying the same procedure as in Appendix B.1, one can obtain Eq. (4.34).

Appendix C

Appendix C

C.1 Scaled cumulant generating function of observables

Here we calculate the scaled cumulant generating function (SCGF) of the observable $J(\mathcal{X}) = \int_0^T dt\, x$ in the long-time limit $T \to \infty$. Note that $J = T\overline{f} + \int_0^T dt\, z$. By imposing periodic boundary conditions on the trajectories, $z(t)$ can be expanded in a discrete Fourier series [271] as

$$z(t) = \sum_{n=-\infty}^{\infty} z_n e^{-i\omega_n t}, \tag{C.1}$$

where the coefficient z_n can be calculated via inverse transforms

$$z_n = \frac{1}{T}\int_0^T dt\, z(t) e^{i\omega_n t}, \tag{C.2}$$

where $\omega_n = 2\pi n/T$. By substituting Eq. (C.1) into the Langevin equation, we obtain

$$(a + be^{i\omega_n \tau} - i\omega_n) z_n = \xi_n, \tag{C.3}$$

with $\langle \xi_n \xi_m \rangle = 2D/T\delta_{n,-m}$. The current J can then be expressed as $J = T\overline{f} + Tz_0 = T\overline{f} + T\xi_0/(a+b)$. Substituting J into the definition of the SCGF, we obtain

$$\begin{aligned} \chi_J(k) &= \lim_{T\to\infty} T^{-1} \ln \left\langle \exp\left(kT(\overline{f} + \xi_0/(a+b)) \right) \right\rangle \\ &= k\overline{f} + \lim_{T\to\infty} T^{-1} \ln \left(\int_{-\infty}^{\infty} d\xi_0\, P(\xi_0) \exp\left[kT\xi_0/(a+b) \right] \right), \end{aligned} \tag{C.4}$$

where $P(\xi_0) = \sqrt{T/(4\pi D)} \exp\left[-T\xi_0^2/(4D) \right]$. Taking the integration in Eq. (C.4), we get $\chi_J(k) = k\overline{f} + Dk^2/(a+b)^2$.

C.2 Detailed derivations in the two-dimensional system

C.2.1 Time-correlation function

Here, we calculate the stationary time-correlation function $\phi_{ij}(z) = \langle x_i(t)x_j(t+z)\rangle$. Using the same method as in Ref. [147] for arbitrary $z \geq 0$, we have

$$\begin{aligned}
\frac{d}{dz}\phi_{11}(z) &= -a\phi_{11}(z) + b\phi_{21}(\tau - z) + \langle x_1(t)\xi_1(t+z)\rangle,\\
\frac{d}{dz}\phi_{12}(z) &= -a\phi_{12}(z) - b\phi_{11}(\tau - z) + \langle x_1(t)\xi_2(t+z)\rangle,\\
\frac{d}{dz}\phi_{21}(z) &= -a\phi_{21}(z) + b\phi_{22}(\tau - z) + \langle x_2(t)\xi_1(t+z)\rangle,\\
\frac{d}{dz}\phi_{22}(z) &= -a\phi_{22}(z) - b\phi_{12}(\tau - z) + \langle x_2(t)\xi_2(t+z)\rangle.
\end{aligned} \tag{C.5}$$

From the Fokker–Planck equation, we have

$$0 = \frac{d}{dt}\langle x_1^2\rangle = -2a\phi_{11}(0) + 2b\phi_{21}(\tau) + 2D. \tag{C.6}$$

On the other hand, from Langevin equation, we also obtain

$$0 = \frac{d}{dt}\langle x_1^2\rangle = -2a\phi_{11}(0) + 2b\phi_{21}(\tau) + 2\langle x_1(t)\xi_1(t)\rangle. \tag{C.7}$$

Comparing Eq. (C.6) and Eq. (C.7), we obtain the relation $\langle x_1(t)\xi_1(t)\rangle = D$. Similarly, we also get $\langle x_2(t)\xi_2(t)\rangle = D$, $\langle x_1(t)\xi_2(t)\rangle + \langle x_2(t)\xi_1(t)\rangle = 0$. Because the noise is irrelevant to the past states of the system, we have $\langle x_i(t)\xi_j(t+z)\rangle = 0$, $\forall z > 0$. Using the Fourier transform $\boldsymbol{g}(\omega) = \int_{-\infty}^{\infty} dt\, e^{i\omega t}\boldsymbol{g}(t)$ for an arbitrary function $\boldsymbol{g}(t)$, we obtain the relation that $\boldsymbol{x}(\omega) = \boldsymbol{H}(\omega)\boldsymbol{\xi}(\omega)$. Here, $\boldsymbol{H}(\omega)$ is a response function matrix in the frequency domain, given by

$$\boldsymbol{H}(\omega) = \frac{1}{(a - i\omega)^2 + b^2 e^{i2\omega\tau}} \times \begin{pmatrix} a - i\omega & be^{i\omega\tau} \\ -be^{i\omega\tau} & a - i\omega \end{pmatrix}. \tag{C.8}$$

The time-correlation function can be calculated via an inverse Fourier transform of the spectral density $\boldsymbol{S}(\omega)$ given by

$$\boldsymbol{S}(\omega) = 2\boldsymbol{H}(\omega)\boldsymbol{D}\boldsymbol{H}^*(\omega), \tag{C.9}$$

where $\boldsymbol{D} = \mathrm{diag}(D, D) \in \mathbb{R}^{2\times 2}$ and $\boldsymbol{H}^*$ is the complex conjugate transpose of $\boldsymbol{H}$. Since $S_{11}(\omega) = S_{22}(\omega)$, $S_{12}(\omega) + S_{21}(\omega) = 0$, we readily obtain

$$\phi_{11}(z) = \phi_{22}(z), \;\; \phi_{12}(z) + \phi_{21}(z) = 0. \tag{C.10}$$

Using the relations in Eq. (C.10), we obtain that for $0 \leq z \leq \tau$

$$\frac{d^2}{dz^2}\phi_{11}(z) = (a^2 - b^2)\phi_{11}(z). \tag{C.11}$$

The solution of time-correlation function $\phi_{11}(z)$ in Eq. (C.11) has the following form:

$$\phi_{11}(z) = \alpha \cosh(cz) + \beta \sinh(cz), \tag{C.12}$$

where $c = \sqrt{a^2 - b^2}$ and $\alpha,\ \beta$ are constants determined via the conditions:

$$\frac{d}{dz}\phi_{11}(z)\bigg|_{z\to 0} = -D, \quad \phi_{12}(z)|_{z\to 0} = 0. \tag{C.13}$$

Finally, we obtain that for $0 \le z \le \tau$

$$\phi_{11}(z) = \phi_{22}(z) = A_{11}^{+} e^{-cz} + A_{11}^{-} e^{cz}, \tag{C.14}$$

$$\phi_{12}(z) = -\phi_{21}(z) = A_{12}\left(e^{-cz} - e^{cz}\right), \tag{C.15}$$

where

$$A_{11}^{\pm} = \frac{D}{2c} \times \frac{(c \pm a)e^{\pm c\tau}}{a\cosh(c\tau) + c\sinh(c\tau)}, \tag{C.16}$$

$$A_{12} = \frac{D}{2c} \times \frac{b}{a\cosh(c\tau) + c\sinh(c\tau)}. \tag{C.17}$$

Because $\phi_{11}(z)$ is an even function and $\phi_{12}(z)$ is an odd function, we readily obtain that for $|z| \le \tau$,

$$\begin{aligned} \phi_{11}(z) &= \phi_{22}(z) = A_{11}^{+} e^{-c|z|} + A_{11}^{-} e^{c|z|}, \\ \phi_{12}(z) &= -\phi_{21}(z) = A_{12}\left(e^{-cz} - e^{cz}\right). \end{aligned} \tag{C.18}$$

C.2.2 Path integral

Because the process is Gaussian, the path probability is given by

$$\mathcal{P}(\mathcal{X}) \propto \exp\left(-\frac{1}{2}\int_0^T dt \int_0^T dt' \begin{bmatrix} x_1(t) & x_2(t) \end{bmatrix} \begin{bmatrix} \Gamma_{11}(t,t') & \Gamma_{12}(t,t') \\ \Gamma_{21}(t,t') & \Gamma_{22}(t,t') \end{bmatrix} \begin{bmatrix} x_1(t') \\ x_2(t') \end{bmatrix}\right), \tag{C.19}$$

where $\Gamma_{ij}(t,t')$ is the inverse of the stationary time-correlation function $\phi_{ij}(z)$ defined via the following relation:

$$\int_0^T ds \begin{bmatrix} \phi_{11}(t-s) & \phi_{12}(t-s) \\ \phi_{21}(t-s) & \phi_{22}(t-s) \end{bmatrix} \begin{bmatrix} \Gamma_{11}(s,t') & \Gamma_{12}(s,t') \\ \Gamma_{21}(s,t') & \Gamma_{22}(s,t') \end{bmatrix} = \begin{bmatrix} \delta(t-t') & 0 \\ 0 & \delta(t-t') \end{bmatrix}. \tag{C.20}$$

Now, we discretize the problem and take the continuum limit at the end. We divide the time interval $[0,T]$ into N equipartitioned intervals with a time step $\epsilon = T/N$, where $t_k = k\epsilon$ $(k = 0,\ldots,N)$ and $x_1^k = x_1(t_k)$, $x_2^k = x_2(t_k)$ (superscripts denote points in a temporal sequence). Equation (C.19) then reads

$$\mathcal{P}(x_1^0, x_2^0, t_0; \ldots; x_1^N, x_2^N, t_N) \propto \exp\left(-\frac{1}{2}\sum_{i,j}\left[x_1^i \Gamma_{11}^{ij} x_1^j + x_1^i \Gamma_{12}^{ij} x_2^j + x_2^i \Gamma_{21}^{ij} x_1^j + x_2^i \Gamma_{22}^{ij} x_2^j\right]\right), \tag{C.21}$$

and Eq. (C.20) corresponds to the following equation:

$$\sum_{p=1}^{2}\sum_{j=0}^{N}\phi_{mp}^{ij}\Gamma_{pn}^{jk}=\delta_{mn}\delta_{ik}, \tag{C.22}$$

where $\phi_{mp}^{ij}\equiv\phi_{mp}(t_j-t_i)$. The matrices Γ_{mn} $(1\le m,\ n\le 2)$ can be analytically calculated and have the following form:

$$\begin{aligned}
&\Gamma_{11}=\Gamma_{22},\ \Gamma_{12}=-\Gamma_{21},\\
&\Gamma_{11}^{0N}=\Gamma_{11}^{N0}=\frac{e^{-Nc\epsilon}\left(A_{11}^{+}A_{11}^{-}+A_{12}^{2}\right)}{(A_{11}^{+}-A_{11}^{-})\left((A_{11}^{-})^2+A_{12}^{2}-\left((A_{11}^{+})^2+A_{12}^{2}\right)e^{-2Nc\epsilon}\right)},\\
&\Gamma_{11}^{ij}=0,\ \forall\ 1<|i-j|<N,\\
&\Gamma_{11}^{ij}=\frac{-e^{-c\epsilon}}{(A_{11}^{+}-A_{11}^{-})(1-e^{-2c\epsilon})},\ \forall\ |i-j|=1,\\
&\Gamma_{11}^{ii}=\frac{1+e^{-2c\epsilon}}{(A_{11}^{+}-A_{11}^{-})(1-e^{-2c\epsilon})},\ \forall\ 0<i<N,\\
&\Gamma_{11}^{00}=\Gamma_{11}^{NN}=\frac{e^{-2c\epsilon}\left[(A_{11}^{-})^2+A_{12}^{2}-\left((A_{11}^{+})^2+A_{12}^{2}\right)e^{-2(N-1)c\epsilon}\right]}{(A_{11}^{+}-A_{11}^{-})\left(1-e^{-2c\epsilon}\right)\left[(A_{11}^{-})^2+A_{12}^{2}-((A_{11}^{+})^2+A_{12}^{2})e^{-2Nc\epsilon}\right]},\\
&\Gamma_{12}^{0N}=-\Gamma_{12}^{N0}=\frac{-A_{12}e^{-Nc\epsilon}}{(A_{11}^{-})^2+A_{12}^{2}-((A_{11}^{+})^2+A_{12}^{2})e^{-2Nc\epsilon}},\\
&\Gamma_{12}^{ij}=0,\ \forall\ |i-j|\neq N.
\end{aligned} \tag{C.23}$$

Using the result in Eq. (C.23), the quadratic form in Eq. (C.21) can be obtained explicitly as

$$\begin{aligned}
&\sum_{i,j}\left[x_1^i\Gamma_{11}^{ij}x_1^j+x_1^i\Gamma_{12}^{ij}x_2^j+x_2^i\Gamma_{21}^{ij}x_1^j+x_2^i\Gamma_{22}^{ij}x_2^j\right]\\
&=\frac{1}{A_{11}^{+}-A_{11}^{-}}\left(\sum_{i=1}^{2}\sum_{k=1}^{N}\frac{(x_i^k-e^{-c\epsilon}x_i^{k-1})^2}{1-e^{-2c\epsilon}}-\frac{1}{\Omega_T}\sum_{i=1}^{2}\left[A_{12}^{2}\left(e^{-Nc\epsilon}x_i^0-x_i^N\right)^2+\left(A_{11}^{+}e^{-Nc\epsilon}x_i^0-A_{11}^{-}x_i^N\right)^2\right]\right)\\
&-\frac{2A_{12}e^{-Nc\epsilon}}{\Omega_T}\left(x_1^0x_2^N-x_1^Nx_2^0\right),
\end{aligned} \tag{C.24}$$

where $\Omega_T=(A_{11}^{-})^2+A_{12}^{2}-((A_{11}^{+})^2+A_{12}^{2})e^{-2cT}$. Taking the continuum limit $\epsilon\to 0,\ N\to\infty$, with $N\epsilon=T$ gives [133]

$$\lim_{\epsilon\to 0}\sum_{k=1}^{N}\frac{(x_i^k-e^{-c\epsilon}x_i^{k-1})^2}{1-e^{-2c\epsilon}}=\frac{1}{2c}\int_0^T dt\ \left(\dot{x}_i(t)+cx_i(t)\right)^2. \tag{C.25}$$

Finally, we obtain the expression of the path probability for $T \le \tau$:

$$\begin{aligned}\mathcal{P}(\mathcal{X}) \propto & \exp\left(-\sum_{i=1}^{2}\int_0^T dt\,\frac{[\dot{x}_i(t)+cx_i(t)]^2}{4D}\right)\\ & \times\exp\left(\frac{c}{2D\Omega_T}\sum_{i=1}^{2}\left\{A_{12}^2\left[e^{-cT}x_i(0)-x_i(T)\right]^2+\left[A_{11}^{+}e^{-cT}x_i(0)-A_{11}^{-}x_i(T)\right]^2\right\}\right)\\ & \times\exp\left(\frac{A_{12}e^{-cT}}{\Omega_T}\left[x_1(0)x_2(T)-x_1(T)x_2(0)\right]\right).\end{aligned} \tag{C.26}$$

C.2.3 Analytical form of the effective forces

We calculate the analytical form of the effective force $\overline{F}_i(\boldsymbol{x})$ from its definition. We note that $\overline{F}_i(\boldsymbol{x})$ cannot be completely determined from the steady-state FPE, i.e., $\sum_{i=1}^{2}\partial_{x_i}[\overline{F}_i(\boldsymbol{x})P(\boldsymbol{x},t)-D\partial_{x_i}P(\boldsymbol{x},t)]=0$. Specifically, if the effective force takes the form $\overline{F}_i(\boldsymbol{x})=\sum_{j=1}^{2}\gamma_{ij}x_j$, then one obtains $\gamma_{11}=\gamma_{22}=-D/\phi_{11}(0)$, $\gamma_{12}+\gamma_{21}=0$. Here, we use the path integral to calculate $\overline{F}_i(\boldsymbol{x})$. From the definition, we have

$$\begin{aligned}\overline{F}_i(\boldsymbol{v}) &= \int d\boldsymbol{u}\,F_i(\boldsymbol{v},\boldsymbol{u})P(\boldsymbol{u},t-\tau|\boldsymbol{v},t)=\int d\boldsymbol{u}\,F_i(\boldsymbol{v},\boldsymbol{u})P(\boldsymbol{v},t;\boldsymbol{u},t-\tau)/P(\boldsymbol{v},t)\\ &= \int d\boldsymbol{u}\,\frac{F_i(\boldsymbol{v},\boldsymbol{u})}{P(\boldsymbol{v},t)}\int_{\boldsymbol{u}}^{\boldsymbol{v}}\mathcal{D}\mathcal{X}\,\mathcal{P}(\mathcal{X}),\end{aligned} \tag{C.27}$$

where the integration is taken over all trajectories $\mathcal{X}$ that start from $\boldsymbol{u}$ at time $t-\tau$ and end at $\boldsymbol{v}$ at time t. The first term in the path probability can be simplified further using the well-known expression of the transition probability for Smoluchowski processes [63, 133]

$$\int_{x(0)}^{x(\tau)}\mathcal{D}\mathcal{X}\,\exp\left(-\int_0^\tau dt\,\frac{[\dot{x}(t)+cx(t)]^2}{4D}\right)\propto\exp\left(-\frac{c}{2D}\frac{[x(\tau)-x(0)e^{-c\tau}]^2}{1-e^{-2c\tau}}\right). \tag{C.28}$$

Consequently, we obtain

$$\overline{F}_i(\boldsymbol{v})=\int d\boldsymbol{u}\frac{F_i(\boldsymbol{v},\boldsymbol{u})}{P(\boldsymbol{v},t)}G(\boldsymbol{v},\boldsymbol{u}), \tag{C.29}$$

where

$$G(\boldsymbol{v},\boldsymbol{u})\propto\exp\left(-\frac{c}{2D}\frac{\|\boldsymbol{v}-\boldsymbol{u}e^{-c\tau}\|^2}{1-e^{-2c\tau}}+\frac{c}{2D\Omega_\tau}\left(A_{12}^2\|e^{-c\tau}\boldsymbol{u}-\boldsymbol{v}\|^2+\|A_{11}^{+}e^{-c\tau}\boldsymbol{u}-A_{11}^{-}\boldsymbol{v}\|^2\right)+\frac{A_{12}e^{-c\tau}}{\Omega_\tau}\left[u_1v_2-u_2v_1\right]\right). \tag{C.30}$$

Taking the integration in Eq. (C.29), we obtain

$$\begin{aligned}\overline{F}_1(\boldsymbol{x}) &= -\frac{c\,(a\cosh(c\tau)+c\sinh(c\tau))}{a\sinh(c\tau)+c\cosh(c\tau)}x_1+\frac{bc}{a\sinh(c\tau)+c\cosh(c\tau)}x_2,\\ \overline{F}_2(\boldsymbol{x}) &= -\frac{c\,(a\cosh(c\tau)+c\sinh(c\tau))}{a\sinh(c\tau)+c\cosh(c\tau)}x_2-\frac{bc}{a\sinh(c\tau)+c\cosh(c\tau)}x_1.\end{aligned} \tag{C.31}$$

C.2.4 Proof of inequality $\langle\sigma_t\rangle \le \langle\Delta Q\rangle/D$

Here we provide a proof of $\langle\sigma_t\rangle \le \langle\Delta Q\rangle/D$ for $T \le \tau$. By simple calculations, we can show that

$$\langle\sigma_t\rangle = \frac{4b^2(1-e^{-2cT})}{[b^2+(c+a)^2e^{2c\tau}]\,e^{-2cT} - [b^2+(c-a)^2e^{-2c\tau}]}. \tag{C.32}$$

For convenience, we define $U \equiv b^2+(c+a)^2e^{2c\tau}$ and $V \equiv b^2+(c-a)^2e^{-2c\tau}$. Then, $\langle\sigma_t\rangle$ can be rewritten as

$$\langle\sigma_t\rangle = \frac{4b^2(1-e^{-2cT})}{Ue^{-2cT}-V}. \tag{C.33}$$

From Eq. (5.43), we also have

$$\frac{\langle\Delta Q\rangle}{D} = 2Tb^2 \times \frac{\cosh(c\tau)}{a\cosh(c\tau)+c\sinh(c\tau)}. \tag{C.34}$$

Therefore, $\langle\sigma_t\rangle \le \langle Q\rangle/D$ is equivalent to

$$\frac{2(1-e^{-2cT})}{Ue^{-2cT}-V} \le T \times \frac{\cosh(c\tau)}{a\cosh(c\tau)+c\sinh(c\tau)}. \tag{C.35}$$

To prove inequality (C.35), we will show that

$$f(T) \le \frac{\cosh(c\tau)}{a\cosh(c\tau)+c\sinh(c\tau)}, \tag{C.36}$$

where

$$f(T) = \frac{2(1-e^{-2cT})}{T(Ue^{-2cT}-V)}. \tag{C.37}$$

First, taking the derivative of $f(T)$, we have

$$\frac{df(T)}{dT} = \frac{e^{2cT}\left(Ue^{-2cT}+Ve^{2cT}-[U+V+2cT(V-U)]\right)}{T^2\left(U-Ve^{2cT}\right)^2}. \tag{C.38}$$

Since $e^z \ge 1+z$, $\forall z \in \mathbb{R}$, we have $Ue^{-2cT}+Ve^{2cT}-[U+V+2cT(V-U)] \ge 0$; thus, $df(T)/dT \ge 0$. Consequently, we obtain $f(T) \le f(\tau)$ for all $T \le \tau$. Therefore, to prove Eq. (C.36), we need to prove only that

$$f(\tau) \le \frac{\cosh(c\tau)}{a\cosh(c\tau)+c\sinh(c\tau)}. \tag{C.39}$$

Inequality (C.39) is equivalent to

$$e^{c\tau}-e^{-c\tau} \le c\tau\left(e^{c\tau}+e^{-c\tau}\right), \tag{C.40}$$

which is always satisfied because for all $z \ge 0$,

$$\begin{aligned} &\frac{d}{dz}\left[z(e^z+e^{-z})-(e^z-e^{-z})\right] = z(e^z-e^{-z}) \ge 0, \\ &\left[z(e^z+e^{-z})-(e^z-e^{-z})\right]\big|_{z=0} = 0. \end{aligned} \tag{C.41}$$

This implies that $\langle\sigma_t\rangle \le \langle\Delta Q\rangle/D$ for $T \le \tau$.

C.3 Analytical calculations in the dragged colloidal particle model

Applying the Laplace transform to Eq. (5.45), we obtain

$$\begin{aligned} &s^2\tilde{x}(s) - sx(0) - v(0) + \tilde{\gamma}(s)(s\tilde{x}(s) - x(0)) + k\tilde{x}(s) \\ &= k\tilde{\lambda}(s) + \tilde{\eta}(s). \end{aligned} \tag{C.42}$$

Here, $\tilde{f}(s) = \int_0^\infty dt\, f(t)e^{-st}$ is the Laplace transform of an arbitrary function $f(t)$. The solution to Eq. (5.45) is

$$x(t) = H(t)x(0) + G(t)v(0) + \int_0^t dt'\, G(t-t')\left[k\lambda(t') + \eta(t')\right], \tag{C.43}$$

where $H(t)$ and $G(t)$ are given by

$$H(t) = \mathcal{L}^{-1}\left\{\frac{\tilde{\gamma}(s) + s}{s^2 + s\tilde{\gamma}(s) + k}\right\}, \tag{C.44}$$

$$G(t) = \mathcal{L}^{-1}\left\{\frac{1}{s^2 + s\tilde{\gamma}(s) + k}\right\}. \tag{C.45}$$

Here, $\mathcal{L}^{-1}\{\cdot\}$ denotes the inverse Laplace transform. We note that $H(t)$ and $G(t)$ satisfy the following differential equations:

$$\dot{H}(t) = -kG(t), \tag{C.46}$$

$$\dot{G}(t) = H(t) - \int_0^t dt'\, \gamma(t-t')G(t'), \tag{C.47}$$

with initial conditions $H(0) = \dot{G}(0) = 1$ and $G(0) = \dot{H}(0) = 0$. Now, we calculate $G(t)$. Since $\tilde{\gamma}(s) = \gamma_0/(s\tau_c + 1)$, we have

$$G(t) = \mathcal{L}^{-1}\left\{\frac{s+a}{s^3 + as^2 + bs + c}\right\}, \tag{C.48}$$

where $a = 1/\tau_c$, $b = k + \gamma_0/\tau_c$, and $c = k/\tau_c$. The roots of the polynomial $s^3 + as^2 + bs + c$ are characterized by the following quantity:

$$Q = -\frac{a^2b^2}{108} + \frac{b^3}{27} + \frac{a^3c}{27} - \frac{abc}{6} + \frac{c^2}{4}. \tag{C.49}$$

In particular, the polynomial has three real roots when $Q < 0$, one real root and two complex roots when $Q > 0$, and a multiple root when $Q = 0$. Here, we consider only the case $Q > 0$ (i.e., the underdamped case). The denominator can be decomposed as

$$s^3 + as^2 + bs + c = (s+p)(s+q+i\omega)(s+q-i\omega), \tag{C.50}$$

where

$$p = \frac{a}{3} - A - B,\ q = \frac{a}{3} + \frac{A+B}{2},\ \omega = \frac{\sqrt{3}}{2}(A-B). \tag{C.51}$$

Here, constants A and B are given by

$$\begin{aligned} A &= \sqrt[3]{-\frac{a^3}{27} + \frac{ab}{6} - \frac{c}{2} + \sqrt{Q}}, \\ B &= \sqrt[3]{-\frac{a^3}{27} + \frac{ab}{6} - \frac{c}{2} - \sqrt{Q}}. \end{aligned} \tag{C.52}$$

Then, $G(t)$ and $H(t)$ can be obtained as

$$\begin{aligned} G(t) &= c_1 e^{-pt} + c_2 e^{-qt} \sin(\omega t + \phi), \\ H(t) &= 1 - k \int_0^t dt' \, G(t'), \end{aligned} \tag{C.53}$$

where

$$c_1 = \frac{a-p}{(p-q)^2 + \omega^2}, \; c_2 = \frac{1}{\omega} \sqrt{\frac{(a-q)^2 + \omega^2}{(p-q)^2 + \omega^2}}, \tag{C.54}$$

$$\sin\phi = \frac{\omega(p-a)}{\sqrt{((a-q)^2 + \omega^2)((p-q)^2 + \omega^2)}}, \tag{C.55}$$

$$\cos\phi = \frac{(a-q)(p-q) + \omega^2}{\sqrt{((a-q)^2 + \omega^2)((p-q)^2 + \omega^2)}}. \tag{C.56}$$

Once the functions $G(t)$ and $H(t)$ are obtained, the fluctuation of the current and the derived bound can be calculated immediately. From Eq. (C.43), we have

$$\langle x(t) \rangle = k \int_0^t dt' \, G(t-t') \lambda(t'), \tag{C.57}$$

$$\langle x(0) x(t) \rangle = H(t) \langle x(0)^2 \rangle. \tag{C.58}$$

Consequently, we obtain the following results:

$$\begin{aligned} H(t) &= 1 - \frac{k c_1 (1 - e^{-pt})}{p} - \frac{k c_2 \left(\omega \cos\phi + q \sin\phi - e^{-qt} \left[\omega \cos(\omega t + \phi) + q \sin(\omega t + \phi)\right]\right)}{q^2 + \omega^2}, \\ \langle x(T) \rangle &= k\alpha \left[\int_0^{T/2} dt \, G(T-t) t + \int_{T/2}^{T} dt \, G(T-t)(T-t) \right] \\ &= \frac{k\alpha c_1 (e^{-pT/2} - 1)^2}{p^2} + \frac{k\alpha c_2}{(q^2 + \omega^2)^2} \Big[2q\omega \left(\cos\phi - 2e^{-qT/2} \cos(\omega T/2 + \phi) + e^{-qT} \cos(\omega T + \phi) \right) \\ &\quad + (q^2 - \omega^2) \left(\sin\phi - 2e^{-qT/2} \sin(\omega T/2 + \phi) + e^{-qT} \sin(\omega T + \phi) \right) \Big], \\ \langle x(T)^2 \rangle &= (k\beta)^{-1} H(T)^2 + \beta^{-1} G(T)^2 + k^2 \left(\int_0^T dt \, G(T-t) \lambda(t) \right)^2 \\ &\quad + \beta^{-1} \frac{\gamma_0}{\tau_c} \int_0^T dt \int_0^T dt' \, G(T-t) G(T-t') e^{-\frac{|t-t'|}{\tau_c}}, \\ \langle \sigma_t \rangle &= k^2 \alpha\beta \left[\int_{T/2}^{T} dt \int_0^t dt' \, G(t-t') \lambda(t') - \int_0^{T/2} dt \int_0^t dt' \, G(t-t') \lambda(t') \right]. \end{aligned} \tag{C.59}$$

Appendix D

Appendix D

D.1 Derivation for discrete measurement and feedback control

First, we note that the joint probability distribution of σ and $\mathcal{O}$, $P(\sigma, \mathcal{O})$, obeys the strong DFT

$$P(\sigma, \mathcal{O}) = e^{\sigma} P(-\sigma, -\mathcal{O}). \tag{D.1}$$

Equation (D.1) can be readily obtained as follows:

$$\begin{aligned}
&P(\sigma, \mathcal{O}) \\
&= \int \mathcal{D}\mathcal{Z}\, \delta(\sigma - \sigma(\mathcal{X}, \mathcal{M}))\delta(\mathcal{O} - \mathcal{O}[\mathcal{X}])\mathcal{P}(\mathcal{X}, \mathcal{M}) \\
&= \int \mathcal{D}\mathcal{Z}\, \delta(\sigma - \sigma(\mathcal{X}, \mathcal{M}))\delta(\mathcal{O} - \mathcal{O}[\mathcal{X}])e^{\sigma(\mathcal{X}, \mathcal{M})}\mathcal{P}(\mathcal{X}^\dagger, \mathcal{M}^\dagger) \\
&= e^{\sigma} \int \mathcal{D}\mathcal{Z}\, \delta(\sigma - \sigma(\mathcal{X}, \mathcal{M}))\delta(\mathcal{O} - \mathcal{O}[\mathcal{X}])\mathcal{P}(\mathcal{X}^\dagger, \mathcal{M}^\dagger) \\
&= e^{\sigma} \int \mathcal{D}\mathcal{Z}^\dagger\, \delta(\sigma + \sigma(\mathcal{X}^\dagger, \mathcal{M}^\dagger))\delta(\mathcal{O} + \mathcal{O}[\mathcal{X}^\dagger])\mathcal{P}(\mathcal{X}^\dagger, \mathcal{M}^\dagger) \\
&= e^{\sigma} P(-\sigma, -\mathcal{O}).
\end{aligned} \tag{D.2}$$

Here, $\mathcal{D}\mathcal{Z} \equiv \mathcal{D}\mathcal{X}\mathcal{D}\mathcal{M}$ and $\mathcal{D}\mathcal{Z}^\dagger \equiv \mathcal{D}\mathcal{X}^\dagger\mathcal{D}\mathcal{M}^\dagger$. Inspired by Ref. [159], where the statistical properties of entropy production were obtained from the strong DFT, we derive the uncertainty relation mainly from Eq. (D.1). By observing that

$$\begin{aligned}
1 &= \int_{-\infty}^{\infty} d\sigma \int_{-\infty}^{\infty} d\mathcal{O}\, P(\sigma, \mathcal{O}) \\
&= \int_{0}^{\infty} d\sigma \int_{-\infty}^{\infty} d\mathcal{O}\, (1 + e^{-\sigma})P(\sigma, \mathcal{O}),
\end{aligned} \tag{D.3}$$

we introduce a probability distribution $Q(\sigma, \mathcal{O}) \equiv (1 + e^{-\sigma})P(\sigma, \mathcal{O})$, which is defined over $[0, \infty) \times (-\infty, \infty)$. The first and second moments of σ and $\mathcal{O}$ can be expressed with respect

to the distribution $Q(\sigma, O)$ as follows:

$$\begin{aligned} \langle \sigma \rangle &= \left\langle \sigma \tanh\left(\frac{\sigma}{2}\right)\right\rangle_Q, \ \langle \sigma^2 \rangle = \langle \sigma^2 \rangle_Q, \\ \langle O \rangle &= \left\langle O \tanh\left(\frac{\sigma}{2}\right)\right\rangle_Q, \ \langle O^2 \rangle = \langle O^2 \rangle_Q, \end{aligned} \tag{D.4}$$

where $\langle \dots \rangle_Q$ denotes the expectation with respect to $Q(\sigma, O)$. By applying the Cauchy–Schwarz inequality to $\langle O \rangle$, we obtain

$$\langle O \rangle^2 = \left\langle O \tanh\left(\frac{\sigma}{2}\right)\right\rangle_Q^2 \leq \langle O^2 \rangle_Q \left\langle \tanh^2\left(\frac{\sigma}{2}\right)\right\rangle_Q. \tag{D.5}$$

The last term in the right-hand side of Eq. (D.5) can be further upper bounded. We observe that

$$\begin{aligned} \left\langle \tanh^2\left(\frac{\sigma}{2}\right)\right\rangle_Q &= \left\langle \tanh^2\left[f\left(\frac{\sigma}{2}\tanh\left(\frac{\sigma}{2}\right)\right)\right]\right\rangle_Q \\ &\leq \tanh^2\left[f\left(\langle\sigma\rangle/2\right)\right]. \end{aligned} \tag{D.6}$$

The equality in Eq. (D.6) is obtained from the fact that $f(x)$ is the inverse function of $x\tanh(x)$. The inequality in Eq. (D.6) can be obtained as follows. First, we show that $\chi(x) = \tanh^2[f(x)]$ is a concave function over $[0, +\infty)$. Indeed, using the relation $f(x)\tanh[f(x)] = x$ and performing simple calculations, we obtain

$$\frac{d^2\chi(x)}{dx^2} = \frac{4\left(4f(x) - \sinh\left[4f(x)\right]\right)}{\left(2f(x) + \sinh\left[2f(x)\right]\right)^3}. \tag{D.7}$$

Since $4f(x) \leq \sinh[4f(x)]$, we have $d^2\chi(x)/dx^2 \leq 0, \ \forall x \geq 0$; thus, implying that $\tanh^2[f(x)]$ is a concave function. Applying Jensen's inequality to this function, we obtain

$$\begin{aligned} &\left\langle \tanh^2\left[f\left(\frac{\sigma}{2}\tanh\left(\frac{\sigma}{2}\right)\right)\right]\right\rangle_Q \\ &\leq \tanh^2\left[f\left(\left\langle\frac{\sigma}{2}\tanh\left(\frac{\sigma}{2}\right)\right\rangle_Q\right)\right] = \tanh^2\left[f\left(\langle\sigma\rangle/2\right)\right]. \end{aligned} \tag{D.8}$$

From Eqs. (D.5) and (D.6), we have

$$\langle O \rangle^2 \leq \langle O^2 \rangle \tanh^2\left[f\left(\langle\sigma\rangle/2\right)\right]. \tag{D.9}$$

By transforming Eq. (D.9), we obtain the derived bound [Eq. (5.64)] for the observable O.

D.2 Derivation for continuous measurement and feedback control

Let $P(x, e, t)$ be the probability distribution function of the joint system [Eqs. (5.65) and (5.66)]. Its time evolution is described by the Fokker–Planck equation as follows:

$$\partial_t P(x, e, t) = -\partial_x J_x(x, e, t) - \partial_e J_e(x, e, t), \tag{D.10}$$

where $J_x(x,e,t) = f(x,x+e)P(x,e,t) - D_x\partial_x P(x,e,t)$ and $J_e(x,e,t) = -eP(x,e,t) - D_e\partial_e P(x,e,t)$ are probability currents. Hereafter, we focus exclusively on the nonequilibrium steady state, for which the probability distribution and currents are $P^{\rm ss}(x,e)$ and $\boldsymbol{J}^{\rm ss}(x,e) \equiv [J_x^{\rm ss}(x,e), J_e^{\rm ss}(x,e)]^\top$, respectively.

We use the Cramér–Rao inequality [33] and the perturbation technique [44] to derive the uncertainty relation for the systems under consideration. Let us consider an auxiliary dynamics described by

$$\begin{aligned} \dot{x} &= f(x,x+e) + \theta \frac{J_x^{\rm ss}(x,e)}{P^{\rm ss}(x,e)} + \xi, \\ \dot{e} &= -e + \theta \frac{J_e^{\rm ss}(x,e)}{P^{\rm ss}(x,e)} + \eta, \end{aligned} \tag{D.11}$$

where θ is a perturbation parameter. When $\theta = 0$, this auxiliary dynamics becomes the original one. Let $P_\theta^{\rm ss}(x,e)$ be the stationary distribution of this auxiliary dynamics; $P_\theta^{\rm ss}(x,e) = P^{\rm ss}(x,e)$ can be easily confirmed. The probability current of the auxiliary dynamics is scaled as follows:

$$J_{\theta,x}^{\rm ss}(x,e) = (1+\theta) J_x^{\rm ss}(x,e). \tag{D.12}$$

Let $\mathcal{X} = \{x(t)\}_{t=0}^{t=\mathcal{T}}$ and $\mathcal{E} = \{e(t)\}_{t=0}^{t=\mathcal{T}}$ be the trajectories of the system states and the noise, respectively. In the auxiliary dynamics, the path probability using the Ito discretisation is expressed as

$$\begin{aligned} \mathcal{P}_\theta(\mathcal{X},\mathcal{E}) \propto P_\theta^{\rm ss}(x(0),e(0)) \exp\left(-\frac{1}{4D_x} \int_0^{\mathcal{T}} dt \left[\dot{x} - f(x,x+e) - \theta \frac{J_x^{\rm ss}(x,e)}{P^{\rm ss}(x,e)} \right]^2 \right) \\ \times \exp\left(-\frac{1}{4D_e} \int_0^{\mathcal{T}} dt \left[\dot{e} + e - \theta \frac{J_e^{\rm ss}(x,e)}{P^{\rm ss}(x,e)} \right]^2 \right). \end{aligned} \tag{D.13}$$

For an arbitrary function $\phi(\mathcal{X})$, we define $\langle \phi \rangle_\theta = \int \mathcal{D}\mathcal{X}\mathcal{D}\mathcal{E}\, \mathcal{P}_\theta(\mathcal{X},\mathcal{E})\phi(\mathcal{X})$ and $\mathrm{Var}_\theta[\phi] = \langle (\phi - \langle \phi \rangle_\theta)^2 \rangle_\theta$. Since $\langle O \rangle_\theta$ is a function of θ, we can consider O as one of its estimators. According to the Cramér–Rao inequality, the precision of this estimator is lower bounded by the Fisher information $\mathcal{I}(\theta)$ as follows:

$$\frac{\mathrm{Var}_\theta[O]}{(\partial_\theta \langle O \rangle_\theta)^2} \geq \frac{1}{\mathcal{I}(\theta)}, \tag{D.14}$$

where $\mathcal{I}(\theta) \equiv -\langle \partial_\theta^2 \ln \mathcal{P}_\theta(\mathcal{X},\mathcal{E}) \rangle_\theta$. Since $\langle O \rangle_\theta = \mathcal{T} \int dx \int de\, \Lambda(x) J_{\theta,x}^{\rm ss}(x,e)$, we have $\langle O \rangle_\theta = (1+\theta)\langle O \rangle$ and, thus, $\partial_\theta \langle O \rangle_\theta = \langle O \rangle$. Moreover, through some algebraic calculations, we obtain

$$\mathcal{I}(0) = \frac{\mathcal{T}}{2} \int dx \int de\, \frac{\boldsymbol{J}^{\rm ss}(x,e)^\top \boldsymbol{D}^{-1} \boldsymbol{J}^{\rm ss}(x,e)}{P^{\rm ss}(x,e)} = \frac{1}{2D_x} \left\langle \int_0^{\mathcal{T}} dt\, f(x,x+e) \circ \dot{x} \right\rangle, \tag{D.15}$$

where $\boldsymbol{D} \equiv \mathrm{diag}(D_x, D_e) \in \mathbb{R}^{2\times 2}$. As shown, the Fisher information is directly proportional to $\langle \sigma \rangle$, i.e. $\mathcal{I}(0) = \langle \sigma \rangle / 2$. By letting $\theta = 0$ in Eq. (D.14), we readily obtain

$$\frac{\mathrm{Var}[O]}{\langle O \rangle^2} \geq \frac{2}{\langle \sigma \rangle}. \tag{D.16}$$

Appendix E

Appendix E

Hereafter, we denote by $\mathfrak{L}(\mathcal{H})$ and $\mathfrak{H}(\mathcal{H})$ the sets of linear and self-adjoint operators, respectively, on a complex Hilbert space $\mathcal{H}$ with dimension $N > 0$. The inner product $\langle \cdot, \cdot \rangle$ is defined as $\langle \boldsymbol{x}, \boldsymbol{y} \rangle = \boldsymbol{x}^\top \boldsymbol{y}$ for $\boldsymbol{x}, \boldsymbol{y} \in \mathbb{R}^{N \times 1}$ (classical case) and $\langle X, Y \rangle = \mathrm{tr}\left\{X^\dagger Y\right\}$ for $X, Y \in \mathfrak{L}(\mathcal{H})$ (quantum case).

E.1 Open quantum systems

E.1.1 Alternative expression of the Lindblad master equation

Here we show that the Lindblad master equation can be written as

$$\dot{\rho} = \mathcal{K}_\rho(-\ln \rho + \ln \rho^{\mathrm{eq}}), \tag{E.1}$$

where $\mathcal{K}_\rho : \nu \mapsto i\beta^{-1}[\nu, \rho] + \mathcal{O}_\rho(\nu)$. The operator $\mathcal{O}_\rho$ is defined by

$$\mathcal{O}_\rho(\nu) \coloneqq \sum_{\mu,\omega} e^{-\beta\omega/2} \alpha_\mu(\omega) [L_\mu(\omega), [\rho]_{\beta\omega}([L_\mu^\dagger(\omega), \nu])]. \tag{E.2}$$

For any density operator $\rho = \sum_n p_n |n\rangle\langle n|$, where $\sum_n p_n = 1$ and $\{|n\rangle\}_n$ are orthonormal eigenvectors, we can express the tilted operator as

$$[\rho]_\theta(X) = e^{-\theta/2} \int_0^1 e^{s\theta} \rho^s X \rho^{1-s} ds = \sum_{n,m} \Phi(e^{\theta/2} p_n, e^{-\theta/2} p_m) \langle n|X|m\rangle |n\rangle\langle m|. \tag{E.3}$$

Here, $\Phi(x, y)$ is the logarithmic mean of two positive numbers x and y, given by $\Phi(x, y) = (x - y)/[\ln(x) - \ln(y)]$ for $x \neq y$ and $\Phi(x, x) = x$. As $\rho^{\mathrm{eq}} = e^{-\beta H}/Z_\beta$ and $[\ln \rho, \rho] = 0$, we have $i\beta^{-1}[-\ln \rho + \ln \rho^{\mathrm{eq}}, \rho] = -i[H, \rho]$. Thus, we need only show that

$$\mathcal{O}_\rho(-\ln \rho + \ln \rho^{\mathrm{eq}}) = \sum_{\mu,\omega} \alpha_\mu(\omega) \left[2L_\mu(\omega) \rho L_\mu^\dagger(\omega) - \left\{L_\mu^\dagger(\omega) L_\mu(\omega), \rho\right\}\right]. \tag{E.4}$$

To this end, we first show that $[\rho]_\theta([X, \ln \rho] - \theta X) = e^{-\theta/2} X\rho - e^{\theta/2} \rho X$ for an arbitrary operator $X \in \mathfrak{L}(\mathcal{H})$ and $\theta \in \mathbb{R}$. This can be achieved through the following transformation:

$$[\rho]_\theta([X, \ln \rho] - \theta X) = e^{-\theta/2} \int_0^1 e^{\theta s} e^{s \ln \rho} (X \ln \rho - \ln \rho X - \theta X) e^{(1-s) \ln \rho} ds \tag{E.5a}$$

$$= -e^{-\theta/2}\int_0^1 \left[e^{\theta s}e^{s\ln\rho}(\ln\rho+\theta)Xe^{(1-s)\ln\rho} + e^{\theta s}e^{s\ln\rho}X(-\ln\rho)e^{(1-s)\ln\rho}\right]ds \tag{E.5b}$$

$$= -e^{-\theta/2}\int_0^1 \frac{d}{ds}\left[e^{(\ln\rho+\theta)s}Xe^{(1-s)\ln\rho}\right]ds \tag{E.5c}$$

$$= e^{-\theta/2}(Xe^{\ln\rho} - e^{\ln\rho+\theta}X) \tag{E.5d}$$

$$= e^{-\theta/2}X\rho - e^{\theta/2}\rho X. \tag{E.5e}$$

Next, applying the relation $[L_\mu^\dagger(\omega), H] = -\omega L_\mu^\dagger(\omega)$, one immediately obtains

$$[\rho]_{\beta\omega}([L_\mu^\dagger(\omega), -\ln\rho + \ln\rho^{\mathrm{eq}}]) = [\rho]_{\beta\omega}([L_\mu^\dagger(\omega), -\ln\rho - \beta H]) \tag{E.6a}$$

$$= -[\rho]_{\beta\omega}([L_\mu^\dagger(\omega), \ln\rho] + \beta[L_\mu^\dagger(\omega), H]) \tag{E.6b}$$

$$= -[\rho]_{\beta\omega}([L_\mu^\dagger(\omega), \ln\rho] - \beta\omega L_\mu^\dagger(\omega)) \tag{E.6c}$$

$$= e^{\beta\omega/2}\rho L_\mu^\dagger(\omega) - e^{-\beta\omega/2}L_\mu^\dagger(\omega)\rho. \tag{E.6d}$$

Consequently, as $L_\mu^\dagger(\omega) = L_\mu(-\omega)$ and $\alpha_\mu(\omega) = e^{\beta\omega}\alpha_\mu(-\omega)$, one can verify Eq. (E.4) as follows:

$$\mathcal{O}_\rho(-\ln\rho + \ln\rho^{\mathrm{eq}}) \tag{E.7a}$$

$$= \sum_{\mu,\omega} e^{-\beta\omega/2}\alpha_\mu(\omega)[L_\mu(\omega), [\rho]_{\beta\omega}([L_\mu^\dagger(\omega), -\ln\rho + \ln\rho^{\mathrm{eq}}])] \tag{E.7b}$$

$$= \sum_{\mu,\omega} e^{-\beta\omega/2}\alpha_\mu(\omega)[L_\mu(\omega), e^{\beta\omega/2}\rho L_\mu^\dagger(\omega) - e^{-\beta\omega/2}L_\mu^\dagger(\omega)\rho] \tag{E.7c}$$

$$= \sum_{\mu,\omega} \alpha_\mu(\omega)\left[-e^{-\beta\omega}L_\mu(\omega)L_\mu^\dagger(\omega)\rho + L_\mu(\omega)\rho L_\mu^\dagger(\omega) + e^{-\beta\omega}L_\mu^\dagger(\omega)\rho L_\mu(\omega) - \rho L_\mu^\dagger(\omega)L_\mu(\omega)\right] \tag{E.7d}$$

$$= \sum_{\mu,\omega} \left\{\alpha_\mu(\omega)\left[L_\mu(\omega)\rho L_\mu^\dagger(\omega) - \rho L_\mu^\dagger(\omega)L_\mu(\omega)\right] + \alpha_\mu(-\omega)\left[L_\mu(-\omega)\rho L_\mu^\dagger(-\omega) - L_\mu^\dagger(-\omega)L_\mu(-\omega)\rho\right]\right\} \tag{E.7e}$$

$$= \sum_{\mu,\omega} \alpha_\mu(\omega)\left[2L_\mu(\omega)\rho L_\mu^\dagger(\omega) - \left\{L_\mu^\dagger(\omega)L_\mu(\omega), \rho\right\}\right]. \tag{E.7f}$$

E.1.2 Properties of the quantum Wasserstein metric

Here we provide several useful properties regarding the defined metric.

Lemma E.1. *The inner product $\langle\cdot, \mathcal{O}_\rho(\cdot)\rangle$ satisfies the conjugate-symmetry condition $\langle\xi, \mathcal{O}_\rho(\nu)\rangle = \langle\nu, \mathcal{O}_\rho(\xi)\rangle^*$ for all operators $\nu, \xi \in \mathfrak{L}(\mathcal{H})$. Here, $*$ denotes the complex conjugate.*

Proof. For an arbitrary operator $X \in \mathfrak{L}(\mathcal{H})$ and $\theta \in \mathbb{R}$, we have

$$\langle\xi, [X, [\rho]_\theta([X^\dagger, \nu])]\rangle = \mathrm{tr}\left\{\xi^\dagger[X, [\rho]_\theta([X^\dagger, \nu])]\right\} \tag{E.8a}$$

$$= \mathrm{tr}\left\{[\xi^\dagger, X][\rho]_\theta([X^\dagger, \nu])\right\} \tag{E.8b}$$

$$= \sum_{n,m} \Phi(e^{\theta/2}p_n, e^{-\theta/2}p_m)\langle n|[X^\dagger, \nu]|m\rangle\langle m|[\xi^\dagger, X]|n\rangle, \tag{E.8c}$$

where we have used Eq. (E.3) in Eq. (E.8c). Swapping ξ and ν, one obtains

$$\langle \nu, [X, [\rho]_\theta([X^\dagger, \xi])]\rangle^* = \sum_{n,m} \Phi(e^{\theta/2}p_n, e^{-\theta/2}p_m)\langle n|[X^\dagger, \xi]|m\rangle^* \langle m|[\nu^\dagger, X]|n\rangle^* \tag{E.9a}$$

$$= \sum_{n,m} \Phi(e^{\theta/2}p_n, e^{-\theta/2}p_m)\langle m|[\xi^\dagger, X]|n\rangle \langle n|[X^\dagger, \nu]|m\rangle \tag{E.9b}$$

$$= \langle \xi, [X, [\rho]_\theta([X^\dagger, \nu])]\rangle. \tag{E.9c}$$

As $\mathcal{O}_\rho(\nu) = \sum_{\mu,\omega} e^{-\beta\omega/2}\alpha_\mu(\omega)[L_\mu(\omega), [\rho]_{\beta\omega}([L_\mu^\dagger(\omega), \nu])]$, Eq. (E.9c) implies that

$$\langle \nu, \mathcal{O}_\rho(\xi)\rangle^* = \langle \xi, \mathcal{O}_\rho(\nu)\rangle. \tag{E.10}$$

□

From Eq. (E.8c), one observes that

$$\langle \xi, [X, [\rho]_\theta([X^\dagger, \xi])]\rangle = \sum_{n,m} \Phi(e^{\theta/2}p_n, e^{-\theta/2}p_m)|\langle n|[X^\dagger, \xi]|m\rangle|^2 \geq 0. \tag{E.11}$$

Therefore, $\langle \xi, \mathcal{O}_\rho(\xi)\rangle \geq 0$ for an arbitrary operator ξ. Equality is attained only when $[L_\mu^\dagger(\omega), \xi] = 0$ for all μ and ω. When ξ is a self-adjoint operator, i.e., $\xi^\dagger = \xi$, we have $\langle \xi, \mathcal{K}_\rho(\xi)\rangle = \langle \xi, \mathcal{O}_\rho(\xi)\rangle \geq 0$.

Proposition E.2. *A self-adjoint operator ν satisfies $\mathcal{K}_\rho(\nu) = 0$ if and only if ν is spanned by $\mathbb{I}_N$.*

Proof. As $\mathcal{K}_\rho(\mathbb{I}_N) = 0$, we need only show that if $\mathcal{K}_\rho(\nu) = 0$, then ν is spanned by $\mathbb{I}_N$. Noting that $0 = \langle \nu, \mathcal{K}_\rho(\nu)\rangle = \langle \nu, \mathcal{O}_\rho(\nu)\rangle$, we find that $\langle \nu, \mathcal{O}_\rho(\nu)\rangle = 0$ only when $[L_\mu^\dagger(\omega), \nu] = 0$ for all μ and ω. As the dynamics of the quantum system are ergodic, this implies that ν is spanned by $\mathbb{I}_N$.

□

Proposition E.3. *$\mathcal{K}_\rho(\nu)$ is a traceless self-adjoint operator for all $\nu \in \mathfrak{H}(\mathcal{H})$.*

Proof. The expression

$$\mathcal{K}_\rho(\nu) = i\beta^{-1}[\nu, \rho] + \mathcal{O}_\rho(\nu) = i\beta^{-1}[\nu, \rho] + \sum_{\mu,\omega} e^{-\beta\omega/2}\alpha_\mu(\omega)[L_\mu(\omega), [\rho]_{\beta\omega}([L_\mu^\dagger(\omega), \nu])] \tag{E.12}$$

is a linear combination of commutators. Therefore, $\mathrm{tr}\{\mathcal{K}_\rho(\nu)\} = 0$ is immediately derived. Note that $(i\beta^{-1}[\nu, \rho])^\dagger = i\beta^{-1}[\nu, \rho]$, so we need only show that $\mathcal{O}_\rho(\nu)$ is self-adjoint. Using the relations $[\rho]_\theta(X)^\dagger = [\rho]_{-\theta}(X^\dagger)$, $[X, Y]^\dagger = [Y^\dagger, X^\dagger]$, $e^{-\beta\omega/2}\alpha_\mu(\omega) = e^{\beta\omega/2}\alpha_\mu(-\omega)$, and $L_\mu^\dagger(\omega) = L_\mu(-\omega)$, we can prove that $\mathcal{O}_\rho(\nu)$ is self-adjoint as follows:

$$\mathcal{O}_\rho(\nu)^\dagger = \sum_{\mu,\omega} e^{-\beta\omega/2}\alpha_\mu(\omega)[L_\mu(\omega), [\rho]_{\beta\omega}([L_\mu^\dagger(\omega), \nu])]^\dagger \tag{E.13}$$

$$= \sum_{\mu,\omega} e^{-\beta\omega/2}\alpha_\mu(\omega)[[\rho]_{\beta\omega}([L_\mu^\dagger(\omega), \nu])^\dagger, L_\mu(\omega)^\dagger] \tag{E.14}$$

$$= \sum_{\mu,\omega} e^{\beta\omega/2}\alpha_\mu(-\omega)[[\rho]_{-\beta\omega}([\nu, L_\mu(\omega)]), L_\mu(-\omega)] \tag{E.15}$$

$$= \sum_{\mu,\omega} e^{\beta\omega/2}\alpha_\mu(-\omega)[L_\mu(-\omega), [\rho]_{-\beta\omega}([L_\mu^\dagger(-\omega), \nu])] \tag{E.16}$$

$$= O_\rho(\nu). \tag{E.17}$$

□

Lemma E.4. *For an arbitrary density operator ρ and traceless self-adjoint operator ϑ, there exists a unique traceless self-adjoint operator ν such that $\vartheta = \mathcal{K}_\rho(\nu)$.*

Proof. Let $\mathcal{B} = \{\chi_{j,k}\}_{1\le j,k\le N}$ denote the set of generalized Gell-Mann matrices, which span the space of operators in the complex Hilbert space $\mathcal{H}$. Specifically, $\chi_{j,k}$ can be expressed as follows:

$$\chi_{j,k} = \begin{cases} E_{k,j} + E_{j,k}, & \text{if } j < k, \\ i(E_{k,j} - E_{j,k}), & \text{if } j > k, \\ \sqrt{\frac{2}{j(j+1)}}\left(\sum_{l=1}^{j} E_{l,l} - jE_{j+1,j+1}\right), & \text{if } j = k < N, \\ N^{-1}\mathbb{I}_N, & \text{if } j = k = N, \end{cases} \tag{E.18}$$

where $E_{j,k}$ denotes a matrix with 1 in the jk-th entry and 0 elsewhere. In this construction, each $\chi_{j,k}$ is a Hermitian matrix and $\mathrm{tr}\{\chi_{j,k}\} = \delta_{jN}\delta_{kN}$ for all (j,k). For convenience, we define a set $\overline{\mathcal{B}} \coloneqq \mathcal{B} \setminus \{\chi_{N,N}\}$. For arbitrary traceless self-adjoint operator X, there exists real coefficients $c_{j,k} \in \mathbb{R}$ such that $X = \sum_{j,k} c_{j,k}\chi_{j,k}$. Taking the trace of both sides of the equation, we obtain $0 = \mathrm{tr}\{X\} = \sum_{j,k} c_{j,k}\mathrm{tr}\{\chi_{j,k}\} = c_{N,N}$. This implies that X can be expressed as a linear combination of matrices in $\overline{\mathcal{B}}$ with all real coefficients.

By propositions E.2 and E.3, $\mathcal{K}_\rho(\chi_{j,k})$ is obviously a nonzero traceless self-adjoint operator for all $(j,k) \neq (N,N)$. We now show that $\{\mathcal{K}_\rho(\chi_{j,k})\}_{(j,k)\neq(N,N)}$ is an independent set, i.e., $\sum_{(j,k)\neq(N,N)} c_{j,k}\mathcal{K}_\rho(\chi_{j,k}) = 0$ only when $c_{j,k} = 0$ for all j,k. Indeed, by the linearity of $\mathcal{K}_\rho$, we have

$$\sum_{(j,k)\neq(N,N)} c_{j,k}\mathcal{K}_\rho(\chi_{j,k}) = \mathcal{K}_\rho\Big(\sum_{(j,k)\neq(N,N)} c_{j,k}\chi_{j,k}\Big) = 0. \tag{E.19}$$

Under proposition E.2, $\sum_{(j,k)\neq(N,N)} c_{j,k}\chi_{j,k}$ must be spanned by $\mathbb{I}_N$ $(= N\chi_{N,N})$, i.e.,

$$\sum_{(j,k)\neq(N,N)} c_{j,k}\chi_{j,k} = -c_{N,N}\chi_{N,N} \tag{E.20}$$

for some $c_{N,N}$. This is equivalent to $\sum_{1\le j,k\le N} c_{j,k}\chi_{j,k} = 0$. As $\mathcal{B}$ is a basis of $\mathcal{H}$, this equivalence requires that $c_{j,k} = 0$ for all j,k.

Because $\{\mathcal{K}_\rho(\chi_{j,k})\}_{(j,k)\neq(N,N)}$ has $N^2 - 1$ elements, we can add another matrix ϕ to form a new basis of $\mathcal{H}$. In terms of the elements of the new basis, $\mathbb{I}_N$ can then be expressed as

$$\mathbb{I}_N = z\phi + \sum_{(j,k)\neq(N,N)} c_{j,k}\mathcal{K}_\rho(\chi_{j,k}), \tag{E.21}$$

where z is some complex number. Taking the trace of both sides of Eq. (E.21), we obtain $N = z\,\mathrm{tr}\{\phi\}$, which indicates that $z \neq 0$. Therefore, ϕ can be expressed in terms of $\mathbb{I}_N$ and

$\{\mathcal{K}_\rho(\chi_{j,k})\}_{(j,k)\neq(N,N)}$ as

$$\phi = z^{-1}\Big[\mathbb{I}_N - \sum_{(j,k)\neq(N,N)} c_{j,k}\mathcal{K}_\rho(\chi_{j,k})\Big]. \tag{E.22}$$

Equation (E.22) implies that an arbitrary matrix can be expressed as a linear combination of elements in the following set:

$$\mathcal{S} \coloneqq \{\mathbb{I}_N\} \cup \{\mathcal{K}_\rho(\chi_{j,k})\}_{(j,k)\neq(N,N)}. \tag{E.23}$$

Equivalently, $\mathcal{S}$ is a basis of $\mathcal{H}$. Consequently, because $\mathcal{K}_\rho(\chi_{j,k})$ is traceless and self-adjoint, an arbitrary traceless self-adjoint operator ϑ can be expressed in terms of $\{\mathcal{K}_\rho(\chi_{j,k})\}_{(j,k)\neq(N,N)}$ with real coefficients $\{c_{j,k}\}$ as

$$\vartheta = \sum_{(j,k)\neq(N,N)} c_{j,k}\mathcal{K}_\rho(\chi_{j,k}) = \mathcal{K}_\rho\Big(\sum_{(j,k)\neq(N,N)} c_{j,k}\chi_{j,k}\Big). \tag{E.24}$$

Defining the traceless self-adjoint operator $\nu \coloneqq \sum_{(j,k)\neq(N,N)} c_{j,k}\chi_{j,k}$, one readily obtains $\vartheta = \mathcal{K}_\rho(\nu)$. Finally, to prove the uniqueness of ν, we assume two traceless self-adjoint operators ν_1 and ν_2 such that $\vartheta = \mathcal{K}_\rho(\nu_1) = \mathcal{K}_\rho(\nu_2)$, then $\mathcal{K}_\rho(\nu_1-\nu_2) = 0$. Applying the result in proposition E.2, we have $\nu_1 - \nu_2 = z\mathbb{I}_N$ for some $z \in \mathbb{C}$. Thus, $zN = \mathrm{tr}\{z\mathbb{I}_N\} = \mathrm{tr}\{\nu_1 - \nu_2\} = 0 \Rightarrow z = 0$, which implies the uniqueness of ν.

□

Lemma E.5. *Given an arbitrary traceless self-adjoint operator ν, the equality $\langle \nu+\lambda\mathbb{I}_N, \mathcal{K}_\rho(\nu+\lambda\mathbb{I}_N)\rangle = \langle \nu, \mathcal{K}_\rho(\nu)\rangle$ holds for an arbitrary number $\lambda \in \mathbb{C}$.*

Proof. Since $\mathcal{K}_\rho(\nu + \lambda\mathbb{I}_N) = \mathcal{K}_\rho(\nu) + \mathcal{K}_\rho(\lambda\mathbb{I}_N) = \mathcal{K}_\rho(\nu)$, we have

$$\begin{aligned}
\langle \nu + \lambda\mathbb{I}_N, \mathcal{K}_\rho(\nu + \lambda\mathbb{I}_N)\rangle &= \langle \nu + \lambda\mathbb{I}_N, \mathcal{K}_\rho(\nu)\rangle && \text{(E.25a)}\\
&= \langle \nu, \mathcal{K}_\rho(\nu)\rangle + \langle \lambda\mathbb{I}_N, \mathcal{K}_\rho(\nu)\rangle && \text{(E.25b)}\\
&= \langle \nu, \mathcal{K}_\rho(\nu)\rangle + \lambda^* \mathrm{tr}\{\mathcal{K}_\rho(\nu)\} && \text{(E.25c)}\\
&= \langle \nu, \mathcal{K}_\rho(\nu)\rangle, && \text{(E.25d)}
\end{aligned}$$

where we have used the traceless property of $\mathcal{K}_\rho$ obtained in proposition E.3. □

E.1.3 Lower bound of the quantum Wasserstein distance in terms of the trace-like distance

Here we derive the lower bound of the quantum Wasserstein distance $\mathcal{W}_\mathrm{q}(\rho_0, \rho_\tau)$ in terms of the trace-like distance. From the definition of the quantum Wasserstein distance, given a fixed positive number $\delta > 0$, there exists a smooth curve $\rho(t)$ with end points ρ_0 and ρ_τ such that

$$\tau \int_0^\tau \langle \nu, \mathcal{K}_\rho(\nu)\rangle dt \leq \mathcal{W}_\mathrm{q}(\rho_0, \rho_\tau)^2 + \delta. \tag{E.26}$$

Here, $\nu(t) \in \mathfrak{H}(\mathcal{H})$ is a traceless self-adjoint operator that satisfies $\dot{\rho}(t) = \mathcal{K}_\rho[\nu(t)]$. Let $\rho(t) = \sum_n p_n(t)|n(t)\rangle\langle n(t)|$ be a spectral decomposition with an orthogonal basis $\langle n(t)|m(t)\rangle = \delta_{nm}$, and define the self-adjoint operator $\phi(t) \coloneqq \sum_n c_n|n(t)\rangle\langle n(t)|$, where $|c_n| \leq 1$ are real constants to be determined later. Evidently, $\phi(t)$ commutes with $\rho(t)$, i.e., $[\phi, \rho] = 0$. Now, using the relations $\dot{\rho} = i\beta^{-1}[\nu, \rho] + \mathcal{O}_\rho(\nu)$ and $\langle \phi, [\nu, \rho]\rangle = 0$, we have

$$\sum_n c_n[p_n(\tau) - p_n(0)] = \mathrm{tr}\left\{\int_0^\tau \phi(t)\dot{\rho}(t)dt\right\} \tag{E.27a}$$

$$= \int_0^\tau \langle \phi, i\beta^{-1}[\nu, \rho] + \mathcal{O}_\rho(\nu)\rangle dt \tag{E.27b}$$

$$= \int_0^\tau \langle \phi, \mathcal{O}_\rho(\nu)\rangle dt \tag{E.27c}$$

$$\leq \left(\int_0^\tau \langle \phi, \mathcal{O}_\rho(\phi)\rangle dt\right)^{1/2} \left(\int_0^\tau \langle \nu, \mathcal{O}_\rho(\nu)\rangle dt\right)^{1/2} \tag{E.27d}$$

$$\leq \left(\tau^{-1}\int_0^\tau \langle \phi, \mathcal{O}_\rho(\phi)\rangle dt\right)^{1/2} \left(\mathcal{W}_{\mathrm{q}}(\rho_0, \rho_\tau)^2 + \delta\right)^{1/2}. \tag{E.27e}$$

The first term in the last inequality (E.27e) can be rewritten as

$$\langle \phi, \mathcal{O}_\rho(\phi)\rangle = \sum_{\mu,\omega} e^{-\beta\omega/2}\alpha_\mu(\omega)\langle \phi, [L_\mu(\omega), [\rho]_{\beta\omega}([L_\mu^\dagger(\omega), \phi])]\rangle \tag{E.28a}$$

$$= \sum_{\mu,\omega} e^{-\beta\omega/2}\alpha_\mu(\omega)\mathrm{tr}\left\{[\phi, L_\mu(\omega)][\rho]_{\beta\omega}([L_\mu^\dagger(\omega), \phi])\right\} \tag{E.28b}$$

$$= \sum_{\mu,\omega} e^{-\beta\omega/2}\alpha_\mu(\omega)\langle [L_\mu^\dagger(\omega), \phi], [\rho]_{\beta\omega}([L_\mu^\dagger(\omega), \phi])\rangle. \tag{E.28c}$$

Before proceeding, we prove the following result.

Proposition E.6. *For an arbitrary operator X, a real number θ, and density operator ρ, the inequality*

$$\langle X, [\rho]_\theta(X)\rangle \leq \frac{1}{2}(e^{\theta/2} + e^{-\theta/2})\|X\|_\infty^2 \tag{E.29}$$

holds, where $\|X\|_\infty$ denotes the spectral norm of the operator X.

Proof. Using Eq. (E.3), we have

$$\langle X, [\rho]_\theta(X)\rangle = \sum_{n,m} \Phi(e^{\theta/2}p_n, e^{-\theta/2}p_m)\langle n|X|m\rangle\langle m|X^\dagger|n\rangle. \tag{E.30}$$

Applying the inequality $\Phi(x, y) \leq (x + y)/2$ and the relation $\sum_n |n\rangle\langle n| = \mathbb{I}_N$, we obtain

$$\langle X, [\rho]_\theta(X)\rangle \leq \frac{1}{2}\sum_{n,m}\left(e^{\theta/2}p_n + e^{-\theta/2}p_m\right)\langle n|X|m\rangle\langle m|X^\dagger|n\rangle \tag{E.31a}$$

$$= \frac{1}{2}\sum_{n,m} e^{\theta/2}p_n\langle n|X|m\rangle\langle m|X^\dagger|n\rangle + \frac{1}{2}\sum_{m,n} e^{-\theta/2}p_m\langle m|X^\dagger|n\rangle\langle n|X|m\rangle \tag{E.31b}$$

$$= \frac{1}{2}\sum_{n} e^{\theta/2}p_n\langle n|XX^\dagger|n\rangle + \frac{1}{2}\sum_{m} e^{-\theta/2}p_m\langle m|X^\dagger X|m\rangle \tag{E.31c}$$

$$\leq \frac{1}{2}\sum_n e^{\theta/2} p_n \|X\|_\infty^2 + \frac{1}{2}\sum_m e^{-\theta/2} p_m \|X\|_\infty^2 \tag{E.31d}$$

$$= \frac{1}{2}(e^{\theta/2} + e^{-\theta/2})\|X\|_\infty^2. \tag{E.31e}$$

Here we applied two facts: $\langle n|XX^\dagger|n\rangle \leq \|X\|_\infty^2$ in Eq. (E.31d) and $\sum_n p_n = 1$ in Eq. (E.31e). □

Returning to our problem, we apply proposition E.6 with $X = [L_\mu^\dagger(\omega), \phi]$ and $\theta = \beta\omega$, and hence obtain

$$\langle [L_\mu^\dagger(\omega),\phi], [\rho]_{\beta\omega}([L_\mu^\dagger(\omega),\phi])\rangle \leq \frac{1}{2}(e^{-\beta\omega/2}+e^{\beta\omega/2})\|[L_\mu^\dagger(\omega),\phi]\|_\infty^2 \leq 2(e^{-\beta\omega/2}+e^{\beta\omega/2})\|L_\mu(\omega)\|_\infty^2. \tag{E.32}$$

Here, we used the inequalities $\|[X,Y]\|_\infty \leq \|XY\|_\infty + \|YX\|_\infty$ and $\|XY\|_\infty \leq \|X\|_\infty\|Y\|_\infty$ for all $X, Y \in \mathfrak{L}(\mathcal{H})$. Consequently, we have

$$\langle \phi, \mathcal{O}_\rho(\phi)\rangle \leq 2\sum_{\mu,\omega} e^{-\beta\omega/2}\alpha_\mu(\omega)(e^{-\beta\omega/2} + e^{\beta\omega/2})\|L_\mu(\omega)\|_\infty^2 = 4\sum_{\mu,\omega}\alpha_\mu(\omega)\|L_\mu(\omega)\|_\infty^2. \tag{E.33}$$

From Eqs. (E.27e) and (E.33), we easily obtain the following inequality:

$$\mathcal{W}_{\mathrm{q}}(\rho_0,\rho_\tau)^2 + \delta \geq \frac{(\sum_n c_n[p_n(\tau) - p_n(0)])^2}{4\tau^{-1}\int_0^\tau \sum_{\mu,\omega}\alpha_\mu(\omega)\|L_\mu(\omega)\|_\infty^2 dt}. \tag{E.34}$$

Setting $c_n = \mathrm{sign}[p_n(\tau) - p_n(0)]$ and taking the limit $\delta \to 0$ in Eq. (E.34), a lower bound of the quantum Wasserstein distance is obtained as

$$\mathcal{W}_{\mathrm{q}}(\rho_0,\rho_\tau) \geq \frac{\sum_n |p_n(\tau) - p_n(0)|}{2\sqrt{\tau^{-1}\int_0^\tau \sum_{\mu,\omega}\alpha_\mu(\omega)\|L_\mu(\omega)\|_\infty^2 dt}}. \tag{E.35}$$

From Eq. (E.35), we wish to bound the Wasserstein distance by the trace-like distance $\mathsf{d}_{\mathrm{T}}(\rho_0,\rho_\tau) = \sum_{n=1}^N |a_n - b_n|$, where $a_1 \leq a_2 \leq \cdots \leq a_N$ and $b_1 \leq b_2 \leq \cdots \leq b_N$ are increasing eigenvalues of ρ_0 and ρ_τ. Given two arrays of real numbers, $\{x_n\}$ and $\{y_n\}$, one can prove that

$$\sum_n |x_n - y_n| \geq \sum_n |x_n - y_{\chi(n)}|, \tag{E.36}$$

where $\{\chi(n)\}$ is a permutation of $\{n\}$ such that $y_{\chi(n)} \geq y_{\chi(m)}$ if $x_n \geq x_m$. Therefore, $\sum_n |p_n(\tau) - p_n(0)| \geq \mathsf{d}_{\mathrm{T}}(\rho_0,\rho_\tau)$, so the bound in terms of the trace-like distance is written as

$$\mathcal{W}_{\mathrm{q}}(\rho_0,\rho_\tau) \geq \frac{\mathsf{d}_{\mathrm{T}}(\rho_0,\rho_\tau)}{2\sqrt{\tau^{-1}\int_0^\tau \sum_{\mu,\omega}\alpha_\mu(\omega)\|L_\mu(\omega)\|_\infty^2 dt}}. \tag{E.37}$$

E.1.4 Lower bound of the entropy production in terms of the average energy-change distance

Here we derive the lower bound of the entropy production ΔS_{tot} in terms of the distance $\mathsf{d}_{\mathrm{E}}(\rho_0,\rho_\tau) = |\mathrm{tr}\{H(\rho_0 - \rho_\tau)\}|$. The Lindblad master equation can be expressed as $\dot\rho(t) = -i[H,\rho(t)] + \mathcal{O}_\rho[\phi(t)]$, where $\phi(t) := -\ln\rho(t) + \ln\rho^{\mathrm{eq}}$. Using the relations $\mathrm{tr}\{H[H,\rho]\} = 0$

and $\Delta S_{\mathrm{tot}} = \int_0^\tau \langle \phi, O_\rho(\phi)\rangle dt$, we obtain

$$|\mathrm{tr}\{H(\rho_0-\rho_\tau)\}| = \left|\mathrm{tr}\left\{H\int_0^\tau \dot{\rho}(t)dt\right\}\right| \tag{E.38a}$$

$$= \left|\int_0^\tau \langle H, O_\rho(\phi)\rangle dt\right| \tag{E.38b}$$

$$\leq \left(\int_0^\tau \langle H, O_\rho(H)\rangle dt\right)^{1/2}\left(\int_0^\tau \langle \phi, O_\rho(\phi)\rangle dt\right)^{1/2} \tag{E.38c}$$

$$= \left(\int_0^\tau \langle H, O_\rho(H)\rangle dt\right)^{1/2}\sqrt{\Delta S_{\mathrm{tot}}}. \tag{E.38d}$$

The first term in Eq. (E.38d) can be rewritten as

$$\langle H, O_\rho(H)\rangle = \sum_{\mu,\omega} e^{-\beta\omega/2}\alpha_\mu(\omega)\langle H, [L_\mu(\omega), [\rho]_{\beta\omega}([L_\mu^\dagger(\omega), H])]\rangle \tag{E.39a}$$

$$= \sum_{\mu,\omega} e^{-\beta\omega/2}\alpha_\mu(\omega)\mathrm{tr}\left\{[H, L_\mu(\omega)][\rho]_{\beta\omega}([L_\mu^\dagger(\omega), H])\right\} \tag{E.39b}$$

$$= \sum_{\mu,\omega} e^{-\beta\omega/2}\alpha_\mu(\omega)\langle [L_\mu^\dagger(\omega), H], [\rho]_{\beta\omega}([L_\mu^\dagger(\omega), H])\rangle. \tag{E.39c}$$

Applying proposition E.6 with $X = [L_\mu^\dagger(\omega), H]$ and $\theta = \beta\omega$, one obtains

$$\begin{aligned}\langle [L_\mu^\dagger(\omega), H], [\rho]_{\beta\omega}([L_\mu^\dagger(\omega), H])\rangle &\leq \frac{1}{2}(e^{-\beta\omega/2}+e^{\beta\omega/2})\|[L_\mu^\dagger(\omega), H]\|_\infty^2 \\ &= \frac{1}{2}(e^{-\beta\omega/2}+e^{\beta\omega/2})\omega^2\|L_\mu(\omega)\|_\infty^2.\end{aligned} \tag{E.40}$$

Consequently, we have

$$\langle H, O_\rho(H)\rangle \leq \frac{1}{2}\sum_{\mu,\omega} e^{-\beta\omega/2}\alpha_\mu(\omega)(e^{-\beta\omega/2}+e^{\beta\omega/2})\omega^2\|L_\mu(\omega)\|_\infty^2 = \sum_{\mu,\omega}\alpha_\mu(\omega)\omega^2\|L_\mu(\omega)\|_\infty^2. \tag{E.41}$$

From Eqs. (E.38d) and (E.41), we readily obtain the following inequality:

$$\Delta S_{\mathrm{tot}} \geq \frac{\mathsf{d}_{\mathrm{E}}(\rho_0,\rho_\tau)^2}{\tau\sum_{\mu,\omega}\alpha_\mu(\omega)\omega^2\|L_\mu(\omega)\|_\infty^2}. \tag{E.42}$$

A tighter bound in terms of the square of the heat current can be analogously obtained. Applying the Cauchy–Schwarz inequality, we have

$$\int_0^\tau |\dot{Q}|dt = \int_0^\tau |\mathrm{tr}\{H\dot{\rho}(t)\}|\,dt \tag{E.43a}$$

$$= \int_0^\tau |\langle H, O_\rho(\phi)\rangle| dt \tag{E.43b}$$

$$\leq \left(\int_0^\tau \langle H, O_\rho(H)\rangle dt\right)^{1/2}\left(\int_0^\tau \langle \phi, O_\rho(\phi)\rangle dt\right)^{1/2} \tag{E.43c}$$

$$= \left(\int_0^\tau \langle H, O_\rho(H)\rangle dt\right)^{1/2}\sqrt{\Delta S_{\mathrm{tot}}}. \tag{E.43d}$$

Subsequently, applying Eq. (E.41), we obtain

$$\Delta S_{\mathrm{tot}} \geq \frac{\left(\int_0^\tau |\dot{Q}|dt\right)^2}{\tau \sum_{\mu,\omega} \alpha_\mu(\omega)\omega^2 \|L_\mu(\omega)\|_\infty^2}. \tag{E.44}$$

This bound is a quantum version of the classical bound reported in Ref. [261], in which the total entropy production is bounded from below by the square of the heat current.

Analogously, we can also derive a lower bound on ΔS_{tot} in terms of the change of entropy ΔS of the system. First, we can bound ΔS from above as

$$\begin{aligned}
|\Delta S| &\leq \int_0^\tau |\mathrm{tr}\{\dot{\rho}(t)\ln\rho(t)\}|dt && \text{(E.45a)}\\
&= \int_0^\tau |\langle \ln\rho, \mathcal{O}_\rho(\phi)\rangle| dt && \text{(E.45b)}\\
&\leq \left(\int_0^\tau \langle \ln\rho, \mathcal{O}_\rho(\ln\rho)\rangle dt\right)^{1/2} \left(\int_0^\tau \langle \phi, \mathcal{O}_\rho(\phi)\rangle dt\right)^{1/2} && \text{(E.45c)}\\
&= \sqrt{\Upsilon}\sqrt{\Delta S_{\mathrm{tot}}}, && \text{(E.45d)}
\end{aligned}$$

where $\Upsilon := \int_0^\tau \langle \ln\rho, \mathcal{O}_\rho(\ln\rho)\rangle dt$. Then, the total entropy production can be bounded from below as

$$\Delta S_{\mathrm{tot}} \geq \frac{|\Delta S|^2}{\Upsilon}. \tag{E.46}$$

Equivalently, the heat dissipated to the environment can be bounded from below as

$$\Delta Q \geq \beta^{-1}\left(-\Delta S + \frac{|\Delta S|^2}{\Upsilon}\right). \tag{E.47}$$

This bound is relevant to the inequality reported in Ref. [13], $\Delta Q \geq Q(\mathcal{S}^{-1}(-\Delta S))$. However, the bound in Eq. (E.47) is not tight in the zero-temperature limit.

E.1.5 Current-dissipation trade-off

Here we derive a trade-off relation between the heat current and dissipation, i.e., we derive an upper bound on the ratio $J^2/\sigma_{\mathrm{tot}}$, where $J := \mathrm{tr}\{H(t)\dot{\rho}(t)\}$ is the heat flow from the heat bath to the system and σ_{tot} is the total entropy production rate, which characterizes the irreversibility. Using the relations $\dot{\rho}(t) = -i[H(t),\rho(t)] + \mathcal{O}_\rho[\phi(t)]$ and $\sigma_{\mathrm{tot}} = \langle \phi(t), \mathcal{O}_\rho[\phi(t)]\rangle$ and applying the Cauchy–Schwarz inequality, we obtain

$$\begin{aligned}
J^2 = |\mathrm{tr}\{H(t)\dot{\rho}(t)\}|^2 &= |\langle H(t), \mathcal{O}_\rho[\phi(t)]\rangle|^2 && \text{(E.48a)}\\
&\leq \langle H(t), \mathcal{O}_\rho[H(t)]\rangle\langle \phi(t), \mathcal{O}_\rho[\phi(t)]\rangle && \text{(E.48b)}\\
&= \langle H(t), \mathcal{O}_\rho[H(t)]\rangle \sigma_{\mathrm{tot}}. && \text{(E.48c)}
\end{aligned}$$

Note that

$$\langle H(t), \mathcal{O}_\rho[H(t)]\rangle = \sum_{\mu,\omega} e^{-\beta\omega/2}\alpha_\mu(\omega)\langle [L_\mu^\dagger(\omega), H(t)], [\rho]_{\beta\omega}([L_\mu^\dagger(\omega), H(t)])\rangle \tag{E.49a}$$

$$= \sum_{\mu,\omega} e^{-\beta\omega/2}\alpha_\mu(\omega)\omega^2\langle L_\mu^\dagger(\omega), [\rho]_{\beta\omega}(L_\mu^\dagger(\omega))\rangle. \tag{E.49b}$$

From Eq. (E.31c), one can prove that

$$\langle H(t), O_\rho[H(t)]\rangle \le \frac{1}{2}\sum_{\mu,\omega} e^{-\beta\omega/2}\alpha_\mu(\omega)\omega^2\left[e^{\beta\omega/2}\mathrm{tr}\left\{L_\mu^\dagger(\omega)L_\mu(\omega)\rho\right\} + e^{-\beta\omega/2}\mathrm{tr}\left\{L_\mu(\omega)L_\mu^\dagger(\omega)\rho\right\}\right] \tag{E.50a}$$

$$= \sum_{\mu,\omega}\alpha_\mu(\omega)\omega^2\mathrm{tr}\left\{L_\mu^\dagger(\omega)L_\mu(\omega)\rho\right\} \tag{E.50b}$$

$$= \mathrm{tr}\left\{\mathsf{L}\rho\right\}, \tag{E.50c}$$

where $\mathsf{L} \coloneqq \sum_{\mu,\omega}\alpha_\mu(\omega)\omega^2 L_\mu^\dagger(\omega)L_\mu(\omega)$. Decomposing $\rho = \rho_{\mathrm{bd}} + \rho_{\mathrm{nd}}$, where

$$\rho_{\mathrm{bd}} = \sum_e \Pi_e\rho\Pi_e, \tag{E.51a}$$

$$\rho_{\mathrm{nd}} = \sum_{e\neq e'} \Pi_e\rho\Pi_{e'}, \tag{E.51b}$$

and Π_e is the projection to the eigenspace of H with eigenvalue e. As $[L_\mu^\dagger(\omega)L_\mu(\omega), H(t)] = 0$, $[L_\mu^\dagger(\omega)L_\mu(\omega), \Pi_e] = 0$ for all e. Therefore, the coherence between eigenstates with different energies vanishes in $\mathrm{tr}\{\mathsf{L}\rho\}$, i.e., $\mathrm{tr}\{\mathsf{L}\rho\} = \mathrm{tr}\{\mathsf{L}\rho_{\mathrm{bd}}\}$. The trade-off relation between the heat current and dissipation is thus obtained as

$$\frac{J^2}{\sigma_{\mathrm{tot}}} \le \langle H, O_\rho(H)\rangle \le \mathrm{tr}\left\{\mathsf{L}\rho_{\mathrm{bd}}\right\}. \tag{E.52}$$

This inequality, known as the current-dissipation trade-off relation [263], implies that the ratio $J^2/\sigma_{\mathrm{tot}}$ is not enhanced by coherence between eigenstates with different energies, but is enhanced by coherence between degenerate energy eigenstates.

E.1.6 Invalidity of the bound in terms of the relative entropy

Here we prove that the total entropy production in thermalization processes cannot be bounded from below by the relative entropy between the initial and final states. In thermalization processes, the dynamics of the density operator are governed by the Lindblad equation

$$\dot\rho = -i[H,\rho] + \sum_{\mu,\omega}\alpha_\mu(\omega)\left[2L_\mu(\omega)\rho L_\mu^\dagger(\omega) - \left\{L_\mu^\dagger(\omega)L_\mu(\omega), \rho\right\}\right]. \tag{E.53}$$

The total entropy production can be explicitly expressed as $\Delta S_{\mathrm{tot}} = S(\rho(0)||\rho^{\mathrm{eq}}) - S(\rho(\tau)||\rho^{\mathrm{eq}})$, where $S(\rho_1||\rho_2) \coloneqq \mathrm{tr}\{\rho_1(\ln\rho_1 - \ln\rho_2)\}$ is the relative entropy of ρ_1 with respect to ρ_2. If the relative entropy satisfies the reverse triangle inequality:

$$S(\rho(0)||\rho^{\mathrm{eq}}) \ge S(\rho(0)||\rho(\tau)) + S(\rho(\tau)||\rho^{\mathrm{eq}}), \tag{E.54}$$

then $\Delta S_{\mathrm{tot}} \ge S(\rho(0)||\rho(\tau))$ and the dissipation can be further bounded by the quantum Fisher information and Wigner–Yanase metrics [214]. However, this inequality holds in the classical

case [228] but not in the general quantum case. As a simple counterexample, consider that $\alpha_\mu(\omega) \to 0$ for all μ and ω. In this vanishing coupling limit, the total entropy production vanishes because the relative entropy is invariant under a unitary transform. On the other hand, $S(\rho(0)||\rho(\tau))$ is always positive because $\rho(t)$ is changed under the internal dynamics; thus $\Delta S_{\rm tot} < S(\rho(0)||\rho(\tau))$.

E.1.7 Quantum Otto heat engine

Consider a quantum Otto heat engine consisting of a two-level atom, whose energy levels (the excited state $|e\rangle$ and the ground state $|g\rangle$) are changed by an external controller. The atom is alternatively coupled with two heat baths at different inverse temperatures $\beta_h < \beta_c$, and undergoes two isochoric and two adiabatic processes. The system Hamiltonian is given by $H(t) = \omega(t)\sigma_z/2$, where $\sigma_z = |e\rangle\langle e| - |g\rangle\langle g|$ is the Pauli matrix in the z direction. The heat engine is cyclically operated as follows:

1. During adiabatic expansion in time τ_a, the frequency changes from ω_h to ω_c, and work is produced due to the change in internal energy. Here, the word *adiabatic* means that the system is isolated from the heat baths and there is no heat exchange during the process, although jumps between energy eigenstates may occur.

2. During the cold isochore in time τ_c, the atom is in contact with the cold bath and the frequency ω_c remains unchanged. In this process, heat Q_c is transferred from the working medium to the cold bath.

3. During adiabatic compression in time τ_a, the frequency is reversed from ω_c to ω_h and work is done on the medium.

4. During the hot isochore in time τ_h, the atom is in contact with the hot bath and the frequency ω_h is fixed. In this process, heat Q_h is extracted from the hot bath by the working medium.

During the adiabatic process, the dynamics of the density matrix are governed by the von Neumann equation

$$\dot{\rho}(t) = -i[H(t), \rho(t)]. \tag{E.55}$$

During an isochoric process $k = h$ or c, the atom is thermalized and the time evolution of the density matrix follows the Lindblad master equation [80]:

$$\dot{\rho}(t) = -i[H_k, \rho(t)] + \mathcal{D}_k[\rho(t)], \tag{E.56}$$

where the dissipator $\mathcal{D}_k[\cdot]$ is defined by

$$\mathcal{D}_k[\rho] = \alpha_k \bar{n}(\omega_k)(2\sigma_+\rho\sigma_- - \{\sigma_-\sigma_+, \rho\}) + \alpha_k(\bar{n}(\omega_k)+1)(2\sigma_-\rho\sigma_+ - \{\sigma_+\sigma_-, \rho\}). \tag{E.57}$$

Here, $H_k = \omega_k\sigma_z/2$, $\sigma_\pm = (\sigma_x \pm i\sigma_y)/2$, α_k is a positive damping rate, and $\bar{n}(\omega_k) = (e^{\beta_k\omega_k} - 1)^{-1}$ is the Planck distribution.

Analytical solution of the density matrix

In the stationary state, the density matrix can be analytically calculated as

$$\rho(t) = (e^{\lambda(t)} + e^{-\lambda(t)})^{-1} e^{\lambda(t)\sigma_z}, \tag{E.58}$$

where $\lambda(t)$ is a periodic function satisfying $\lambda(t+\tau) = \lambda(t)$ with $\tau = 2\tau_a + \tau_h + \tau_c$. In the following analysis, we determine the analytical form of $\lambda(t)$. For any operators X and Y, one can prove that

$$e^{-\lambda X} Y e^{\lambda X} = \sum_{n=0}^{\infty} \frac{(-\lambda)^n}{n!} [X,Y]_n, \tag{E.59}$$

where the nested commutator is recursively defined as $[X,Y]_n = [X,[X,Y]_{n-1}]$ and $[X,Y]_0 = Y$. Using the relations $[\sigma_z,\sigma_+] = 2\sigma_+$ and $[\sigma_z,\sigma_-] = -2\sigma_-$, one readily obtains

$$[\sigma_z,\sigma_+]_n = (+2)^n \sigma_+, \tag{E.60a}$$

$$[\sigma_z,\sigma_-]_n = (-2)^n \sigma_-. \tag{E.60b}$$

Subsequently,

$$e^{-\lambda\sigma_z}\sigma_+ e^{\lambda\sigma_z} = \sum_{n=0}^{\infty} \frac{(-\lambda)^n (2)^n}{n!} \sigma_+ = e^{-2\lambda}\sigma_+ \Leftrightarrow e^{\lambda\sigma_z}\sigma_+ = e^{2\lambda}\sigma_+ e^{\lambda\sigma_z}, \tag{E.61a}$$

$$e^{-\lambda\sigma_z}\sigma_- e^{\lambda\sigma_z} = \sum_{n=0}^{\infty} \frac{(-\lambda)^n (-2)^n}{n!} \sigma_- = e^{2\lambda}\sigma_- \Leftrightarrow e^{\lambda\sigma_z}\sigma_- = e^{-2\lambda}\sigma_- e^{\lambda\sigma_z}. \tag{E.61b}$$

Noting that $\sigma_+\sigma_- = (\mathbb{I}_2 + \sigma_z)/2$ and $\sigma_-\sigma_+ = (\mathbb{I}_2 - \sigma_z)/2$, the dissipator term can be calculated as

$$\mathcal{D}_k[e^{\lambda\sigma_z}] = \alpha_k \bar{n}(\omega_k)(2\sigma_+ e^{\lambda\sigma_z}\sigma_- - \{\sigma_-\sigma_+, e^{\lambda\sigma_z}\}) + \alpha_k(\bar{n}(\omega_k)+1)(2\sigma_- e^{\lambda\sigma_z}\sigma_+ - \{\sigma_+\sigma_-, e^{\lambda\sigma_z}\}) \tag{E.62a}$$

$$= 2\left[\alpha_k \bar{n}(\omega_k)(e^{-2\lambda}\sigma_+\sigma_- - \sigma_-\sigma_+) + \alpha_k(\bar{n}(\omega_k)+1)(e^{2\lambda}\sigma_-\sigma_+ - \sigma_+\sigma_-)\right] e^{\lambda\sigma_z} \tag{E.62b}$$

$$= \alpha_k \Big[\bar{n}(\omega_k)(e^{-2\lambda}-1) + (\bar{n}(\omega_k)+1)(e^{2\lambda}-1) + \left\{\bar{n}(\omega_k)(e^{-2\lambda}+1) - (\bar{n}(\omega_k)+1)(e^{2\lambda}+1)\right\}\sigma_z\Big] e^{\lambda\sigma_z}. \tag{E.62c}$$

Inserting Eqs. (E.58) and (E.62) into Eq. (E.56), we obtain

$$\left[-\frac{e^{\lambda}-e^{-\lambda}}{e^{\lambda}+e^{-\lambda}} + \sigma_z\right]\dot{\lambda}(t) = \alpha_k\Big[\bar{n}(\omega_k)(e^{-2\lambda}-1) + (\bar{n}(\omega_k)+1)(e^{2\lambda}-1) \tag{E.63}$$

$$+ \left\{\bar{n}(\omega_k)(e^{-2\lambda}+1) - (\bar{n}(\omega_k)+1)(e^{2\lambda}+1)\right\}\sigma_z\Big], \tag{E.64}$$

which is satisfied if $\lambda(t)$ obeys the following differential equation:

$$\dot{\lambda}(t) = \alpha_k\left[\bar{n}(\omega_k)(e^{-2\lambda}+1) - (\bar{n}(\omega_k)+1)(e^{2\lambda}+1)\right]. \tag{E.65}$$

This equation can be analytically solved for $\lambda(t)$. The result is

$$\lambda(t) = \begin{cases} \lambda(\tau_a), & \text{if } 0 \le t < \tau_a, \\ \frac{1}{2}\ln\left[\frac{\bar{n}(\omega_c)e^{2\alpha_c(2\bar{n}(\omega_c)+1)(t-\tau_a)}-z_c}{(\bar{n}(\omega_c)+1)e^{2\alpha_c(2\bar{n}(\omega_c)+1)(t-\tau_a)}+z_c}\right], & \text{if } \tau_a \le t < \tau_a+\tau_c, \\ \lambda(2\tau_a+\tau_c), & \text{if } \tau_a+\tau_c \le t < 2\tau_a+\tau_c, \\ \frac{1}{2}\ln\left[\frac{\bar{n}(\omega_h)e^{2\alpha_h(2\bar{n}(\omega_h)+1)(t-2\tau_a-\tau_c)}-z_h}{(\bar{n}(\omega_h)+1)e^{2\alpha_h(2\bar{n}(\omega_h)+1)(t-2\tau_a-\tau_c)}+z_h}\right], & \text{if } 2\tau_a+\tau_c \le t < \tau, \end{cases} \tag{E.66}$$

where the constant z_k can be explicitly determined through the boundary conditions as

$$z_c = [2\bar{n}(\omega_c)+1]\left(\frac{\bar{n}(\omega_c)}{2\bar{n}(\omega_c)+1} - \frac{\bar{n}(\omega_h)}{2\bar{n}(\omega_h)+1}\right) \Bigg/ \left[1+\frac{1-e^{-2\alpha_c(2\bar{n}(\omega_c)+1)\tau_c}}{e^{2\alpha_h(2\bar{n}(\omega_h)+1)\tau_h}-1}\right], \tag{E.67a}$$

$$z_h = [2\bar{n}(\omega_h)+1]\left(\frac{\bar{n}(\omega_h)}{2\bar{n}(\omega_h)+1} - \frac{\bar{n}(\omega_c)}{2\bar{n}(\omega_c)+1}\right) \Bigg/ \left[1+\frac{1-e^{-2\alpha_h(2\bar{n}(\omega_h)+1)\tau_h}}{e^{2\alpha_c(2\bar{n}(\omega_c)+1)\tau_c}-1}\right]. \tag{E.67b}$$

Thermodynamics and efficiency

For each $1 \le i \le 4$, let ρ_i denote the density matrix at the beginning of process i. Note that the density matrix is unchanged during the adiabatic processes, i.e., $\rho_1 = \rho_2$ and $\rho_3 = \rho_4$. During an isochoric process, a heat quantity $Q_c = \mathrm{tr}\{H_c(\rho_2-\rho_3)\}$ is transferred to the cold bath, or a heat quantity $Q_h = \mathrm{tr}\{H_h(\rho_1-\rho_4)\}$ is extracted from the hot bath. The total work W extracted from the working medium is

$$-W = \int_0^{\tau_a} \mathrm{tr}\{\partial_t H(t)\rho(t)\}\,dt + \int_{\tau_a+\tau_c}^{\tau-\tau_h} \mathrm{tr}\{\partial_t H(t)\rho(t)\}\,dt = \mathrm{tr}\{\rho_1(H_c-H_h)\} + \mathrm{tr}\{\rho_3(H_h-H_c)\}. \tag{E.68}$$

By conservation of energy, we have $-W+Q_h-Q_c=0$. The efficiency η is then defined as

$$\eta := \frac{W}{Q_h} = 1 - \frac{Q_c}{Q_h}. \tag{E.69}$$

The total entropy produced during the isochoric processes is

$$\Delta S^h_{\mathrm{tot}} = \Delta S_h - \beta_h Q_h \ge 0, \tag{E.70a}$$

$$\Delta S^c_{\mathrm{tot}} = \Delta S_c + \beta_c Q_c \ge 0, \tag{E.70b}$$

where $\Delta S_h = \mathrm{tr}\{\rho_4 \ln \rho_4\} - \mathrm{tr}\{\rho_1 \ln \rho_1\}$ and $\Delta S_c = \mathrm{tr}\{\rho_2 \ln \rho_2\} - \mathrm{tr}\{\rho_3 \ln \rho_3\}$ are the changes in the von Neumann entropy during the hot and cold isochoric processes, respectively. As $\Delta S_h + \Delta S_c = 0$, $\beta_c Q_c - \beta_h Q_h \ge 0$ follows from the second law of thermodynamics. Using this inequality, one can prove that η cannot exceed the Carnot efficiency, given by

$$\eta \le 1 - \frac{\beta_h}{\beta_c} =: \eta_{\mathrm{C}}. \tag{E.71}$$

In the following, we tighten the bound on the efficiency. According to Eqs. (7.56) and (7.57), the total entropy productions during the isochoric processes are bounded from below by the

distances $\mathsf{d}_{\mathrm{T}}(\cdot,\cdot)$ and $\mathsf{d}_{\mathrm{E}}(\cdot,\cdot)$ as follows:

$$\Delta S^h_{\mathrm{tot}} = \Delta S_h - \beta_h Q_h \geq \max\left\{\frac{\mathsf{d}_{\mathrm{T}}(\rho_1,\rho_4)^2}{4\tau_h \mathcal{A}^h_{\mathrm{T}}}, \frac{\mathsf{d}_{\mathrm{E}}(\rho_1,\rho_4)^2}{\tau_h \mathcal{A}^h_{\mathrm{E}}}\right\}, \tag{E.72}$$

$$\Delta S^c_{\mathrm{tot}} = \Delta S_c + \beta_c Q_c \geq \max\left\{\frac{\mathsf{d}_{\mathrm{T}}(\rho_2,\rho_3)^2}{4\tau_c \mathcal{A}^c_{\mathrm{T}}}, \frac{\mathsf{d}_{\mathrm{E}}(\rho_2,\rho_3)^2}{\tau_c \mathcal{A}^c_{\mathrm{E}}}\right\}. \tag{E.73}$$

Here, $\mathcal{A}^k_{\mathrm{T}} := \alpha_k(2\bar{n}(\omega_k)+1)$ and $\mathcal{A}^k_{\mathrm{E}} := \omega_k^2\alpha_k(2\bar{n}(\omega_k)+1)$ for $k = h$ or c. From Eqs. (E.72) and (E.73), we obtain

$$\beta_c Q_c - \beta_h Q_h \geq \max\left\{\frac{\mathsf{d}_{\mathrm{T}}(\rho_1,\rho_4)^2}{4\tau_h \mathcal{A}^h_{\mathrm{T}}}, \frac{\mathsf{d}_{\mathrm{E}}(\rho_1,\rho_4)^2}{\tau_h \mathcal{A}^h_{\mathrm{E}}}\right\} + \max\left\{\frac{\mathsf{d}_{\mathrm{T}}(\rho_2,\rho_3)^2}{4\tau_c \mathcal{A}^c_{\mathrm{T}}}, \frac{\mathsf{d}_{\mathrm{E}}(\rho_2,\rho_3)^2}{\tau_c \mathcal{A}^c_{\mathrm{E}}}\right\} =: \mathfrak{g}. \tag{E.74}$$

Consequently, a tighter bound on η is obtained as

$$\eta \leq \eta_{\mathrm{C}} - \frac{\mathfrak{g}}{\beta_c Q_h} =: \eta_{\mathrm{G}}. \tag{E.75}$$

E.2 Classical Markov jump processes

E.2.1 Alternative expression of the classical master equation

We now show that the master equation $\dot{\boldsymbol{p}} = \mathsf{R}\boldsymbol{p}$ can be expressed as $\dot{\boldsymbol{p}} = \mathsf{K}_p \boldsymbol{f}$, where $\mathsf{R} = [R_{mn}]$ with $R_{nn} = -\sum_{m(\neq n)} R_{mn}$, $\mathsf{K}_p = \sum_{1\leq n<m\leq N} R_{nm} p_m^{\mathrm{eq}} \Phi\left(\frac{p_n}{p_n^{\mathrm{eq}}}, \frac{p_m}{p_m^{\mathrm{eq}}}\right) \mathsf{E}_{nm}$, and $\boldsymbol{f} = -\nabla_{\boldsymbol{p}} D(\boldsymbol{p}||\boldsymbol{p}^{\mathrm{eq}})$. Here, $\nabla_{\boldsymbol{p}} := [\partial_{p_1}, \ldots, \partial_{p_N}]^{\top}$. Specifically, we need to show that

$$(\mathsf{K}_p \boldsymbol{f})_n = \sum_{m(\neq n)} [R_{nm} p_m - R_{mn} p_n] \tag{E.76}$$

holds for all n. Indeed, using the relations $f_n = -(\ln p_n - \ln p_n^{\mathrm{eq}} - 1)$ and $R_{nm} p_m^{\mathrm{eq}} = R_{mn} p_n^{\mathrm{eq}}$, Eq. (E.76) can be verified as follows:

$$(\mathsf{K}_p \boldsymbol{f})_n = \sum_{m(\neq n)} R_{nm} p_m^{\mathrm{eq}} \Phi\left(\frac{p_n}{p_n^{\mathrm{eq}}}, \frac{p_m}{p_m^{\mathrm{eq}}}\right) (\mathsf{E}_{nm} \boldsymbol{f})_n \tag{E.77a}$$

$$= \sum_{m(\neq n)} R_{nm} p_m^{\mathrm{eq}} \Phi\left(\frac{p_n}{p_n^{\mathrm{eq}}}, \frac{p_m}{p_m^{\mathrm{eq}}}\right) (f_n - f_m) \tag{E.77b}$$

$$= \sum_{m(\neq n)} R_{nm} p_m^{\mathrm{eq}} \frac{p_n/p_n^{\mathrm{eq}} - p_m/p_m^{\mathrm{eq}}}{\ln p_n - \ln p_n^{\mathrm{eq}} - \ln p_m + \ln p_m^{\mathrm{eq}}} (\ln p_m - \ln p_m^{\mathrm{eq}} - \ln p_n + \ln p_n^{\mathrm{eq}}) \tag{E.77c}$$

$$= \sum_{m(\neq n)} R_{nm} p_m^{\mathrm{eq}} \left(\frac{p_m}{p_m^{\mathrm{eq}}} - \frac{p_n}{p_n^{\mathrm{eq}}}\right) \tag{E.77d}$$

$$= \sum_{m(\neq n)} [R_{nm} p_m - R_{mn} p_n]. \tag{E.77e}$$

E.2.2 Properties of the matrix K_p

The matrix K_p is symmetric and positive semi-definite. Its properties are given below.

Lemma E.7. *For an arbitrary distribution* $\boldsymbol{p}$ *satisfying* $p_n > 0$ *for all* n, $\ker(\mathsf{K}_p) = \{\boldsymbol{v} \in \mathbb{R}^{N\times 1} \mid \boldsymbol{v} \propto \mathbf{1}\}$.

Proof. As the system is irreducible, there exists a set of $N-1$ unordered pairs, $\mathcal{Y} = \{(i,j) \mid R_{ij} \neq 0\}$, such that for arbitrary states $n \neq m$, there is a path $n = i_0 \to i_1 \to \cdots \to i_k = m$ and $(i_l, i_{l+1}) \in \mathcal{Y}$ for all $0 \le l \le k-1$. Assuming $\boldsymbol{v} \in \ker(\mathsf{K}_p)$, we have

$$0 = \langle \boldsymbol{v}, \mathsf{K}_p \boldsymbol{v}\rangle = \sum_{1\le n<m\le N} R_{nm} p_m^{\mathrm{eq}} \Phi\left(\frac{p_n}{p_n^{\mathrm{eq}}}, \frac{p_m}{p_m^{\mathrm{eq}}}\right)(v_m - v_n)^2. \tag{E.78}$$

This expression means that $v_i - v_j = 0$ for all $(i,j) \in \mathcal{Y}$, or equivalently, $\boldsymbol{v} \propto \mathbf{1}$. □

Lemma E.8. *There exists a vector* $\boldsymbol{v}$ *for which* $\dot{\boldsymbol{p}} = \mathsf{K}_p \boldsymbol{v}$. *Such a vector is unique under the condition* $\langle \mathbf{1}, \boldsymbol{v}\rangle = 0$.

Proof. For any $\boldsymbol{v}$ satisfying $\mathsf{K}_p \boldsymbol{v} = 0$ [i.e., $\boldsymbol{v} \in \ker(\mathsf{K}_p)$], then $\boldsymbol{v} \propto \mathbf{1} \Rightarrow \boldsymbol{v}^\top \dot{\boldsymbol{p}} = 0$; equivalently, $\dot{\boldsymbol{p}} \in \ker(\mathsf{K}_p)^\perp$. According to the Fredholm alternative, the equation $\dot{\boldsymbol{p}} = \mathsf{K}_p \boldsymbol{v}$ always has a nonzero solution $\boldsymbol{v}$. Defining $\overline{\boldsymbol{v}} := \boldsymbol{v} - N^{-1}\langle \mathbf{1}, \boldsymbol{v}\rangle \mathbf{1}$, we can write $\dot{\boldsymbol{p}} = \mathsf{K}_p \overline{\boldsymbol{v}}$ and $\langle \mathbf{1}, \overline{\boldsymbol{v}}\rangle = 0$. Assume that there exist two solutions $\boldsymbol{v}_1$ and $\boldsymbol{v}_2$ satisfying $\langle \mathbf{1}, \boldsymbol{v}_1\rangle = \langle \mathbf{1}, \boldsymbol{v}_2\rangle = 0$. We then have $\mathsf{K}_p(\boldsymbol{v}_1 - \boldsymbol{v}_2) = 0 \Rightarrow \boldsymbol{v}_1 - \boldsymbol{v}_2 = c\mathbf{1}$ for some $c \in \mathbb{R}$. Moreover, $\langle \mathbf{1}, \boldsymbol{v}_1 - \boldsymbol{v}_2\rangle = 0 \Rightarrow Nc = 0 \Rightarrow c = 0$, which proves the uniqueness of $\boldsymbol{v}$. □

E.2.3 Geodesic equation of the modified Wasserstein distance

We here derive the geodesic equation that determines the shortest path between two distributions $\boldsymbol{p}_0$ and $\boldsymbol{p}_\tau$. To this end, we consider the following functional, which is minimized along the geodesic path $\{\boldsymbol{p}(t)\}_{0\le t\le\tau}$:

$$\mathcal{J}[\boldsymbol{p}(t)] = \int_0^\tau \langle \boldsymbol{v}(t), \mathsf{K}_p \boldsymbol{v}(t)\rangle dt, \tag{E.79}$$

where $\boldsymbol{v}(t)$ and $\boldsymbol{p}(t)$ are related through $\dot{\boldsymbol{p}}(t) = \mathsf{K}_p \boldsymbol{v}(t)$. Consider an arbitrary perturbation path $\{\boldsymbol{q}(t)\}_{0\le t\le\tau}$ that satisfies $\boldsymbol{q}(0) = \boldsymbol{q}(\tau) = 0$ and $\sum_n q_n(t) = 0$ for all $0 \le t \le \tau$. Because the functional $\mathcal{J}[\boldsymbol{\gamma}(t)]$ is minimized when $\boldsymbol{\gamma} = \boldsymbol{p}$, the function $\Theta(\epsilon) = \mathcal{J}[\boldsymbol{p}(t) + \epsilon \boldsymbol{q}(t)]$ has a minimum at $\epsilon = 0$, so $\Theta'(0) = 0$. The functional evaluated at $\boldsymbol{\gamma} = \boldsymbol{p} + \epsilon \boldsymbol{q}$ can be written as

$$\mathcal{J}[\boldsymbol{p}(t) + \epsilon \boldsymbol{q}(t)] = \int_0^\tau \langle \boldsymbol{\vartheta}(t), \mathsf{K}_{p+\epsilon q} \boldsymbol{\vartheta}(t)\rangle dt, \tag{E.80}$$

where $\boldsymbol{\vartheta}(t)$ is determined from $\dot{\boldsymbol{p}}(t) + \epsilon \dot{\boldsymbol{q}}(t) = \mathsf{K}_{p+\epsilon q} \boldsymbol{\vartheta}(t)$. From Eq. (E.80), we have

$$0 = \Theta'(0) = \int_0^\tau \left[\langle \partial_\epsilon \boldsymbol{\vartheta}(t), \mathsf{K}_p \boldsymbol{v}(t)\rangle + \langle \boldsymbol{v}(t), \partial_\epsilon \mathsf{K}_{p+\epsilon q} \boldsymbol{v}(t)\rangle + \langle \boldsymbol{v}(t), \mathsf{K}_p \partial_\epsilon \boldsymbol{\vartheta}(t)\rangle\right]_{\epsilon=0} dt. \tag{E.81}$$

Hereafter, we omit the notation of evaluating at $\epsilon = 0$ for conciseness. The first and third terms in Eq. (E.81) are equal by symmetry of K_p; that is, $\langle \partial_\epsilon \boldsymbol{\vartheta}(t), \mathsf{K}_p \boldsymbol{v}(t)\rangle = \langle \boldsymbol{v}(t), \mathsf{K}_p \partial_\epsilon \boldsymbol{\vartheta}(t)\rangle$. Taking the partial derivative of both sides of $\dot{\boldsymbol{p}}(t) + \epsilon \dot{\boldsymbol{q}}(t) = \mathsf{K}_{p+\epsilon q} \boldsymbol{\vartheta}(t)$ with respect to ϵ and

evaluating at $\epsilon = 0$, we obtain

$$\dot{\boldsymbol{q}}(t) = \partial_\epsilon \mathsf{K}_{p+\epsilon q}\boldsymbol{v}(t) + \mathsf{K}_p \partial_\epsilon \boldsymbol{\vartheta}(t) \Rightarrow \langle \boldsymbol{v}(t), \mathsf{K}_p \partial_\epsilon \boldsymbol{\vartheta}(t)\rangle = \langle \boldsymbol{v}(t), \dot{\boldsymbol{q}}(t)\rangle - \langle \boldsymbol{v}(t), \partial_\epsilon \mathsf{K}_{p+\epsilon q}\boldsymbol{v}(t)\rangle. \tag{E.82}$$

From Eqs. (E.81) and (E.82), we have

$$0 = \int_0^\tau \left[2\langle \boldsymbol{v}(t), \dot{\boldsymbol{q}}(t)\rangle - \langle \boldsymbol{v}(t), \partial_\epsilon \mathsf{K}_{p+\epsilon q}\boldsymbol{v}(t)\rangle\right] dt = -\int_0^\tau \left[2\langle \dot{\boldsymbol{v}}(t), \boldsymbol{q}(t)\rangle + \langle \boldsymbol{v}(t), \partial_\epsilon \mathsf{K}_{p+\epsilon q}\boldsymbol{v}(t)\rangle\right] dt. \tag{E.83}$$

Since

$$\partial_\epsilon \mathsf{K}_{p+\epsilon q} = \sum_{1\le n<m\le N} R_{nm} p_m^{\mathrm{eq}} \partial_\epsilon \Phi\left(\frac{p_n + \epsilon q_n}{p_n^{\mathrm{eq}}}, \frac{p_m + \epsilon q_m}{p_m^{\mathrm{eq}}}\right) \mathsf{E}_{nm}, \tag{E.84}$$

we have

$$\langle \boldsymbol{v}(t), \partial_\epsilon \mathsf{K}_{p+\epsilon q}\boldsymbol{v}(t)\rangle = \sum_{m,n} R_{mn}[v_m(t) - v_n(t)]^2 \Psi\left(\frac{p_n(t)}{p_n^{\mathrm{eq}}(t)}, \frac{p_m(t)}{p_m^{\mathrm{eq}}(t)}\right) q_n(t) = \langle \boldsymbol{r}(t), \boldsymbol{q}(t)\rangle, \tag{E.85}$$

where $\Psi(x,y) = [x - \Phi(x,y)]/[x(\ln x - \ln y)]$ and

$$r_n(t) \coloneqq \sum_m R_{mn}[v_m(t) - v_n(t)]^2 \Psi\left(p_n(t)/p_n^{\mathrm{eq}}(t), p_m(t)/p_m^{\mathrm{eq}}(t)\right). \tag{E.86}$$

From Eqs. (E.83) and (E.85), we have

$$\int_0^\tau \langle 2\dot{\boldsymbol{v}}(t) + \boldsymbol{r}(t), \boldsymbol{q}(t)\rangle dt = 0. \tag{E.87}$$

Because $\{\boldsymbol{q}(t)\}_{0\le t\le\tau}$ is an arbitrary perturbation path, the term in the inner product must be zero, i.e., $\dot{\boldsymbol{v}}(t) + \boldsymbol{r}(t)/2 = 0$. Finally, the geodesic equation that determines the shortest path between states $\boldsymbol{p}_0$ and $\boldsymbol{p}_\tau$ is obtained as follows:

$$\begin{cases} \dot{\boldsymbol{p}}(t) - \mathsf{K}_p \boldsymbol{v}(t) = 0, \\ \dot{\boldsymbol{v}}(t) + \dfrac{1}{2}\boldsymbol{r}(t) = 0, \end{cases} \tag{E.88}$$

with boundary conditions $\boldsymbol{p}(0) = \boldsymbol{p}_0$ and $\boldsymbol{p}(\tau) = \boldsymbol{p}_\tau$.

E.2.4 Lower bound of the modified Wasserstein distance in terms of the total variation distance

Here we derive the lower bound of the Wasserstein distance in terms of the total variation distance, $\mathsf{d}_{\mathrm{V}}(\boldsymbol{p},\boldsymbol{q}) = \sum_n |p_n - q_n|$. In variational form, the distance $\mathsf{d}_{\mathrm{V}}(\boldsymbol{p},\boldsymbol{q})$ can be expressed as

$$\mathsf{d}_{\mathrm{V}}(\boldsymbol{p},\boldsymbol{q}) = \max_{\|\boldsymbol{w}\|_\infty \le 1} \{\boldsymbol{w}^\top(\boldsymbol{p} - \boldsymbol{q})\} = \max_{\|\boldsymbol{w}\|_\infty \le 1} \langle \boldsymbol{w}, \boldsymbol{p} - \boldsymbol{q}\rangle, \tag{E.89}$$

where the maximum is taken over all real vectors $\boldsymbol{w} = [w_1, \ldots, w_N]^\top$ and $\|\boldsymbol{w}\|_\infty \coloneqq \max_n |w_n|$. Equality is attained when $w_n = \mathrm{sign}(p_n - q_n)$. Here, the sign function $\mathrm{sign}(x)$ of x is defined as $\mathrm{sign}(x) = 1$ for $x \ge 0$ and -1 otherwise. By definition of the modified Wasserstein distance,

given a fixed positive number $\delta > 0$, there exists a smooth curve $\boldsymbol{p}(t)$ with end points $\boldsymbol{p}_0$ and $\boldsymbol{p}_\tau$ such that

$$\tau \int_0^\tau \langle \boldsymbol{v}, \mathsf{K}_p \boldsymbol{v} \rangle dt \leq \mathcal{W}_{\mathrm{c}}(\boldsymbol{p}_0, \boldsymbol{p}_\tau)^2 + \delta. \tag{E.90}$$

Here, $\boldsymbol{v}(t) \in \mathbb{R}^{N\times 1}$ is determined from $\dot{\boldsymbol{p}}(t) = \mathsf{K}_p \boldsymbol{v}(t)$. For an arbitrary vector $\boldsymbol{w}$ with $\|\boldsymbol{w}\|_\infty \leq 1$, we have

$$\langle \boldsymbol{w}, \boldsymbol{p}_\tau - \boldsymbol{p}_0 \rangle = \int_0^\tau \langle \boldsymbol{w}, \mathsf{K}_p \boldsymbol{v} \rangle dt \tag{E.91a}$$

$$\leq \left(\int_0^\tau \langle \boldsymbol{w}, \mathsf{K}_p \boldsymbol{w} \rangle dt \right)^{1/2} \left(\int_0^\tau \langle \boldsymbol{v}, \mathsf{K}_p \boldsymbol{v} \rangle dt \right)^{1/2} \tag{E.91b}$$

$$\leq \left(\tau^{-1} \int_0^\tau \langle \boldsymbol{w}, \mathsf{K}_p \boldsymbol{w} \rangle dt \right)^{1/2} \left(\mathcal{W}_{\mathrm{c}}(\boldsymbol{p}_0, \boldsymbol{p}_\tau)^2 + \delta \right)^{1/2}. \tag{E.91c}$$

To further bound the first term in Eq. (E.91c), we apply the inequalities $\Phi(x, y) \leq (x + y)/2$ and $(w_n - w_m)^2 \leq 4$, and obtain

$$\langle \boldsymbol{w}, \mathsf{K}_p \boldsymbol{w} \rangle = \sum_{m>n} R_{nm} p_m^{\mathrm{eq}} \Phi\left(\frac{p_n}{p_n^{\mathrm{eq}}}, \frac{p_m}{p_m^{\mathrm{eq}}} \right) \langle \boldsymbol{w}, \mathsf{E}_{nm} \boldsymbol{w} \rangle \tag{E.92a}$$

$$= \sum_{m>n} R_{nm} p_m^{\mathrm{eq}} \Phi\left(\frac{p_n}{p_n^{\mathrm{eq}}}, \frac{p_m}{p_m^{\mathrm{eq}}} \right) (w_n - w_m)^2 \tag{E.92b}$$

$$\leq 2 \sum_{m>n} R_{nm} p_m^{\mathrm{eq}} \left(\frac{p_n}{p_n^{\mathrm{eq}}} + \frac{p_m}{p_m^{\mathrm{eq}}} \right) \tag{E.92c}$$

$$= 2 \sum_{m>n} [R_{nm} p_m + R_{mn} p_n]. \tag{E.92d}$$

Consequently, we have

$$\mathcal{W}_{\mathrm{c}}(\boldsymbol{p}_0, \boldsymbol{p}_\tau)^2 + \delta \geq \frac{\langle \boldsymbol{w}, \boldsymbol{p}_0 - \boldsymbol{p}_\tau \rangle^2}{2\tau^{-1} \int_0^\tau \sum_{m>n} [R_{nm}(t) p_m(t) + R_{mn}(t) p_n(t)] dt}. \tag{E.93}$$

Taking the maximum over all $\boldsymbol{w}$ and the limit $\delta \to 0$, we obtain

$$\mathcal{W}_{\mathrm{c}}(\boldsymbol{p}_0, \boldsymbol{p}_\tau)^2 \geq \frac{\mathsf{d}_{\mathrm{V}}(\boldsymbol{p}_0, \boldsymbol{p}_\tau)^2}{2\mathcal{A}_{\mathrm{V}}}, \tag{E.94}$$

where $\mathcal{A}_{\mathrm{V}} \coloneqq \tau^{-1} \int_0^\tau \sum_{m\neq n} R_{mn}(t) \gamma_n(t) dt$ is the average dynamical activity along the geodesic path $\{\gamma(t)\}_{0\leq t\leq \tau}$. The dynamical activity characterizes the time scale of the system. As it indicates the time-symmetric changes in the system, it plays important roles in nonequilibrium phenomena [52]. From Eqs. (7.64) and (E.94), the classical speed limits of the state transformation are obtained as

$$\tau \geq \frac{\mathcal{W}_{\mathrm{c}}(\boldsymbol{p}(0), \boldsymbol{p}(\tau))^2}{\Delta S_{\mathrm{tot}}} \geq \frac{\mathsf{d}_{\mathrm{V}}(\boldsymbol{p}(0), \boldsymbol{p}(\tau))^2}{2\Delta S_{\mathrm{tot}} \mathcal{A}_{\mathrm{V}}}. \tag{E.95}$$

These inequalities imply a trade-off relation between the time needed to transform the system state and the physical quantities such as entropy production and dynamical activity. Specifically, a fast transformation necessitates high dissipation and frenesy. The last bound

in the inequality (E.95) is analogous to, but distinct from, a bound derived in Ref. [92]. In the earlier study, $\mathcal{A}_{\mathrm{V}}$ is replaced by the average dynamical activity along the path described by the time evolution of the system.

We can derive a bound that is tighter than Eq. (E.94). First, we divide the set of states $\mathcal{N} = \{1, \ldots, N\}$ into two subsets $\mathcal{N} = \mathcal{X}_- \cup \mathcal{X}_+$, where

$$\mathcal{X}_- := \{n \mid 1 \le n \le N,\ p_n(0) < p_n(\tau)\}, \tag{E.96}$$

$$\mathcal{X}_+ := \{n \mid 1 \le n \le N,\ p_n(0) \ge p_n(\tau)\}. \tag{E.97}$$

For convenience, we define $\mathrm{par}(n) := -1$ if $n \in \mathcal{X}_-$ and $\mathrm{par}(n) := 1$ if $n \in \mathcal{X}_+$. Then, $\mathsf{d}_{\mathrm{V}}(\boldsymbol{p}_0, \boldsymbol{p}_\tau) = \langle \boldsymbol{w}, \boldsymbol{p}_0 - \boldsymbol{p}_\tau \rangle$, where $w_n = \mathrm{par}(n)$. From Eq. (E.92b), noticing that $(w_n - w_m)^2 = 0$ if n and m belong to the same subset $\mathcal{X}_-$ or $\mathcal{X}_+$, and $(w_n - w_m)^2 = 4$ if n and m belong to different subsets, we have

$$\langle \boldsymbol{w}, \mathsf{K}_p \boldsymbol{w} \rangle \le 2 \sum_{m>n \ \&\ \mathrm{par}(m)\neq\mathrm{par}(n)} R_{nm} p_m^{\mathrm{eq}} \left(\frac{p_n}{p_n^{\mathrm{eq}}} + \frac{p_m}{p_m^{\mathrm{eq}}} \right) \tag{E.98a}$$

$$= 2 \sum_{m\in\mathcal{X}_-,\, n\in\mathcal{X}_+} [R_{mn} p_n + R_{nm} p_m] = 2 \sum_{\mathrm{par}(m)\neq\mathrm{par}(n)} R_{mn} p_n. \tag{E.98b}$$

Subsequently, we obtain a tighter bound as

$$\mathcal{W}_{\mathrm{c}}(\boldsymbol{p}_0, \boldsymbol{p}_\tau)^2 \ge \frac{\mathsf{d}_{\mathrm{V}}(\boldsymbol{p}_0, \boldsymbol{p}_\tau)^2}{2\mathcal{A}_{\mathrm{V}}^{\mathrm{par}}}, \tag{E.99}$$

where $\mathcal{A}_{\mathrm{V}}^{\mathrm{par}} := \tau^{-1} \int_0^\tau \sum_{\mathrm{par}(m)\neq\mathrm{par}(n)} R_{mn}(t) \gamma_n(t) dt$ is the average of the *partial* dynamical activity along the geodesic path $\{\boldsymbol{\gamma}(t)\}_{0\le t\le\tau}$. Since $\mathcal{A}_{\mathrm{V}}^{\mathrm{par}}$ involves only transition rates between states in $\mathcal{X}_-$ and $\mathcal{X}_+$, $\mathcal{A}_{\mathrm{V}}^{\mathrm{par}} \le \mathcal{A}_{\mathrm{V}}$.

Following the same approach (i.e., applying Eq. (E.91) for the path described by the system dynamics), we obtain

$$\langle \boldsymbol{w}, \boldsymbol{p}_\tau - \boldsymbol{p}_0 \rangle = \int_0^\tau \langle \boldsymbol{w}, \mathsf{K}_p \boldsymbol{h} \rangle dt \tag{E.100a}$$

$$\le \left(\int_0^\tau \langle \boldsymbol{w}, \mathsf{K}_p \boldsymbol{w} \rangle dt \right)^{1/2} \left(\int_0^\tau \langle \boldsymbol{h}, \mathsf{K}_p \boldsymbol{h} \rangle dt \right)^{1/2} \tag{E.100b}$$

$$= \left(\int_0^\tau \langle \boldsymbol{w}, \mathsf{K}_p \boldsymbol{w} \rangle dt \right)^{1/2} \sqrt{\Delta S_{\mathrm{tot}}}. \tag{E.100c}$$

Analogously, we can prove that

$$\tau \ge \frac{\mathsf{d}_{\mathrm{V}}(\boldsymbol{p}(0), \boldsymbol{p}(\tau))^2}{2\Delta S_{\mathrm{tot}} \mathcal{A}^{\mathrm{par}}}, \tag{E.101}$$

where $\mathcal{A}^{\mathrm{par}} := \tau^{-1} \int_0^\tau \sum_{\mathrm{par}(m)\neq\mathrm{par}(n)} R_{mn}(t) p_n(t) dt$ is the average of the *partial* dynamical activity along the path described by the time evolution of the system. Obviously, Eq. (E.101) is tighter than the bound reported in Ref. [92]. The newly obtained bound indicates that the speed of the state transformation is not constrained by the total dynamical activity, but by the partial dynamical activity induced by transitions between states in $\mathcal{X}_-$ and $\mathcal{X}_+$.

Bibliography

[1]E. Fermi, *Thermodynamics* (Dover Publications, 1956).

[2]K. Sekimoto, "Langevin equation and thermodynamics", Prog. Theor. Phys. Supp. **130**, 17–27 (1998).

[3]U. Seifert, "Stochastic thermodynamics, fluctuation theorems and molecular machines", Rep. Prog. Phys. **75**, 126001 (2012).

[4]C. Van den Broeck and M. Esposito, "Ensemble and trajectory thermodynamics: A brief introduction", Physica A **418**, 6–16 (2015).

[5]L. Onsager, "Reciprocal relations in irreversible processes. I.", Phys. Rev. **37**, 405–426 (1931).

[6]L. Onsager, "Reciprocal relations in irreversible processes. II.", Phys. Rev. **38**, 2265–2279 (1931).

[7]U. Seifert, "Entropy production along a stochastic trajectory and an integral fluctuation theorem", Phys. Rev. Lett. **95**, 040602 (2005).

[8]J. Goold, M. Huber, A. Riera, L. del Rio, and P. Skrzypczyk, "The role of quantum information in thermodynamics—a topical review", J. Phys. A **49**, 143001 (2016).

[9]S. Vinjanampathy and J. Anders, "Quantum thermodynamics", Contemp. Phys. **57**, 545–579 (2016).

[10]S. Deffner and S. Campbell, *Quantum Thermodynamics* (Morgan & Claypool Publishers, 2019).

[11]R. Landauer, "Irreversibility and heat generation in the computing process", IBM J. Res. Dev. **5**, 183–191 (1961).

[12]J. Goold, M. Paternostro, and K. Modi, "Nonequilibrium quantum Landauer principle", Phys. Rev. Lett. **114**, 060602 (2015).

[13]A. M. Timpanaro, J. P. Santos, and G. T. Landi, "Landauer's principle at zero temperature", Phys. Rev. Lett. **124**, 240601 (2020).

[14]G. T. Landi and M. Paternostro, "Irreversible entropy production, from quantum to classical", arXiv preprint arXiv:2009.07668 (2020).

[15]D. J. Evans, E. G. D. Cohen, and G. P. Morriss, "Probability of second law violations in shearing steady states", Phys. Rev. Lett. **71**, 2401–2404 (1993).

[16]G. Gallavotti and E. G. D. Cohen, "Dynamical ensembles in nonequilibrium statistical mechanics", Phys. Rev. Lett. **74**, 2694–2697 (1995).

[17]G. E. Crooks, "Entropy production fluctuation theorem and the nonequilibrium work relation for free energy differences", Phys. Rev. E **60**, 2721–2726 (1999).

[18]C. Jarzynski, "Hamiltonian derivation of a detailed fluctuation theorem", J. Stat. Phys. **98**, 77–102 (2000).

[19]D. J. Evans and D. J. Searles, "The fluctuation theorem", Adv. Phys. **51**, 1529–1585 (2002).

[20]P. Gaspard, "Fluctuation theorem for nonequilibrium reactions", J. Chem. Phys. **120**, 8898–8905 (2004).

[21]A. C. Barato and U. Seifert, "Thermodynamic uncertainty relation for biomolecular processes", Phys. Rev. Lett. **114**, 158101 (2015).

[22]T. R. Gingrich, J. M. Horowitz, N. Perunov, and J. L. England, "Dissipation bounds all steady-state current fluctuations", Phys. Rev. Lett. **116**, 120601 (2016).

[23]J. M. Horowitz and T. R. Gingrich, "Proof of the finite-time thermodynamic uncertainty relation for steady-state currents", Phys. Rev. E **96**, 020103(R) (2017).

[24]A. Dechant and S.-i. Sasa, "Current fluctuations and transport efficiency for general Langevin systems", J. Stat. Mech.: Theory Exp., 063209 (2018).

[25]K. Proesmans and C. V. den Broeck, "Discrete-time thermodynamic uncertainty relation", Europhys. Lett. **119**, 20001 (2017).

[26]B. K. Agarwalla and D. Segal, "Assessing the validity of the thermodynamic uncertainty relation in quantum systems", Phys. Rev. B **98**, 155438 (2018).

[27]P. Pietzonka, A. C. Barato, and U. Seifert, "Universal bounds on current fluctuations", Phys. Rev. E **93**, 052145 (2016).

[28]M. Polettini, A. Lazarescu, and M. Esposito, "Tightening the uncertainty principle for stochastic currents", Phys. Rev. E **94**, 052104 (2016).

[29]J. P. Garrahan, "Simple bounds on fluctuations and uncertainty relations for first-passage times of counting observables", Phys. Rev. E **95**, 032134 (2017).

[30]A. C. Barato, R. Chetrite, A. Faggionato, and D. Gabrielli, "Bounds on current fluctuations in periodically driven systems", New J. Phys. **20**, 103023 (2018).

[31]K. Macieszczak, K. Brandner, and J. P. Garrahan, "Unified thermodynamic uncertainty relations in linear response", Phys. Rev. Lett. **121**, 130601 (2018).

[32]K. Brandner, T. Hanazato, and K. Saito, "Thermodynamic bounds on precision in ballistic multiterminal transport", Phys. Rev. Lett. **120**, 090601 (2018).

[33]Y. Hasegawa and T. Van Vu, "Uncertainty relations in stochastic processes: An information inequality approach", Phys. Rev. E **99**, 062126 (2019).

[34]H.-M. Chun, L. P. Fischer, and U. Seifert, "Effect of a magnetic field on the thermodynamic uncertainty relation", Phys. Rev. E **99**, 042128 (2019).

[35]T. Koyuk and U. Seifert, "Operationally accessible bounds on fluctuations and entropy production in periodically driven systems", Phys. Rev. Lett. **122**, 230601 (2019).

[36]I. D. Terlizzi and M. Baiesi, "Kinetic uncertainty relation", J. Phys. A **52**, 02LT03 (2019).

[37]A. C. Barato, R Chetrite, A Faggionato, and D Gabrielli, "A unifying picture of generalized thermodynamic uncertainty relations", J. Stat. Mech.: Theory Exp., 084017 (2019).

[38]D. Gupta and A. Maritan, "Thermodynamic uncertainty relations in a linear system", Eur. Phys. J. B **93**, 28 (2020).

[39]Y. Hasegawa and T. Van Vu, "Fluctuation theorem uncertainty relation", Phys. Rev. Lett. **123**, 110602 (2019).

[40]F. Carollo, R. L. Jack, and J. P. Garrahan, "Unraveling the large deviation statistics of Markovian open quantum systems", Phys. Rev. Lett. **122**, 130605 (2019).

[41]Y. Hasegawa, "Quantum thermodynamic uncertainty relation for continuous measurement", Phys. Rev. Lett. **125**, 050601 (2020).

[42]G. Guarnieri, G. T. Landi, S. R. Clark, and J. Goold, "Thermodynamics of precision in quantum nonequilibrium steady states", Phys. Rev. Research **1**, 033021 (2019).

[43]K. Proesmans and J. M. Horowitz, "Hysteretic thermodynamic uncertainty relation for systems with broken time-reversal symmetry", J. Stat. Mech.: Theory Exp., 054005 (2019).

[44]A. Dechant and S.-i. Sasa, "Fluctuation-response inequality out of equilibrium", Proc. Natl. Acad. Sci. U.S.A. **117**, 6430–6436 (2020).

[45]G. Falasco, M. Esposito, and J.-C. Delvenne, "Unifying thermodynamic uncertainty relations", New J. Phys. **22**, 053046 (2020).

[46]A. M. Timpanaro, G. Guarnieri, J. Goold, and G. T. Landi, "Thermodynamic uncertainty relations from exchange fluctuation theorems", Phys. Rev. Lett. **123**, 090604 (2019).

[47]V. T. Vo, T. Van Vu, and Y. Hasegawa, "Unified approach to classical speed limit and thermodynamic uncertainty relation", Phys. Rev. E **102**, 062132 (2020).

[48]Y. Hasegawa, "Thermodynamic uncertainty relation for general open quantum systems", Phys. Rev. Lett. **126**, 010602 (2021).

[49]J. Li, J. M. Horowitz, T. R. Gingrich, and N. Fakhri, "Quantifying dissipation using fluctuating currents", Nat. Commun. **10**, 1666 (2019).

[50]S. K. Manikandan, D. Gupta, and S. Krishnamurthy, "Inferring entropy production from short experiments", Phys. Rev. Lett. **124**, 120603 (2020).

[51]S. Otsubo, S. Ito, A. Dechant, and T. Sagawa, "Estimating entropy production by machine learning of short-time fluctuating currents", Phys. Rev. E **101**, 062106 (2020).

[52]C. Maes, "Frenesy: Time-symmetric dynamical activity in nonequilibria", Phys. Rep. **850**, 1–33 (2020).

[53]T. Van Vu and Y. Hasegawa, "Uncertainty relations for underdamped Langevin dynamics", Phys. Rev. E **100**, 032130 (2019).

[54]T. Van Vu and Y. Hasegawa, "Thermodynamic uncertainty relations under arbitrary control protocols", Phys. Rev. Research **2**, 013060 (2020).

[55]T. Van Vu and Y. Hasegawa, "Uncertainty relations for time-delayed Langevin systems", Phys. Rev. E **100**, 012134 (2019).

[56]T. Van Vu and Y. Hasegawa, "Uncertainty relation under information measurement and feedback control", J. Phys. A **53**, 075001 (2020).

[57]T. Van Vu and Y. Hasegawa, "Generalized uncertainty relations for semi-Markov processes", J. Phys.: Conf. Ser. **1593**, 012006 (2020).

[58]T. Van Vu, V. T. Vo, and Y. Hasegawa, "Entropy production estimation with optimal current", Phys. Rev. E **101**, 042138 (2020).

[59]T. Van Vu and Y. Hasegawa, "Geometrical bounds of the irreversibility in Markovian systems", Phys. Rev. Lett. **126**, 010601 (2021).

[60]F. Verstraete, M. M. Wolf, and J. I. Cirac, "Quantum computation and quantum-state engineering driven by dissipation", Nat. Phys. **5**, 633–636 (2009).

[61]R. Kosloff and A. Levy, "Quantum heat engines and refrigerators: Continuous devices", Annu. Rev. Phys. Chem. **65**, 365–393 (2014).

[62]K. Sekimoto, *Stochastic Energetics*, Vol. 799 (Springer, Berlin, 2010).

[63]H. Risken, *The Fokker-Planck Equation: Methods of Solution and Applications*, 2nd ed. (Springer, Berlin, 1989).

[64]C. Gardiner, *Stochastic Methods* (Springer-Verlag, Berlin Heidelberg, 2009).

[65]T. Hatano and S.-i. Sasa, "Steady-state thermodynamics of Langevin systems", Phys. Rev. Lett. **86**, 3463–3466 (2001).

[66]C. Van den Broeck and M. Esposito, "Three faces of the second law. II. Fokker-Planck formulation", Phys. Rev. E **82**, 011144 (2010).

[67]M. Esposito and C. Van den Broeck, "Three detailed fluctuation theorems", Phys. Rev. Lett. **104**, 090601 (2010).

[68]D. J. Evans and D. J. Searles, "Equilibrium microstates which generate second law violating steady states", Phys. Rev. E **50**, 1645–1648 (1994).

[69]J. Kurchan, "Fluctuation theorem for stochastic dynamics", J. Phys. A **31**, 3719–3729 (1998).

[70]D. J. Searles and D. J. Evans, "Fluctuation theorem for stochastic systems", Phys. Rev. E **60**, 159–164 (1999).

[71]J. L. Lebowitz and H. Spohn, "A Gallavotti–Cohen-type symmetry in the large deviation functional for stochastic dynamics", J. Stat. Phys. **95**, 333–365 (1999).

[72]C. Maes and F. Redig, "Positivity of entropy production", J. Stat. Phys. **101**, 3–15 (2000).

[73]C. Jarzynski, "Nonequilibrium equality for free energy differences", Phys. Rev. Lett. **78**, 2690–2693 (1997).

[74]C. Jarzynski, "Equilibrium free-energy differences from nonequilibrium measurements: A master-equation approach", Phys. Rev. E **56**, 5018–5035 (1997).

[75]R. J. Harris and G. M. Schütz, "Fluctuation theorems for stochastic dynamics", J. Stat. Mech.: Theory Exp. **2007**, P07020 (2007).

[76]E. M. Sevick, R. Prabhakar, S. R. Williams, and D. J. Searles, "Fluctuation theorems", Annu. Rev. Phys. Chem. **59**, 603–633 (2008).

[77]M. M. Mansour and F. Baras, "Fluctuation theorem: A critical review", Chaos **27**, 104609 (2017).

[78]V. Y. Chernyak, M. Chertkov, and C. Jarzynski, "Path-integral analysis of fluctuation theorems for general Langevin processes", J. Stat. Mech.: Theory Exp. **2006**, P08001 (2006).

[79]T. Speck and U. Seifert, "Integral fluctuation theorem for the housekeeping heat", J. Phys. A **38**, L581 (2005).

[80]H.-P. Breuer and F. Petruccione, *The Theory of Open Quantum Systems* (Oxford University Press, New York, 2002).

[81]M. Esposito, K. Lindenberg, and C. V. den Broeck, "Entropy production as correlation between system and reservoir", New J. Phys. **12**, 013013 (2010).

[82]G. Lindblad, "On the generators of quantum dynamical semigroups", Commun. Math. Phys. **48**, 119–130 (1976).

[83]S. Pigolotti, I. Neri, E. Roldán, and F. Jülicher, "Generic properties of stochastic entropy production", Phys. Rev. Lett. **119**, 140604 (2017).

[84]M. Matsuo and S.-i. Sasa, "Stochastic energetics of non-uniform temperature systems", Physica A **276**, 188–200 (2000).

[85]A. Celani, S. Bo, R. Eichhorn, and E. Aurell, "Anomalous thermodynamics at the microscale", Phys. Rev. Lett. **109**, 260603 (2012).

[86]S. Bo and A. Celani, "Entropy production in stochastic systems with fast and slow time-scales", J. Stat. Phys. **154**, 1325–1351 (2014).

[87]V. Lecomte, C. Appert-Rolland, and F. van Wijland, "Chaotic properties of systems with Markov dynamics", Phys. Rev. Lett. **95**, 010601 (2005).

[88]M. Merolle, J. P. Garrahan, and D. Chandler, "Space-time thermodynamics of the glass transition", Proc. Natl. Acad. Sci. U.S.A **102**, 10837–10840 (2005).

[89]V. Lecomte, C. Appert-Rolland, and F. van Wijland, "Thermodynamic formalism for systems with Markov dynamics", J. Stat. Phys. **127**, 51–106 (2007).

[90]J. P. Garrahan, R. L. Jack, V. Lecomte, E. Pitard, K. van Duijvendijk, and F. van Wijland, "First-order dynamical phase transition in models of glasses: An approach based on ensembles of histories", J. Phys. A **42**, 075007 (2009).

[91]C. Maes, "Frenetic bounds on the entropy production", Phys. Rev. Lett. **119**, 160601 (2017).

[92]N. Shiraishi, K. Funo, and K. Saito, "Speed limit for classical stochastic processes", Phys. Rev. Lett. **121**, 070601 (2018).

[93]Y. Fily and M. C. Marchetti, "Athermal phase separation of self-propelled particles with no alignment", Phys. Rev. Lett. **108**, 235702 (2012).

[94]M. C. Marchetti, J. F. Joanny, S. Ramaswamy, T. B. Liverpool, J. Prost, M. Rao, and R. A. Simha, "Hydrodynamics of soft active matter", Rev. Mod. Phys. **85**, 1143–1189 (2013).

[95]T. Speck, J. Bialké, A. M. Menzel, and H. Löwen, "Effective Cahn-Hilliard equation for the phase separation of active Brownian particles", Phys. Rev. Lett. **112**, 218304 (2014).

[96]T. F. F. Farage, P. Krinninger, and J. M. Brader, "Effective interactions in active Brownian suspensions", Phys. Rev. E **91**, 042310 (2015).

[97]U. Marini Bettolo Marconi and C. Maggi, "Towards a statistical mechanical theory of active fluids", Soft Matter **11**, 8768–8781 (2015).

[98]E. Fodor, C. Nardini, M. E. Cates, J. Tailleur, P. Visco, and F. van Wijland, "How far from equilibrium is active matter?", Phys. Rev. Lett. **117**, 038103 (2016).

[99]D. Mandal, K. Klymko, and M. R. DeWeese, "Entropy production and fluctuation theorems for active matter", Phys. Rev. Lett. **119**, 258001 (2017).

[100]C. Nardini, E. Fodor, E. Tjhung, F. van Wijland, J. Tailleur, and M. E. Cates, "Entropy production in field theories without time-reversal symmetry: Quantifying the non-equilibrium character of active matter", Phys. Rev. X **7**, 021007 (2017).

[101]H. K. Lee, C. Kwon, and H. Park, "Fluctuation theorems and entropy production with odd-parity variables", Phys. Rev. Lett. **110**, 050602 (2013).

[102]R. E. Spinney and I. J. Ford, "Entropy production in full phase space for continuous stochastic dynamics", Phys. Rev. E **85**, 051113 (2012).

[103]R. E. Spinney and I. J. Ford, "Nonequilibrium thermodynamics of stochastic systems with odd and even variables", Phys. Rev. Lett. **108**, 170603 (2012).

[104]A. Imparato and L. Peliti, "Fluctuation relations for a driven Brownian particle", Phys. Rev. E **74**, 026106 (2006).

[105]A. Dechant, "Multidimensional thermodynamic uncertainty relations", J. Phys. A **52**, 035001 (2019).

[106]L. P. Fischer, P. Pietzonka, and U. Seifert, "Large deviation function for a driven underdamped particle in a periodic potential", Phys. Rev. E **97**, 022143 (2018).

[107]M. L. Rosinberg, G. Tarjus, and T. Munakata, "Heat fluctuations for underdamped Langevin dynamics", Europhys. Lett. **113**, 10007 (2016).

[108]G Falasco and M Baiesi, "Nonequilibrium temperature response for stochastic overdamped systems", New J. Phys. **18**, 043039 (2016).

[109]J. Zinn-Justin, *Quantum Field Theory and Critical Phenomena*, 4th (Clarendon Press, 2002).

[110]R. L. Jack, J. P. Garrahan, and D. Chandler, "Space-time thermodynamics and subsystem observables in a kinetically constrained model of glassy materials", J. Chem. Phys. **125**, 184509 (2006).

[111]W. De Roeck and C. Maes, "Symmetries of the ratchet current", Phys. Rev. E **76**, 051117 (2007).

[112]M. Baiesi, C. Maes, and B. Wynants, "Nonequilibrium linear response for Markov dynamics, I: Jump processes and overdamped diffusions", J. Stat. Phys. **137**, 1094 (2009).

[113]R. L. Jack and P. Sollich, "Large deviations of the dynamical activity in the East model: analysing structure in biased trajectories", J. Phys. A **47**, 015003 (2014).

[114]C. Maes and A. Salazar, "Active fluctuation symmetries", New J. Phys. **16**, 015019 (2014).

[115]P. Pietzonka and U. Seifert, "Universal trade-off between power, efficiency, and constancy in steady-state heat engines", Phys. Rev. Lett. **120**, 190602 (2018).

[116]J. M. Horowitz, "Multipartite information flow for multiple Maxwell demons", J. Stat. Mech.: Theory Exp., P03006 (2015).

[117]R. Filliger and P. Reimann, "Brownian gyrator: A minimal heat engine on the nanoscale", Phys. Rev. Lett. **99**, 230602 (2007).

[118]K.-H. Chiang, C.-L. Lee, P.-Y. Lai, and Y.-F. Chen, "Electrical autonomous Brownian gyrator", Phys. Rev. E **96**, 032123 (2017).

[119]A. Argun, J. Soni, L. Dabelow, S. Bo, G. Pesce, R. Eichhorn, and G. Volpe, "Experimental realization of a minimal microscopic heat engine", Phys. Rev. E **96**, 052106 (2017).

[120]A. Dechant, N. Kiesel, and E. Lutz, "Underdamped stochastic heat engine at maximum efficiency", Europhys. Lett. **119**, 50003 (2017).

[121]V. Blickle and C. Bechinger, "Realization of a micrometre-sized stochastic heat engine", Nat. Phys. **8**, 143 (2012).

[122]V. Holubec and A. Ryabov, "Cycling tames power fluctuations near optimum efficiency", Phys. Rev. Lett. **121**, 120601 (2018).

[123]P. P. Potts and P. Samuelsson, "Thermodynamic uncertainty relations including measurement and feedback", Phys. Rev. E **100**, 052137 (2019).

[124]S. Ito and A. Dechant, "Stochastic time evolution, information geometry, and the Cramér-Rao bound", Phys. Rev. X **10**, 021056 (2020).

[125]D. M. Busiello and S. Pigolotti, "Hyperaccurate currents in stochastic thermodynamics", Phys. Rev. E **100**, 060102 (2019).

[126]D. Bratsun, D. Volfson, L. S. Tsimring, and J. Hasty, "Delay-induced stochastic oscillations in gene regulation", Proc. Natl. Acad. Sci. U.S.A. **102**, 14593–14598 (2005).

[127]W. Mather, M. R. Bennett, J. Hasty, and L. S. Tsimring, "Delay-induced degrade-and-fire oscillations in small genetic circuits", Phys. Rev. Lett. **102**, 068105 (2009).

[128]B. Novák and J. J. Tyson, "Design principles of biochemical oscillators", Nat. Rev. Mol. Cell Biol. **9**, 981 (2008).

[129]S. Kim, S. H. Park, and H.-B. Pyo, "Stochastic resonance in coupled oscillator systems with time delay", Phys. Rev. Lett. **82**, 1620–1623 (1999).

[130]C. Masoller, "Distribution of residence times of time-delayed bistable systems driven by noise", Phys. Rev. Lett. **90**, 020601 (2003).

[131]K. Lichtner, A. Pototsky, and S. H. L. Klapp, "Feedback-induced oscillations in one-dimensional colloidal transport", Phys. Rev. E **86**, 051405 (2012).

[132]S. A. M. Loos and S. H. L. Klapp, "Heat flow due to time-delayed feedback", Sci. Rep. **9**, 2491 (2019).

[133]M. L. Rosinberg, T. Munakata, and G. Tarjus, "Stochastic thermodynamics of Langevin systems under time-delayed feedback control: Second-law-like inequalities", Phys. Rev. E **91**, 042114 (2015).

[134]M. L. Rosinberg, G. Tarjus, and T. Munakata, "Stochastic thermodynamics of Langevin systems under time-delayed feedback control. II. Nonequilibrium steady-state fluctuations", Phys. Rev. E **95**, 022123 (2017).

[135]H. Touchette and S. Lloyd, "Information-theoretic limits of control", Phys. Rev. Lett. **84**, 1156–1159 (2000).

[136]H. Touchette and S. Lloyd, "Information-theoretic approach to the study of control systems", Physica A **331**, 140–172 (2004).

[137]T. Sagawa and M. Ueda, "Second law of thermodynamics with discrete quantum feedback control", Phys. Rev. Lett. **100**, 080403 (2008).

[138]T. Sagawa and M. Ueda, "Generalized Jarzynski equality under nonequilibrium feedback control", Phys. Rev. Lett. **104**, 090602 (2010).

[139]J. M. Horowitz and J. M. R. Parrondo, "Thermodynamic reversibility in feedback processes", Europhys. Lett. **95**, 10005 (2011).

[140]T. Sagawa and M. Ueda, "Nonequilibrium thermodynamics of feedback control", Phys. Rev. E **85**, 021104 (2012).

[141]D Hartich, A. C. Barato, and U Seifert, "Stochastic thermodynamics of bipartite systems: transfer entropy inequalities and a Maxwell's demon interpretation", J. Stat. Mech.: Theory Exp., P02016 (2014).

[142]A. C. Barato and U. Seifert, "Unifying three perspectives on information processing in stochastic thermodynamics", Phys. Rev. Lett. **112**, 090601 (2014).

[143]J. M. Parrondo, J. M. Horowitz, and T. Sagawa, "Thermodynamics of information", Nat. Phys. **11**, 131 (2015).

[144]P. P. Potts and P. Samuelsson, "Detailed fluctuation relation for arbitrary measurement and feedback schemes", Phys. Rev. Lett. **121**, 210603 (2018).

[145]V. Serreli, C.-F. Lee, E. R. Kay, and D. A. Leigh, "A molecular information ratchet", Nature **445**, 523 (2007).

[146]B. Lau, O. Kedem, J. Schwabacher, D. Kwasnieski, and E. A. Weiss, "An introduction to ratchets in chemistry and biology", Mater. Horiz. **4**, 310–318 (2017).

[147]T. D. Frank, P. J. Beek, and R. Friedrich, "Fokker-Planck perspective on stochastic delay systems: Exact solutions and data analysis of biological systems", Phys. Rev. E **68**, 021912 (2003).

[148]T. D. Frank, "Delay Fokker-Planck equations, Novikov's theorem, and Boltzmann distributions as small delay approximations", Phys. Rev. E **72**, 011112 (2005).

[149]A. Gomez-Marin, J. M. R. Parrondo, and C. Van den Broeck, "Lower bounds on dissipation upon coarse graining", Phys. Rev. E **78**, 011107 (2008).

[150]E. Roldán and J. M. R. Parrondo, "Entropy production and Kullback-Leibler divergence between stationary trajectories of discrete systems", Phys. Rev. E **85**, 031129 (2012).

[151]G. Diana and M. Esposito, "Mutual entropy production in bipartite systems", J. Stat. Mech.: Theory Exp., P04010 (2014).

[152]P. Gaspard, "Time-reversed dynamical entropy and irreversibility in Markovian random processes", J. Stat. Phys. **117**, 599–615 (2004).

[153]E. H. Trepagnier, C. Jarzynski, F. Ritort, G. E. Crooks, C. J. Bustamante, and J. Liphardt, "Experimental test of Hatano and Sasa's nonequilibrium steady-state equality", Proc. Natl. Acad. Sci. U.S.A. **101**, 15038–15041 (2004).

[154]D. Collin, F. Ritort, C. Jarzynski, S. B. Smith, I. Tinoco Jr, and C. Bustamante, "Verification of the Crooks fluctuation theorem and recovery of RNA folding free energies", Nature **437**, 231 (2005).

[155]S. Schuler, T. Speck, C. Tietz, J. Wrachtrup, and U. Seifert, "Experimental test of the fluctuation theorem for a driven two-level system with time-dependent rates", Phys. Rev. Lett. **94**, 180602 (2005).

[156]C. Tietz, S. Schuler, T. Speck, U. Seifert, and J. Wrachtrup, "Measurement of stochastic entropy production", Phys. Rev. Lett. **97**, 050602 (2006).

[157]D. Andrieux, P. Gaspard, S. Ciliberto, N. Garnier, S. Joubaud, and A. Petrosyan, "Entropy production and time asymmetry in nonequilibrium fluctuations", Phys. Rev. Lett. **98**, 150601 (2007).

[158]C. Aron, G. Biroli, and L. F. Cugliandolo, "Symmetries of generating functionals of Langevin processes with colored multiplicative noise", J. Stat. Mech.: Theory Exp., P11018 (2010).

[159]N. Merhav and Y. Kafri, "Statistical properties of entropy production derived from fluctuation theorems", J. Stat. Mech.: Theory Exp., P12022 (2010).

[160]N. Shiraishi, "Finite-time thermodynamic uncertainty relation do not hold for discrete-time Markov process", arXiv preprint arXiv:1706.00892 (2017).

[161]U. Küchler and B. Mensch, "Langevins stochastic differential equation extended by a time-delayed term", Stochastics and Stochastic Rep. **40**, 23–42 (1992).

[162]R. van Zon and E. G. D. Cohen, "Stationary and transient work-fluctuation theorems for a dragged Brownian particle", Phys. Rev. E **67**, 046102 (2003).

[163]T. Mai and A. Dhar, "Nonequilibrium work fluctuations for oscillators in non-Markovian baths", Phys. Rev. E **75**, 061101 (2007).

[164]O. Paredes-Altuve, E. Medina, and P. J. Colmenares, "Extracting work from a single reservoir in the non-Markovian underdamped regime", Phys. Rev. E **94**, 062111 (2016).

[165]B. Ghosh and S. Chaudhury, "Fluctuation theorems for total entropy production in generalized Langevin systems", Physica A **466**, 133–139 (2017).

[166]T. Ohkuma and T. Ohta, "Fluctuation theorems for non-linear generalized Langevin systems", J. Stat. Mech.: Theory Exp., P10010 (2007).

[167]L. Schimansky-Geier, M. Kschischo, and T. Fricke, "Flux of particles in sawtooth media", Phys. Rev. Lett. **79**, 3335–3338 (1997).

[168]J. A. Freund and L. Schimansky-Geier, "Diffusion in discrete ratchets", Phys. Rev. E **60**, 1304–1309 (1999).

[169]F. J. Cao, L. Dinis, and J. M. R. Parrondo, "Feedback control in a collective flashing ratchet", Phys. Rev. Lett. **93**, 040603 (2004).

[170]E. Craig, N. Kuwada, B. Lopez, and H. Linke, "Feedback control in flashing ratchets", Ann. Phys. **17**, 115–129 (2008).

[171]A. Mogilner and G. Oster, "The polymerization ratchet model explains the force-velocity relation for growing microtubules", Eur. Biophys. J. **28**, 235–242 (1999).

[172]Z. Siwy and A. Fuliński, "Fabrication of a synthetic nanopore ion pump", Phys. Rev. Lett. **89**, 198103 (2002).

[173]A. Kundu, "Nonequilibrium fluctuation theorem for systems under discrete and continuous feedback control", Phys. Rev. E **86**, 021107 (2012).

[174]J. M. Horowitz and M. Esposito, "Thermodynamics with continuous information flow", Phys. Rev. X **4**, 031015 (2014).

[175]J. M. Horowitz and H. Sandberg, "Second-law-like inequalities with information and their interpretations", New J. Phys. **16**, 125007 (2014).

[176]L Dinis, J. M. R Parrondo, and F. J Cao, "Closed-loop control strategy with improved current for a flashing ratchet", Europhys. Lett. **71**, 536–541 (2005).

[177]M. Feito and F. J. Cao, "Information and maximum power in a feedback controlled Brownian ratchet", Eur. Phys. J. B **59**, 63–68 (2007).

[178]F. Cao, M. Feito, and H. Touchette, "Information and flux in a feedback controlled Brownian ratchet", Physica A **388**, 113–119 (2009).

[179]Y. Zhou and J.-D. Bao, "Optimal number of disperse states in the model of Brownian motors", Physica A **343**, 515–524 (2004).

[180]A. Braggio, J. König, and R. Fazio, "Full counting statistics in strongly interacting systems: Non-Markovian effects", Phys. Rev. Lett. **96**, 026805 (2006).

[181]C. Flindt, T. c. v. Novotný, A. Braggio, M. Sassetti, and A.-P. Jauho, "Counting statistics of non-Markovian quantum stochastic processes", Phys. Rev. Lett. **100**, 150601 (2008).

[182]H.-P. Breuer and B. Vacchini, "Quantum semi-Markov processes", Phys. Rev. Lett. **101**, 140402 (2008).

[183]E. Barkai, R. S. Eisenberg, and Z. Schuss, "Bidirectional shot noise in a singly occupied channel", Phys. Rev. E **54**, 1161–1175 (1996).

[184]Y. Hasegawa, "Multidimensional biochemical information processing of dynamical patterns", Phys. Rev. E **97**, 022401 (2018).

[185]M. Gorissen and C. Vanderzande, "Ribosome dwell times and the protein copy number distribution", J. Stat. Phys. **148**, 628–636 (2012).

[186]G. Knoops and C. Vanderzande, "Motion of kinesin in a viscoelastic medium", Phys. Rev. E **97**, 052408 (2018).

[187]Y. Sughiyama, S. Nakashima, and T. J. Kobayashi, "Fitness response relation of a multitype age-structured population dynamics", Phys. Rev. E **99**, 012413 (2019).

[188]H. Wang and H. Qian, "On detailed balance and reversibility of semi-Markov processes and single-molecule enzyme kinetics", J. Math. Phys. **48**, 013303 (2007).

[189]C. Maes, K. Netočný, and B. Wynants, "Dynamical fluctuations for semi-Markov processes", J. Phys. A **42**, 365002 (2009).

[190]M. E. Fisher and A. B. Kolomeisky, "Simple mechanochemistry describes the dynamics of kinesin molecules", Proc. Natl. Acad. Sci. U.S.A **98**, 7748–7753 (2001).

[191]T. Van Vu and Y. Hasegawa, "Diffusion-dynamics laws in stochastic reaction networks", Phys. Rev. E **99**, 012416 (2019).

[192]L. S. Tsimring, "Noise in biology", Rep. Prog. Phys. **77**, 026601 (2014).

[193]T. Van Vu and Y. Hasegawa, "An algebraic method to calculate parameter regions for constrained steady-state distribution in stochastic reaction networks", Chaos **29**, 023123 (2019).

[194]B. Lander, J. Mehl, V. Blickle, C. Bechinger, and U. Seifert, "Noninvasive measurement of dissipation in colloidal systems", Phys. Rev. E **86**, 030401(R) (2012).

[195]I. A. Martínez, G. Bisker, J. M. Horowitz, and J. M. R. Parrondo, "Inferring broken detailed balance in the absence of observable currents", Nat. Commun. **10**, 3542 (2019).

[196]J. Mehl, B. Lander, C. Bechinger, V. Blickle, and U. Seifert, "Role of hidden slow degrees of freedom in the fluctuation theorem", Phys. Rev. Lett. **108**, 220601 (2012).

[197]N. Shiraishi and T. Sagawa, "Fluctuation theorem for partially masked nonequilibrium dynamics", Phys. Rev. E **91**, 012130 (2015).

[198]A. Quarteroni, R. Sacco, and F. Saleri, *Numerical Mathematics* (Springer, New York, 2007).

[199]D. T. Gillespie, "Exact stochastic simulation of coupled chemical reactions", J. Phys. Chem. **81**, 2340–2361 (1977).

[200]K. Hayashi, H. Ueno, R. Iino, and H. Noji, "Fluctuation theorem applied to F_1-ATPase", Phys. Rev. Lett. **104**, 218103 (2010).

[201]P. Salamon and R. S. Berry, "Thermodynamic length and dissipated availability", Phys. Rev. Lett. **51**, 1127–1130 (1983).

[202]G. Ruppeiner, "Riemannian geometry in thermodynamic fluctuation theory", Rev. Mod. Phys. **67**, 605–659 (1995).

[203]E. H. Feng and G. E. Crooks, "Length of time's arrow", Phys. Rev. Lett. **101**, 090602 (2008).

[204]B. B. Machta, "Dissipation bound for thermodynamic control", Phys. Rev. Lett. **115**, 260603 (2015).

[205]G. M. Rotskoff, G. E. Crooks, and E. Vanden-Eijnden, "Geometric approach to optimal nonequilibrium control: Minimizing dissipation in nanomagnetic spin systems", Phys. Rev. E **95**, 012148 (2017).

[206]S. Ito, "Stochastic thermodynamic interpretation of information geometry", Phys. Rev. Lett. **121**, 030605 (2018).

[207]S. B. Nicholson, A. del Campo, and J. R. Green, "Nonequilibrium uncertainty principle from information geometry", Phys. Rev. E **98**, 032106 (2018).

[208]S. J. Large, R. Chetrite, and D. A. Sivak, "Stochastic control in microscopic nonequilibrium systems", Europhys. Lett. **124**, 20001 (2018).

[209]M. Scandi and M. Perarnau-Llobet, "Thermodynamic length in open quantum systems", Quantum **3**, 197 (2019).

[210]C. Cafaro and P. M. Alsing, "Information geometry aspects of minimum entropy production paths from quantum mechanical evolutions", Phys. Rev. E **101**, 022110 (2020).

[211]S. J. Bryant and B. B. Machta, "Energy dissipation bounds for autonomous thermodynamic cycles", Proc. Natl. Acad. Sci. U.S.A. **117**, 3478–3483 (2020).

[212]S.-i. Amari and H. Nagaoka, *Methods of Information Geometry*, Vol. 191 (Oxford University Press, New York, 2000).

[213]S. Deffner and E. Lutz, "Generalized Clausius inequality for nonequilibrium quantum processes", Phys. Rev. Lett. **105**, 170402 (2010).

[214]L. Mancino, V. Cavina, A. De Pasquale, M. Sbroscia, R. I. Booth, E. Roccia, I. Gianani, V. Giovannetti, and M. Barbieri, "Geometrical bounds on irreversibility in open quantum systems", Phys. Rev. Lett. **121**, 160602 (2018).

[215]G. E. Crooks, "Measuring thermodynamic length", Phys. Rev. Lett. **99**, 100602 (2007).

[216]D. A. Sivak and G. E. Crooks, "Thermodynamic metrics and optimal paths", Phys. Rev. Lett. **108**, 190602 (2012).

[217]C. Villani, *Optimal Transport: Old and New* (Springer, Berlin, Heidelberg, 2008).

[218]E. Aurell, C. Mejía-Monasterio, and P. Muratore-Ginanneschi, "Optimal protocols and optimal transport in stochastic thermodynamics", Phys. Rev. Lett. **106**, 250601 (2011).

[219]E. Aurell, K. Gawędzki, C. Mejía-Monasterio, R. Mohayaee, and P. Muratore-Ginanneschi, "Refined second law of thermodynamics for fast random processes", J. Stat. Phys. **147**, 487–505 (2012).

[220]A. Dechant and Y. Sakurai, "Thermodynamic interpretation of Wasserstein distance", arXiv preprint arXiv:1912.08405 (2019).

[221]D. P. Pires, M. Cianciaruso, L. C. Céleri, G. Adesso, and D. O. Soares-Pinto, "Generalized geometric quantum speed limits", Phys. Rev. X **6**, 021031 (2016).

[222]S. Deffner, "Geometric quantum speed limits: a case for Wigner phase space", New J. Phys. **19**, 103018 (2017).

[223]K. Funo, N. Shiraishi, and K. Saito, "Speed limit for open quantum systems", New J. Phys. **21**, 013006 (2019).

[224]H. J. D. Miller, M. Scandi, J. Anders, and M. Perarnau-Llobet, "Work fluctuations in slow processes: Quantum signatures and optimal control", Phys. Rev. Lett. **123**, 230603 (2019).

[225]K. Brandner and K. Saito, "Thermodynamic geometry of microscopic heat engines", Phys. Rev. Lett. **124**, 040602 (2020).

[226]J. M. Deutsch, "Eigenstate thermalization hypothesis", Rep. Prog. Phys. **81**, 082001 (2018).

[227]K. Ptaszyński and M. Esposito, "Entropy production in open systems: The predominant role of intraenvironment correlations", Phys. Rev. Lett. **123**, 200603 (2019).

[228]N. Shiraishi and K. Saito, "Information-theoretical bound of the irreversibility in thermal relaxation processes", Phys. Rev. Lett. **123**, 110603 (2019).

[229]L. Mandelstam and I. Tamm, "The uncertainty relation between energy and time in non-relativistic quantum mechanics", J. Phys. USSR **9**, 249–254 (1945).

[230]N. Margolus and L. B. Levitin, "The maximum speed of dynamical evolution", Physica D **120**, 188–195 (1998).

[231]A. del Campo, I. L. Egusquiza, M. B. Plenio, and S. F. Huelga, "Quantum speed limits in open system dynamics", Phys. Rev. Lett. **110**, 050403 (2013).

[232]M. M. Taddei, B. M. Escher, L. Davidovich, and R. L. de Matos Filho, "Quantum speed limit for physical processes", Phys. Rev. Lett. **110**, 050402 (2013).

[233]S. Deffner and S. Campbell, "Quantum speed limits: from Heisenberg's uncertainty principle to optimal quantum control", J. Phys. A **50**, 453001 (2017).

[234]M. Okuyama and M. Ohzeki, "Quantum speed limit is not quantum", Phys. Rev. Lett. **120**, 070402 (2018).

[235]B. Shanahan, A. Chenu, N. Margolus, and A. del Campo, "Quantum speed limits across the quantum-to-classical transition", Phys. Rev. Lett. **120**, 070401 (2018).

[236]J. M. Lee, *Introduction to Smooth Manifolds*, 1st ed., Vol. 218 (Springer-Verlag, New York, 2003).

[237]J. Dolbeault, B. Nazaret, and G. Savaré, "A new class of transport distances between measures", Calc. Var. Partial Dif. **34**, 193–231 (2008).

[238]E. A. Morozova and N. N. Chentsov, "Markov invariant geometry on manifolds of states", J. Sov. Math. **56**, 2648–2669 (1991).

[239]D. Petz, "Monotone metrics on matrix spaces", Linear Algebra Appl. **244**, 81–96 (1996).

[240]F. Hiai and D. Petz, "Riemannian metrics on positive definite matrices related to means", Linear Algebra Appl. **430**, 3105–3130 (2009).

[241]W. K. Wootters, "Statistical distance and Hilbert space", Phys. Rev. D **23**, 357–362 (1981).

[242]S. L. Braunstein and C. M. Caves, "Statistical distance and the geometry of quantum states", Phys. Rev. Lett. **72**, 3439–3443 (1994).

[243]F. Kubo and T. Ando, "Means of positive linear operators", Math. Ann. **246**, 205–224 (1980).

[244]A. Uhlmann, "Density operators as an arena for differential geometry", Rep. Math. Phys. **33**, 253–263 (1993).

[245]P. Gibilisco and T. Isola, "Wigner-Yanase information on quantum state space: The geometric approach", J. Math. Phys. **44**, 3752 (2003).

[246]M. G. A. Paris, "Quantum estimation for quantum technology", Int. J. Quantum Inf. **7**, 125–137 (2009).

[247]M. Gelbrich, "On a formula for the L^2-Wasserstein metric between measures on Euclidean and Hilbert spaces", Math. Nachr. **147**, 185–203 (1990).

[248]J.-D. Benamou and Y. Brenier, "A computational fluid mechanics solution to the Monge-Kantorovich mass transfer problem", Numer. Math. **84**, 375–393 (2000).

[249]V. Gorini, A. Kossakowski, and E. C. G. Sudarshan, "Completely positive dynamical semigroups of N-level systems", J. Math. Phys. **17**, 821–825 (1976).

[250]D. A. Lidar, "Lecture notes on the theory of open quantum systems", arXiv preprint arXiv:1902.00967 (2019).

[251]R. Alicki and K. Lendi, *Quantum Dynamical Semigroups and Applications* (Springer, Berlin, 1987).

[252]P. Strasberg, G. Schaller, T. Brandes, and M. Esposito, "Quantum and information thermodynamics: A unifying framework based on repeated interactions", Phys. Rev. X **7**, 021003 (2017).

[253]R. Jordan, D. Kinderlehrer, and F. Otto, "The variational formulation of the Fokker-Planck equation", SIAM J. Math. Anal. **29**, 1–17 (1998).

[254]J. Maas, "Gradient flows of the entropy for finite Markov chains", J. Funct. Anal. **261**, 2250–2292 (2011).

[255]E. A. Carlen and J. Maas, "Gradient flow and entropy inequalities for quantum Markov semigroups with detailed balance", J. Funct. Anal. **273**, 1810–1869 (2017).

[256]C. Rouzé and N. Datta, "Concentration of quantum states from quantum functional and transportation cost inequalities", J. Math. Phys. **60**, 012202 (2019).

[257]J. Agredo and F. Fagnola, "On quantum versions of the classical Wasserstein distance", Stochastics **89**, 910–922 (2017).

[258]F. Golse, C. Mouhot, and T. Paul, "On the mean field and classical limits of quantum mechanics", Commun. Math. Phys. **343**, 165–205 (2016).

[259]G. D. Palma and D. Trevisan, "Quantum optimal transport with quantum channels", arXiv preprint arXiv:1911.00803 (2019).

[260]Y. Chen, T. T. Georgiou, L. Ning, and A. Tannenbaum, "Matricial Wasserstein-1 distance", IEEE Control Syst. Lett. **1**, 14–19 (2017).

[261]N. Shiraishi, K. Saito, and H. Tasaki, "Universal trade-off relation between power and efficiency for heat engines", Phys. Rev. Lett. **117**, 190601 (2016).

[262]A. J. Short and T. C. Farrelly, "Quantum equilibration in finite time", New J. Phys. **14**, 013063 (2012).

[263]H. Tajima and K. Funo, "Superconducting-like heat current: Effective cancellation of current-dissipation trade off by quantum coherence", arXiv preprint arXiv:2004.13412 (2020).

[264]O. Abah, J. Roßnagel, G. Jacob, S. Deffner, F. Schmidt-Kaler, K. Singer, and E. Lutz, "Single-ion heat engine at maximum power", Phys. Rev. Lett. **109**, 203006 (2012).

[265]R. Kosloff and Y. Rezek, "The quantum harmonic Otto cycle", Entropy **19**, 136 (2017).

[266]M. Kloc, P. Cejnar, and G. Schaller, "Collective performance of a finite-time quantum Otto cycle", Phys. Rev. E **100**, 042126 (2019).

[267]M. Ramezani, F. Benatti, R. Floreanini, S. Marcantoni, M. Golshani, and A. T. Rezakhani, "Quantum detailed balance conditions and fluctuation relations for thermalizing quantum dynamics", Phys. Rev. E **98**, 052104 (2018).

[268]M. Scandi, H. J. D. Miller, J. Anders, and M. Perarnau-Llobet, "Quantum work statistics close to equilibrium", Phys. Rev. Research **2**, 023377 (2020).

[269]H. J. D. Miller, G. Guarnieri, M. T. Mitchison, and J. Goold, "Quantum fluctuations hinder finite-time information erasure near the Landauer limit", Phys. Rev. Lett. **125**, 160602 (2020).

[270]A. van den Bos, *Parameter Estimation for Scientists and Engineers* (Wiley-Interscience, New York, 2007).

[271]M. L. Rosinberg and J. M. Horowitz, "Continuous information flow fluctuations", Europhys. Lett. **116**, 10007 (2016).